MET-EGFR Dimerisation in Lung Adenocarcinoma is Dependent on EGFR Mutations and Altered by MET Kinase Inhibition

Lee, Richard William

Awarding institution:
King's College London

MET-EGFR Dimerisation in Lung Adenocarcinoma is Dependent on *EGFR* Mutations and Altered by MET Kinase Inhibition

A thesis submitted to

King's College London for the degree of

Doctor of Philosophy

Dr Richard William Lee

Asthma, Allergy & Lung Biology

King's College London

2017

This thesis is dedicated to my grandparents who knew lung cancer as a 'shadow' before EGFR and to my wife and children for helping me to 'work hard, play hard'.

Acknowledgements

This project was made possible with the generous support of the Medical Research Council and the NIHR Biomedical Research Centre (BRC) at Guy's Hospital. Beyond financial and educational resources, the BRC also enacted a valuable program of engagement events, so I could see the value of sharing research with primary school children, the unsuspecting public of Peckham library and senior research leaders.

A first word of gratitude is owed to my supervisors Professors George Santis and Tony Ng for their commitment to my fellowship in lung cancer. A special thank you to George who has provided a clinical repose for every difficulty and an engaging mentorship that has not tired since welcoming me into the department nearly a decade ago. His unnerving experience in choosing the right path has been instrumental to reaching this point. Tony likewise has inspired an intellectual foray into the many depths of EGFR and its dimers and back on the long road between basic science and better health.

Another heartfelt thank you to my 'maestra y comandante', Dr Elena Ortiz-Zapater whose extensive post-doctoral experience ploughed through the large xenograft experiment and a number of other hurdles which would not have been achievable without her efforts. Her demand for high calibre work and relentless effort gave me an appreciation of "team science" and when to set my own objectives. She designed the original H1975 model and I acknowledge direct contributions in the figures where appropriate. A firm 'cheers' is also needed for Dr Gregory Weitsman who supervised many visits to the microscope, often without daylight, with a 'blue roll' lecture in optical biophysics and spent many more hours remotely shutting down the laser, long after the last train home. Thanks also to Dr Moonim (MM) and the St Thomas' pathology services for guidance and assistance with cell block preparation and tissue staining and to Dr Neat and the Genetics Department for help with *MET* copy number analysis.

Finally, good scientists need good coffee and colleagues with whom to share it. Alex, Claire and Siva were always wise and encouraging. Along with Lyn, Sara, Will, Elena, Wei and Fatin, the lab was a warmer place with good friends and Western blots more fun with Radio 4 and *WhatsApp.* The last word is owed to those closest to me. The most sincere gratitude goes to my wife who has shown patience, listened to science and politics and ultimately realised a deadline. Finally to my wonderful children whom I hope will one day read a few of these words as experts in their own fields and attribute value to medicine, science and cancer research in general.

Abstract

Prognosis in advanced stage lung cancer is extremely poor with few effective therapies. EGFR tyrosine kinase inhibitors (TKIs) have high response rates in patients with activating *EGFR* mutations and are now an established part of therapy in selected patients. Such advances herald a previously unprecedented enthusiasm for the possibilities of targeted therapy. Acquired resistance however is widespread - the *EGFR* T790M mutation in particular represents approximately 50% of these. *MET* amplification is also an important route of resistance and preclinical data suggests synergy between therapies targeting these two receptors. We hypothesized that *EGFR* mutation status determines the EGFR-MET interaction and response to MET inhibition. We tested this hypothesis by using cells derived from NCI-H1975, which possess L858R and T790M *EGFR* mutations. This cell model and a derived murine xenograft experiment provided a platform with which to test these ideas by using assays of tumorigenicity *in vitro*; tumour growth/stroma formation *in vivo* and a selective MET kinase inhibitor, SGX523. EGFR-MET interaction was assessed by a Förster Resonance Energy Transfer (FRET) Fluorescence Lifetime Imaging Microscopy (FLIM) assay developed as part of this thesis that quantified EGFR-MET dimer formation.

SGX523 significantly reduced cell proliferation, xenograft tumour growth and ERK phosphorylation in the presence of the *EGFR* L858R-T790M mutations but not with *EGFR* L858R alone where SGX523 reduced stroma formation but not growth. SGX523 reduced EGFR-MET dimerisation in the EGFR L858R-T790M mutant but increased EGFR-MET interaction in the presence of EGFR L858R alone. Little effect was seen with EGFR WT in response to SGX523 for any of these indices. This thesis provides novel data for the mechanistic understanding of EGFR-MET heterodimerisation and the accompanying discussion explores how this is relevant for EGFR and MET targeted therapies.

Table of Contents

Table of Figures

Table of Tables

Abbreviations

Abbreviation	Meaning
ADC	Analogue to digital converter
ALK	Anaplastic lymphoma kinase
APS	Ammonium persulfate
AR	Amphiregulin
ATP	Adenosine triphosphate
BrdU	5'-Bromodeoxyuridine
BSA	Bovine serum albumin
CCD	Charge-coupled device
CD31	Cluster of differentiation 31
CK5/6	Cytokeratin 5/6
Co-IP	Co-Immunoprecipitation
CO2	Carbon dioxide
Cy5	Cyanine 5
D/P	Dye: Protein ratio
ddPCR	Digital droplet polymerase chain reaction
DNA	Deoxyribonucleic acid
DTT	Dithiothreitol
EC	Extracellular
EDTA	Ethylenediaminetetraacetic acid
EGF	Epidermal Growth Factor
EGFR	Epidermal Growth Factor Receptor
EGTA	Ethylene glycol tetraacetic acid
EMT	Epithelial–mesenchymal transition
ERK	Extracellular signal-Regulated Kinases
FBS	Fetal bovine serum
FDA	US Food and Drug Administration
FFPE	Formalin fixed paraffin embedded
FISH	Fluorescence In Situ Hybridisation
FLIM	Fluorescence lifetime imaging
FRET	Forster Resonance Energy Transfer
GAPDH	Glyceraldehyde 3-phosphate dehydrogenase
GBM	Glioblastoma Multiforme
GFP	Green fluorescence protein

H	Hours
H&E	Haematoxylin and eosin
HB-EGF	Heparin-binding EGF-like growth factor
HEPES	N-2-hydroxyethylpiperazine-N-2-ethane sulfonic acid
HER	Human Epidermal growth factor Receptor
HGF	Hepatocyte Growth Factor
HNSCC	Head and neck squamous cell carcinoma
IASLC	International Association for the Study of Lung Cancer
IC	Intracellular
IF	Immunofluorescence
IHC	Immunohistochemistry
IP	Immunoprecipitation
JAK	Janus kinase
JM	Juxtamembrane
Kb	Kilobases
K_{cat}	Turnover number
KDa	Kilodaltons
Ki	Inhibitor constant
Km	Michaelis constant
KRAS	V-Ki-ras2 Kirsten rat sarcoma viral oncogene homolog
MAPK	Mitogen-activated protein kinases
MT	Masson's trichrome
NaF	Sodium fluoride
NCI	National Cancer Institute
NICE	National Institute of Clinical Excellence
NS	Not significant
NSCLC	Non-Small Cell Lung Cancer
PAGE	Polyacrylamide gel electrophoresis
PI3K	Phosphoinositide 3-kinase
RT	Room temperature
RT-PCR	Reverse transcription polymerase chain reaction
S-phase	Synthesis phase
SD	Standard Deviation
SDS	Sodium Dodecyl Sulphate
SEM	Standard Error of the Mean
shEGFR	Short hairpin - EGFR
SOX2	SRY (sex determining region Y)-box 2

STAT	Signal transducer and activator of transcription
TBS	Tris buffered saline
TCSCP	Time-correlated single-photon counting
TEMED	Tetramethylethylenediamine
TGF	Transforming Growth Factor
TKI	Tyrosine Kinase Inhibitor
TNM	Tumour, Node, Metastasis (Staging)
TTF1	Thyroid transcription factor 1
UCCC	University of Colorado Cancer Center
V	Volts
WB	Western blot
WT	Wildtype
X546	Alexa Fluor 546
α-SMA	Anti-smooth muscle actin

Chapter 1. Introduction

1.1 Lung cancer Background

Lung cancer was diagnosed in 45,500 patients in the UK in 2013 with 35,400 lung cancer deaths recorded in the UK in 2012. Worldwide, lung cancer is the commonest cause of cancer deaths; in 2012 these totalled 1.6 million. These statistics are staggering for a disease where prognosis is extremely poor with a median survival of six months - only 5% of patients survive 10 or more years (Cancer research UK data, accessed April 2016). The outlook is bleak for such patients, particularly since most present with advanced stage, incurable disease. Potentially curative surgery is in fact available for fewer than 20% of cases. Unfortunately, in the inoperable, success in chemotherapy is usually limited to months and sustained remission is rare. Approximately one third of lung cancer patients may receive no anti-cancer therapy at all (The National Lung Cancer Audit 2015, Royal College of Physicians).

An inextricable nihilism has therefore surrounded lung cancer care in recent decades. Whilst prognosis has improved in other cancers such as breast cancer (e.g. increased 5 year survival from 75% to 91% between 1975 and 2011), likely as a result of improved understanding of disease mechanisms and therapeutic improvements, the statistics around lung cancer survival remain sobering (12%, 1975; 18%, 2011) (Siegel, Miller et al. 2016). This can be attributed to a poor understanding of lung cancer historically and a gloomy pessimism, which accepted that treatment in most cases would be futile. The assumption that lung cancer was a single disease with simplistic histopathological classifications that shared clinical features and therefore equal approaches to treatment is now out-dated. The considerable effort to overcome these challenges is essential to improve prospects for future generations.

Lung cancer is in fact a broad entity. According to the 2015 World Health Organisation classification, lung cancer can be categorised into Small cell and Non-Small Cell Lung Cancer (NSCLC) based on histopathological appearances of cells and tissue architecture, in addition to immunohistochemical markers. The majority (80%) of lung cancers are NSCLC, which includes the commonest subtypes adenocarcinoma and squamous cell carcinoma (Reck, Heigener et al. 2013). Lung adenocarcinoma is more usually seen towards the lung peripheries and demonstrates a neoplastic glandular appearance with cells that characteristically stain positively for thyroid transcription factor 1 (TTF1), keratin 7 and mucin (Chen, Fillmore et al. 2014). Conversely, squamous cell carcinoma more usually arises in the proximal airways and is defined by the presence of intercellular 'desmosomes', keratin production and p40, p63,

Cytokeratin 5/6 (CK5/6), SRY-Box2 (SOX2) and desmoglein immunostaining. Squamous cell lung cancer is also more usually associated with smoking and chronic inflammation and is typically associated with a more diffuse mutational burden than adenocarcinoma (Travis, Brambilla et al. 2013, Chen, Fillmore et al. 2014).

Finally other forms of lung cancer not explored further here include small cell lung cancer, a more aggressive tumour defined by the relatively small size and volume of cytoplasm, with hyperchromatic nuclei and diffuse necrosis and presence of neuroendocrine features; carcinoid which express neuroendocrine features to varying extents and finally, large cell and adenosquamous lung cancer (Chen, Fillmore et al. 2014). The discussion within this thesis will largely be limited to the non-small cell lung cancer cell types and the experiments conducted within systems representing lung adenocarcinoma.

1.2 The Limitations of Current Lung Cancer Therapy

Presently, the most important determinant of effective treatment in lung cancer is based on “tumour stage”, for example, invasiveness of tumour margins and anatomical spread. The International Association for the Study of Lung defines these phase specific features of lung cancer, which group together prognostically into a set of recommendations, which it submits to the Union for International Cancer Control (UICC) and the American Joint Committee on Cancer (AJCC) who mandate a classification most recently updated in the latter part of 2016 and effected in early 2017. This 'IASLC' classification, known as “TNM staging” of the tumour, now in its eighth incarnation provides a classification system for lung tumours based on (T)umour characteristics, lymph (N)ode involvement and (M)etastatic deposits (Travis, Brambilla et al. 2011, Goldstraw, Chansky et al. 2016). Stage I, II and some stage III groups have the best chance of surgical cure assuming the patient has sufficient physiological reserve to endure surgery or alternatively withstand radical radiotherapeutic approaches. Unfortunately the remainder are unlikely to be cured and can at best hope for prolonged treatment response with optimal systemic therapy, which typically includes platinum based combinations but increasingly molecularly targeted approaches including immunotherapy.

Immunotherapy with PDL1 inhibitors such as nivolumab and pembrolizumab represents a new class of therapy, which impairs the ability of the tumour to defend itself against the host immune response. In these trials PDL1 can be utilised as a biomarker to predict response to such agents although a number of trials have also

shown response irrespective of PDL1 status (Brahmer, Reckamp et al. 2015, Spigel, Reckamp et al. 2015, Herbst, Baas et al. , Herbst, Baas et al. 2016, Johnson 2016, Kindler, Karrison et al. 2017, Lievense, Sterman et al. , Rittmeyer, Barlesi et al.).

Significant efforts have been made to achieve early diagnosis where existing treatment might be more effective, for example through lung cancer screening programs (Ruparel and Janes 2016, Yousaf-Khan, van der Aalst et al. 2017). In addition, addressing the most important risk factor, smoking, through efforts such as legislating against smoking in public and plain packaging has been a priority. There does however remain a significant proportion of the population who are not affected by such changes (Peto, Darby et al. 2000). Lung cancer also remains an important disease in never smokers who account for 10-25% of sufferers of lung cancer and is the seventh commonest cause of cancer deaths in this group (Couraud, Zalcman et al. 2012). Furthermore as preventative efforts to reduce smoking prevalence come into fruition (albeit with several decades lag period) the proportion of case in non-smokers rises (Cancer Genome Atlas Research 2014).

Therapeutic advances in the lung cancer literature have focused *firstly*, on enhanced, minimally invasive diagnostics and biomarker development, which has supported other important efforts into early diagnosis/therapy; *secondly*, on stage-specific "personalized therapy" consisting of novel pharmacological agents and extending to radical surgical and radiotherapeutic techniques, where curative treatment is feasible and targeted multimodal therapy in locally advanced or metastatic disease where cure is not possible (Reck, Heigener et al. 2013); and *thirdly*, on study of resistance mechanisms in search of novel therapeutic avenues to tackle recurrence. The diagnostic and therapeutic pathway for each is likely to diverge as our understanding of therapy in each subtype broadens.

One of the most important developments in lung cancer research in recent years has been the recognition of the potential to further sub-classify lung cancer according to genomic aberrations and molecular biomarkers against which stratified therapy could be employed. A number of clinically relevant mutations have now been discovered, including those in *EGFR*, *KRAS*, *ALK-ROS* rearrangements, *RET*, *BRAF* and *HER2* (Cancer Genome Atlas Research 2014, Sholl, Aisner et al. 2015). Most success in targeted agents has been observed in lung adenocarcinoma and one of the greatest sources for optimism and the most significant advances in lung cancer research this

decade has been the development of targeted agents against the Epidermal Growth Factor Receptor (EGFR) (Devarakonda, Morgensztern et al. 2015).

1.3 The Human Epidermal Growth Factor Receptor Family

The Human Epidermal Growth Factor Receptor (HER) family also known as by the related avian viral erythroblastosis oncogene *ErbB* consist of 4 cell surface receptor tyrosine kinases (*ErbB1-4* or HER1-4) which includes the prototypical Epidermal Growth Factor Receptor (EGFR or 'HER1'). Many tissue types express HER family members; some co-express multiple receptor types, although for unknown reasons, certain HER family members are more common in one type of cancer rather than another. For example, EGFR is important in lung cancer, glioblastoma multiforme (GBM) and head and neck squamous cell carcinoma (HNSCC), albeit with quite different genetic differences. Meanwhile, HER2 and HER3 are the most significant receptors in breast cancer (Holbro, Beerli et al. 2003). All play important roles in normal physiological conditions; lead to organ defects and non-viability in knockout mice and when dysregulated are important mediators of tumorigenesis in a number of solid cancers. As a consequence there is growing interest in these receptors as therapeutic targets in lung and other tumour types (Yarden and Sliwkowski 2001, Hynes and Lane 2005, Fujita 2013, Hansen and Siu 2013, Mitsui, Yonezawa et al. 2014).

The HER receptors are similar in their composition of the large extracellular ligand binding domain, hydrophobic transmembrane region and cytoplasmic tyrosine kinase domain which includes a juxtamembrane region and carboxyl-terminal regulatory tyrosine residues which serve as docking sites for downstream signaling proteins. The 620 amino acid extracellular region consists of 4 domains made up from a tandem repeat of a leucine rich domain (190 amino acids) and a cysteine rich domain (120 amino acids). Within this, domains I and III are beta-helix solenoid structures, which are within the leucine-rich region and can bind a single ligand simultaneously. Domain II and IV meanwhile are cysteine-rich and linked by disulphide bonds. The initial three of these domains share up to 20% sequence homology with the insulin-like growth receptor although unlike HER1, this receptor does not bind ligand with high affinity (Garrett, McKern et al. 1998, Lemmon 2009).

Dimerisation is essential to HER family activation. This can be homo- or hetero-dimeric. EGFR and HER4 undergo homodimerisation and are capable of auto-phosphorylation. Meanwhile, HER2 which lacks an identifiable ligand and HER3 which

has weak or no tyrosine kinase activity (Steinkamp et al, 2014) must heterodimerise to become activated (Yarden and Sliwkowski 2001). Partnering selectivity in such dimerisation appears to be hierarchical. Heterodimeric pairings in general are perceived to lead to more tumorigenic outcomes than their homodimeric counterparts and this is thought to be particularly true for those that include HER2 or HER3 partners. The HER2-HER3 dimer is thought to be the most oncogenic HER pair despite each individually being handicapped by the apparent lack of ligand/kinase domain respectively (Citri, Skaria et al. 2003). It is not clear why this should be the case, but one hypothesis suggests that the lack of competition from homodimers for these obligate heterodimers may be important (Lemmon 2009). HER1-HER4 heterodimers are recognized and may influence cellular behaviour such as migration but appear to form less frequently (Yarden and Sliwkowski 2001, Kiuchi, Ortiz-Zapater et al. 2014)

An asymmetric activator-receiver model where each of a pair of HER receptors is dedicated to either activating or being activated in the process of phosphorylation and signal transduction, appears to be the basis of activation for the HER family in general (Zhang, Gureasko et al. 2006). In their inactive, unbound state, the default HER family structure is to adopt a closed, tethered conformation. Ligand binding to extracellular domain then promotes a conformational change to an extended structure that reveals the dimerisation arm. This engages another ligand-bound receptor molecule, overcoming the resting auto-inhibited state with subsequent activation of the kinase domain and propagation of downstream signaling through molecules containing SH2-like domains in a manner resembling cyclin-dependent kinases (Yarden and Sliwkowski 2001, Zhang, Gureasko et al. 2006). Interestingly, ErbB receptors are unique in this sense compared with other RTK in that the ligand forms no part of the dimer interface, which is instead receptor mediated (Lemmon, Schlessinger et al. 2014)

Signal processing by the HER family receptors is mediated by additional effectors such as by Ras- or Shc-driven activation of MAPK (proliferation) or the PI3K-AKT (cell survival) pathways. Loss of HER-mediated activation of these signals promotes BCL-2 driven apoptosis (Yarden and Sliwkowski 2001, Arteaga and Engelman 2014). HER3 in particular is an important mediator of PI3K-AKT signaling as it has six consensus binding sites for the P85 subunit. HER2 alone can activate ERK but requires HER3 for PI3K signaling, hence the importance of the HER2-HER3 dimer. Similarly HER3 mediated AKT signaling is likely to be important in aberrant EGFR signaling. Src kinases, JAK/STAT and WNT are also likely to play a role (Arteaga and Engelman 2014).

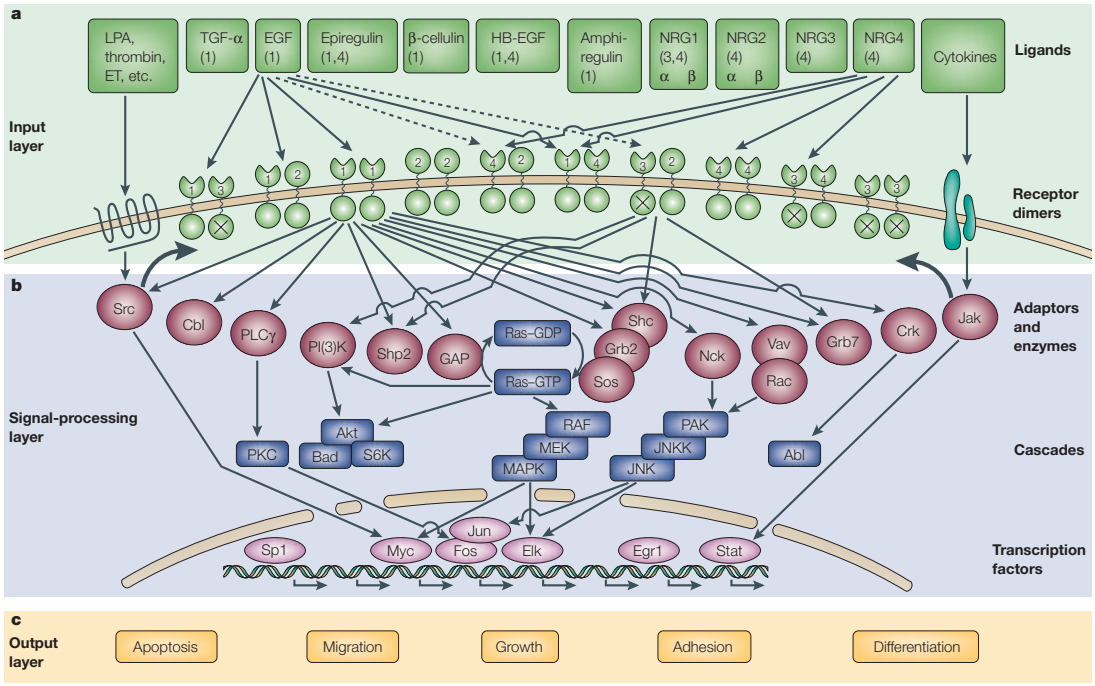

Figure 1.1 Signalling heterogeneity in the HER signaling network.
A range of ligands activate the HER receptors (green squares). There are 10 potential dimerisation partnerships between the 4 HER family members which results in various possibilities for multi-functionality and signaling specificity (green circles). Each HER (ErbB) dimer pair in the cell surface membrane (input layer) can give rise to multiple unique downstream signals with MAPK and PI3K-AKT being of particular importance (Red circles/blue squares). A range of phenotypical outcomes is thus determined through the control of these signaling mediators by the respective HER receptor pairing - output layer (yellow squares). Reproduced from (Yarden and Sliwkowski 2001).

1.4 The Epidermal Growth Factor Receptor (EGFR)

EGFR is the most important HER family receptor in Non-Small Cell Lung Cancer (NSCLC) and has rapidly become established as one of the most clinically relevant oncogenes in this tumour type. Over 60% of NSCLC tumours express EGFR and overexpression is associated with increased growth, metastasis and poor differentiation (Franklin, Veve et al. 2002, Herbst 2004).

EGFR, a 170KDa glycoprotein is prototypical of the HER receptors and there is significant structural and functional overlap. Like the other HER molecules, EGFR has a structure that consists of an extra-cellular domain, which receives ligand signal in the form of EGF but is also responsive to transforming growth factor-β (TGF-β), heparin-binding EGF-like growth factor (HB-EGF), amphiregulin (AR), betacellulin (BTC), epi-regulin (EPR), and epigen. There is in addition a transmembrane domain; a juxtamembrane (JM) region, which is likely to form an integral, dimer-stabilising component of the activated state of EGFR; a tyrosine kinase domain, the enzymatic

core of the receptor and an intracellular domain where tyrosine residues are found which can become phosphorylated by kinase activity, and act as docking sites to facilitate binding of signal mediators (Schlessinger 2002, Harris, Chung et al. 2003, Hubbard 2009).

The *EGFR* gene lies on the short arm of chromosome 7 at the 7p12 locus consisting of approximately 200,000 base pairs containing 30 exons (Reiter, Threadgill et al. 2001). A number of genetic aberrations have been described which dysregulate EGFR function. Increased *EGFR* copy number is reported in up to 45% of lung cancers whilst *EGFR* mutations have been described in up to two thirds. It is not clear whether one event precedes the other, although it is likely that both events increases genomic instability and both are correlated with EGFR overexpression (Liang, Zhang et al. 2010). Increased *EGFR* copy number is also highly prevalent in head and neck squamous cell carcinoma (HNSCC) and glioblastoma multiforme (GBM). In GBM the *EGFRvIII* mutation in the extracellular domain drives ligand independent signaling. A clearly dominant *EGFR* mutation has not been established in HNSCC (Kalyankrishna and Grandis 2006, Hatanpaa, Burma et al. 2010, Worsham, Ali et al. 2012).

EGFR mutations are of established importance in lung cancer clinical practice. Mutations found within the tyrosine kinase domain encoded by exons 18-21 of the *EGFR* gene are of particular relevance. This region gives rise to an important part of the ATP binding pocket. As seen in figure 1.2, the most frequently recognized are deletions in exon 19, within codons 746-750 (the ELREA motif) and a point mutation at codon 858 (L858R), which together account for 90% of these mutations. Other larger deletions or combined deletions/substitutions are also recognized and 3-5% of mutations occur at codon 719 (G719X). Another 1-3% are insertion mutations in exon 20. A subset of mutations including T790M on exon 20 are rarer but become more important with exposure to EGFR therapy (see later).

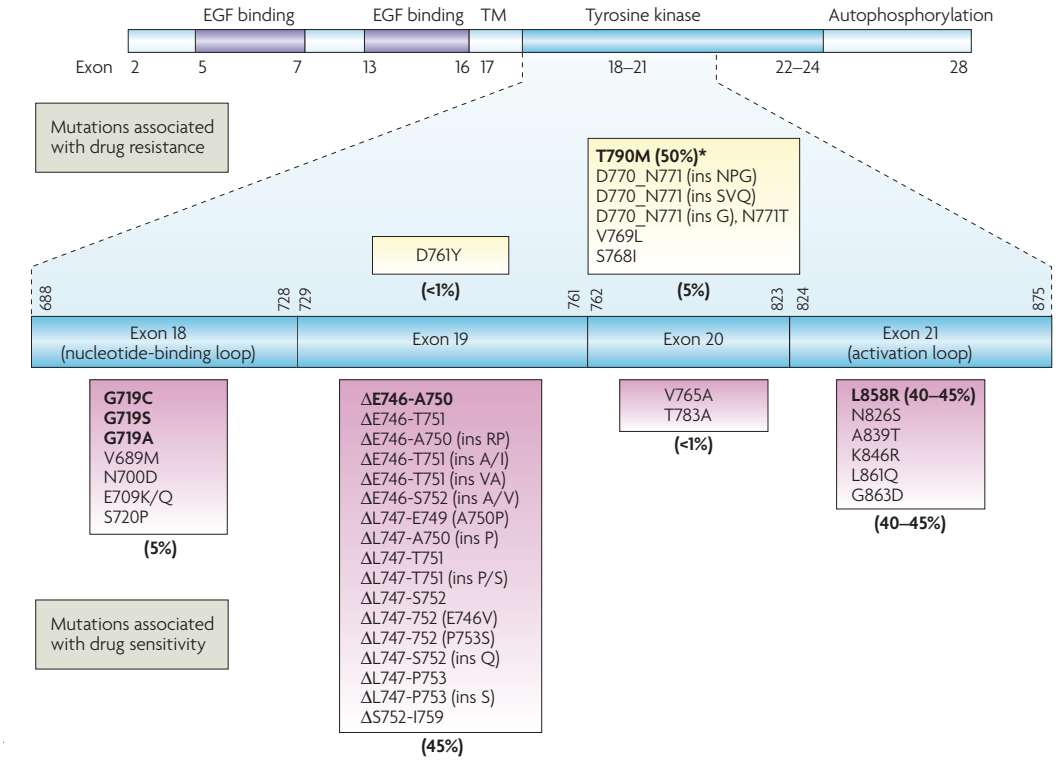

Figure 1.2 The *EGFR* gene exons and corresponding functional regions.
EGFR mutations are common in the kinase domain encoding region within exons 18-21, which alter residues important for ATP interaction with its binding pocket. As a consequence, mutations result in either increased sensitivity to EGFR TKI (purple boxes) or treatment resistance (yellow boxes). Adapted from Sharma 2007 (Sharma, Bell et al. 2007).

Many *EGFR* kinase domain mutations result in constitutive kinase domain activity that causes *EGFR* to act as an oncogenic driver in tumour cells (Sharma, Bell et al. 2007, Suda, Onozato et al. 2009, Mitsudomi and Yatabe 2010). L858R, a Leucine substitution (also labelled L834R in alternative nomenclature) for example, lies in the activation loop and results in kinase activity that is 50 times more active than the wildtype (WT) form (Yun, Boggon et al. 2007). Interestingly there appears to be a difference in activity between these activating mutations. The del19 mutant is 10-fold more active than WT. Additionally L858R and del19 mutations differ in their affinity for ATP with the del19 *EGFR* having a 10-fold higher *Km* ATP than L858R and a higher auto-phosphorylation rate (Carey, Garton et al. 2006, Yun, Boggon et al. 2007). Double mutants, such as L858R combined with T790M are also recognized which modulate the behaviour of the initial mutation, which as in the case of T790M can increase the affinity for ATP which appears to change the dynamics of EGFR activation and have important consequences for susceptibility to agents targeted at these regions of the receptor as discussed below (Yun, Mengwasser et al. 2008).

As with other HER family members, EGFR must dimerise to function. EGFR can become activated by *homo*-dimerisation of two collocated EGFR monomers, brought together by ligand interaction (Bublil, Pines et al. 2010). The extra-cellular domain, suppresses a propensity of the kinase domains to dimerise and become activated until ligand binding. Under normal resting conditions, EGFR WT is inactive in an auto-inhibited state until binding of the EGF ligand. Ligand binding results in autophosphorylation of key tyrosine residues within the cytoplasmic domain which then interact with signaling molecules containing SH2 like domains that propagate the onward signal downstream towards the nucleus (Yarden and Sliwkowski 2001). An important aspect of EGFR dimerisation is its asymmetric nature, whereby the N-lobe of an 'activator' kinase engages and allosterically activates the C lobe of its receiving partner. Figure 1.3 shows a schematic of this process. This activator-receiver model of dimerisation resembles the activation of cyclin-dependent kinases and has been highlighted as an important basis of activation for the entire HER family (Zhang, Gureasko et al. 2006).

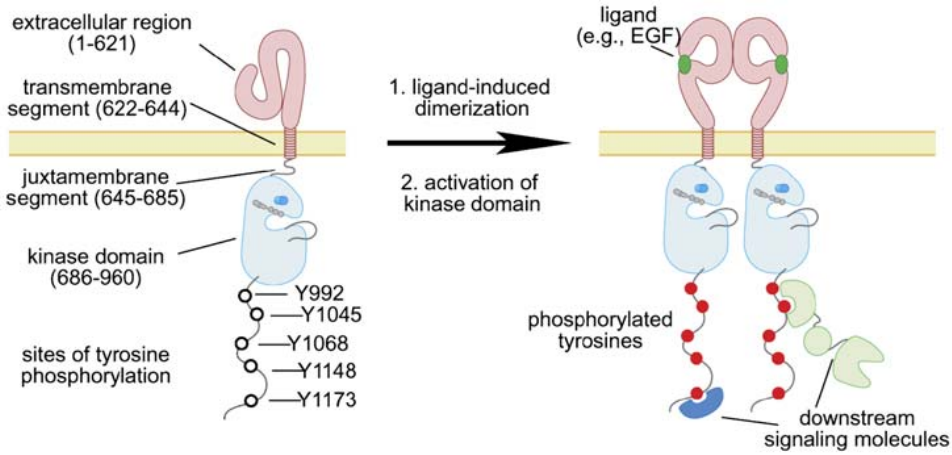

Figure 1.3 Schematic of EGFR activation with ligand-induced dimerisation
EGFR consists of an extracellular region and transmembrane/juxtamembrane segments (pink) bound to a kinase domain (blue), which acts to phosphorylate downstream tyrosine residues (--Y) which then serve as important docking sites for downstream signaling proteins. Conformational changes arising as a result of ligand binding or activating mutations encourage receptor-receptor dimerisation which are important to tyrosine phosphorylatio and subsequent signal transduction. Adapted from Zhang et al (Zhang, Gureasko et al. 2006).

It is thought that activating EGFR kinase domain mutations induce conformational changes that disrupt auto-inhibitory interactions that alter the dimerisation interface and would otherwise stabilize the inactive state, thus resulting in a conformation that favours transactivation and constitutive kinase activity leading to increased and sustained tyrosine residue phosphorylation (Yun, Boggon et al. 2007). It is also apparent that such mutations can interfere with intrinsic disorder, which would also favour transactivation (Shan, Eastwood et al. 2012). The L858R mutant EGFR has also been shown to possess a greater tendency to dimerisation than WT EGFR. Data from the literature suggests that EGFR L858R preferentially forms dimers and higher order oligomers than WT EGFR in light scattering and gel electrophoresis assays of molecular weight and that dimerisation is a more important consequence of the L858R mutation than catalytic potency is on EGFR signaling (Shan, Eastwood et al. 2012). Since allosteric interactions between partner EGFR molecules appear to be necessary for activation - even in the absence of ligand, this mechanism of asymmetric dimerisation may be sufficient for activation (Wang, Longo et al. 2011). In addition *EGFR* mutations result in differing abilities to dimerise within homodimeric versus heterodimeric pairings. This important observation might influence cell phenotype and which downstream pathway is activated. For example an EGFR-HER3 pairing versus an EGFR-EGFR pairing may preferentially activate AKT/STAT pathways in preference to MAPK (Mitsudomi and Yatabe 2010, Littlefield and Jura 2013).

1.5 EGFR Targeted Therapy

EGFR mutations are important clinically, predominantly as a tool to predict responsiveness to treatment (Shan, Eastwood et al. 2012). Initial study of EGFR directed therapy with agents such as the first generation EGFR tyrosine kinase inhibitors (TKI) gefitinib or erlotinib, noted a response in as few as 8-15% of Caucasians with lung cancer which was as high as 30-40% of Eastern Asian patients. These are low molecular weight ATP mimetics that reversibly bind EGFR in a specific and competitive manner (Lynch, Bell et al. 2004, Paez, Janne et al. 2004, Suda, Onozato et al. 2009). Young, female, 'never smokers' and adenocarcinoma classification were identified as clinical features that predict clinical response with subsequent identification that such *EGFR* mutations are enriched in this population (Sharma, Bell et al. 2007). One of the most important observations in EGFR targeted therapy was that response rates to these drugs were most striking in patients with the presence of an *EGFR* activating mutation in whom it was thereafter confirmed that EGFR TKI are most effective. For example, del19 or L858R saw responses in up to

80% of patients, compared to 10% in those without such mutations (Sharma, Bell et al. 2007, Gazdar 2009, Mok, Wu et al. 2009).

This increased sensitivity of EGFR mutants to EGFR TKI is likely to result from conformational differences arising from these mutations that increase the tendency for the receptor to be in the active state to which these EGFR TKI preferentially bind (Gazdar 2009). In addition it appears that significant structural alterations arise as result of these mutations at key TKI binding residues, which alters their tendency to bind and dissociate in favour of ATP (Carey, Garton et al. 2006, Kumar, Petri et al. 2008, Rosell, Carcereny et al. 2012). Four classes of EGFR inhibitors are recognised, as defined by their target binding site in the kinase domain that target the active (type I) or inactive conformations (type II) and those which inhibit the kinase allosterically (type III) or through interference of kinase regulators (type IV) (Muller, Chaikuad et al. 2015).

EGFR targeted therapy is important in a number of other solid tumour types. Interestingly, *EGFR* mutations typical in GBM are extracellular and induce a conformation not responsive to gefitinib or erlotinib, but instead by lapatinib, an EGFR/HER2 inhibitor that recognizes the inactive kinase conformation (Park, Liu et al. 2012, Vivanco, Robins et al. 2012). Here, TKI which recognise the active kinase can induce disabled "quasi-dimers". These dimers differ from ligand-induced dimers in that they appear to depend only upon the kinase domain interface rather being held by intra- and extra-cellular regions (Bublil, Pines et al. 2010). Again in HNSCC, gefitinib/erlotinib are not used – instead a monoclonal antibody inhibitor of EGFR, cetuximab is the only FDA approved EGFR targeted therapy (Cassell and Grandis 2010). A clear role for cetuximab and other monoclonal inhibitors of EGFR (e.g. necitumumab) in lung cancer have not been established (Pirker and Filipits 2012) (Thatcher, Hirsch et al.). The multiplicity of EGFR as a target and yet its refractoriness to a single therapeutic agent across tumour types provides interesting biological insights to its role in different tissue types.

Clinical assays that can identify activating *EGFR* kinase domain mutations from routine clinical biopsies are hence a vital part of the treatment of patients with EGFR targeted therapy. Use of partner tests in this way improves the efficacy and cost effectiveness of these costly agents. Presence of such mutations is an internationally approved selection criterion for EGFR TKI and by guiding rationalised therapy by regulatory bodies such as National Institute of Clinical Excellence (NICE Guidance TA162 2008). Treatment with EGFR TKI in patients with WT EGFR was associated with less

favourable prognosis in these trials and hence clinically EGFR TKI are not routinely used in these cases, although the evidence remains unclear as to best management of such WT patients with regards to TKI (Lee, Hahn et al. 2014).

1.6 Resistance to EGFR TKI

Despite the rapidly evolving role and potential capability for dramatic clinical responses, EGFR TKI as with most HER family targeted therapies are almost universally prone to treatment resistance. A standardised criteria of EGFR TKI resistance requires that a patient with an *EGFR* sensitising mutation or whom has shown benefit from EGFR TKI, develops progressive disease during or immediately following such treatment (Jackman, Pao et al. 2010). Drug resistance can either be primary i.e. it exists prior to starting treatment, arising either through germ-line or somatic mutations or be acquired through exposure to treatment. Acquired resistance to TKI often arises when either when a mutated form of EGFR evolves which is no longer sensitive to the EGFR TKI of choice – for example through structural alteration of its TKI binding site to preclude binding or through changes to the competitive nature of TKI binding versus ATP. Another common route of TKI resistance is seen when the tumour escapes dependency or 'addiction' to the pathway targeted by the TKI in question. This 'kinase switch', allows signaling to be sustained via an alternative pathway as can be seen in gene amplification of *MET*, *HER2* or *MAPK*). Alternatively dysregulation of downstream signaling (e.g. *PIK3CA* or *BRAF* mutations) and transformation to an alternative phenotype (e.g. Epithelial-Mesenchymal Transition or conversion to small cell lung cancer) are also important (The Cancer Genome Atlas Research 2014, Stewart, Tan et al. 2015). See Table 1.

The T790M mutation is the most important mechanism of resistance to first generation EGFR TKI (~50%). This mutation results in increased affinity for ATP relative to EGFR TKI hence rendering them ineffective (Yun, Mengwasser et al. 2008)(NICE TA162 2008). Interestingly T790M has also been reported to increase EGFR activity *in vitro* and has been identified in hereditary lung cancer in TKI naïve patients (Bell, Gore et al. 2005, Godin-Heymann, Bryant et al. 2007). It is thus plausible that T790M alone or in combination with other activating mutations provides a survival advantage in TKI-naïve patients. Only recently has this detail of the origin of T790M in the evolution of resistance been clarified. Whilst T790M may arise during treatment, T790M positive clones have been observed to exist prior to TKI exposure and thus expand upon treatment with EGFR TKI therapy. This is of importance as the response to third generation EGFR-TKI differs between the two forms and provides evidence that multi-

target treatment regimes may be required to pre-empt resistance (Maheswaran, Sequist et al. 2008, Hata, Niederst et al. 2016). A number of other EGFR TKI resistance mutations have also been observed on exon 20 e.g. D770-N771 (see figure 1.2) and also exon 19 (D761Y) indicating structural relevance of these residues for EGFR TKI binding (Gazdar 2009).

Some of the most convincing evidence for a kinase switch leading to EGFR resistance was observed in data that suggested that activation of MET can bypass EGFR signaling via HER3 activation in order to sustain downstream PI3K/AKT signaling (Engelman, Zejnullahu et al. 2007, Campbell, Amin et al. 2010). The literature that associates EGFR TKI resistance with HER family dimer formation is not well established, however the HER3 receptor is of considerable importance in breast cancer therapy and is implicated in the response to the widely utilized trastuzumab (Herceptin) which targets HER2 (ERBB2), another key signaling mediator in this type of cancer (Holbro, Beerli et al. 2003, Claus, Patel et al. 2014). HER2 has also been linked to EGFR TKI resistance in lung cancer directly (Takezawa, Pirazzoli et al. 2012).

Another important route of resistance includes phenotypical change for example epithelial-mesenchymal transition (EMT) or conversion to Small Cell Lung Cancer. This route accounts for resistance EGFR TKI in approximately 10% of patients and the original activating *EGFR* mutation can be detected at the time of the small cell biopsy excluding a *de novo* tumour. These observations have raised interesting questions about a possible mutual cell of origin of both cancer types (Oser, Niederst et al. 2015). In EMT meanwhile, tumour cells acquire mesenchymal features such as loss of E-Cadherin, and increased expression of vimentin, fibronectin and N-cadherin, which is associated with increased motility and invasiveness (Morgillo, Della Corte et al. 2016).

Table 1. Summary of mechanisms of EGFR TKI resistance

Mechanism	Estimated frequency
EGFR Target changes (e.g. T790M)	60%
Small Cell Lung Cancer Conversion	10%
***MET* amplification**	5-10%
***HER2* amplification**	8-13%
Epithelial-Mesenchymal Transition	1-2%
Others: BRAF, PI3K	2-3%
Unknown	15-20%

Adapted from Camidge et al (Camidge, Pao et al. 2014)

It is inevitable that legion other resistance mechanisms are yet to be discovered e.g. undetected mutations, chromosomal rearrangements or more complex resistance mechanisms (e.g. receptor recycling/degradation, crosstalk) to account for the remaining cases of resistance. Decoding these is of obvious interest as it could provide novel avenues to broaden the use of EGFR TKI in the context of relapse. The important role of tumour heterogeneity in resistance is also increasingly recognized (Burrell and Swanton 2014, de Bruin, McGranahan et al. 2014).

A major focus of research in this area is now to identify and surpass routes of treatment resistance and to better understand the mechanistic features of TKI treatment. Much attention has been placed upon the T790M mutation and hence alternative structural approaches to EGFR inhibition. Second-generation EGFR inhibitors that bound EGFR irreversibly and thus not susceptible to ATP competition e.g. afatinib were not successful in early trials due to dose-limiting toxicity although afatinib remains of interest and demonstrated encouraging results in brain metastatic lung cancer. Subsequent "third generation" approaches have targeted the mutated sensitized and resistant (T790M) forms of EGFR directly e.g. rociletinib and AZD9291 (Cross, Ashton et al. 2014, Park, Tan et al. 2016, Schuler, Wu et al. 2016). Although such approaches are likely to encounter similar difficulties when further *EGFR* mutations arise, the success of these agents in clinical trials with response rates of up to 60% and prolonged control is encouraging and will increase the possibilities for patient fitness for further lines of treatment available now and in the development pipeline. Of further note, rociletinib was also beneficial in T790M-negative patients highlighting further work that is needed in this important area of the literature (Pao and Chmielecki 2010, Sequist, Soria et al. 2015, Yu, Tian et al. 2015, Tan, Cho et al. 2016).

1.7 Mesenchymal-Epithelial Transition (MET) Receptor

Another key player in this network of receptors is MET, a receptor tyrosine kinase found on the cell surface, which has seen a growing interest in the lung cancer literature. MET, also known as the Hepatocyte Growth Factor Receptor is encoded by a proto-oncogene located on chromosome 7q31 consisting of 21 exons and 120Kb. The transcribed peptide is synthesized as a 190KDa glycosylated peptide that is cleaved to 50KDa and 140KDa alpha and beta chains respectively (Ma, Maulik et al. 2003).

Derailment of normal MET signaling is associated with 'invasive growth' – a growth program important for morphogenesis in early embryonic development (Boccaccio and Comoglio 2006). A parallel thus exists between a role for MET in embryogenesis such as during formation of the gastrula, where separation of the endoderm, mesoderm and ectoderm requires cell motility and branching and a similar invasiveness of cancer cells at the tumour front. Sacrifice of proliferative behaviour of tumour cells in favour of acquisition of properties that can facilitate cell migration and invasion is known as Epithelial Mesenchyme Transition' (EMT) – a process with which MET is well associated (Boccaccio and Comoglio 2006).

HGF, the cognate ligand of MET, also known as scatter factor, stimulates a number of cellular processes leading to growth, motility and invasion. HGF is secreted from cells derived from a mesenchymal origin including stroma, fibroblasts and monocytes, reinforcing the importance of MET in the interaction of the tumour with the microenvironment. HGF has also been shown to induce EGFR resistance highlighting how this ligand of MET could tie together the MET signaling pathway with EGFR (Yano, Wang et al. 2008).

Like EGFR, MET is thought to become activated by dimerisation. The stoichiometry of this reaction in relation to HGF is not well understood but is thought to involve a seven-bladed propeller structure known as the Sema domain to which HGF binds. The Sema domain would then be responsible for mediating receptor cross-linking and thereafter activation (Gherardi, Youles et al. 2003, Wickramasinghe and Kong-Beltran 2005). Whilst this region is critical for ligand binding it may also allow ligand-independent MET activation in the context of *MET* amplification (Kong-Beltran, Stamos et al.). The juxtamembrane region of MET is also of importance in regulation of catalytic function, as with HER family proteins, mutations in this region result in altered cell morphology, proliferation and motility in small cell lung cancer cell (Ma, Kijima et al. 2003). Mutations affecting these Sema and juxtamembrane regions have been detected in lung cancer specimens although have not yet been translated into the context of biomarker trials or partner therapeutics (Ma, Jagadeeswaran et al. 2005).

The evidence for a potential clinical role of MET in lung cancer is strong. MET has been linked to tumorigenesis, propensity to metastasis and poor outcomes in a number of solid cancers (Gelsomino, Facchinetti et al. 2014). MET is also widely overexpressed in lung cancer cell lines and clinical specimens. A number of studies have reported MET overexpression by immunohistochemistry in particular at the

tumour front. Strong MET staining by immunohistochemistry correlates to earlier progression and increased expression of MET is also seen in brain metastases and as already discussed is an important resistance mechanism to EGFR TKI (Ma, Jagadeeswaran et al. 2005, Zucali, Ruiz et al. 2008, Benedettini, Sholl et al. 2010).

1.8 MET Biomarkers

According to the literature, MET is frequently overexpressed in lung cancer, but assays of protein expression haven't been translatable into clinical assays. *MET* amplification is currently viewed as being the most suitable clinical biomarkers of MET activity in NSCLC. This can be measured using real-time polymerase chain reaction (RT-PCR), comparative genomic hybridization or fluorescence in situ hybridization (FISH). FISH is one of the most widely employed approaches, because of reliability, selective measurement of tumour cells (rather than stroma) and its suitability to be applied to archival formalin-fixed paraffin embedded (FFPE) tissue as is routine for clinical specimens (Go, Jeon et al. 2010). Two criteria are recognized, the Cappuzzo scoring system sets a threshold of 5 copies to define amplification whilst the University of Colorado Cancer Center (UCCC) considers *MET* copy number as a ratio against a control locus on the same chromosome e.g. *Cep7*. Because copy number can be increased in isolation but not meet these criteria, later clinical studies have favoured a definition based on copy number ratio (Bean, Brennan et al. 2007, Okuda, Sasaki et al. 2008, Cappuzzo, Janne et al. 2009, Go, Jeon et al. 2010).

MET amplification predicts poor survival and has been associated with a higher incidence of metastatic disease with increased *MET* copy number observed in intracranial metastatic tumours (Bean, Brennan et al. 2007, Benedettini, Sholl et al. 2010). Mutations are also recognized in *MET*, most in relation to exon 14. These may be more frequent in an older population and moreso in smokers than with *EGFR* (Awad, Oxnard et al. 2016). Whilst such *MET* mutations have been shown to induce tumorigenesis, they are in comparison rarer events in clinical series and their significance prognostically and how they relate to *MET* amplification remains poorly defined (Cancer Genome Atlas Research 2014, Awad, Oxnard et al. 2016). Interestingly none of the patients in the aforementioned series had *EGFR* mutations unlike *MET* amplification which is implicated in up to 20% of patients with acquired resistance to EGFR TKI (Bean, Brennan et al. 2007, Tanaka, Sueoka-Aragane et al. 2012). Clinically these indices are of greatest potential interest in the context of selecting therapies that inhibit MET signaling.

1.9 MET Targeted Therapy

Therapeutic agents targeted at MET are broadly divided into three groups (Gherardi, Birchmeier et al. 2012): 1) Small molecule kinase inhibitors such as crizotinib and tivantinib (ARQ197); 2) Antibody based approaches which interrupt HGF binding at the MET extracellular domain for example onartuzumab (METMab). 3) Other agents which specifically target HGF. MET inhibitors have been validated experimentally in a number of *in vitro* and *in vivo* models of extra-thoracic cancer, including primary brain malignancies (Guessous, Zhang et al. 2010), gastric cancer (Kawakami, Okamoto et al. 2013, Wiehr, von Ahsen et al. 2013), triple negative breast cancer (Sohn, Liu et al. 2014), ovarian cancer (Zillhardt, Christensen et al. 2010), and hepatocellular carcinoma (Steinway, Dang et al. 2015).

Inhibition of MET alone or synergistic blockade with EGFR has been demonstrated within such systems representing thoracic malignancy (Tang, Du et al. 2008, Zhang, Staal et al. 2010, Xu, Kikuchi et al. 2012). Preclinical models of MET therapy in lung cancer include use of the small molecule inhibitor crizotinib which can overcome HGF/MET-mediated EGFR-TKI resistance in a number of NSCLC cell lines including H1975, HCC827 and PC-9 cell lines (Chen, Zhou et al. 2013). Similar studies have confirmed this *in vitro* effect with tivantinib (ARQ197)(Fong, Jacobs et al. 2013), PHA-665752 (Christensen, Schreck et al. 2003) and also the multi-kinase agents sunitinib and cabozantinib (Gridelli, Maione et al. 2007, Yakes, Chen et al. 2011). Similarly monoclonal antibody approaches such as onartuzumab (METMab) to block MET receptor signaling through impaired HGF binding, have also been validated *in vitro* (Surati, Patel et al. 2011, Ekert, Johnson et al. 2014, Vigna and Comoglio 2014).

In patients, data on sole treatment with MET inhibition is limited to early phase trials but include the use of crizotinib in tumours with *MET* amplification or exon 14 skipping which suggest crizotinib could be more effective in such cases but again a clear subgroup which derives benefit has not been defined (Camidge, Ou et al. 2014, Paik, Drilon et al. 2015, Vassal, Ledeley et al. 2015). Despite the pre-clinical data suggesting that combination (EGFR and MET) treatment could be beneficial against tumour growth, efficacy of dual treatment with such combined regimes have not been reproduced clinically (Zhang, Staal et al. 2013). Even the most advanced agents in development, onartuzumab ('METMab') – a MET neutralizing antibody which prevents HGF binding to MET in proximity to the Sema domain (Merchant, Ma et al. 2013); and tivantinib (ARQ197) - a small molecule inhibitor of MET which manipulates kinase conformation to prevent kinase activation, have failed in phase III clinical trials which

have included EGFR-TKI combinations (Gelsomino, Facchinetti et al. 2014, Pérol 2014, Scagliotti, von Pawel et al. 2015)

There is good evidence for interaction between EGFR and MET that support a combined approach: Both have been shown to be co-expressed in lung cancer cell lines (Tang, Du et al. 2008); crosstalk has also been observed between EGFR and MET signaling pathways in addition to direct co-immunoprecipitation between this two receptors (Jo, Stolz et al. 2000, Tang, Du et al. 2008, Wang, Li et al. 2010). There does hence remain hope that as with similar attempts to harness the EGFR pathway, an un-identified opportunity to isolate subgroups of patients who can benefit from this approach awaits discovery, perhaps through personalized (patient-specific), combination treatment dictated by an individual tumour interactome (Chmielecki and Pao 2010). Further themes of uncertainty in the literature include the relevance of MET inhibition in T790M-mediated resistance, and the role of MET inhibition in EGFR-driven lung cancers in patients not already exposed to EGFR-TKI (Pérol 2014). Any potential progress with this agents will require more accurate patient selection and mechanistic understanding, as was the case for EGFR targeted therapy prior to the elucidation of the mutations now widely employed in clinical practice (Lynch, Bell et al. 2004).

1.10 FRET-FLIM Imaging to Understand Receptor Crosstalk

An evolving theme in the literature is that our understanding of tumour biology needs to move on from assays based on single mutations that represent a tumour “on” or “off” signal to a deeper understanding of tumour behaviour based on molecular signaling, crosstalk and epigenetic dysregulation of malignant cells. This thesis describes use of a comparatively new technology known as Forster Resonance Energy Transfer (FRET) to better understand the interaction between EGFR and MET. By using nano-proximity microscopy platforms such as Fluorescence Life Time Imaging (FLIM) to image protein-protein interactions at the subcellular level it is possible to measure FRET to quantify interactions between proteins at the 5-10nm scale.

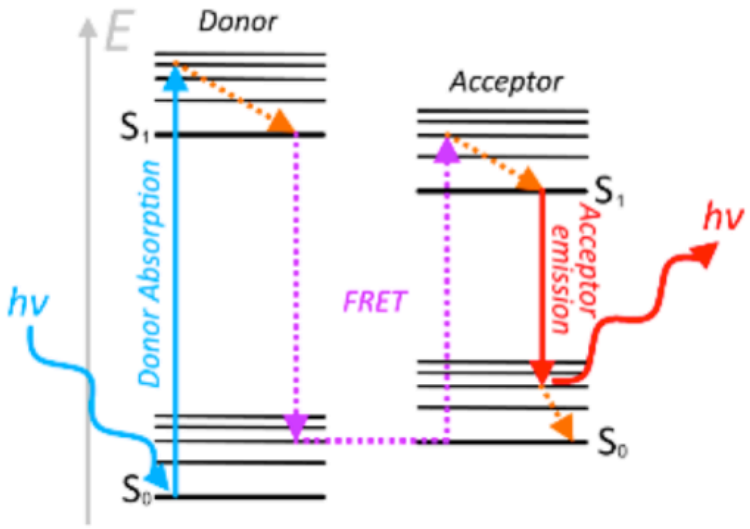

Figure 1.4 Jablonski demonstrating principle of FRET-FLIM.
The excitation of a donor fluorophore raises an electron to a higher energy state (blue arrow). Fluorescence decay of this unstable results in emission of photon of a longer wavelength and with less energy. When in close proximity to an appropriate acceptor, energy is transferred from the donor to the acceptor (FRET – Førster Resonance Energy Transfer). The donor lifetime (tau) becomes shorter which can be compared in the presence and absence of an acceptor fluorophore to derive FRET efficiency which is proportional to molecular proximity. Adapted from Hochreiter et al 2015 (Hochreiter, Garcia et al. 2015).

Fluorophores are used as labelling tools in various biological applications. The fluorescence group within a fluorophore, once excited, emits light at a longer wavelength as it returns to its ground state. Each fluorophore has a specific lifetime within which it remains within the excited state. Fluorescence lifetime (tau) of a donor fluorophore will be reduced in the immediate presence of an excess of a spectrally related acceptor fluorophore. FRET describes this energy transfer observed when two fluorophores are within nanometre proximity. By directly conjugating two such fluorophores (e.g. Alexa 546 and cyanine 5) to antibodies against proteins of interest, an assay can be constructed to monitor interaction between two such proteins in various biological conditions by quantifying FRET efficiency which is inversely proportional to the distance, R between the molecules according to the formula (Lakowicz 2013):

$$FRET_{efficiency} = 1/ [1 + (R/R_0)^6]$$

Receptors such as the HER family which undergo dimerisation are well suited to such technologies since one partner from each pair can be targeted by a labelled antibody. FRET FLIM has thus been employed to quantify the relationship between HER2-HER3

and other HER family dimer pairs with regards to the basic biology of these receptors, their role in resistance and as a biomarker of treatment response (Patel, Kiuchi et al. 2011). EGFR related interactions have been explored but to the best of our knowledge there have been no such reports of the ability to explore EGFR and MET interaction by this means. An assay based on such an interaction would be well positioned to explore the effects of mutations that determine TKI sensitivity and resistance and enable us to observe at a molecular level the effect of targeted drugs in an *in vitro*, and *in vivo* environment to better understand the effect that they are having.

1.11 Aims:

The aim of this project is to better understand the mechanisms that underlie resistance to EGFR TKI with specific consideration of the putative role of MET activation and how we might use MET inhibitors as a means to overcome such resistance. This work explores EGFR and MET crosstalk using derivatives of NCI-H1975 lung adenocarcinoma cells established in the laboratory that recapitulate EGFR-TKI treatment groups based on the presence or absence of the L858R and T790M mutations. This project investigates the consequence of these mutations for lung adenocarcinoma with the hypothesis that *EGFR* mutation status could influence the crosstalk between EGFR and MET and the efficiency of MET inhibition therapy.

Finally, this work develops a novel FRET-FLIM approach to quantify the EGFR-MET interaction and explore how such an assay could be predictive of response to MET inhibition. Based on these studies we believe that imaging and quantification of EGFR-MET interaction at the membrane may act as biomarker to select for and predict responses to drugs targeting MET in lung cancer.

1.12 Main scientific objectives:

1. To establish and characterise *in vitro* and *in vivo*, lung cancer models based on NCI-H1975 to represent the mutational phenotypes of EGFR (*EGFR* mutated: activating and resistance mutations and wild-type).
2. To determine the role of hetero-dimerisation of EGFR and MET using FLIM/FRET imaging within this cell model and in excised tissues from an immuno-deficient xenograft mouse model.
3. To quantify the effect of MET inhibition in the EGFR-MET crosstalk and in the tumoural properties exhibited *in vitro* within this model.

Chapter 2. Materials and Methods

2.1 Cell Lines

NCI-H1975 lung adenocarcinoma cells were purchased from ATCC. HEK293T and MCF-7 cells were a kind gift from Tony Ng. All cell lines were cultured at 37°C in a humidified incubator in 5% CO2. H1975 lung adenocarcinoma cells were cultured in RPMI-1640 (Invitrogen) and Phoenix Ampho HEK293T cells and MCF-7 cells were maintained in Dulbecco´s modified Eagle medium (Invitrogen). All medium was supplemented with 10% Fetal Bovine Serum (FBS), penicillin/streptomycin and L-Glutamine (Gibco). For serum-starved conditions, FBS was omitted or cells were cultured in Optimem (Invitrogen). The $H1975^{L858R}$ and $H1975^{WT}$ cells were previously established in the lab. Briefly, a GFP tagged short hairpin (shRNA) against *EGFR* obtained from Sigma (siMission) was used to produce lentiviral particles in HEK293T cells. After transduction, stable cells expressing shEGFR-GFP were selected with puromycin (1.5 µg/ml) for 5 days. After selection, a pcDNA3 construct containing WT *EGFR* or L858R *EGFR* was transfected in the cells with Fugene HD (Roche) following manufacturer's instructions. Selection was performed for 5 days with G418 (50 µg/ml). Ongoing culture of $H1975^{L858R}$ and $H1975^{WT}$ cells was in the presence of G418 (50 µg/ml) and puromycin (1.5 µg/ml).

2.2 Transfections

Plasmids encoding EGFR and MET were a kind gift from Tai Kiuchi and Peter Parker respectively. For overexpression assays, transient transfections were performed according to the manufacturers' instructions with Fugene6 for MCF-7 cells and FugeneHD for H1975 or H1975 derived cells (Promega). Briefly cells were allowed to grow for 24 hours. 0.6 micrograms of each plasmid DNA per well was used for 24 well plates and 2.5 micrograms per 60mm dish and incubated with Optimem/FuGene at RT for 30minutes. The Optimem/DNA/FuGene mix was then added to cells and incubated for 24-48hours.

2.3 Cell Pellets

Pellets were prepared from MCF-7 cells with or without MET overexpression by amplifying cells to confluence in 2 x T175 plates per cell line. These were then decanted into 3 x 60mm dishes for transfection. The next day, FFPE cell blocks were prepared for testing antibody specificity in FFPE tissue. This was performed in the St Thomas' Hospital Cytopathology laboratory for consistency with standard clinical methods. Briefly, cells were transferred into a 50ml centrifuge tube and spun down for

5 minutes at 200g to form a pellet. Supernatant was then aspirated off, and the cell pellet covered in plasma followed by thrombin to form a thrombus encapsulating the cells. The pellet was then carefully removed from the Falcon and placed in filter paper folded to fit inside a biopsy cassette with a lid and placed in formalin. This was processed overnight, as standard, through a dehydrating alcohols-xylene gradient, followed by embedding in molten paraffin wax.

2.4 Antibodies

2.4.1 Primary Antibodies:

The table describes a list of primary antibodies used for various applications.

Table 2. Summary of primary antibodies.

Target	Source	Use
Phospho-EGFR (Y1173 53A5)	Cell signaling	WB
total EGFR (Ab-15)	Thermo Scientific	IF/FRET
total EGFR (038B1)	Cell signaling	WB
Total EGFR (SC120)	Santa Cruz	IP
Total EGFR (Ab-5)	Millipore	FRET
Phospho-MET (Y1234 D26)	Cell signaling	WB
Phospho-MET	AbCAM	IHC
Total MET (D1C2)	Cell signaling	WB/FRET
Total MET (AF276)	R+D systems	IF
BrdU	Abcam	IF
hsc70 (SC7298)	Santa Cruz	WB
GAPDH (6C5)	Genetex	WB
Phospho-histone H3	Millipore	IHC
Smooth muscle actin (SMA)	Anaspec	IHC
CD31	Abcam	IHC
Phosphor-AKT	Cell signaling	WB
Total AKT	Cell signaling	WB
Phospho ERK	Cell signaling	WB
Total ERK	Cell signaling	WB
Phospho FAK	Cell signaling	WB
FAK	Cell signaling	WB

Abbreviations in table: WB – Western Blotting; IHC – Immunohistochemistry; IF Immunofluorescence; FRET (Forster Resonance Energy Transfer).

2.4.2 Secondary Antibodies:

For immunohistochemistry, peroxidase-conjugated (Envision+) anti-rabbit and anti-mouse immunoglobulin reagents from Dako were used for 1h.

For Western Blotting, we used Anti-Mouse or Anti-Rabbit, immunoglobulin/HRP (Dako)

For Immunofluorescence, we used Anti-Mouse or Anti-Rabbit, Alexa Fluor 488, 568 or 647 (Life technologies).

2.5 Antibody Labelling

For FRET, donor antibodies were kindly labelled by Dr Gregory Weitsman. Alexa Fluor 546 was used for donor antibodies and Cyanine 5 dyes (GE Healthcare) for acceptors, both prepared in N,N-Dimethylformamide according to the manufacturers instructions. The antibody of interest and dye were combined in a Bicine buffer (pH 8.6, 1M) and size-exclusion chromatography used to remove excess dye (Zeba^{TM} Spin Desalting microcolumns, Thermo Scientific). A 10µl aliquot of the labelled antibody was used to determine labelling reaction: Absorption was measured at 280nm and 558nm for Alexa 546 and 280nm and 650 nm for Cy5 with the following formulas used to generate the dye:protein ratios (see table):

$$\text{(Alexa 546 D/P)} = [1.64\ (A558)\ ] / [A280 - (0.12 \times A558)].$$

$$\text{(Cy5 D/P)} = [0.68\ (A650)\ ] / [A280 - (0.05 \times A650)]$$

Target dye:protein was aimed for 3:1 for acceptor fluorophore (Cy5)-labelled protein, and 1:1 for donor fluorophore (Alexa 546).

Table 3. Directly labelled antibodies employed in FRET-FLIM imaging

Target	Clone	Manufacturer	Dye	D:P	Concentration	Use	IC/EC
EGFR	Ab-5	Millipore	x546	0.9	0.25mcg/ml	*in vitro*	EC
MET	AF276	R+D	cy5	5.4	10mcg/ml	*in vitro*	EC
EGFR	Ab-15	Thermo Scientific	x546	0.9	0.5mcg/ml	*in vivo*	IC
EGFR	Ab-15	Thermo Scientific	cy5	3.5	10mcg/ml	*in vivo*	IC
MET	D1C2	Cell signaling	x546	0.8	0.5mcg/ml	*in vivo*	IC
MET	D1C2	Cell signaling	cy5	2.6	10mcg/ml	*in vivo*	IC

IC – Intracellular epitopes, EC – Extracellular epitopes. X546 – Alexa Fluor 546, cy5 – Cyanine 5.

2.6 Ligands and Drugs

Recombinant Human Epidermal Growth Factor (EGF) and recombinant Human Growth Factor (HGF) were purchased from Peprotech. For ligand dependent assays, cells were starved overnight in growth factor deficient medium and either left unstimulated or exposed to EGF (100ng/ml) and/or HGF (25ng/ml) for 15 minutes or 15, 30 and 60 minutes in ligand time-course experiments.

SGX523 was purchased from Selleck and solubilised in 100% dimethyl sulfoxide (DMSO) and used at 5uM. In the xenograft experiment SGX523 was administered by gavage at 60 mg/kg of SGX523 (equilibrated suspensions in 0.5% Methocell A4M). Erlotinib was purchased from Cayman chemicals and reconstituted in DMSO for use at 10uM. For *in vitro* work drugs were added to culture medium at greater than 12 hours before cell lysis or fixation.

2.7 Immunoblotting

Cells were lysed in in 120uL of sample lysis buffer: TrisHCl (pH6.8), SDS (2.5%), DTT (1:40), bromophenol blue (0.02%). Proteins were separated by Sodium Dodecyl Sulphate (SDS)-polyacrylamide gel electrophoresis (PAGE). A stacking gel (5%) was used for sample loading (see Table). 1.5mm Gels were used with 10 or 15 lanes. SDS-PAGE was with 8% or 10% gels (see Table) in Tris-Glycine SDS running Buffer (Life Technologies). Samples were electrophoresed at 100V until the running front had crossed the stacking gel and then at 160V for approximately 60-90 minutes or complete resolution. Separated gels were transferred to nitrocellulose membranes (Bio-Rad) in Tris-Glycine Transfer Buffer (Life Technologies) with 10% Methanol at 40V for 90minutes. Membranes were blocked in 5% BSA in 0.1% TBS TWEEN and then exposed overnight in primary antibody (see table 1) in 5% BSA solution. Membranes were washed and exposed in secondary HRP conjugated antibodies before developing with the ECL/ECL2 blotting system on a Biorad ‘bioanalyser’.

Protein extracts from xenograft tumours was obtained by mechanically homogenizing tumour material as follows. Xenograft tumours were snap-frozen in liquid nitrogen and thawed on the day of tissue homogenisation. RIPA buffer (50mM Trish-Hcl pH 7.4, 1% NP-40, 0.1% SDS, 150mM NaCl, 2mM EDTA, 50mM NaF. 0.5% Na-deoxycholate, with protease inhibitor cocktail) was prepared as a homogenisation buffer. Tissue homogenisation was then performed using a "Bullet blender" (Next Advance) with zirconium silicate beads (1.0 mm diameter) at half of the volume as the tissue with two volumes of homogenisation buffer (90 sec blending at room temperature).

Supernatants were taken off, centrifuged at 13,000g and the resulting supernatants were used for further analysis.

Table 4. Running Gels

Stock solutions	**8%**	**10%**
	(ml)	(ml)
H2O	23.2	19.8
30% Acrylamide mix	13.3	16.7
1.5M Tris (pH8.8)	12.5	12.5
10% SDS	0.5	0.5
10% Ammonium persulfate	0.5	0.5
TEMED	0.03	0.02

Loading gel recipe with appropriate volumes for 4 gels of 1.5mm (50ml).

Table 5. Stacking gels

Stock solutions	**5% (stacking)**
	(ml)
H2O	5.5
30% Acrylamide mix	1.3
1M Tris (pH6.8)	1
10% SDS	0.08
10% Ammonium persulfate	0.08
TEMED	0.08

Stacking gel recipe with approprirate volumes for 4 gels (1.5mm), TEMED-Tetramethylethylenediamine , H2O-Water, SDS- Sodium Dodecyl Sulphate

2.8 Immunoprecipitation

Cells were grown to 80% confluence then lysed in IP lysis buffer (50mM Tris-HCl pH 7.4, 150mM NaCl, 1mM EDTA, 1mM EGTA, 10% glycerol, 1% Triton X-100, 10mM NaF, 1mM Na3VO4, 10mM N-ethylmaleimide, 0.01µM Calyculin A) with Protease inhibitor cocktail set I (Roche). Samples were scraped on ice with a cell-scraper and centrifuged to remove cellular debris. Cell lysates were pre-cleared with Protein A/G beads for 30 minutes at 4^{o}C (Alpha Diagnostic international) then centrifuged to remove the beads. Pre-cleared samples were then incubated overnight at 4^{o}C with gentle shaking in the presence of anti-EGFR antibody (Santa Cruz) or irrelevant mouse

IgG before finally adding washed Protein A/G beads for 1 hour (Alpha Diagnostic International Inc.). Beads and complexes were washed in IP buffer then Immune complexes were collected by heat dissociation (95^{o}C for 10 minutes) in sample buffer (1X as above) and beads discarded by centrifugation. After centrifugation, the immunoprecipitates were washed and subjected to SDS-PAGE and run on WB as described above.

2.9 Immunofluorescence and confocal microscopy

Cells were plated on glass coverslips at 50-60% confluence and incubated in normal growth medium for 24 hours. Cells were then either received fresh medium or were starved overnight in serum-free medium for ligand stimulation experiments. Cells were washed with Phosphate Buffered Saline (PBS) and fixed in 4% Paraformaldehyde (PFA) in PBS for 15 minutes at room temperature (RT). Permeabilisation was performed with Triton-100 (0.2%) for 10 minutes at RT. Cells were blocked in 1% BSA TBS and stained with primary antibody diluted in blocking buffer overnight at 4C. For secondary antibodies, dilutions were made in TBS and applied in the dark for 1 hour at room temperature. Coverslips were mounted on microscope slides with FluorSave Reagent (Calbiochem). Cells were imaged using the LSM 510 META confocal laser-scanning microscope (Carls Zeiss, Germany), equipped with 63x plan-APOCHROMAT oil immersion objective. Confocal images were analysed using the Zeiis LSM Image Browser.

2.10 Immunohistochemistry

FFPE tissue was cut in 3-5mm sections and mounted onto glass slides. On the day of staining, slides were baked at 60°C for 2 hours and rehydrated through a xylene to ethanol gradient. Antigen retrieval was performed in citrate buffer (0.1M, pH 6) at 120 ºC for 10 min. Slides were allowed to cool, washed in TBS then blocked in hydrogen peroxide (3%) followed by blocking in TBS-Tween 0.1% + 1% BSA + 1% FBS. Primary antibodies were added overnight at 4ºC. As secondary antibodies, peroxidase-conjugated (Envision+) anti-rabbit and anti-mouse Ig reagents from Dako were used for 1h. Non-immune (Santa Cruz Biotechnology) or pre-immune rabbit serum was used as negative controls. Reactions were developed using diaminobenzidine (DAB) as chromogenic substrate.

Specimens were then dehydrated through an ethanol to xylene gradient before mounting in DPX mountant (Sigma-Aldrich) and allowed to set before imaging. Images from digitalized scans of the glass slide specimens were obtained at magnification ×20

(0.45 μ m/pixel resolution) using a Hamamatsu Nanozoomer 2.0 HT. All quantifications were done using Image J. Alternatively, for direct staining of tissue we used either Haematoxylin and Eosin stain or Masson's trichrome stain. Collagen staining was reviewed and validated by a histopathologist.

2.11 Cell Proliferation Assay

Cell proliferation was determined by a 5'-Bromodeoxyuridine (BrdU) based cell proliferation assay. Cells were plated to 70% confluence on coverslips in a 24-well plate and incubated at 37C in the presence of BrdU (Abcam) for 3 hours. Coverslips were then prepared for immunofluorescence staining as described above with an added 15 minute DNA denaturation step using 1.5M Hydrochloric Acid (HCl). Anti-BrdU primary antibody was applied for 2 hours (1:150), followed by Alexa-546 conjugated mouse secondary. Nuclei were counterstained with Hoechst. Images were obtained LSM510 microscope (Carl Zeiss) and quantified in ImageJ using a macro to automate cell counting for red versus blue nuclei. At least 5 fields per condition were obtained at 20X objective.

2.12 Random Cell migration assays

Cells were plated to 20% confluence in 6 well plates in the presence or absence of SGX523 and incubated overnight in a time-lapse microscopy chamber set at 37C in the presence of HEPES. 18 hours of images were recorded every 10 minutes and tracked for migration in ImageJ using Cell tracker. Quantification of random migration velocity of cells was made ± response to pre-treatment with SGX523 and analysed by Mathematica notebook.

2.13 Soft-agar growth assay

Anchorage-independent growth was evaluated using soft agar embedded colonies. $1x10^4$ cells were plated in complete DMEM containing 0.3% soft agar in 6-cm plates over a solidified DMEM containing 0.7% soft agar layer. Medium was added twice a week to maintain humidity. After 5 weeks, colonies were stained with MTT (0.5 mg/ml) for 3 hours at 37ºC and imaged by confocal microscopy and colonies counted in ImageJ. The assay was repeated in the presence or absence of SGX523.

2.14 Wound healing assay

H1975 ± shEGFR L858R/WT cells were plated to confluence in wells of a 6 well plate and a horizontal wound made through the middle of wells using a micropipette. Images were obtained by bright field microscopy with a field of view aligned to the wound

centre at equal distances across the wound. Wound closure was calculated by imaging wounds a 0, 2, 8, 20 and 28 hours and calculating % closure with ImageJ.

2.15 Fluorescence in situ hybridization (FISH)

Cells were plated on coverslips and fixed with Carnoy's fixative (3:1 methanol to acetic acid). After washing with PBS, incubation with the MET/cep7 FISH probe was performed for 16 hours at 36^{o}C after a 5minute denaturation at 72°C. The coverslips were washed in 0.4xSSC at 72°C for 5 minutes, followed by 2 minutes in 4xSSC/Tween and two rounds of 2 minutes in PBS at room temperature. The coverslips were then mounted onto slides with DAPI counterstain and analysed using a fluorescence microscope.

2.16 Digital Droplet PCR

Cells were plated for confluence and DNA extracted from cells using a DNeasy Blood and Tissue Kit (Qiagen) according to manufacturers protocol. Digital Droplet PCR was performed using reference primers/probe sets validated on the Bio-Rad QX100 mdPCR system (Bio-Rad) using commercially available reference standards (Pinheiro, Coleman et al. 2012). Data was analysed using Quantasoft (Bio-Rad) software. Droplets were scored as positive or negative based on relative fluorescence intensity in FAM or VIC/HEX channels.

2.17 Generation of xenograft model

All animal work was conducted in accordance with institutional guidelines. H1975$^{L858R/T790M}$, H1975^{L858R} and H1975^{WT} cell lines (3x10^{6}) were injected subcutaneously into the two posterior flanks of BALB/c nude mice (Charles River Laboratories). For each cell line, 16 female 5 weeks old mice were used. Mice were followed weekly and tumours allowed growing for 13 days after injection. Tumours were measured with a calliper in long and short axes recorded three times per week. Tumour volume was determined by the formula 4 x A x B^{2} (A, long axis, B short axis). At day 14th after injection mice were divided randomly in two groups (6 animals/group) and vehicle or SGX523 (drug treatment) was started. 60 mg/kg of SGX523 (equilibrated suspensions in 0.5% Methocell A4M) was administered for 12 days, daily, by oral gavage. Mice were culled on either day 1 or day 12 of treatment using CO2 to give short or long treatment groups and tumours were removed aseptically with dissecting scissors and weighed. Tumours were immediately subjected to either freezing in liquid nitrogen or formalin fixation and dehydration for embedding in a FFPE block for later staining.

All animals were maintained under specific pathogen-free conditions and handled in accordance with the Institutional Committees on Animal Welfare of the UK Home Office (The Home Office Animals Scientific Procedures Act, 1986). All animal experiments were approved by the Ethical Review Process Committee at King's College London and carried out under license from the Home Office, UK. The protocol used followed the Arrive Guidelines. A time-line diagram of the experiment can be found in Chapter 4, Figure 4.9.

2.18 Single Photon Lifetime Imaging

Coverslips or FFPE tissue were prepared as described as above for immunofluorescence except for modification of the antigen retrieval process for FFPE tissue being performed overnight in a water bath at 65ºC in Antigen retrieval buffer provided by Dr Weitsman (Unpublished) and with the added step of quenching of autofluorescence by 15 minute immersion in sodium borohydride (1mg/ml). Donor antibodies were directly labelled with Alexa-Fluor 546 and acceptors with Cyanine 5 respectively, as described below. Antibody specificity was confirmed in cells expressing *EGFR* or *MET* constructs respectively.

For *in vitro* experiments, two cover slips were prepared for each experimental condition – the first ("Donor alone") was stained for EGFR alone using an Alexa Fluor 546-conjugated mAb to EGFR (Ab-5, Thermo Scientific) whilst the next ("Donor + Acceptor") for EGFR and additionally MET (recognized by a Cy5-conjugated monoclonal antibody to MET (AF276, R+D). For FFPE samples from the xenograft and human experiments two slides were prepared, the first ("Donor alone") with EGFR alone but now using EGFR (Ab-15)-Alexa546 and the second ("Donor + Acceptor") using in addition to EGFR, MET (D1C2)-Cyanine 5. Please see earlier paragraph describing Antibodies and labelling. The reverse pair MET (D1C2)-Alexa546 with EGFR (Ab-15)-Cy5 was tested as discussed in Chapter 4, but was not optimized further.

Samples were imaged on a custom-built open automated single photon microscope (Galileo) as previously published (Barber, Tullis et al. 2014), with a 20X air objective (Nikon) and a CCD camera. A 553nm Fianium Laser provides fluorescence excitation (BDL-473_SMC, Becker and Hickl) in the form of optical pulses of 40ps at 40MHz. FLIM was performed using a PMT detector (PMH-100, Becker and Hickl) and time-correlated single-photon counting (TCSPC) electronics (SPC830, Becker & Hickl). Single photon, time-resolved fluorescence is detected at 593±10nm using a

photomultiplier tube (PMH-100, Becker and Hickl) with a 200ps time resolution and 20x (NA0.75) objective. This system is automated with a motorized microscope stage (Märzhauser GmbH, Wetzler, Germany), closed-loop objective lens mount with a 500µm range of travel (Piezosystem Jena GmbH, Jena, Germany) and a motorized filter cube selector.

Points for each coverslip or slide were defined manually, logging x,y,z coordinates which were then used for imaging the automation facility. Points were focused using the high precision (auto-focus in 0.2µm lateral resolution) computer-controlled objective stage (Piezo-system). Imaging was then performed sequentially in the Cy3 cube for Alexa-546 detection and the Cy5 cube for Cyanine 5 staining. Epifluorescence images were saved for each point in both channels and then the microscope switched automatically to laser-scanning mode to acquire the single photon data and save time-resolved images. FLIM images have 256 x 256 pixel resolutions and ADC was set to 64 time channels.

FRET Analysis was performed in the Tri2 software written by Dr Barber which allows exponential fitting for time resolved analysis based on the Levenburg-Marquardt algorithm with instrumental response iterative reconvolution capabilities (http://users.ox.ac.uk/~raob0009/software.html). This program outputs files with fitting parameters for each images pixel into Excel format including a distribution of lifetime, and an average lifetime, from which FRET efficiency can be calculated using the following equation:

$$\text{FRET efficiency} = 1 - \tau(\text{donor + acceptor})/\tau(\text{donor}),$$

Here, τ(tau) is the fluorescence lifetime of the donor fluorophore, in the presence or absence of acceptor. All *in vitro* data was fitted with a single exponential decay analysis. To analyse FRET in tissue xenografts samples, batch analysis of tri-exponential data fitting was performed followed by application of dedicated algorithm that masks autofluorescent lifetime measurements.

2.19 Statistical Analysis

Statistical differences were determined by student T test for parametric data, with ANOVA comparison for more than two groups. Probability of $P<0.05$ was considered significant. Graphs and statistics were prepared in GraphPad Prism or Microsoft Excel. Where possible, three or more consistent replicates (N=3) were performed for each experiment. This is shown in each figure. In experiments where optimization steps were consistent with the final result, N is shown accordingly. Averages of multiple experiments are shown with the standard error of the mean (SEM). Where plots of a single experiment were clearer, Standard deviation (SD) is used and labelled accordingly.

In the case of the xenograft experiment there were a total of 48 mice divided between the three mutant cell lines (see Chapter 4, Figure 4.9). In the treatment part of the experiment, culling was divided between day 1 and 12 to enable comparison between short and long groups (N=8 tumours). In the case of analysis of phosphor-Histone H3 and CD31, short and long groups were combined to simplify analysis as no differences were seen at short and long time points, thus allowing us to reduce the number of comparisons to mutant types or treatment i.e. this equated to approximately N=16 tumours per condition (2 tumours per mice). For the preparation of growth curves with and without treatment, tumour volumes were normalized and compared to day 1 post treatment. For immunohistochemistry, quantification was performed in ImageJ using a macro to score % threshold area (brown staining in representative image) in relation to background tissue for 6-10 views per section. Averages were then plotted alongside SEM bars shown. (**$p<0.001$).

Chapter 3. EGFR Mutants in Lung Adenocarcinoma

3.1 Introduction

The identification of activating *EGFR* kinase domain mutations as oncogenic drivers in lung cancer have been one of the most important discoveries in thoracic oncology in the last decade, both for our mechanistic understanding of the tumorigenesis of lung adenocarcinoma but also for the parallel development of EGFR targeted tyrosine kinase inhibitors (TKI). The *EGFR* exon 21 mutation L858R, and in-frame exon 19 deletions dominate and lead to impressive responses but which are usually short-lived, for example through T790M mediated resistance (Sharma, Bell et al. 2007). Whilst primarily used to predict response to small molecule tyrosine kinase inhibitors (TKI) such as erlotinib, such mutations are oncogenes in their own right and have consequences for EGFR signaling, recycling and dimerisation beyond their modulation of drug sensitivity (Pines, Köstler et al. 2010).

3.1.1 EGFR Mutants in Lung Adenocarcinoma: Beyond TKI response

The conformation of the EGFR L858R mutant closely resembles the activated WT receptor (Yun, Boggon et al. 2007). Like most activating *EGFR* mutations, the position of L858R at the active site of the kinase domain, in the activation loop (see Figure 3.1, L858 = L834)(Lynch, Bell et al. 2004), disrupts stabilizing interactions which maintain the inactive conformation of the WT EGFR thus promoting the active conformation (Yun, Boggon et al. 2007). Structural alterations have also been shown for other EGFR mutants including del19 and T790M that likewise are associated with an increase in EGFR activity and signaling and phenotype (Mulloy, Ferrand et al. 2007). Tumour cell dependence on EGFR signaling (oncogene addiction) evolves that explains the efficacy of EGFR TKI (Sharma, Bell et al. 2007).

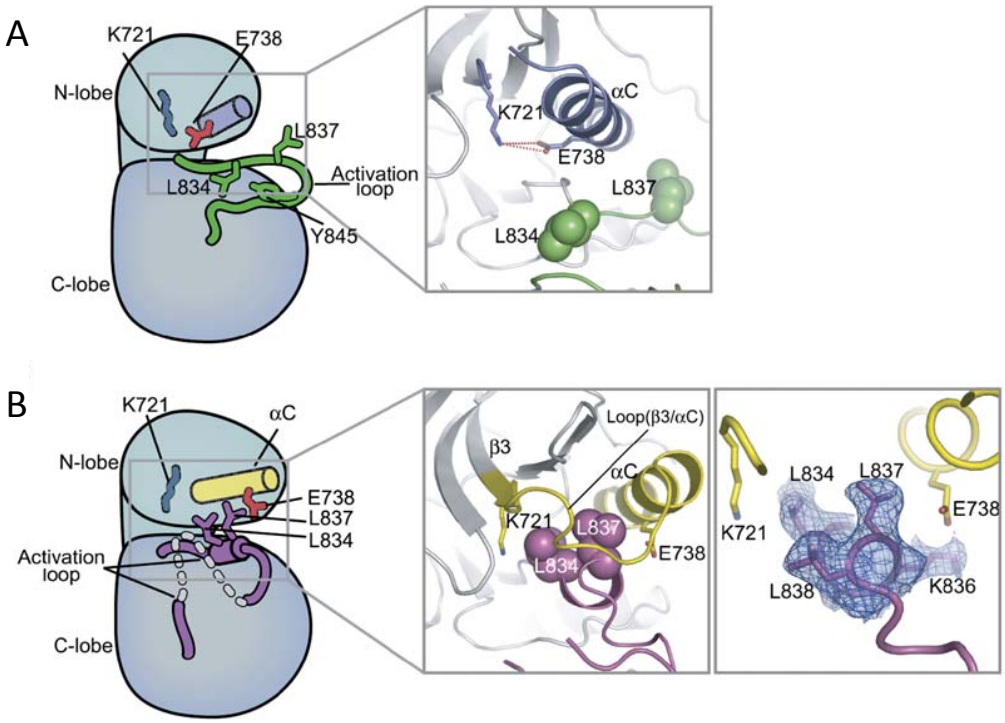

Figure 3.1 The kinase domain of the Epidermal Growth Factor Receptor
Active (A) and Inactive (B) States of EGFR Kinase Domain. A) L834 (an alternative nomenclature for L858, the site of the common L858R mutation) is found within the activation loop (green). In the active state, L858 is exposed and the activation loop is ejected and thus accesible. K721 and E738 are able to interact in an evolutionarily conserved ionic bridge important for catalysis. (Red and blue bars in left-hand schematic view). B. In the inactive state, L858 is packed against the alpha-C loop (yellow rod) which interupts pairing of K721 and E738 (right-hand box). Adapted from Zhang et al. (Zhang, Gureasko et al. 2006).

Some authors suggest that the EGFR L858R mutant is the most active, whilst others argue that acquisition of T790M results in greater catalytic activity – either way both are considerably more active than EGFR WT (Godin-Heymann, Bryant et al. 2007, Yun, Boggon et al. 2007, Yun, Mengwasser et al. 2008). Furthermore, whilst T790M is recognized to augment EGFR activity alone, it is synergistic *in cis* with L858R with enhanced anchorage independent growth and xenograft growth (Politi, Zakowski et al. 2006, Godin-Heymann, Bryant et al. 2007). This data and a number of other *in vitro* and *in vivo* models demonstrate the transforming nature of such mutations beyond their role in determining TKI response (Sordella, Bell et al. 2004, Amann, Kalyankrishna et al. 2005, Greulich, Chen et al. 2005, Regales, Balak et al. 2007). In human studies too, L858R, del19 and T790M can determine survival irrespective of treatment modality (Sequist, Joshi et al. 2007, Rosell, Carcereny et al. 2012, Karachaliou, Mayo-de Las Casas et al. 2015).

3.1.2 EGFR Mutants in a dimer-dependent model of EGFR activation

As discussed in chapter 1, dimerisation and transphosphorylation between two EGFR molecules is key to activation. Union of an activator and receiver EGFR kinase in a homodimeric (i.e. another EGFR monomer) or heterodimeric (e.g. another HER family member) partnership are required to achieve phosphorylation of key tyrosine residues required for intracellular signaling. Mutant forms of EGFR appear to have different tendencies to dimerisation and can influence the configuration of the dimer formed i.e. WT versus mutant EGFR or other partner (Red Brewer, Yun et al. 2013). One can hypothesise that each EGFR dimer arrangements has the potential to produce a different downstream signal.

3.1.3 EGFR mutants and downstream signal transduction

Downstream signal transduction from EGFR is primarily mediated through PI3K and AKT, inhibition of which is seen in EGFR sensitised cell lines treated with gefitinib (Engelman, Janne et al. 2005). Whilst EGFR can activate AKT via Gab1, it is thought that the dominant pathway through which this occurs is via dimerisation with HER3, which has multiple PI3K binding sites (Sordella, Bell et al. 2004). A HER3 "kinase switch" from EGFR is thought to augment the role of the PI3K-AKT pathway as a driver pathway (Engelman, Zejnullahu et al. 2007). This may account for ligand-independent AKT phosphorylation seen in the presence of the *EGFR* L858R mutant (Sordella, Bell et al. 2004, Noro, Gemma et al. 2006). Activation of the RAS-ERK-MAPK pathway via Grb2/SOS is also seen with mutant EGFR (Ercan, Xu et al. 2012) although whilst there is crosstalk between these signal transducers e.g. through the activation/relief of positive/negative feedback signaling, it is not clear whether one downstream pathway can become dominant (Turke, Song et al. 2012).

3.1.4 EGFR mutants and the tumour micro-environment

The interaction between tumour cells and the surrounding stroma, through creating a 'tumour microenvironment' is also vital for tumorigenesis, local spread and metastasis, as well as treatment resistance (Hanahan and Weinberg 2011). EGFR is important in this bidirectional relationship between tumour and stromal cells as well as being implicated in metastasis to distant sites such as brain and bone (Wood, Pernemalm et al. 2014). The importance of the tumour microenvironment is highlighted further by the association between resistance to EGFR targeted therapy and epithelial-to-mesenchymal transition (EMT) (Singh and Settleman 2010, Sequist, Waltman et al. 2011). Finally stromal expression of EGFR is also recognised and provides a further means by which EGFR targeted therapies may not achieve the intended effect (Weber, Fukino et al. 2005).

3.1.5 Aims

The aim of this chapter was to investigate the effect of *EGFR* mutations that are most commonly seen clinically (L858R and T790M) using a cell model based on NCI-H1975, to understand the effects of these mutants *in vitro* and *in vivo*.

My objective was to characterise a model derived from an EGFR-TKI resistant lung adenocarcinoma cell line by knockdown and reconstitution of EGFR with EGFR WT or L858R forms to isolate the changes between cell lines to EGFR. This avoided other confounding mutations and genomic aberrations such as can be seen when comparing distinct cell lines according to their mutational status.

To understand the impact of these *EGFR* mutations we selected assays of cellular appearance and behaviour alongside EGFR conformation, activation, dimerisation, downstream signaling and regulation.

3.2 Results

3.2.1 Validation of an *in vitro* model of *EGFR* mutation status

This work is based on NCI-H1975 derived model, previously developed by the Santis group to represent a translational model of three clinically relevant forms of *EGFR* (Ortiz-Zapater, Lee et al. 2017). Briefly, the model was created by modification of the NCI-H1975 cell line (hereafter described as 'H1975 $^{L858R/T790M}$') that harbours the L858R and T790M (L858R/T790M) double mutated form of *EGFR*: These H1975$^{L858R/T790M}$ cells were subjected to lentiviral shRNA knockdown of *EGFR*, followed by their transfection with pcDNA3 plasmids encoding wild-type (WT) *EGFR* or *EGFR* with the L858R activating mutation to generate the 'H1975^{WT}' and 'H1975^{L858R}' cell lines respectively. The parental H1975$^{L858R/T790M}$ cell line thus represented patients with lung adenocarcinoma and EGFR TKI resistance whilst H1975^{L858R}, portrayed the activated mutant form, which typically responds to EGFR TKI. At the conception of this project I set out to validate this model and understand its significance in the study of EGFR mutants in lung adenocarcinoma.

On initial inspection by bright field microscopy, striking differences were apparent in the morphology of each cell population - the H1975$^{L858R/T790M}$ parental cells, (i.e. EGFR L858R-T790M) were elongated and branching, with a fibroblast-like appearance, forming mesh-like monolayers with gaps between cells. In contrast, H1975^{L858R} (i.e. EGFR L858R) and H1975^{WT} (i.e. EGFR WT) cells were larger both in cytoplasm and nucleus, more rounded and epithelial in appearance, forming also better tessellated monolayers (Figure 3.2A).

To confirm that the modified cell lines had a genetic constitution consistent with the expected mutants, cDNA derived from each cell type was analysed by digital droplet PCR (ddPCR) - a recently developed technology that allows selective enrichment of rare somatic mutations for either detection or quantification (Day, Dear et al. 2013). Using this technique, relative allele frequency (*EGFR* L858R vs. T790M) in each of the cell lines was quantified. We confirmed that L858R and T790M probes were equally represented (80%) in the H1975$^{L858R/T790M}$ parental cells as expected from the literature, which describes that the mutations are expected to arise in *cis* (Pao, Miller et al. 2005). In addition, the relative allele frequency for both L858R and T790M probes were markedly reduced in the H1975^{WT} cells (Approx. 30%), consistent with effective knockdown following shEGFR treatment. Meanwhile, the H1975^{L858R} cells had near complete abrogation of events for the T790M probe whilst demonstrating a high relative allele frequency for the *EGFR* L858R mutation validating the design of this L858R

mutated cell line (Figure 3.2B). Total EGFR protein levels were similar between the cell lines as shown by lysates in the immunoblot in Figure 3.2C.

L858R and T790M *EGFR* mutations are expected to result in constitutive activation of the tyrosine kinase domain (Kancha, von Bubnoff et al. 2009). Erlotinib meanwhile is expected to inhibit tyrosine phosphorylation in activated EGFR (L858R) but not in the presence of T790M (Pao, Miller et al. 2005). Using Western blot (WB) analysis, in Figure 3.2D we compared basal phospho-EGFR in the three lines and phospho-EGFR response to EGF in the presence of the EGFR TKI erlotinib. Starved cells retained basal EGFR phosphorylation in the presence of either EGFR L858R or L858R-T790M in keeping with constitutive, ligand-independent activation in the presence of these mutations, as previously described (Kancha, von Bubnoff et al. 2009). Phosphorylation of EGFR was increased in response to EGF stimulation in all three cell lines reflecting the ongoing influence of EGF, even in the presence of "activating" *EGFR* mutations. This Western blot demonstrates that the modified $H1975^{L858R}$ and $H1975^{WT}$ cells became sensitive to erlotinib upon elimination of the T790M mutated form of *EGFR* from their genomes.

We next visualised the cells using immunofluorescence confocal microscopy to assess EGFR localization in the absence or presence of its natural ligand EGF at different time points. EGFR staining was identified with an EGFR targeted antibody, detected with Alexa Fluor 546 secondary antibody staining. As seen in Figure 3.3, we saw internalisation of EGFR (stained red), from the lace-like membrane pattern to a cytoplasmic pattern within 15 minutes of EGF application in $H1975^{L858R/T790M}$ and $H1975^{WT}$ cells in the top and bottom rows respectively. In the $H1975^{L858R}$ cells, EGFR membrane staining persists strongly at 15 minutes and is only partially internalised after 60 minutes. This is indicative of delayed EGFR internalization in the presence of the EGFR L858R mutant alone, consistent with previous reports that the EGFR L858R can escape endocytosis. Given that the signaling of EGFR is dependent upon EGF from the extracellular environment, the persistent expression of EGFR at the cell membrane is an important determinant of EGFR activity (Shtiegman, Kochupurakkal et al. 2007).

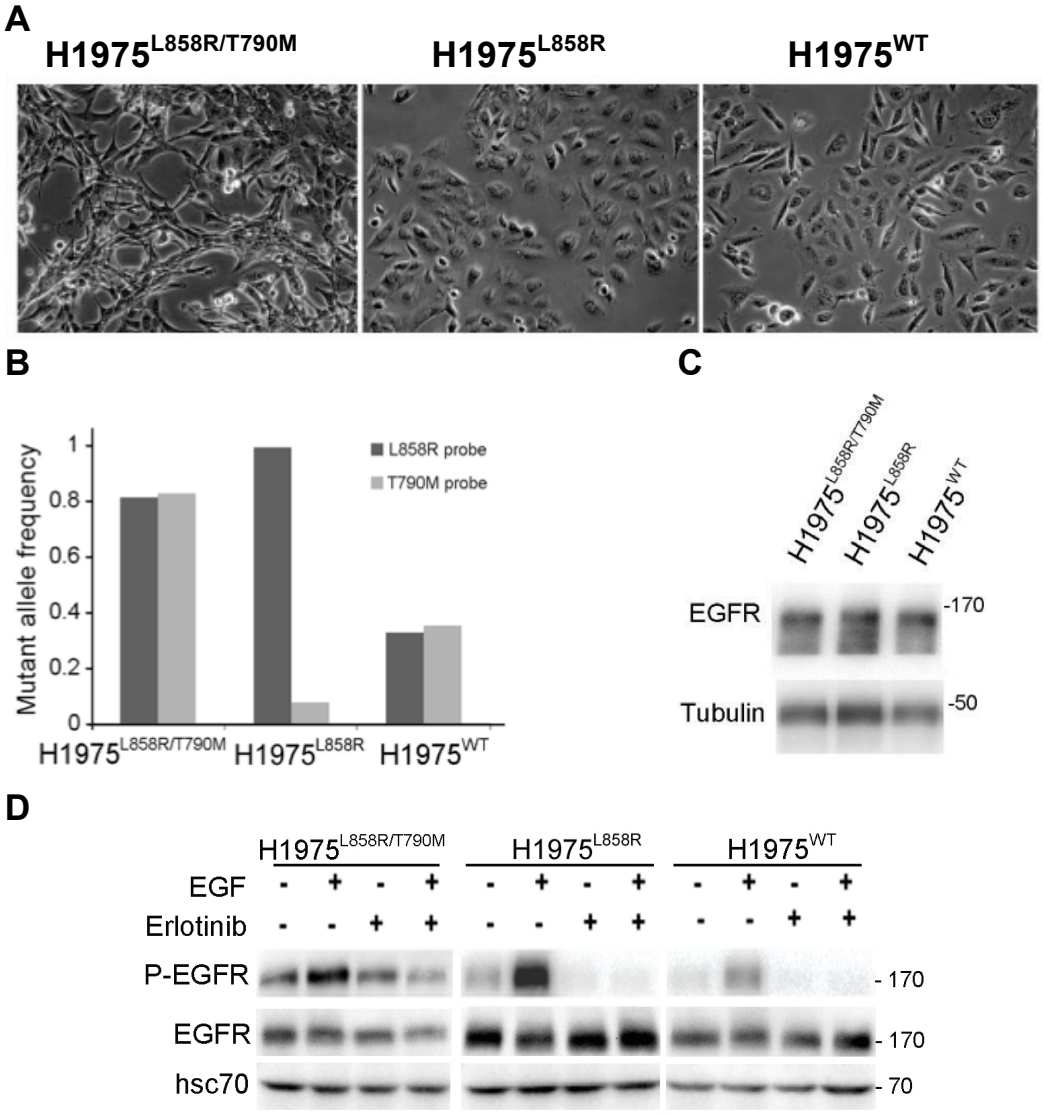

Figure 3.2 H1975 EGFR mutants differ in appearance and response to EGFR-TKI
A) Bright field microscopy with a 20X objective showing appearances of $H1975^{L858R/T790M}$ cells compared with $H1975^{L858R}$ and $H1975^{WT}$ cells. There is a mesh-like confluence of elongated $H1975^{L858R/T790M}$ cells compared with rounded $H1975^{L858R}$ and $H1975^{WT}$ cells, which formed more tightly packed monolayers. B) Digital Droplet PCR of relative L858R-T790M mutation frequency shows copy number of these mutations in each cell line. Both mutations are at equivalent levels in the $H1975^{L858R/T790M}$ cell line; There is dominance of L858R in the sensitised $H1975^{L858R}$ cell line versus relatively lower frequency of both mutations in the H1975 WT cells (N=2). C) Western Blot Analysis showing equal expression of Total EGFR (170KDa) in protein lysates from each cell line. Tubulin is provided as a loading control. D) Western Blot Analysis of Phosphorylated EGFR (170KDa) in the presence of EGF (100ng/mL) with or without erlotinib (10μM) in H1975 derivative cells. EGFR phosphorylation response to EGF was used as a positive control and blockade by erlotinib for each cell line as a marker of EGFR TKI resistance. phospho-EGFR signal was inhibited by erlotinib in $H1975^{L858R}$ and $H1975^{WT}$ cells but not $H1975^{L858R/T790M}$. hsc70 was used as a loading control (N=3). White block lines divide blots performed in different experiments.

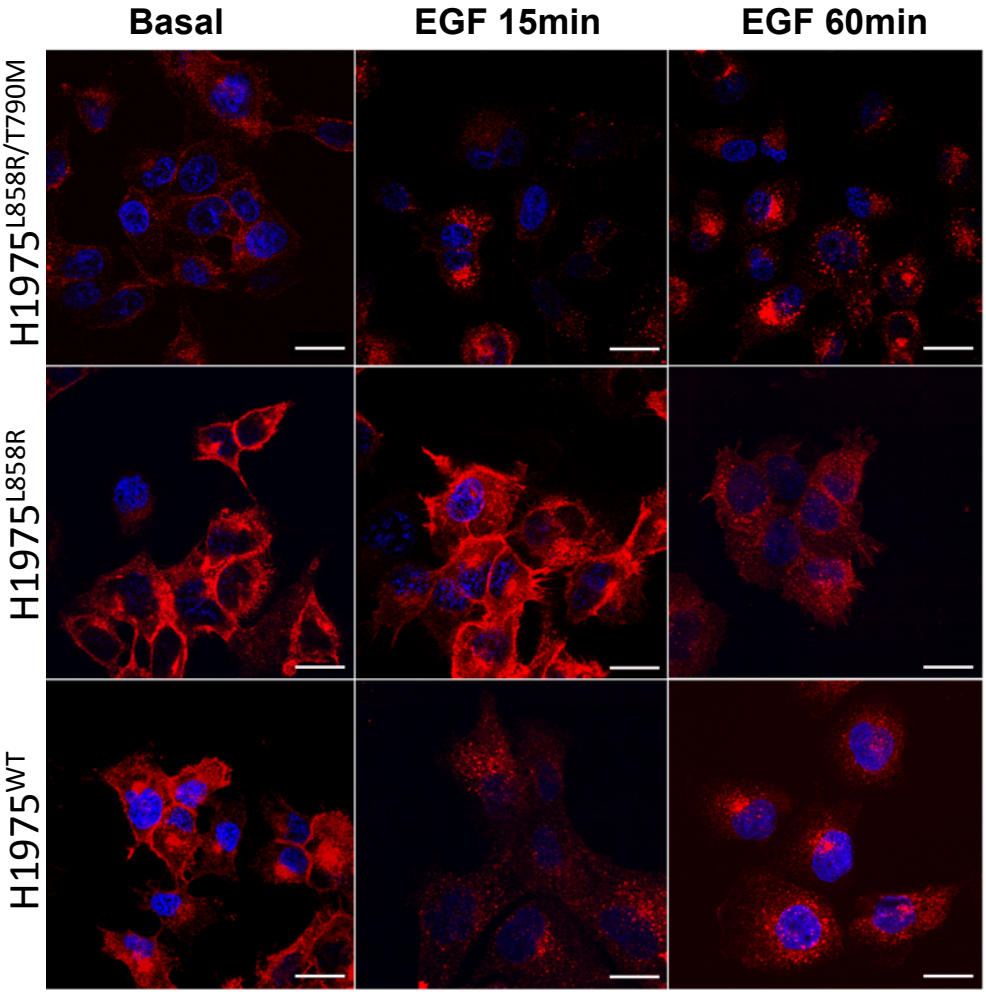

Figure 3.3 H1975 EGFR mutants differ in internalisation

H1975 derivative cells were plated to sub-confluence, starved, exposed to Epidermal Growth Factor (EGF, 100ng/ml) for 15 minutes or 60 minutes and fixed for staining for EGFR. Mouse Alexa Fluor 546 (Red) secondary antibody reveals EGFR as red with a Hoechst (blue) nuclear counterstain. A membrane-predominant pattern of staining was seen as red demarcation of cell boundaries whereas a cytoplasmic pattern consistent with internalisation of EGFR, is shown by a more granular staining pattern. Internalisation of EGFR was seen in $H1975^{L858R/T790M}$ and $H1975^{WT}$ cells by 15 minutes after application of EGF to starved cells. This was delayed in $H1975^{L858R}$ cells and still incomplete by 60 minutes where membrane pattern staining can still be seen. Imaging performed by confocal microscopy and images prepared in ImageJ, Scale bar 20μm, N=3. (Final figure kindly constructed by Dr. E. Ortiz-Zapater).

3.2.2 The *EGFR* L858R 'Activating' mutation is associated with a proliferative phenotype in lung adenocarcinoma

In view of the differences we had observed up until this point, we anticipated that we would also see phenotypical consequences arising from the different EGFR mutants within this model. As demonstrated in Figure 3.4 (Quantification in A, representative images in B), we compared the proliferation rate of the three different cells lines using a BromodeoxyUridine (BrdU) incorporation assay. A higher number of nuclei stained pink (red and blue channel co-localisation) representing BrdU incorporation in the $H1975^{L858R}$ cell line suggested that this cell line had the most nuclei in active cell cycle and hence was the most proliferative. On the contrary, the $H1975^{L858R/T790M}$ cells from which the others were derived were the least proliferative with fewest nuclei with BrdU uptake relative to nuclei showing only the blue Hoechst counterstain. The $H1975^{WT}$ cells were intermediary between the $H1975^{L858R/T790M}$ and $H1975^{L858R}$ forms.

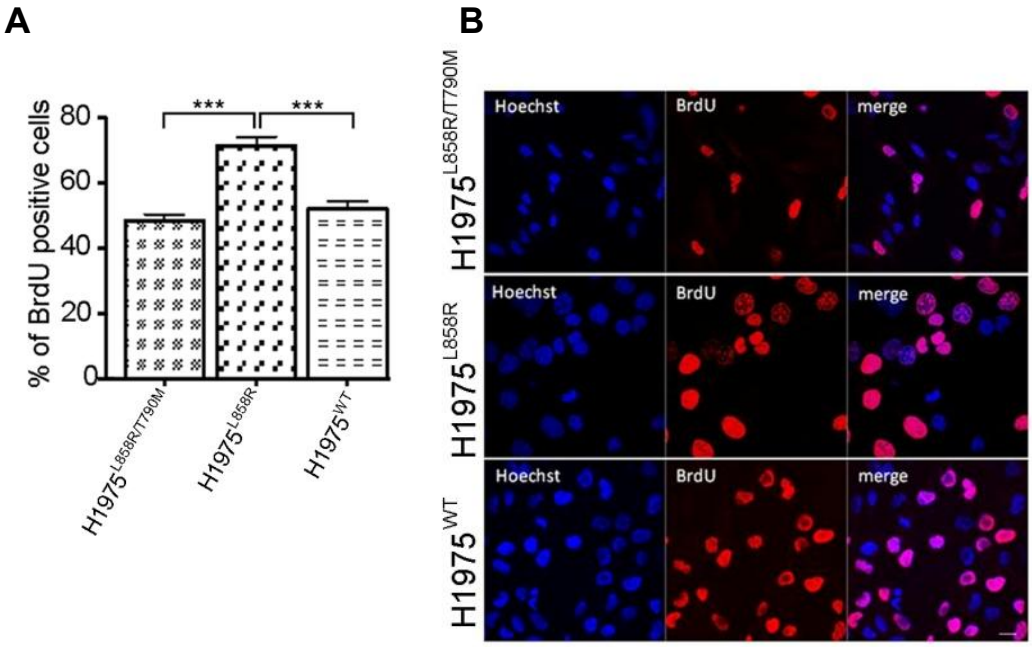

Figure 3.4 *In vitro* assays: $H1975^{L858R}$ cells are the most proliferative.
A & B) BrdU Proliferation assay. Quantification was performed in ImageJ using a macro to count number of nuclei in red (BrdU+ve) versus blue (all nuclei) channels for 5-10 views per section, with a threshold approach to separate nuclei from background. Averages are plotted as a percentage of BrdU positive nuclei. SEM bars are shown (*** $p < 0.005$, N=5). Representative images are shown for each of the three cell lines grown at 60% confluence on coverslips after 24 hours. The BrdU positive nuclei (Anti-BrdU, Mouse Alexa Fluor 546) in the red channel show cycling cells, and in the blue channel is the counterstain (Hoechst dye) to indicate nuclei of all cells as a denominator. $H1975^{L858R}$ cells show greatest % positive BrdU stained nuclei compared with the other cell lines (middle row). Scale bar, 20μm.

Using a soft agar growth assay as a measure of growth in an anchorage-independent manner, we confirmed again that H1975^{L858R} was the most proliferative with the greatest number of colonies and H1975$^{L858R/T790M}$ the least, but this time within a 3D environment (Figure 3.5). This trend was similar for both large and small colonies of the tumour cells (significant only for small colonies). Colony numbers represent persistence of cells seeded within the anchorage-independent environment and therefore represent tumour cell survival in the absence of an adherent surface. Larger colonies are also an indicator of a larger number of cells and thus cell divisions which give a surrogate therefore of proliferation rate, again in an environment devoid of an adherent surface.

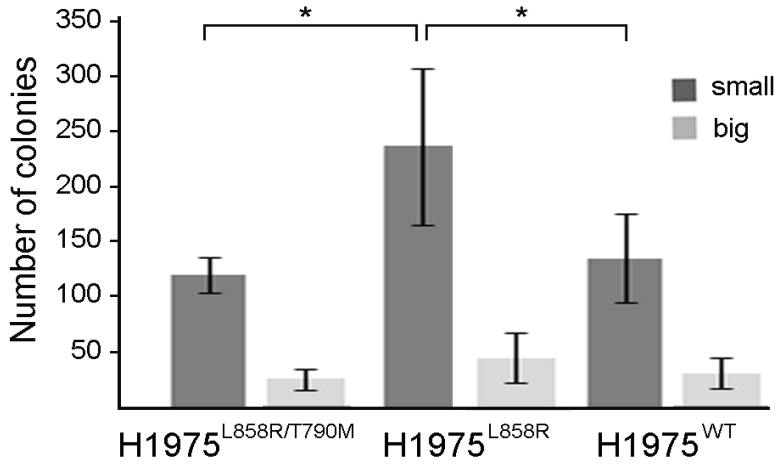

Figure 3.5 *In vitro* assays: H1975^{L858R} cells produce most colonies.
Anchorage-independent Agar Growth Assay. Colony formation in H1975 derived cell lines. The graph shows the number of colonies after 3 weeks of growth. Quantification was performed in ImageJ using a macro to count number of colonies per field of view for 5-10 views per section, using a threshold approach to separate nuclei from background. Small colonies were defined as 100-1500mm circularity, and large colonies, >1500mm circularity. Average numbers of each colony type for the three cell lines are plotted. Number of colonies represents cell survival. Larger colonies suggest higher number of cell divisions/proliferation. The number of small colonies was significantly greater in H1975^{L858R} cells than the other cell lines as indicated by the dark grey bars. SD Error bars shown (*p< 0.001), N=4. (Agar data kindly provided by Dr. E. Ortiz-Zapater).

3.2.3 Effect of EGFR mutational status on tumour cell migration

The ability of tumour cells to migrate is an important cancer hallmark, which allows locally invasive growth and metastasis, which are also clinically important prognostic indicators in lung cancer. The *in vitro* model allowed comparison of the ability of the cells to migrate independently, using firstly a wound closure assay and secondly, an assay of random cell migration by time-lapse microscopy. In both cases, we could observe that the H1975$^{L858R/T790M}$ cell line was the most migratory. Firstly, in the wound closure assay, cells moved to close a wound made with a pipette tip in a confluent monolayer representing cell movement away from an injured front of confluent cells. Here, H1975$^{L858R/T790M}$ cells migrated faster into the wound to mitigate its closure as measured by reduction in wound area (mm^2) per hour compared with the H1975^{L858R} and H1975^{WT} cells (Figure 3.6). The H1975^{L858R} wounds healed the most slowly. Secondly, in the random migration assay, shown in Figure 3.7, where cells were plated to low confluence, then visualized and quantified by time-lapse microscopy in a humidified chamber, we saw greatest velocity (microns per microsecond) in H1975$^{L858R/T790M}$ cells in comparison to the H1975^{L858R} cells which showed only membrane ruffling with minimal migration and the H1975^{WT} which were again intermediate. Thus in both assays whether or not in close contact with surrounding cells, the H1975$^{L858R/T790M}$ cells were more migratory.

In summary the *in vitro* proliferation experiments showed that the H1975^{L858R} cell line was the most proliferative, suggesting that the expression of the *EGFR* L858R mutant alone is capable of inducing proliferation but that this advantage is lost in the presence of the T790M mutation, which conferred a proliferative disadvantage in comparison to the WT or L858R mutant forms of *EGFR*. The reverse was seen in the migration assays where both random migration and wound closure were fastest in the H1975$^{L858R/T790M}$ cell line suggesting that the double mutant *EGFR* L858R-T790M induces a migratory phenotype that is not present with *EGFR* L858R.

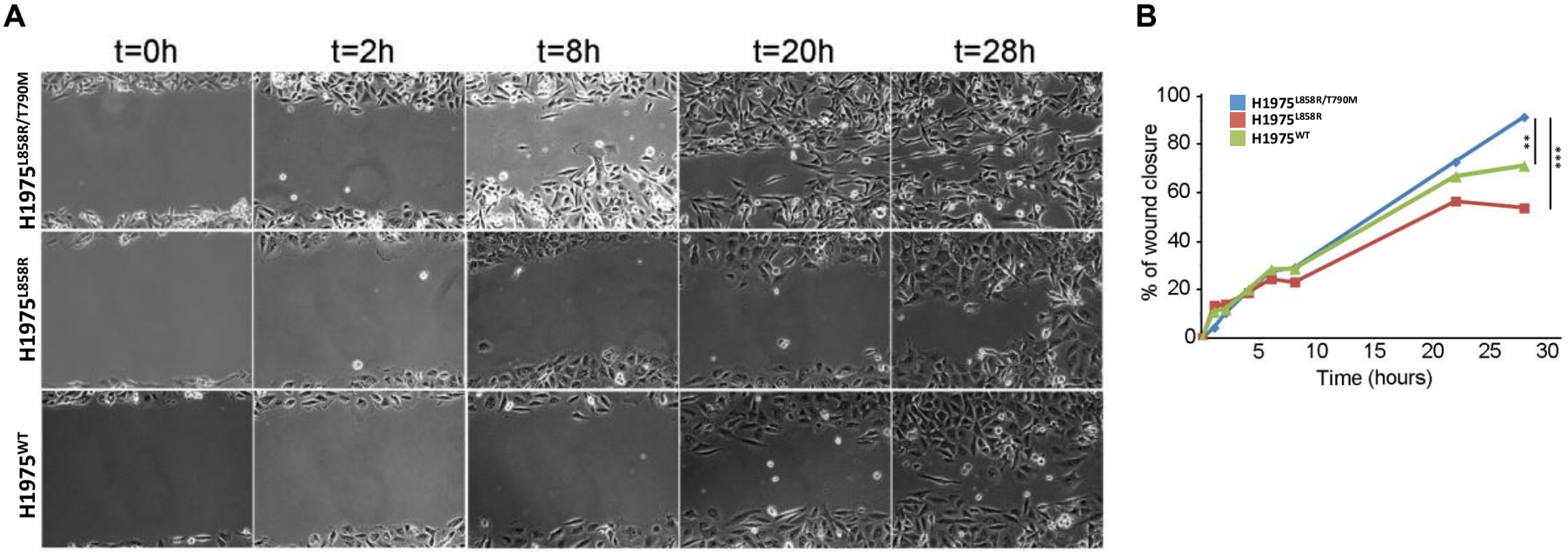

Figure 3.6 H1975$^{L858R/T790M}$ Tumour cells show greatest wound closure rate.

A) Wound Healing Assay. Cells plated to sub-confluence were injured in a line through the centre of a well with a 20µl pipette tip and imaged at 0, 2, 8, 20 and 28 hours (h) by bright-field microscopy. B) The line graph shows quantified wound closure as percentage of surface area of the wound at each time point quantified using ImageJ. H1975$^{L858R/T790M}$ cells (top row of images, blue line) showed most rapid closure of wound and H1975^{L858R} cells the slowest (middle row of images, red line).(** $p<0.005$, *** $p<0.0005$, N=4 experiments), 2 fields per condition per time point. (Data and images for final replicate kindly provided by Dr. E. Ortiz-Zapater).

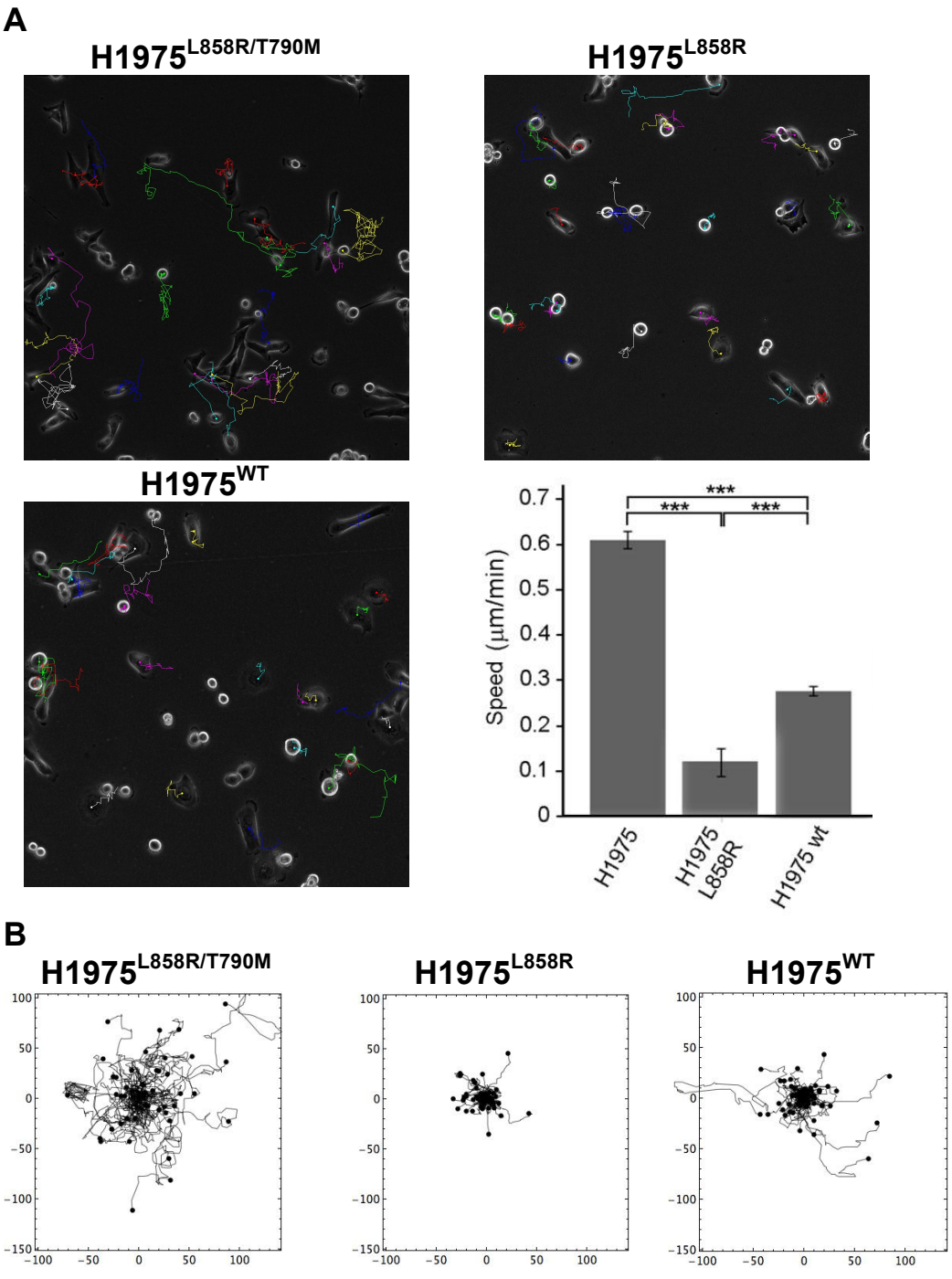

Figure 3.7 H1975$^{L858R/T790M}$ Tumour cells show greatest random cell migration.
A) Representative images of cell tracks (each coloured differently) for a single field of view at the end of the timelapse data file. Tracks were made manually in ImageJ by isolating the centre of each cell of interest per frame and analysed by Mathematica notebook (6 fields of view, 10 cells per image). Bar graph showing speed quantification of random migration velocity of cells over 18h. SD bars shown, ***p < 0.0001, N=3. B) Representative rose plots shown with tracks for all cells (n = 75, 46, 73) normalised to a common origin at the centre of the blot (velocity is µm/minute: x and y axis on plots are in µm. Cells with the greatest migrational velocity are shown by longer tracks as seen for H1975$^{L858R/T790M}$ in the left-most box which had the greatest migrational velocity with a corresponding value in the bar graph that exceeded the other cell lines.

3.2.4 Effect of *EGFR* mutational status on xenograft growth

We wanted to validate whether the same observations could be reproduced in an *in vivo* setting by using a murine xenograft model based on the H1975 derived mutant cell lines. 3 x 10^6 $H1975^{L858R/T790M}$, $H1975^{L858R}$ and $H1975^{WT}$ cells were injected into the flanks of 5-week old female, immunosuppressed, nude, BalbC mice and tumours were allowed to grow for 2 weeks. We thus had three tumour types representative of the same three clinically important forms of EGFR tested within the *in vitro model* but now with the added contribution of local factors within an *in vivo* tumour microenvironment. The model provided bilateral tumours in 8 mice per condition thus giving 16 tumours for each of the three mutant cell lines.

Tumour volumes were measured and charted every 2 days and weights of dissected tumours were recorded for culled mice. Tumour growth, shown by the increase in average volume (mm^3) per day after cell injection was most striking in tumours coming from the $H1975^{L858R}$ xenografts indicated by the red line compared with the green and blue lines representing $H1975^{WT}$ and $H1975^{L858R/T790M}$ respectively, the latter of which had the lowest gradient demonstrating the slow increase in tumour volume in these xenografts (Figure 3.8). Dissected tumours from the $H1975^{L858R}$ cell line also showed the highest average weight with the points corresponding to each tumour plotted inside of their error bars for each tumour type (Figure 3.8B). $H1975^{L858R/T790M}$ derived tumours in comparison had the lowest average culled tumour weights matching the lower incremental volume change in Figure 3.8A. $H1975^{WT}$ derived tumours were again intermediary between $H1975^{L858R/T790M}$ and $H1975^{L858R}$.

We further validated this pattern of increased growth in the $H1975^{L858R}$ xenografts by staining for the mitotic marker phospho-Histone H3 as an index of proliferation (Figure 3.9A and B). Greatest numbers of nuclei with phosphorylated Histone H3 staining (brown nuclei) were observed in the $H1975^{L858R}$ derived tumours suggesting a higher rate of mitosis in these xenografts. The percentage of brown stained nuclei in proportion to Haematoxylin counterstained nuclei are plotted for quantification in the graph beneath. $H1975^{L858R/T790M}$ derived xenografts meanwhile showed the lowest proportion of phospho-Histone H3 staining suggesting that these were the least proliferative tumours in line again with the volume and weight data. Overall, these findings were in keeping with the *in vitro* results reinforcing the hypothesis that the H1975L858R cells and tumours with the activated EGFR L858R mutant alone were the most proliferative, whilst H1975L858R/T790M was the least proliferative.

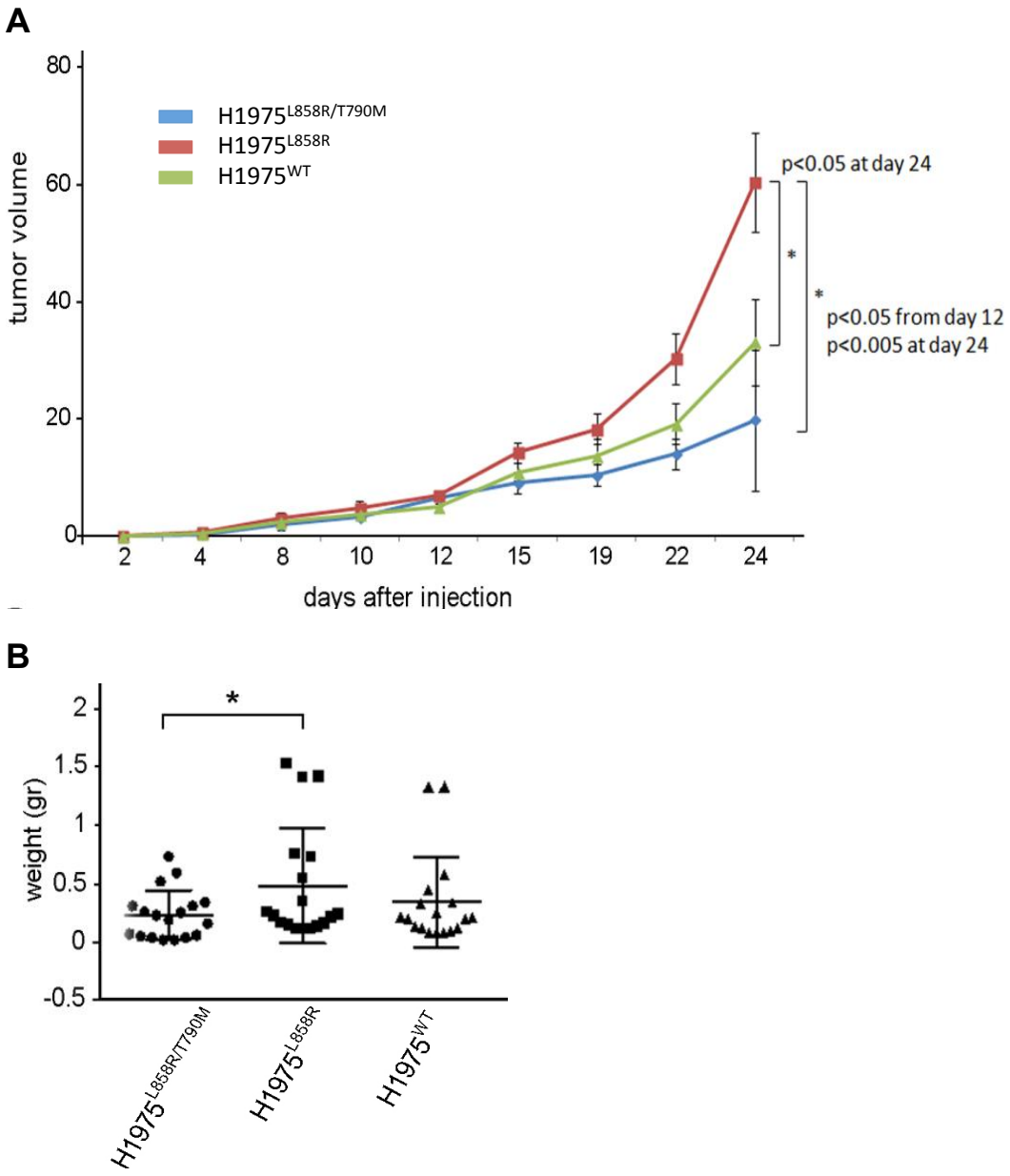

Figure 3.8 H1975^{L858R} xenograft tumours show fastest growth

Xenograft tumour growth curves. 3x10^6 cells were injected into both flanks of immunocompromised BALB/c nude mice and tumours allowed to grow for 24 days. N=16 tumours (8 mice, bilateral tumours) per condition. A) At the indicated times, tumour volumes were measured using a calliper and calculated using the equation 0.4xAxB^2 (A, the long axis and B, the short axis of the tumour). H1975^{L858R} tumours (red line) were largest and H1975$^{L858R/T790M}$ (blue line) were smallest with consistent separation throughout. SD bars shown. B) Tumours from culled mice were dissected and weighed and were compared between the different xenografts. Tumours from the H1975^{L858R} cell line were signinificantly heavier than those coming from the H1975$^{L858R/T790M}$ cells. SEM bars shown (*p = 0.05).

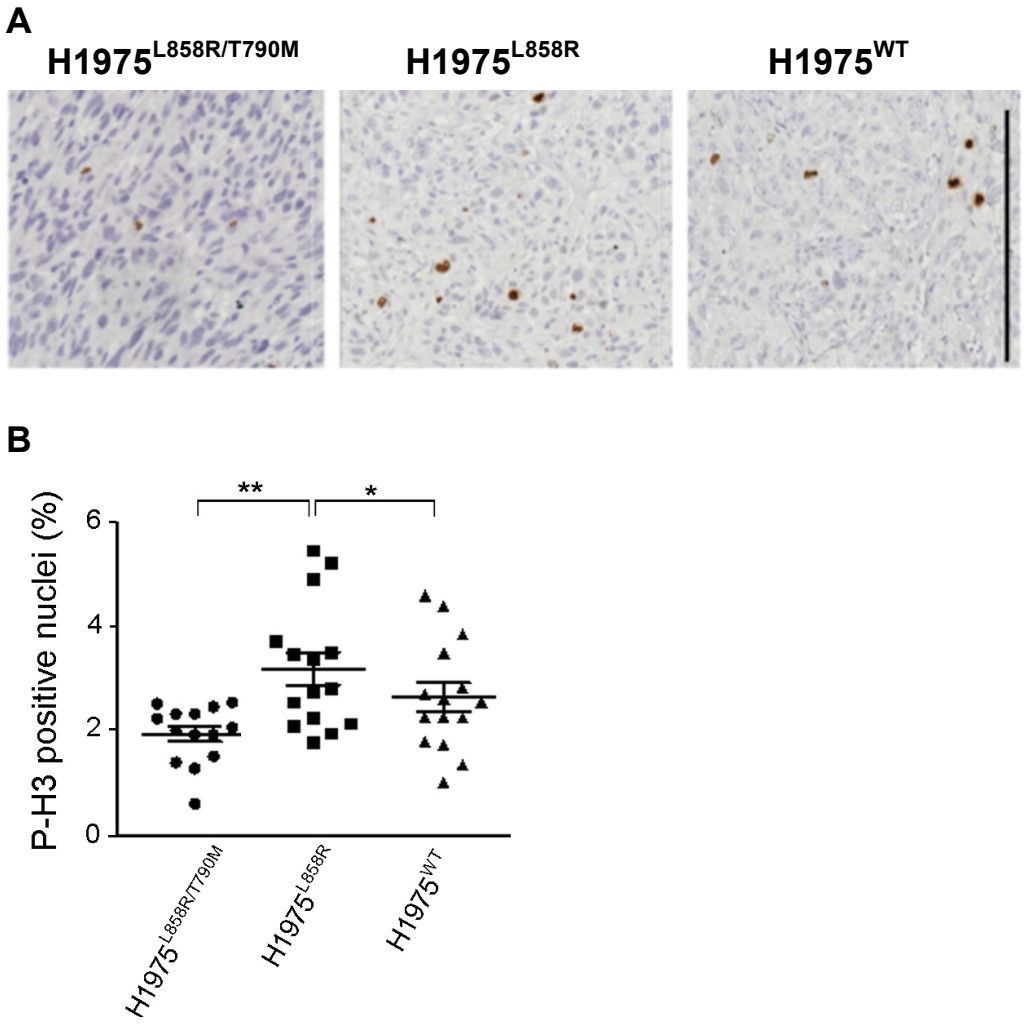

Figure 3.9 H1975^{L858R} xenograft tumours show most proliferation
3x10^6 cells were injected into both flanks of immunocompromised BALB/c nude mice and tumours allowed to grow for 24 days before culling. N=16 tumours (8 mice, bilateral tumours) per condition. A) & B) Representative images and quantification. Tumour immunohistochemistry for phospho-Histone H3 staining of xenografts tumors coming from each H1975 derived cell line as a marker of proliferation. Quantification was performed in ImageJ using a macro to score % threshold area (brown staining in representative image) in relation to background tissue for 6-10 views per section. Averages are plotted. There was sginficantly more phospho-Histone H3 staining in H1975^{L858R} tumours than the other 2 xenograft types. The number of cells stained in the images and the percentage score on the charts highlights the relatively low frequency of staining for this marker. Scale bar, 400μm. SEM bars shown indicate the variability in relation to this low mean score (*p<0.05, **p<0.001).

3.2.5 Effect of *EGFR* mutational status on tumour stroma *in vivo*

In light of the clear differences we had observed in the appearances of the cells *in* vitro, we also expected that the murine tumours would differ in architecture and may offer further explanation of the differences that we had observed in proliferation. Examining the tumours using Haematoxylin and Eosin (H&E) staining as shown in Figure 3.10E, we could make observations about the basic morphology of the tumour cells and see that the adjacent stromal tissue in each xenograft type was very different. H1975$^{L858R/T790M}$ derived xenografts gave rise to dense, cellular tumours, with tightly aligned cells, oriented in similar directions. Conversely, H1975^{L858R} cells gave rise to tumours with abundant intra-tumoural stromal tissue deposition with highly segregated cells that appeared to have a greater stromal component (see Figure 3.10). We also noticed on examination of the H&E staining that necrosis appeared greatest in H1975^{L858R} derived tumours and less so in H1975$^{L858R/T790M}$ tumours (Figure 3.10).

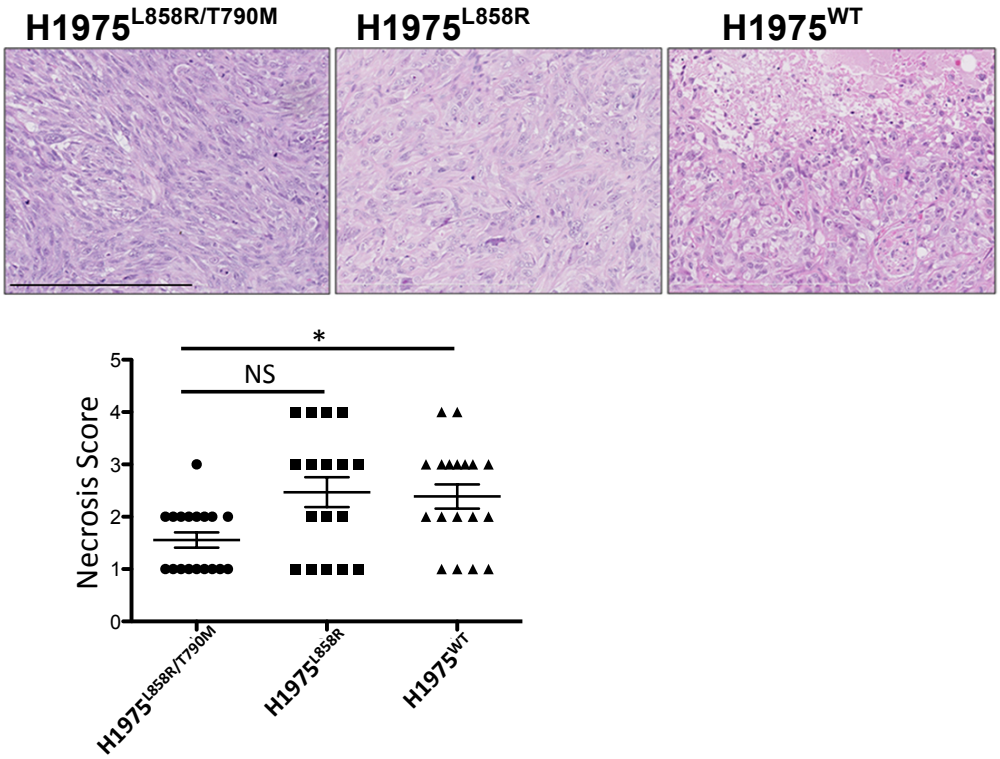

Figure 3.10 H1975^{L858R} xenograft tumour appearances differ

Representative images of Haematoxylin and Eosin (H&E) staining showing the differences in architecture between the different xenografts. Differences in the cellular and stromal appearances in the different tumours are presented visually. Quantification of necrosis was performed in ImageJ by defining a score of based on proportion of entire section occupied by necrotic tissue. Tightly packed cells in the H1975$^{L858R/T790M}$ tumours differed from those of the stroma-rich H1975^{L858R} which were separated by strands of pink stromal tissue. H1975^{WT} were more clearly necrotic as shown by lack of cellular features at the top of the third image and the right hand column on the graph. Scale bar, 400μm. SEM bars shown. (*$p<0.05$, N=16 tumours per condition).

To understand if the *EGFR* mutations resulted in differences in the interaction of the tumour cells with the encapsulating stroma we again addressed the tumours coming from the same xenograft model. We stained the stromal compartment within the tumours, for collagen deposition (MT, Masson's trichrome staining) as well as anti-smooth muscle actin staining (α-SMA), (see Figure 3.11A). As shown in the quantifications in Figure 3.11B and C, the H1975^{L858R} tumours possessed the most substantial collagen deposition (MT) shown in green against the H&E background and a similarly increased proportion of a-SMA positive cells stained brown as a marker of activated fibroblasts. These features of stromal cells and collagen deposition would be consistent with a greater degree of interaction with the stroma in the H1975^{L858R} xenografts. These markers were both significantly lower in the H1975$^{L858R/T790M}$ tumours in comparison suggesting that there was less stromal tissue in these tumours.

We hypothesized that this might relate to the augmented proliferative capacity of the tumours outstripping vascular supply, so sought to quantify neo-angiogenesis with CD31 staining. Using the % of cd31 staining (brown cells) in the tumour sections as a marker of endothelial cells we saw the greatest proportion of cd31 positive areas representing regions of new blood vessels in the tumours coming from the H1975^{WT} and from the H1975^{L858R} cells compared with those from the H1975$^{L858R/T790M}$ cell line (Figure 3.12).

In summary, in addition to greatest growth and proliferation, the xenograft tumours coming from the H1975^{L858R} cell line demonstrated markedly more prominent stromal components in comparison to the H1975$^{L858R/T790M}$ tumours, which were lowest in all these aspects. These results provided an interesting contrast between the H1975^{L858R} cells in which the EGFR L858R mutant produced a proliferative phenotype and H1975$^{L858R/T790M}$, which possessed in addition, the T790M resistance mutation, which produced a migratory phenotype. H1975^{WT} tumours were intermediary between these two cell types except in neovascularization where in this regard, H1975^{WT} had the greatest scores, potentially highlighting an important role for EGFR in interacting with new vessel formation.

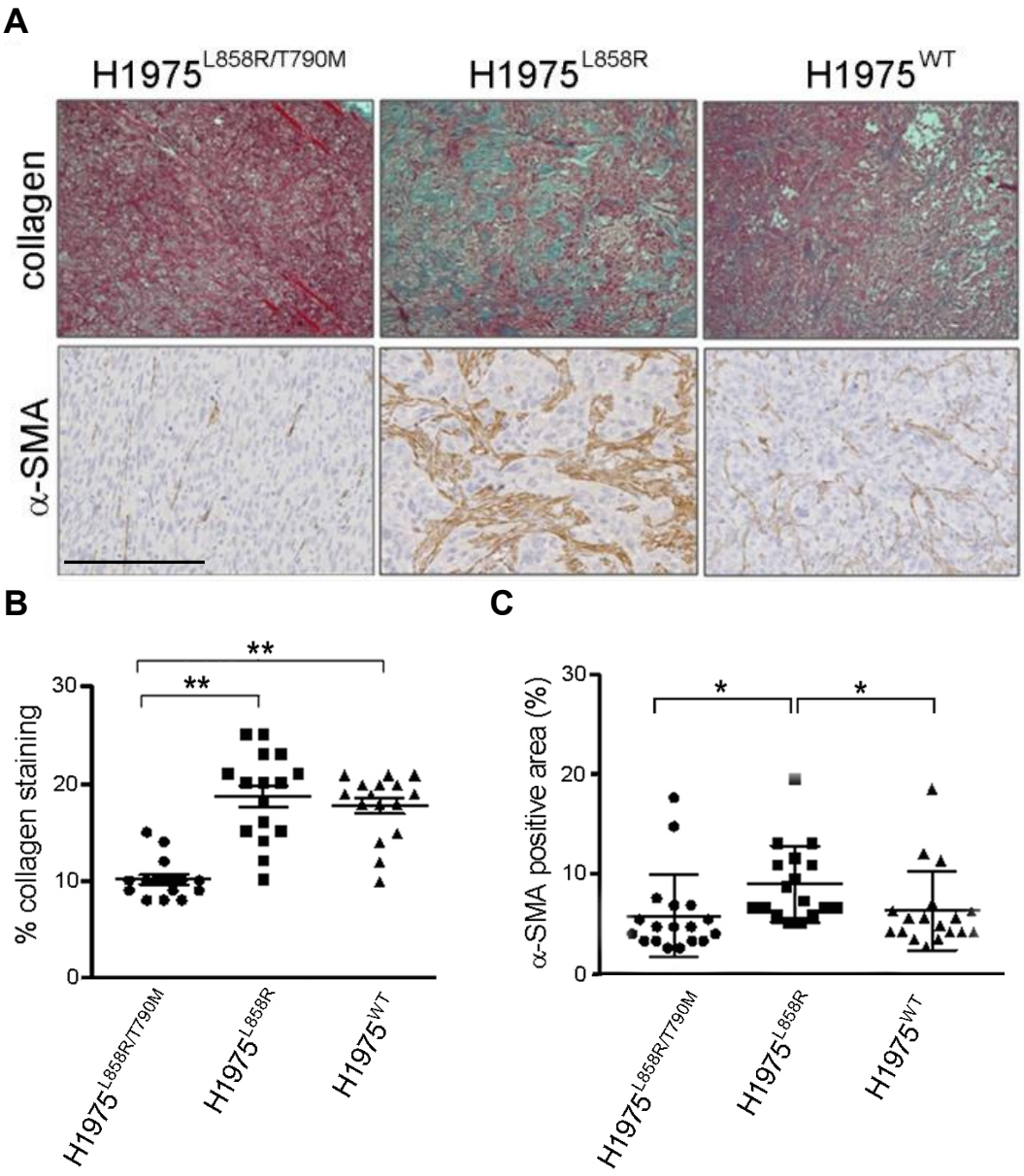

Figure 3.11 L858R mutant xenografts tumours show increased stroma
Immunohistochemistry with Masson's trichrome (MT) or anti-smooth muscle actin (α-SMA) for collagen from mice xenograft tumours (N=16 tumours per condition). A) Representative images show collagen (green with MT) and anti-smooth muscle actin (brown) stained areas were most notable in the H1975^{L858R} xenografts. B & C) For Masson's trichrome, dominance of collagen-rich features (green) were scored by a consultant histopathologist (MM) and plotted using Prism Graph Pad. α-SMA quantification was performed in ImageJ using a macro to score % threshold area (brown staining in representative image) in relation to background tissue for 6-10 views per tumour. Averages plotted. % Collagen staining and α-SMA were significantly greater in H1975^{L858R} xenografts. Scale bar, 400μm. SEM bars shown (*p<0.05, **p<0.001).

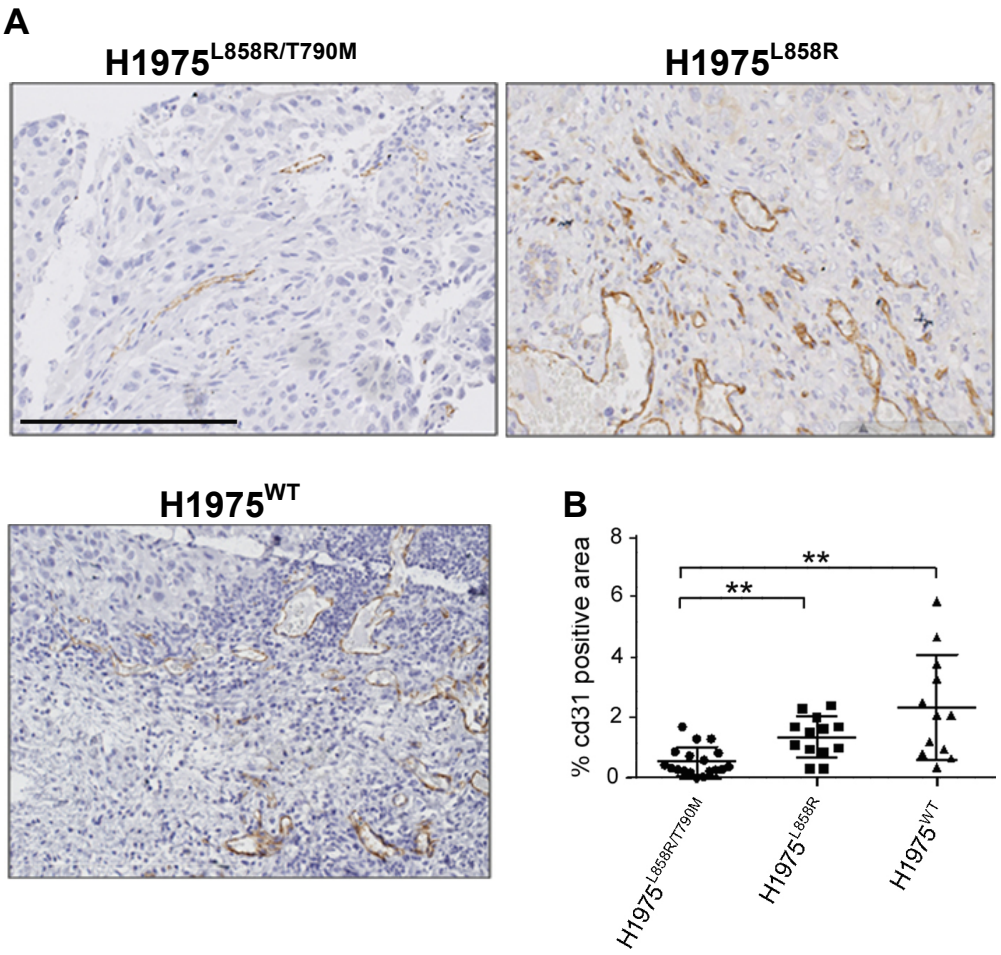

Figure 3.12 H1975^{WT} xenografts tumours have greatest angiogenesis
Immunohistochemistry xenograft tumours stained for cd31. A) Representative images for each tumour type. Brown stained cells represent endothelium and demarcate new vessel formation within xenograft tumours. Tissue architecture counterstained with haematoxylin. B) Percentage area was quantified in ImageJ as a marker of extent of new vessel formation. Quantification was performed in ImageJ using a macro to score % threshold area (brown staining in representative image) in relation to background tissue for 6-10 views per section. Averages plotted. This marker of neo-angiogenesis was greatest in the H1975^{WT} derived tumours and lowest in H1975$^{L858R/T790M}$. Scale Bar, 400µm. SEM bars are shown. Of note these are wider in the H1975^{WT} compared with the other tumour types which give a better approximation to the mean (**p<0.001, N=16 tumours per condition).

3.3 Discussion

The aim of this chapter was to understand the effects of *EGFR* mutations using a model based on a lung adenocarcinoma cell line and derived tumours. We have used assays of cell phenotype to compare the EGFR mutants using cell model and have thereafter derived xenografts to establish the veracity of literature that suggests there is a difference between them. It is not clear if this merely reflects the EGFR activation levels induced by the respective mutation or alternatively the modulation of the capacity of EGFR for signaling in another manner, for example through altered receptor recycling and downstream signaling or through allosteric interactions between partner molecules in EGFR dimers (Arteaga 2007, Shtiegman, Kochupurakkal et al. 2007). The discussion considers the characteristics of EGFR in the context of the different *EGFR* mutations that might explain this.

3.3.1 Creating a model of EGFR L858R and T790M mutations *in vitro*.

The use of the NCI-H1975 cell line is well established in the lung cancer literature since it provides a good experimental model of EGFR TKI treatment resistance (Sharma, Bell et al. 2007). This cell line represents patients who have acquired constitutive EGFR activity (and enhanced EGFR TKI sensitivity) through acquisition of the *EGFR* L858R mutation, who additionally have gained the *EGFR* T790M resistance mutation. The L858R and T790M mutations are two of the most commonly encountered *EGFR* mutations, which are used within the routine treatment algorithm for lung adenocarcinoma.

We have used the H1975 model since we wanted lung adenocarcinoma cells with focus on the significance of these *EGFR* L858R and T790M mutations. By developing derivative cell lines based on the NCI-H1975 parent cell line in this way, we were able to specifically address the role of these three forms of EGFR which are amongst the most commonly encountered in the clinical environment: i.e. EGFR WT versus L858R (activating) ± T790M (resistance). We used assays assessing cell function and EGFR signaling to understand the concepts underlying current clinical approaches. This approach was chosen to be able to assess differences between the cell lines based solely on the *EGFR* mutation status without being confounded by the presence of other driver or passenger genomic aberrations present in alternative, commercially-available cell lines, representing other TKI sensitive or resistant cell lines derived from different patients or tumour material. Limitations of these alternative approaches consist of other sensitising/resistance *EGFR* mutations when our intention was to focus on L858R/T790M, which other than del19 are two of the most relevant *EGFR* sensitising and resistance mutations respectively. We did consider the merits of a CRISPR

approach to achieve purer cell populations. However, the validation steps described and the tumour cell heterogeneity inherent to our approach could offer a good reflection of the clinical situation and CRISPR may not influence cells with increased genome copy (since not all copies may be edited) as effectively as a short-hairpin approach where excess EGFR is then re-introduced. In addition, having a WT form of EGFR at our disposal within the same system provided a robust internal control against which to compare the mutant forms.

3.3.2 Validating an H1975-derived model EGFR mutant lung cancer.

Bright field microscopy confirmed that each of the cell lines were clearly different after manipulation of EGFR. $H1975^{L858R}$ and $H1975^{WT}$ cells were rounded, and tightly packed having acquired a more epithelial appearance than the parental $H1975^{L858R/T790M}$ cell line, which was elongated and more typical of a mesenchymal appearance (Figure 3.2A). $H1975^{WT}$ showed greater similarity in appearance to $H1975^{L858R}$ than $H1975^{L858R/T790M}$ suggesting an important difference between the presence of *EGFR* L858R-T790M and *EGFR* L858R alone in terms of cell phenotype.

We validated the appropriate allelic frequency of each mutated form of EGFR relative to control probes using digital droplet PCR (ddPCR), thus demonstrating satisfactory design of the model with cDNA content in each cell line dominated by the expected EGFR form. Such techniques serve a useful purpose in our model to establish the effective manipulation of the genetic content of our tumour cells (Day, Dear et al. 2013). In the case of the $H1975^{L858R/T790M}$ parental line, both L858R and T790M mutants were dominant and present in equal concentrations in line with the supposition that they exist in *cis* with allelic dilution of the WT *EGFR* by selective amplification of the mutant form. In the case of the modified lines, for $H1975^{WT}$ we saw equal suppression of both mutants and consistent with the dominance of the L858R mutation in *EGFR* L858R-driven tumours, ddPCR analysis of the $H1975^{L858R}$ cells showed that L858R events dominated in this cell line with near complete elimination of T790M. There remained a possibility that EGFR molecules with the L858R-T790M mutation persisted. The ddPCR in this respect is reassuring but also highlights the difficulty of the short hairpin approach where complete elimination of the activity of parental *EGFR* L858R-T790M is not possible. We anticipated for the purposes of the model that this was unlikely to be significant since EGFR WT genetic material subsequently transfected would exceed this. In any case we went on to ensure also that an appropriate response to erlotinib treatment was seen in EGFR phosphorylation by immunoblotting protein lysates of each cell line.

The three cell lines indeed recapitulated the clinical scenario when subjected to treatment with the EGFR TKI erlotinib when EGFR phosphorylation was used as a marker for activation. We saw, as expected, inhibition of this kinase activity with erlotinib in the H1975^{L858R} cells but not H1975$^{L858R/T790M}$ cells with the T790M mutation (see Figure 3.2D). There was no remaining phosphorylation signal in the H1975^{WT} cell line suggesting that no significant levels of functionally active EGFR L858R-T790M protein were present. EGFR protein levels were comparable between each of the cell lines as demonstrated by the Western blot shown in Figure 3.2C. From the same Western blots we also verified the constitutive, ligand-independent activation of tyrosine kinase activity in the L858R and L858R-T790M mutated forms of EGFR which would be consistent with the expected behaviour of activating *EGFR* mutations. H1975^{WT} only showed phosphorylation in response to stimulation with Epidermal Growth Factor (EGF), the natural ligand for EGFR. All three of the cell lines in addition showed increase in the phosphorylated EGFR signal in response to stimulation with EGF, highlighting the continued ligand-dependence even in the event of constitutive activation (Red Brewer, Yun et al. 2013)(see Figure 3.2D).

Finally, the murine xenograft model provided an *in vitro* context for the behaviour of tumour cells. In particular this gave information of tumour proliferation within a 3-dimensional architecture of a tumour and gave us the option to compare the stromal and vascular components in response to the genetic differences between the cells. Whilst the mouse model is not a true representation of lung adenocarcinomas found within a human tissue environment with differences expected between murine and human host factors and additionally a subcutaneous tumour model in comparison with an orthotopic model, it does however add detail to the *in vitro* data in these approximations of the tumour microenvironment.

3.3.3 Effect of *EGFR* mutations on *in vitro* tumour cell characteristics

We observed that the *EGFR* L858R mutation alone resulted in increased proliferation within the BrdU incorporation assay that was not the case with the addition of the T790M mutation. BrdU staining is highest in cell nuclei with actively replicating DNA and thus represents cells in S-Phase as a marker of proliferation. This is consistent with an increased catalytic activity of the L858R mutant form of EGFR. Similarly the agar colony formation assays, which represent the ability of tumour cells to grow independently of attachment, a tumorigenic trait in itself, showed greatest numbers of both small and large colonies in the H1975$^{L858R/T790M}$ cell line. Here number of colonies overall are a marker of survival, whereas the size and number of larger colonies give an indication of frequency of cell division whereby higher rates of cell division give rise

to larger colonies consisting of greater numbers of cells and is therefore more closely related to proliferation. These results are consistent with increased proliferation in the presence of the *EGFR* L858R mutation. H1975$^{L858R/T790M}$ was the least proliferative cell line, with the fewest colonies in the agar colony forming assay and hence highlights that this mutation impedes the activity of the L858R towards proliferation (Figure 3.4 and Figure 3.5). Wound healing and random cell migration assays suggested that the presence of EGFR L858R did not cause the same capacity for migration as did the double mutant form, EGFR L858R-T790M as found in the H1975$^{L858R/T790M}$ cell line, which was the most migratory cell line (Figure 3.6 and Figure 3.7). Cells expressing EGFR WT demonstrated an intermediate phenotype between the two mutant forms for both proliferation and migration suggesting that they polarised towards opposite phenotypes.

Existing work that has studied the effects of *EGFR* mutations on the biological characteristics of *in vitro* models demonstrate that activating mutations of *EGFR* in general increase the proliferative capacities of lung cancer cells and other *in vitro* models in terms of viability and anchorage independent growth models similar to those which we have employed. Such results are thus consistent with our EGFR L858R activated cells (Sordella, Bell et al. 2004, Greulich, Chen et al. 2005). EGFR L858R mutants within other models such as the A549, H1299 and CL1-0 (NSCLC) cell lines increase tumour cell migration and invasiveness compared to WT EGFR but do not give us information on how this differs from L858R-T790M (Tsai, Chang et al. 2015, Hung, Chen et al. 2016). Direct comparison between the phenotypical effects of L858R versus T790M independently or *in cis* are unfortunately not common in the literature and additionally studies have been conducted in non-'lung cancer' cell lines (Godin-Heymann, Bryant et al. 2007, Uchida, Hirano et al. 2007). Previous comparison of the L858R±T790M mutants has in an agar colony-forming assay using NIH3T3 cells suggested that the presence of L858R and T790M combined resulted in the greatest number of colonies. This cell line however is fibroblast derived and thus is difficult to compare directly with the epithelial H1975 (Godin-Heymann, Bryant et al. 2007). We chose H1975 in this respect as we considered it important to compare these mutations in the context of a cell line of established relevance to EGFR TKI resistance in lung cancer.

This conflicting data also highlights that relative enzyme activities of the EGFR L858R versus L858R-T790M mutants are not clearly defined. The same authors suggest that T790M enhances the tumorigenic properties of the L858R mutation and that this mutant is a 'stronger mutation' (Godin-Heymann, Bryant et al. 2007). This may reflect

the different behaviour of EGFR in our model compared to that of others. For example the relative dominance of other growth factor receptors and downstream signaling proteins in different cell lines may alter the effects of EGFR. Context of EGFR activity appears to be more important therefore than specific kinase activity or expression levels of the receptor as elaborated on in the paragraphs below. Our data confirm this notion that the L858R and L858R-T790M mutations were each polarizing and induced changes dependent on an exact characteristic of this mutation rather than the degree of phosphorylation present.

3.3.4 Effect of *EGFR* mutations on xenograft tumour characteristics

Differences observed between proliferation of the our H1975 derived cell lines *in vitro* were recapitulated *in vivo* – the $H1975^{L858R}$ tumours grew most quickly with greatest volumes throughout the experiment. $H1975^{L858R/T790M}$ was conversely the slowest growing cell type (Figure 3.8). This was most noticeable after the full 24 days of the experiments although a separation of the curves appeared approximately two weeks after injection of the cells. This most likely represents the time taken to amass a recordable difference in cell-doubling time in terms of cell number. Tumour weights at the end of the experiment at time of sacrifice and proliferation rate as defined by proportion of cells with phospho-Histone H3 staining as a marker for mitosis followed a similar pattern (Figure 3.9). These results thus provided internal validity between the *in vitro* and *in vivo* systems used to test the effects of the *EGFR* mutations. We additionally scored the tumours for necrosis (Figure 3.10), which were highest in the $H1975^{WT}$ and the $H1975^{L858R}$ tumours. This may in part reflect the proliferative capacity of the cells where the rapid tumour growth out of proportion to supporting stroma predisposes to necrosis. This does not explain the $H1975^{WT}$ finding however. $H1975^{WT}$ tumours may potentially lack adaptation to stimulate a supportive stroma.

Findings of others consistent with this data include studies indicating increased tumour growth in murine xenografts derived from A549 and NIH3T3 cells transfected with *EGFR* L858R (Greulich, Chen et al. 2005, Hung, Chen et al. 2016); lung tumour formation in transgenic mice with tetracycline inducible expression of EGFR L858R (Politi, Zakowski et al. 2006); and increased latency of xenograft tumours with the addition of T790M to L858R (Regales, Balak et al. 2007). Again these data are focused on L858R more than T790M and the results of Godin-Heymann *et. al.* conflict with our observations, since they observed steepest growth curves for the double mutant cell lines with T790M combined with either L858R or del19 (Godin-Heymann, Bryant et al. 2007).

Further analysis of the stroma, using other markers, which included Masson's trichrome staining and anti-smooth muscle actin to delineate the tumour cells from surrounding collagen and fibroblasts, highlighted other important differences between the EGFR kinase domain mutants in the *in vivo* environment (Figure 3.11). Tumour cells in H1975^{L858R} xenografts were highly interspersed with stromal tissue, positive for staining of collagen (Masson's trichrome) and anti-smooth muscle actin. This stroma tissue appeared to encapsulate 'packets' of tumour cells. Our interpretation was that the proliferative capacity for the EGFR L858R mutant led to increased interaction with the surrounding stroma in the *in vivo* environment and that these cells grow most effectively in cooperation with the stroma suggesting a paracrine effect from the tumour on the stroma. Looking for other differences in the consequences of these *EGFR* mutations *in vivo,* we also quantified anti-CD31, a marker of angiogenesis, which thus represents new blood vessel formation. This was most prominent in H1975^{WT} tumours and thereafter H1975^{L858R} although it was not clear what was driving this trait (Figure 3.12).

Themes in the literature regarding interaction between EGFR mutants and the stroma focus on the tumorigenic effect of ligands coming from the stroma or the potential for tumour associated immune responses. Other data reports that disease spread (malignant pleural effusions) is increased in the presence of L858R (Tsai, Chang et al. 2015). In general there is limited data from direct assessment of the effect of *EGFR* mutations in animal models, which instead must be inferred from data on experiments assessing TKI response in such models. For example Hepatocyte Growth Factor (HGF), the ligand of the MET receptor, a related tyrosine kinase receptor frequently dysregulated in lung cancer (see Chapter 4), can mediate EGFR-TKI resistance in murine models (Nakagawa, Takeuchi et al. 2012) with MET inhibition a means of demonstrating that EGFR TKI resistance is related to HGF activity (Tang, Du et al. 2008). Patient data similarly supports a role for ligands such as HGF in resistance to therapy against EGFR (Yano, Wang et al. 2008).

An important influence of ligands such as EGF and HGF on the tumour microenvironment is plausible which through both autocrine and paracrine effects could provide a control mechanism for coordination of tumour cells traits within the wider tumour. Such theoretical differences in secreted ligand may result from the increased number of cells present in a more proliferative cell line or be related to another change in cell biology arising from EGFR that changes ligand interaction (Riemenschneider,

Bell et al. 2005, Wang, Li et al. 2009). Further study of ligands was outside the scope of this project.

In summary, the ability to examine the EGFR mutants in an *in vivo* xenograft model highlighted an important difference of tumour cell behaviour between the different EGFR mutants with regards to tumour cell growth and also interaction with surrounding stroma. This indicated that in addition to the intrinsic differences between how the cells behaved *in vitro*, there were also consequences for the tumour microenvironment (Wilson, Fridlyand et al. 2012, Junttila and de Sauvage 2013, Feldman and Yarden 2014).

3.3.5 What are the potential mechanisms to link *EGFR* mutations and tumour cell characteristics?

In order to understand how *EGFR* mutations lead to the differences we observed in both *in vitro* and *in vivo* traits, we looked at mechanistic differences between EGFR mutants and considered how these could be implicated.

3.3.5.1 TKI Sensitising *EGFR* mutations alter EGFR activation

We looked first to the current literature on EGFR conformational changes arising from *EGFR* mutations and their consequences for EGFR activation. The accepted mechanism of EGFR activation is homodimerisation, driven by ligand binding (Capuani, Conte et al. 2015). It is recognized that dimerisation is asymmetric and requires that an allosterically active C lobe of an activator kinase induces a conformational change in the receiver-competent N lobe of its partner. Usually, the extracellular domain suppresses dimerisation, maintaining an inactive state until ligand binding (Zhang, Gureasko et al. 2006). *EGFR* kinase domain mutations such as del19 or L858R can result in constitutive activation of EGFR through their positioning around the active site where they disrupt hydrophobic interactions that exist to protect the auto-inhibited inactive conformation of EGFR (Yun, Boggon et al. 2007). EGFR kinetics analyses suggest that these changes arising from the L858R mutation result in constitutive kinase activity 50X more active than WT (Yun, Boggon et al. 2007).

It is not clear why the increased EGFR activity of the L858R mutant is so much greater than the augmentation (10x) seen with other mutants such as G719S, which is a less commonly observed kinase domain mutation (2-3%). Particularly since both resemble the active conformation of the WT receptor. This does however raise interesting mechanistic questions about the consequences of such mutations arising at different positions within the kinase domain on EGFR function. This may be explicable in terms

of enzyme kinetics - the Michaelis constant (K_m), a marker of the concentration of substrate required for catalysis according to the Michaelis-Menten equation, a surrogate of enzyme affinity for peptide substrate, is halved for EGFR L858R compared with EGFR WT. Furthermore the 'turnover number' (K_{cat}) which represents the rate of substrate molecules converted to product, is elevated to a greater extent in the presence of L858R compared with G719S. Consequently there is an order of magnitude difference in the second order rate constant $K_{cat}/K_{m,}$ an overall marker of enzyme efficiency between WT and each mutant form (Yun, Boggon et al. 2007). Similar data is not available for deletion in exon 19 mutants.

3.3.5.2 The T790M TKI resistance mutation alters EGFR activation

T790M is located within hydrophobic residues at the posterior aspect of the ATP binding pocket, which restores the affinity of EGFR for ATP to near WT levels (Yun, Mengwasser et al. 2008). Increased binding affinity of ATP to the EGFR L858R-T790M mutant relative to EGFR L858R. The K_{cat}/K_m [ATP] is five-fold higher than for the single mutant suggesting that the kinetics of the two mutants differ substantially (Yun, Mengwasser et al. 2008). The presence of the T790M mutation alone confers only a modest change from *EGFR* WT, whereas when combined with activating mutations such as L858R, EGFR activity is more substantially altered (Godin-Heymann, Bryant et al. 2007). Despite differences in phosphorylation kinetics and functional behaviour, structural similarities between these mutants suggest that these differences arise from different energy costs to transition between forms rather than due to the mutations' direct effect on EGFR structure. EGFR L858R-T790M is the least stable in its inactive state followed by L858R and finally WT (Gajiwala, Feng et al. 2013).

Another hypothesis is that the phosphorylation pattern of EGFR tyrosine residues differs between the activating EGFR mutants e.g. del 19 vs. L858R; L858R-T790M and additionally that this is further modulated by EGF ligand binding (Guha, Chaerkady et al. 2008). For example, higher degrees of phosphorylation are seen at residues Y1068, Y1086, and Y1173 in the L858R-T790M mutant form of EGFR (Yen, Liu et al. 2015). Thus the re-positioning of key residues with each mutation could determine the phosphorylation pattern and with it, a unique downstream pathways specific to a particular phosphorylation site (Figure 3.14)(Sordella, Bell et al. 2004, Morandell, Stasyk et al. 2008).

Our data both matches and conflicts others in the literature, where there is disagreement about the relative tumorigenicity of the T790M mutant form of EGFR. This may reflect the contextual differences of non-tumour/lung cell models in

comparison to the H1975 cell line (Godin-Heymann, Bryant et al. 2007). With this in mind, although the proliferative capacity for $H1975^{L858R}$ could be sufficient to cause an increased kinase activity or capacity for phosphorylation of the EGFR-L858R mutant, given that we observed very distinct phenotypes for $H1975^{L858R/T790M}$ and $H1975^{L858R}$ both in terms of proliferation and migration and additionally stromal deposition, it seems likely that the catalytic activity of EGFR alone is not sufficient to explain the differences observed in phenotype.

3.3.5.3 EGFR mutant-specific dimers could function differently

An important evolving concept in the EGFR literature is that receptor dimerisation is essential for EGFR signaling and intracellular effect. In WT EGFR, Binding of EGF releases auto-inhibitory interactions that render the receptor in a state competent for dimerisation. Here EGF is thought to promote EGFR homodimer formation through firstly proximity that facilitates transphosphorylation and then stabilization of the activated conformation by these phosphorylation events (Hubbard 2006).

The L858R mutation induces changes in the EGFR ectodomain structure that render the single mutant L858R form of EGFR in an extended, dimerisation-competent conformation which has also been shown to encourage EGFR homodimerisation (Valley, Arndt-Jovin et al. 2015, Valley, Arndt-Jovin et al. 2015). This is believed to increase dimerisation ability by suppressing local intrinsic disorder in the catalytic region of the receiver kinase (Shan, Eastwood et al. 2012, Sutto and Gervasio 2013). Crystal studies of the double mutant EGFR L858R-T790M (monomerised with V948R) suggest a conformation of EGFR in which the dimer interface is nearly identical to that of the active WT EGFR and the oncogenic L858R mutant (Gajiwala, Feng et al. 2013). Both L858R and L858R-T790M mutant EGFR retain dependence on an intact asymmetric dimerisation interface for full activation suggesting that neither mutation is capable of generating a signal as a monomer (Red Brewer, Yun et al. 2013).

Other features of EGFR consistent with an allosteric model of activation include the interaction between the alpha-H helix of the activator EGFR monomer with the alpha-C helix of the receiver, which initiates the switch to the active conformation. This results in freeing of the activation loop to activate its partner heterodimer molecule (Lemmon, Schlessinger et al. 2014). Thereafter the juxtamembrane (JM) region's c-terminal portion latches the activated kinase domain of the receiver to the activator which is further augmented by the N-terminal segment, which then engages the transmembrane region of the activated receptor (Jura, Endres et al. 2009).

The potential role for dimerisation in the differences in cell phenotype that we observed is highlighted by evidence that different EGFR mutants are “specialised” in this way – kinase mutant forms of EGFR behave preferentially as ‘receivers’ when expressed with WT EGFR and can then hyperphosphorylate the WT conformation (Red Brewer, Yun et al. 2013). Here, the authors report that combining the L858R ± T790M mutants or WT EGFR with mutations known to disrupt the asymmetric dimerisation interface showed that N lobe disrupting mutations which could set the direction of asymmetric activation were less effective in the presence of T790M. EGFR L858R-T790M then appeared to be more effective in signaling when acting as an acceptor compared with a donor (Red Brewer, Yun et al. 2013). Our data that the different EGFR mutants give rise to different traits is consistent with this data. Figure 3.13 suggests how putative combinations of EGFR ‘homodimeric’ pairings (single versus double mutant EGFR versus WT) could populate the pool of EGFR in each cell line. Certain pairings may be more frequent based both on structural tendency to interact and thereafter ability of a given dimer pair to activate the EGFR signal. This may suggest that the WT EGFR persists alongside mutant EGFR acting in synergy with them (Red Brewer, Yun et al. 2013).

Since EGFR heterodimerisation is also possible, other HER family members may be important to the differences induced by the EGFR mutants. Previous studies have shown that cell proliferation and tumorigenesis are enhanced in tumour xenografts co-expressing HER family *heterodimers*, e.g. EGFR-HER2, EGFR-HER4 or HER2-HER4, compared to those expressing single receptors (Alaoui-Jamali, Song et al. 2003). This indicates that in addition to the well-characterized HER2-HER3 pair, the most oncogenic in breast cancer (Holbro, Beerli et al. 2003), EGFR heterodimerisation is important to oncogenic signaling. This may also account for differences between our results and those of others, whereby EGFR mutants transfected into cell lines without a natural pool of HER family receptors are unlikely to behave as they do in lung cancer cell lines.

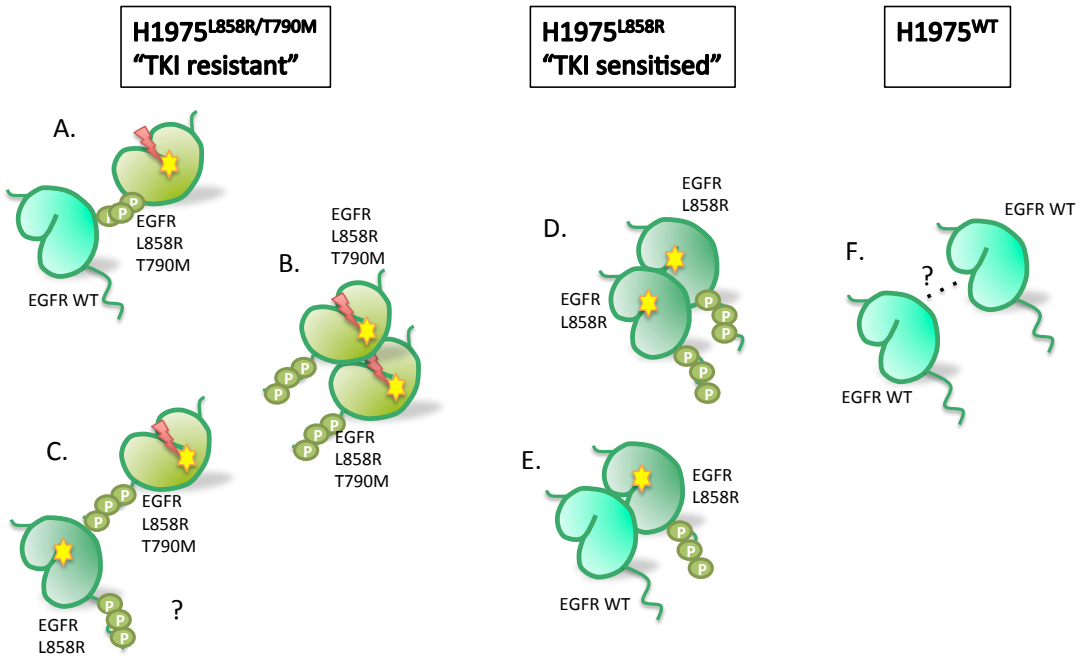

Figure 3.13 EGFR homodimerisation in H1975 derived model
A number of possible configurations of EGFR homodimers are possible between EGFR WT and each of the EGFR mutants we included in our model). If, as suggested by the literature, the L858R-T790M mutations exist in *cis*, the pairing of EGFR remaining chromosome could give rise to EGFR WT/EGFR L858R-T790M heterodimers (A) or through selective upregulation of the double mutant, exist as EGFR L858R-T790M homodimers (B). If EGFR-L858R persists, for example through increased EGFR copy number it is conceivable that a EGFR L858R-T790M/ EGFR L858R heterodimer could be observed (C). In the case of $H1975^{L858R}$ we would expect either homodimerisation of EGFR L858R (D) or heterodimerisation between EGFR L858R/EGFR WT (E). In the case of $H1975^{WT}$ a ligand-induced EGFR WT homodimer would be expected. It is possible that any of these interactions can be bi-directional, for example in A – the mutant form could activate the WT or vice versa. However, it is likely that a particular direction would be favourable and could alter the signaling consequence observed (Littlefield and Jura 2013).

3.3.5.4 Is there a role for defective EGFR L858R internalization?

We were interested to observe that the pattern of immunofluorescence staining of EGFR after EGF stimulation for different times in our cell lines differed. $H1975^{WT}$ cells demonstrated rapid internalization following ligand stimulation. However, in $H1975^{L858R}$, EGFR showed persistent membrane staining suggestive of delayed or defective internalization even after EGF treatment (Figure 3.3). Comparing this with $H1975^{L858R/T790M}$ cells where we saw internalization, this provides a further mechanism by which EGFR L858R-T790M could differ in signal intensity/specificity beyond the capacity for phosphorylation. This defective internalisation may augment the EGFR signal due to reduced degradation/recycling to non-signaling cell compartments. This may contribute to the constitutive phosphorylation that we saw in EGFR mutants, which

could result in prolonged EGFR signaling compared with a more transient phosphorylation in EGFR WT potentially as a result of protection from phosphatase activity. This accumulation of EGFR at the membrane or within other nearby signaling compartments and accompanying increased EGFR activity is likely to be an important factor in the increased transforming capacity of EGFR in the presence of this mutant and also its availability to encounter other EGFR or HER family molecules which may become enriched and available for interaction at the membrane.

These results are consistent with a previously reported defective clathrin-mediated endocytosis in L858R mutated EGFR, also a recognised mechanism that precedes receptor recycling and degradation (Murthy, Basu et al. 1986, Kirisits, Pils et al. 2007). Other authors have shown co-localisation of mutant EGFR with endosomal markers whereby $H1975^{L858R/T790M}$ show constitutive endocytosis, which renders them more likely to interact with SRC (Chung, Raja et al. 2009). Shtiegman *et al* related such defective ligand-induced internalization of mutant EGFR to differences in c-cbl mediated ubiquitinylation, a well recognized regulatory, post-translational modification (Lemmon and Schlessinger 2010). Shtiegman *et al* also suggested that differences in EGFR dimerisation in this mutant could be attributable to heterodimerisation with another ErbB receptor, such as HER2 could be the cause of such a delay in internalisation. We anticipate that in our model another receptor known to be important in lung cancer, for example HER3 or MET might be more important (Engelman, Zejnullahu et al. 2007). Little is known of the significance of the acquisition of T790M to this process. Although the authors also saw defective ubiquitinylation in similar assays with EGFR L858R-T790M they did not compare whether EGFR L858R differed from EGFR L858R-T790M in this respect (Shtiegman, Kochupurakkal et al. 2007). According to our observations EGFR L858R-T790M differed from EGFR L858R in this respect (Shtiegman, Kochupurakkal et al. 2007).

3.3.5.5 Could this be explained by differences in downstream signaling?

As discussed above, the literature suggests that different EGFR phosphorylation signatures arise from each mutant and this can be linked to different tumoural traits, phenotypes and signaling pathways (see Figure 3.14) (Morandell, Stasyk et al. 2008).

In the case of proliferation, the increased rate of cell division and growth noted in the $H1975^{L858R}$ versus $H1975^{WT}$ cells could be mediated by increases in AKT or ERK signaling, both of which are linked to survival and growth. There are existing reports that driver mutations in EGFR select for EGFR-TKI efficacy by their dependence on anti-apoptotic pathways (e.g. AKT), more so than on proliferative pathways such as ERK. Additionally EGFR L858R has been reported in the literature to activate ERK less effectively than EGFR WT (Lazzara, Lane et al. 2010). The migratory phenotype we associated with the $H1975^{L858R/T790M}$ cell line as well as a reduction in proliferation may result in a different propensity to activate AKT, ERK in favour of another mediating pathway such as FAK.

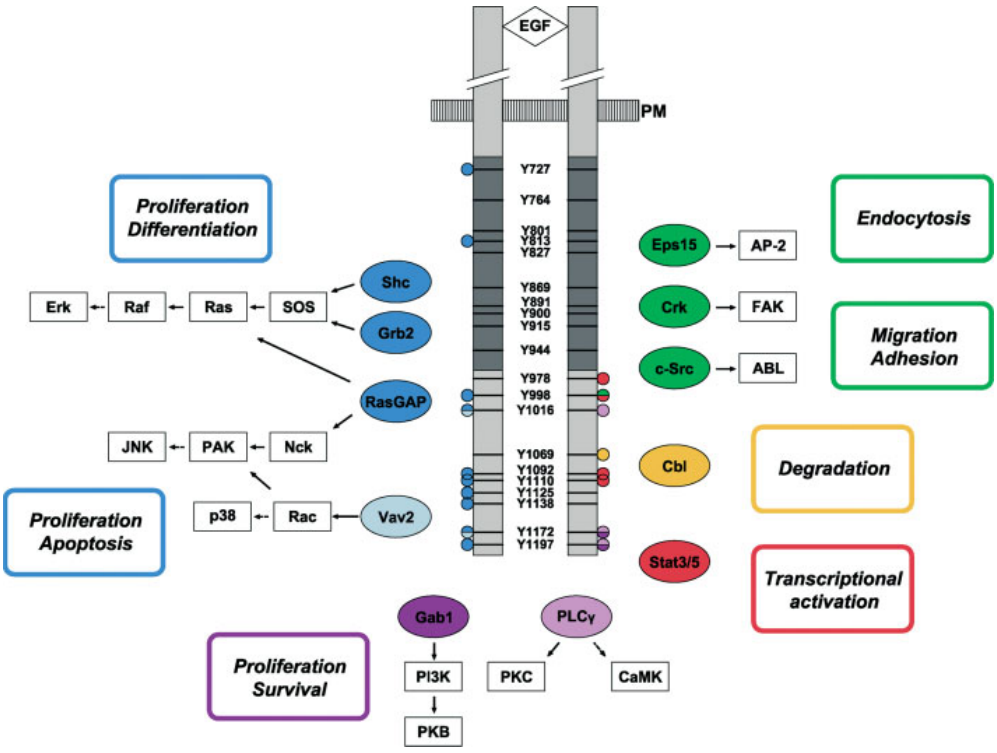

Figure 3.14 EGFR phosphorylation sites determine specificity for downstream signaling pathways

Phosphorylation of specific tyrosine residues upon phosphorylation are associated with particular downstream adaptor proteins. The figure gives examples of Tyrosine residues of EGFR homodimer and known mediators (multicolour ovals) alongside their accompanying signaling pathways and functional roles. Activating mutations and dimerisation can influence the pattern of phosphorylation and therefore downstream signaling. Adapted from Morandell et. al. (Morandell, Stasyk et al. 2008).

3.4 Conclusions

In conclusion, the commonly encountered *EGFR* mutations, L858R and T790M, which determine EGFR sensitivity/resistance respectively, have additional consequences for lung adenocarcinoma both *in vitro* and *in vivo.* Within a H1975 derived model, the L858R mutation was associated with a proliferative phenotype and an increase in markers of stromal activity in tumour xenografts. The L858R-T790M mutation meanwhile led to a more migratory phenotype and resulted in slower proliferation rates and smaller tumours in the murine model.

These observations combined with the importance of dimerisation in the EGFR family of proteins in general, prompted us to consider if these differences in EGFR and the phenotypic observations made might be unified by the tendency of the differentially mutated forms of EGFR to dimerise with another receptor. This would fit into our model of mutation-specific dimerisation by providing a mechanism by which downstream signaling and phenotype might vary with *EGFR* mutation status. Specifically, it would be plausible that if the activation of each of specific tyrosine residues by its dedicated kinase, i.e. SRC, EGFR/another ErbB or MET was altered by the ability of EGFR to dimerise, then a particular function role could be exaggerated. Sequestration at the membrane may provide an additional layer of regulation to this process.

According to the literature, dimerisation between EGFR and itself and other ErbB family members differs depending on the *EGFR* mutation present as discussed in Section 3.3.5.3. We can hypothesise that dimerisation of EGFR with another receptor which has an increased capacity to activate the PI3K/AKT pathway, for example HER3, may lead to a dominance of signaling through this downstream pathway (Arteaga 2007). Alternatively, in other mutant forms of EGFR such as EGFR-L858R-T790M which is reported to engage HER3 less readily, the importance of another partner molecule such as MET may be augmented with the resultant change in the signaling pathway affected (Wang, Ma et al. 2015). This would be an important determinant of tumour responsiveness to other receptor tyrosine kinase inhibitors, which would provide valuable information to avoid and circumvent treatment resistance.

Chapter 4. Understanding the role of MET in EGFR mutant lung adenocarcinoma

4.1 Introduction

4.1.1 The overlapping role of *EGFR* and *MET* oncogenes

The MET tyrosine kinase receptor initiates signaling events in multiple biological processes. In cancer, over-expression, amplification or mutation of *MET* is associated with invasive growth, tumour progression and metastasis (Olivero, Rizzo et al. 1996, Boccaccio and Comoglio 2006, Beau-Faller, Ruppert et al. 2008, Cappuzzo, Janne et al. 2009, Cappuzzo, Marchetti et al. 2009, Benedettini, Sholl et al. 2010). The recognised link between the tumorigenic effects of MET and a proposed crosstalk between MET and other membrane-based receptors such as EGFR is also believed to contribute to EGFR TKI resistance. EGFR-MET crosstalk is supported by MET and EGFR co-expression in lung cancer cell lines (Tang, Du et al. 2008), crosstalk between EGFR and MET in assays of signaling pathways and direct co-immunoprecipitation experiments (Jo, Stolz et al. 2000, Tang, Du et al. 2008, Wang, Li et al. 2010).

The phenotypical effects of EGFR-MET crosstalk have been demonstrated in assays of proliferation, cell migration and wound healing (Xu and Yu 2007). EGFR inhibition has also been shown to inhibit HGF-MET induced invasiveness and scattering (Bonine-Summers, Aakre et al. 2007). In an important *in vitro* model of *MET* amplification, the HCC827 cell line (*EGFR* del 19) can be driven to MET-mediated acquired EGFR TKI resistance through prolonged culture in the presence of EGFR inhibitors (Turke, Zejnullahu et al. 2010). In these EGFR-TKI resistant HCC827 cells, gefitinib still suppressed cell migration and anchorage independent growth suggesting ongoing dependence on EGFR even in the context of a switch to MET as a driver (La Monica, Caffarra et al. 2013). It is reported that in this and other EGFR mutant cell lines, EGFR TKI inhibit the EGFR-MET interaction and suppress MET phosphorylation. Reduction in MET expression however was not observed in EGFR WT cell lines such as H1666 and no phosphorylation of MET is seen in this cell line (Guo, Villen et al. 2008). EGFR activation by ligand or mutation has also been associated with increased levels of MET expression (Xu, Nilsson et al. 2010). These observations therefore support the importance of activated EGFR to the tumorigenicity of MET.

The main role of EGFR-MET crosstalk has previously been discussed primarily as a resistance pathway to EGFR TKI therapy in EGFR activated tumours mainly, in the context of MET amplification (Bean, Brennan et al. 2007). It is not known whether *MET* amplified tumours represent a unique subset of tumours in which EGFR and MET are

co-activated or if MET is important in lung cancer in general. It is also not clear how EGFR-MET synergism relates to EGFR activating mutations and where MET fits into tumour signaling in a non-amplified state. Finally MET mutations bring further opportunity to this area (Matsubara, Ishikawa et al. 2010). This chapter explores these unmet needs in the potential targeting of MET.

4.1.2 What is the role of MET targeted therapy in EGFR mutant NSCLC?

Despite the promising pre-clinical data supporting plausible blockade of MET as a therapeutic strategy in EGFR TKI resistant NSCLC, these agents have not yet realized clinical use outside of trials (Feng, Thiagarajan et al. 2012, Gherardi, Birchmeier et al. 2012, Menis, Levra et al. 2013). Early data suggested that EGFR-MET *combination* treatment could be beneficial against tumour growth and hence many trials have focused on dual therapy with EGFR TKI (Tang, Du et al. 2008, Zhang, Staal et al. 2010). The most promising agents in phase III trials, even in combination with EGFR TKI, have not provided evidence for MET inhibition (Pérol 2014, Scagliotti, von Pawel et al. 2015).

We had the opportunity to study SGX523 (6-[6-(1-methyl-1H-pyrazol-4-yl)-[1,2,4] triazolo-[4,3-b]pyridazin-3-ylsulfanyl]-quinoline), an orally available, small molecule, ATP-competitive TKI which shows high affinity for the less active, un-phosphorylated form of MET (Ki = 2.7 nmol/L) compared with the active phospho-MET (Ki = 23 nmol/L). This is indicative of a drug that targets the inactive conformation and has shown 'exquisitely' high selectivity for WT MET with minimal off target effects on other kinases as demonstrated against a panel of 213 protein kinases when used at 1000nM/L, with a 'Karaman' score of 0.005 (Buchanan, Hendle et al. 2009). An important observation regarding the drug-bound structure of MET in the presence of SGX523 is that the conformation resembles that more usually seen for inhibitors that target the active conformation, with a "DFG-in" structure. Such orientations can be important determinants of how kinase domains interact with related molecules. SGX523 has shown inhibition of proliferation and growth in lung cancer models *in vitro* and *in vivo* and acts synergistically with EGFR inhibitors (Guessous, Zhang et al. 2010, Zhang, Staal et al. 2010). Unfortunately, clinical development has ceased because of nephrotoxic metabolites detected in phase I safety trials, not observed in animal studies (Infante, Rugg et al. 2013)

Although no longer suitable for use in a clinical environment, this agent demonstrates potential as an experimental tool to target the MET pathway with high fidelity, without 'off target' effects on other receptor tyrosine kinases such as EGFR (Buchanan, Hendle

et al. 2009). For this reason it provided an ideal agent to use for these studies to truly isolate the manipulation of the experimental condition to MET and enable us to compare the exact contribution of each of these related kinases to EGFR-MET crosstalk independent to that of EGFR activity which could then be modulated separately (Buchanan, Hendle et al. 2009).

4.1.3 Could an EGFR-MET FRET assay add to existing clinical management?

This area remains highly experimental but critics of failed studies have highlighted the need for novel predictive biomarkers to best select such therapies. *MET* amplification outperforms tissue immunostaining although the lack of success of MET targeted therapy suggests this approach is inadequate (Tanaka, Sueoka-Aragane et al. 2012). Whilst MET mutations are also evolving as a possible means to target MET based therapy, these appear to represent a different population of patients. Finally although combination therapy are increasingly considered, there is unfortunately no data on whether crosstalk between related drug targets such as EGFR and MET could reliably direct such approaches.

A novel approach in kinase receptor derived biomarkers includes Förster Resonance Energy Transfer (FRET) assays using fluorescence lifetime imaging microscopy (FLIM) to analyse the interaction between pairs of molecules (Kelleher, Fruhwirth et al. 2009). This is a gold standard technique for measuring protein proximity within the typically <10nm range (Ng, Squire et al. 1999, Ng, Parsons et al. 2001, Parsons, Keppler et al. 2002). Fluorescence Life Time Imaging (FLIM) is well suited to analysis of the interaction between EGFR and MET, as discussed in Chapter 1. Using FLIM, it is possible to measure FRET to quantify interactions between EGFR and MET at the nanometre scale to establish the potential role that crosstalk might play in lung cancer. Such data could be used prognostically to group patients according to EGFR-MET interacting or not. Furthermore, it could help characterise/predict response to EGFR or MET targeted therapy.

4.1.4 Aims

To address these themes and gain mechanistic insight into the role of MET in the context of EGFR mutant lung cancer and also to better understand therefore the potential circumstances where MET targeted therapy might be relevant we selected a highly specific small molecule kinase inhibitor of MET, SGX523.

The two main objectives therefore are to establish whether

1) *EGFR* mutations directly influence EGFR-MET binding/dimerisation.
2) *EGFR* mutations determine the effect of MET inhibition.

This chapter focuses on the possibility of a direct interaction between EGFR and MET. We chose to conduct our studies in the model developed in Chapter 3, based on the H1975 cell line which is the stereotypical model of EGFR resistance acquired by the T790M route to better understand the significance of MET in the context of the L858R activating mutation and the T790M mutation more commonly associated with EGFR TKI resistance.

We hypothesised that outcomes from MET inhibition would be influenced by *EGFR* mutation status both at the level of the cell biology and also in terms of cell behaviour. This would also address an important clinical question at the bench. We have explored this hypothesis by evaluating the response of lung cancer cells with *EGFR* WT or activating mutations, to the MET inhibitor SGX523 using the *in vitro* and murine xenograft model based on the NCI-H1975 derived lung adenocarcinoma cell lines and associated assays, which were validated in chapter 3.

4.2 Results

4.2.1 *MET* copy, protein and localisation are unchanged by *EGFR* mutation status

To assess if EGFR-MET interaction is modified by *EGFR* mutations, we studied the MET receptor using the same modified NCI-H1975 lung adenocarcinoma cell lines that we investigated in Chapter 3. We observed no differences in basal MET protein levels between the cell lines as evidenced by the Western blot whereby the double band representing total MET (140KDa) were of equal intensity in all three cell lines. Tubulin was used as a loading control (Figure 4.1A). Given that clinically, *MET* copy number is perceived to be the preferred marker of activation of MET signaling and MET therapeutic effect (Tanaka, Sueoka-Aragane et al. 2012), we assessed *MET* copy number using *MET/cep7* fluorescence *in situ* hybridization (FISH) probes. We calculated both the mean copy number of *MET* and additionally the ratio of *MET* to chromosome 7 centromere signals (Figure 4.1B). The latter approach defines amplification in terms of a "Copy number ratio" standardized to a control probe – in this case 'Cep7' (Chromosome 7 enumeration probe). *MET*/cep7 ratio, as shown in Fig 4.1B as the number of red spots per green control spots was equal (<1) in all three cell lines. MET copy number (the total number of red spots) was increased in all three cell lines, whilst copy number ratio was equal given chromosome 7 polyploidy.

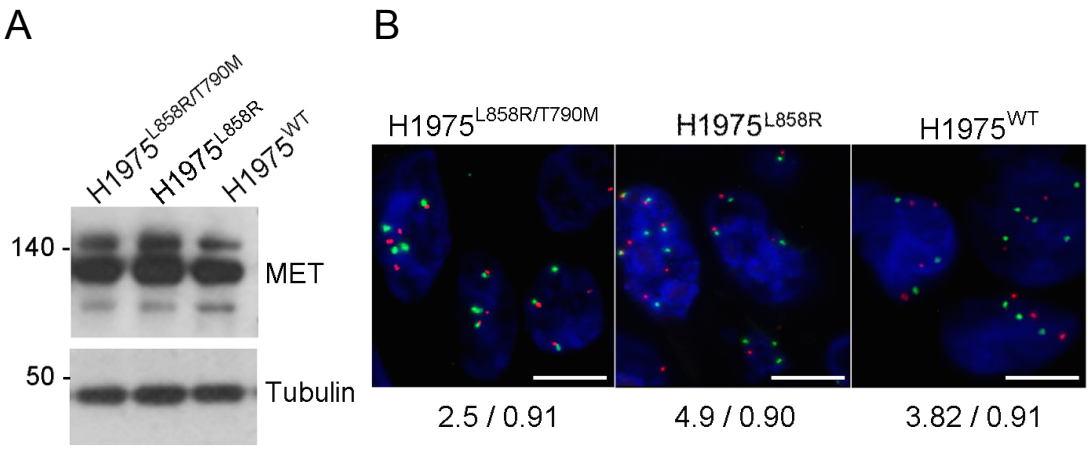

Figure 4.1 MET expression/genomic copy is high in H1975 derived cells
A) Western blot (WB) of total MET in H1975 derived cells is shown as equally represented double bands at 140KDa. Tubulin levels are shown as loading control.
B) *MET* (7q31) copy number analysis is by FISH in the three H1975 derived cell lines using the Leica Kreatech *MET* (7q31)/SE7 FISH probe (KBI-10719). *MET* is visualised in the red channel, Chromosome 7 (Cep7) centromere in green. Scale bar, 10 μm. Average copy number/ratio *MET*:Cep7 below image. The Ratio is equal in all cases with minor change apparent in *MET* copy number. N=30 cells.

4.2.2 EGFR-MET binding is influenced by *EGFR* mutations in lung cancer

In view of the anticipated possibility of crosstalk between the EGFR and MET pathways, we wanted to test our cell lines for EGFR-MET interaction and assess whether this was influenced by *EGFR* mutation status. By undertaking immunofluorescence staining of our cells, we could show that both proteins co-localised similarly at the membrane in each of the three cell types as shown by the demarcation of the cell membrane by the EGFR (red) and MET (green) stains respectively with a crisp yellow perimeter to the cells where the two receptors co-localised (Figure 4.2A). Staining was not seen at the cell nucleus and cytoplasm consistent with the main site of action of these receptors being at the cell membrane. Direct co-immunoprecipitation (Co-IP) between these two receptors as suggested by the literature was confirmed by the data presented in Figure 4.2B below. Pairs of samples are presented for each cell type; the first lane of each pair corresponds to irrelevant immunoglobulin which acts as a negative control, where no band is detected. Conversely, a signal is detected at 170KDa corresponding to EGFR in the samples where an EGFR antibody was used for immunoprecipitation, showing that the EGFR protein was efficiently immunoprecipitated with the EGFR Antibody. In support of an important interaction between *EGFR* mutations and crosstalk with MET, the same samples immuno-blotted with MET antibody showed a band at 140KDa corresponding to detection of MET as an EGFR-MET complex in these lanes. Input lanes are shown as a positive control to confirm that lysates contained EGFR and MET prior to subjecting the samples to the immunoprecipitation reaction.

Co-immunoprecipitation also showed that bands representing amount of total MET protein were of greatest intensity in the lanes corresponding to $H1975^{L858R/T790M}$ lysates EGFR co-immunoprecipitate. In the same blot in comparison, the lanes corresponding to $H1975^{L858R}$ and $H1975^{WT}$ cells showed a weaker intensity of band consistent with a reduction in the co-immunoprecipitation between these two proteins in the latter cell lines (Figure 4.2B). This provides evidence of potential differential interaction between MET and the different mutated forms of EGFR.

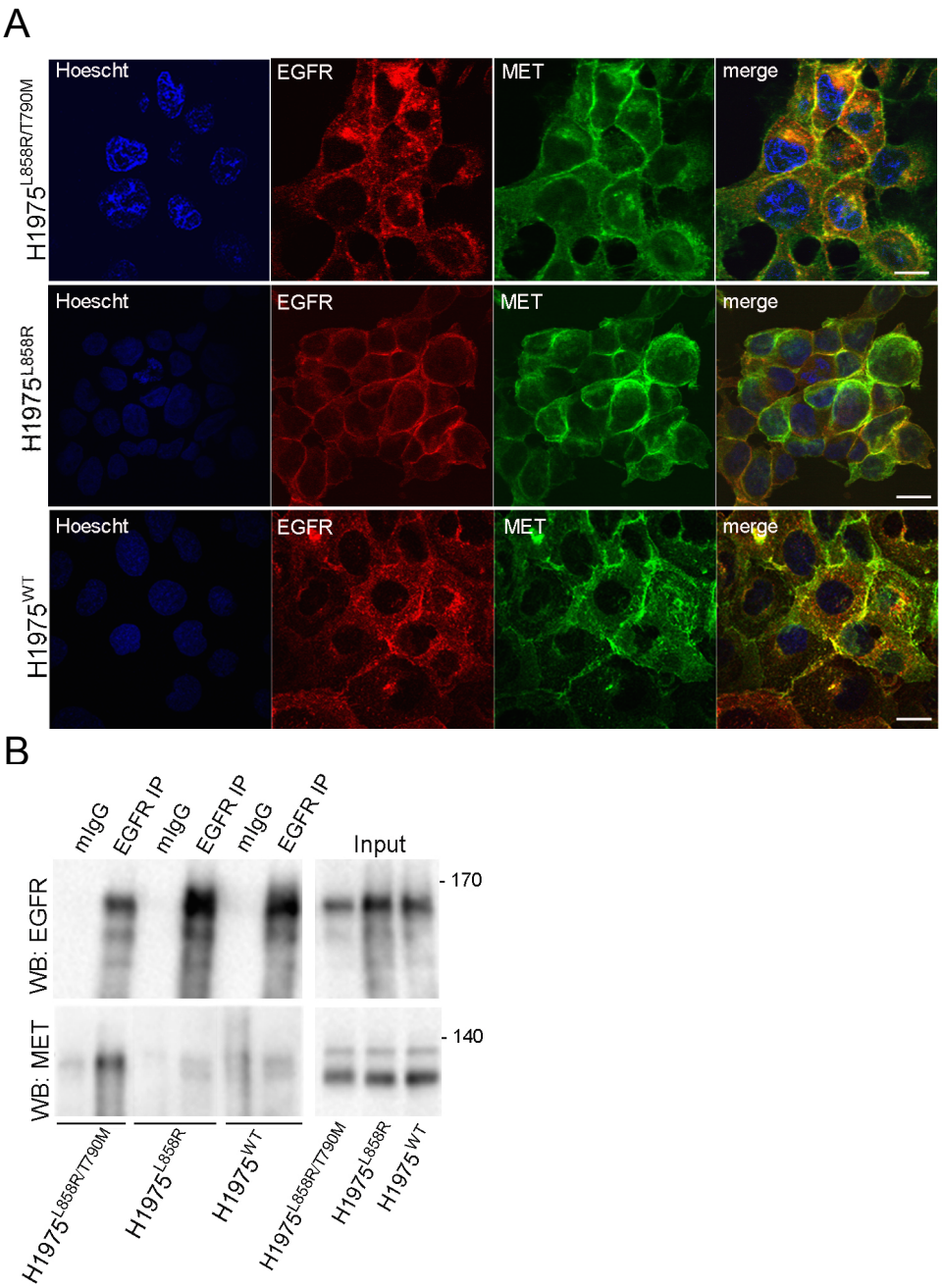

Figure 4.2. EGFR MET interaction differs with *EGFR* mutation status

A) Immunofluorescence of EGFR (red channel) and MET (green channel) in H1975 derived cells. Demarcation of cell periphery by immunofluoresence indicates receptor localisation to the membrane. Cell peripheries are similarly demarcated by both stains with yellow membrane staining on the merge channels suggesting EGFR and MET co-localisation at the membrane. Hoechst dye (blue channel) acts as nuclear counterstain. Merge panels show colocalised pixels as yellow. Scale bar, 20 μm. N=3. Co-immunoprecipitation (IP) of EGFR in H1975 derived cell lines. EGFR antibody was used to immunoprecipitate. EGFR (170KDa) and MET (140KDa) levels are shown in both bound and input fractions to highlight EGFR-MET binding or as positive control for presence of these proteins prior to the IP reaction. MET signal (bottom panel) coming from the lane with the sample immunoprecipiated with EGFR is most prominent in H19757$^{L858R/T790M}$ suggesting EGFR and MET might interact in this cell line. N=4 (Final IP blot kindly Provided by Dr. E. Ortiz-Zapater).

4.2.3 Validating an EGFR-MET FRET assay *in vitro*

To further validate a direct protein interaction between MET and EGFR as suggested by these experiments, we employed a Förster Resonance Energy Transfer (FRET) assay to analyse the interaction between EGFR and MET. We labelled antibodies known to be reliable for staining against EGFR (Ab-5) and MET (AF276) as discussed in Chapter 2 Methods and subjected them to validation in cells manipulated to overexpress EGFR or MET. This was usually compared with an unlabelled primary antibody and secondary fluorophore conjugated not expected to cross-react with the labelled species. For example in Figure 4.3, we see how the control MET (D1C2) antibody with Rabbit secondary (Alexa Fluor 546) compared with the directly labelled MET (AF276)-Cyanine 5 antibody co-localised.

Figure 4.4A shows the Lifetime heat maps and intensity images for EGFR and MET staining. The intensity images for the Alexa Fluor 546 (EGFR) and Cyanine 5 (MET) channels confirm appropriate membrane pattern staining that is similar between the cell lines. The heat maps demonstrate the degree of FRET for each condition – Red represents high FRET (%) i.e. where there is greatest EGFR-MET interaction versus Blue where the interaction is weakest. This reflects the fact that lifetime is measured in the donor fluorophore channel. Fluorescence lifetime falls when donor and acceptor fluorophores are co-localised i.e. at cellular locations where there is direct interaction between the EGFR and MET receptors since bound to the fluorescently labelled antibodies corresponding to these neighbouring fluorophores. Our results show that highest FRET efficiency between MET and EGFR occurred in $H1975^{L858R/T790M}$ cells. In contrast, significantly lower FRET efficiency was seen in the $H1975^{L858R}$ and $H1975^{WT}$ cells. These results demonstrate that EGFR and MET can interact directly at the cell membrane and that the level of interaction is significantly higher in $H1975^{L858R/T790M}$ compared to $H1975^{L858R}$ and $H1975^{WT}$ cells. Quantification for averaged data from multiple replicates is shown in Figure 4.4B.

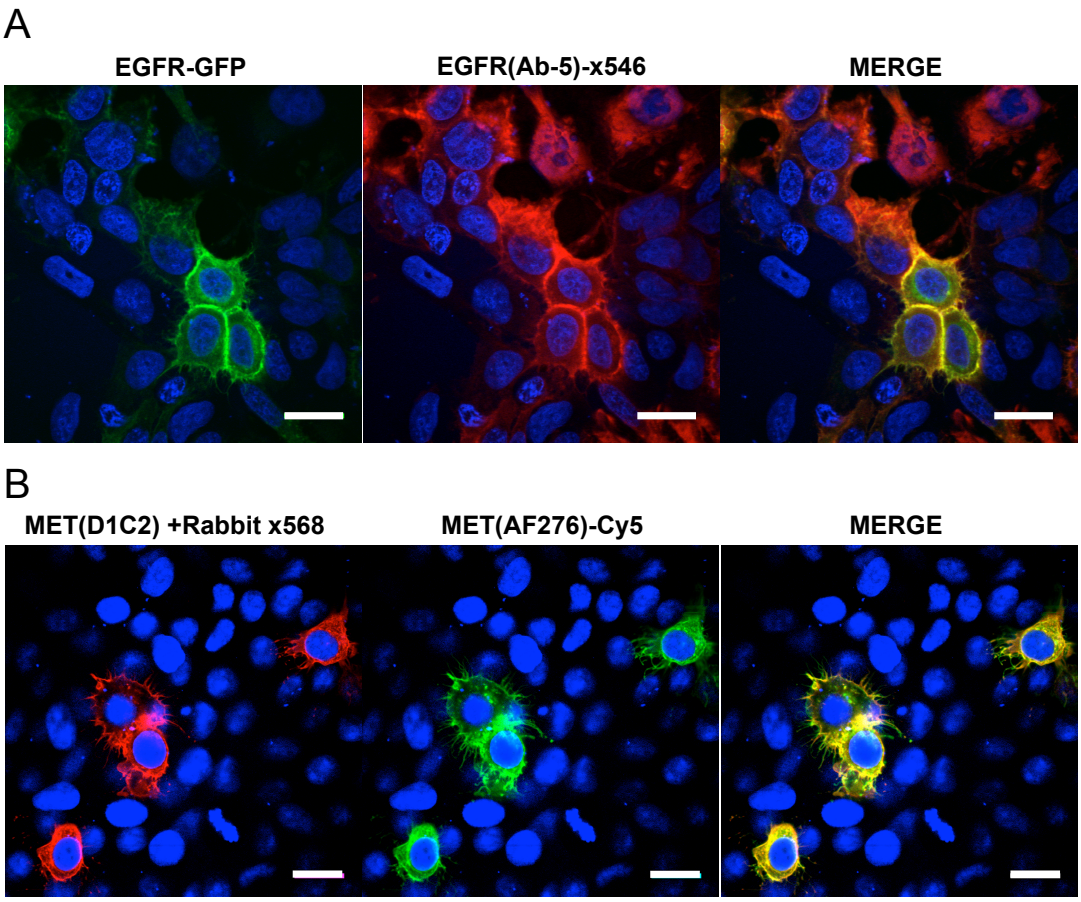

Figure 4.3. Validation of EGFR-MET FRET antibodies for *in vitro* use
Example antibody validation steps. MCF-7 cells, which lack endogenous EGFR/MET are shown transfected with EGFR-GFP or MET and exposed to fluorophore labelled antibodies against EGFR or MET respectively. Hoechst counterstain (blue) used to demonstrate cell nuclei. A) MCF-7 EGFR-GFP+ cells stained on coverslips with EGFR (Ab-5)-Alexa Fluor 546 directly labelled antibody. The first panel shows the green channel for GFP-containing EGFR construct. The red panel shows labelled antibody. Colocalised signal in yellow shows overlap confirming equivalent staining even after fluorophore labelling. B) MCF-7 MET+ cells stained on coverslips with MET (AF276)-Cyanine5 directly labelled antibody shows specific staining pattern confirmed by MET (D1C2) revealed with Rabbit secondary-Alexa Fluor 546. Scale bar, 20μm. Both EGFR and MET antibodies demonstrate specific staining unimpaired by fluorophore labelling.

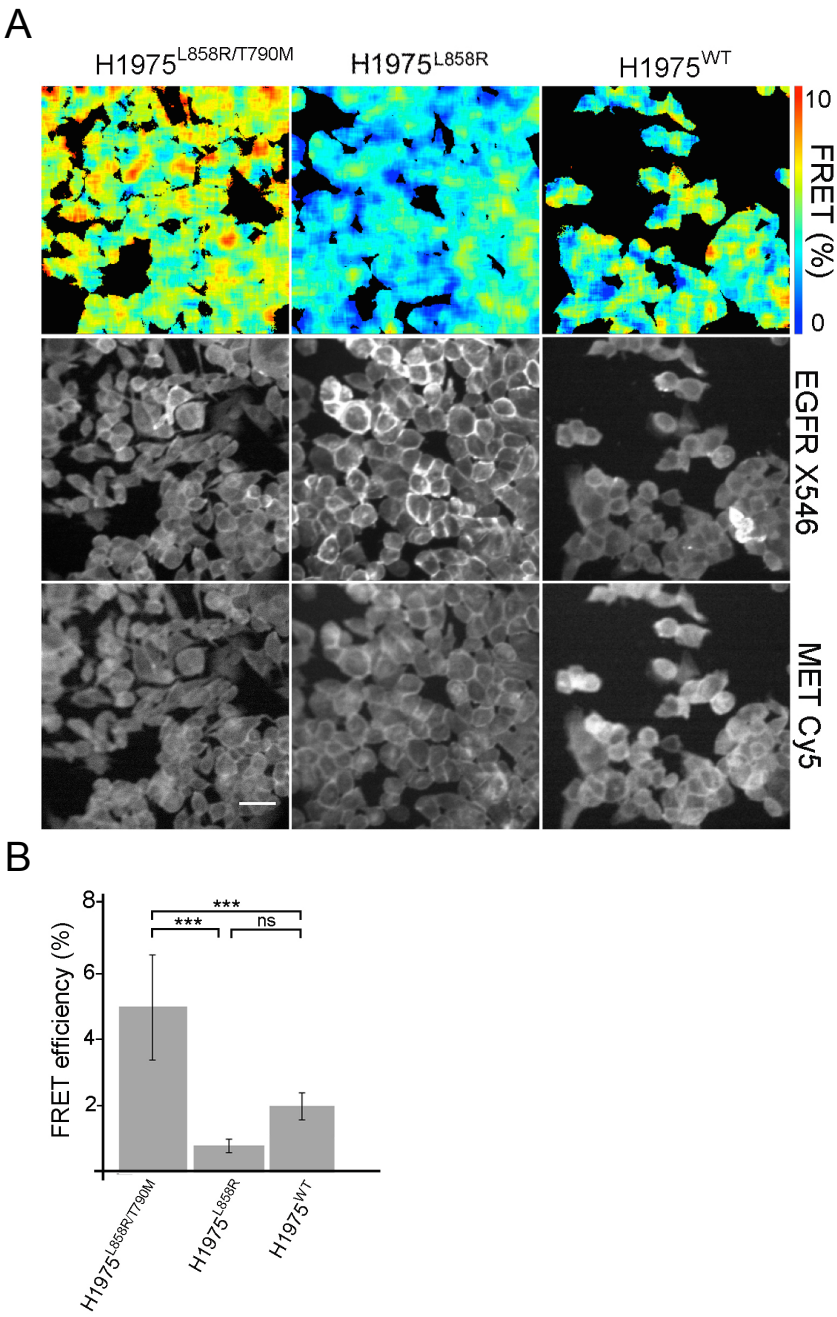

Figure 4.4. EGFR-MET binding *in vitro* vs. EGFR mutant status

A) Fluorescence lifetime imaging performed in the three H1975 derived cell lines plated to sub-confluence on coverslips. Representative pseudocolour lifetime images showing FRET efficiency accompanied by corresponding grayscale donor (EGFR-Alexa Fluor 546) and acceptor (MET-Cyanine 5) intensity images. Pseudocolour images demonstrate different patterns for each EGFR mutant. Scale bar, 50μm. B) Bar chart shows quantification of average FRET efficiency representing interaction between EGFR and MET in each of the cell lines. Interaction between EGFR and MET is greatest in $H1975^{L858R/T790M}$ and lowest in $H1975^{L858R}$. FRET measurement data obtained by time-resolved analysis in Tri2 for 3-5 fields of view per condition per experiment imaged. SEM bars shown (***p<0.0005, N=6). Quantification in Excel and GraphPad Prism.

4.2.4 SGX523 results in effective and sustained blockade of phospho-MET

Having demonstrated the importance of EGFR-MET interaction in our model, we wanted to explore the therapeutic effect of MET inhibition on the model and how it could differ according to the presence of EGFR mutants. We utilized SGX523, as a MET kinase inhibitor because of its extremely high specificity. Although not in clinical development because of renal toxicity, its selectivity ensured that we were manipulating MET without off-target effects and set about validating its activity in our models *in vitro* and *in vivo* (Buchanan, Hendle et al. 2009). In the first instance it was important to verify the efficacy of SGX523 in the blockade of MET phosphorylation. The western blots in Figure 4.5 show an increase in the intensity of the bands corresponding to MET phosphorylation from a basal state with the addition of its cognate ligand, Hepatocyte Growth Factor (HGF). Subsequently at all time points, there are no bands visible for phosphorylated MET once samples had been treated with SGX523. Corresponding lysates were electrophoresed and blotted to total MET antibody to confirm that MET was expressed in these samples and were equivalent between the conditions to allow appropriate comparison (Figure 4.5 A).

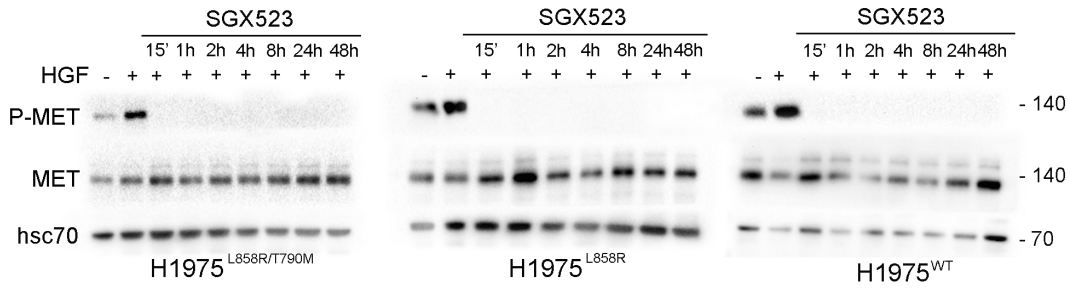

Figure 4.5. SGX523 effectively inhibits MET phosphorylation *in vitro*

WB of phospho- and total MET from cell lysates of the untreated H1975 derived cell lines treated with HGF (25ng/mL) for 15 min ± pre-treatment with SGX523 (5mM) for the indicated times. Phopshorylated (P-MET) and Total MET (140KDa) levels are shown in separate blots. Lanes with samples exposed to SGX523 are indicated by their respective time points. hsc70 was used as loading control (70KDa), N=2. Images prepared on the Biorad analyser, scanned with Biorad Image Lab. In these blots we can see that in all cell lines, HGF increased basal phospho-MET signal. SGX523 completely inhibited MET phosphorylation immediately and without recovery by 48h in all cell lines.

4.2.5 *In vitro* effects of MET inhibition on cell proliferation and migration

In order to assess the functional consequences of MET kinase inhibition, we assessed proliferative responses to drug treatment after 24h. We only observed a significant decrease in the proliferation rate after MET inhibition in H1975$^{L858R/T790M}$ cells (Figure 4.6) where the percentage of BrdU incorporating cells (red channel) was reduced. Representative images are shown and quantified in the bar graph. We found that the proliferation of H1975^{L858R} cells were not significantly inhibited by SGX523 in a BrdU incorporation assay, as evidenced (Figure 4.6) by a lack of change in the number of BrdU positive nuclei labelled by an anti-BrdU antibody with subsequent application of Alexa Fluor 546 conjugated secondary antibodies. In this figure we see that the percentage of red "proliferating" nuclei stained for BrdU, as a proportion of the number of all blue, Hoechst counter-stained nuclei is unchanged after treatment (Figure 4.6).

We also assessed proliferation in a 3D environment using an anchorage independent growth assay. In the presence of SGX523, there was a significant decrease in the number of colonies in the case of H1975$^{L858R/T790M}$ cells and in the number of large colonies in the H1975^{L858R} cells. SGX523 had no effect in the 2D or 3D proliferation rate in the case of the H1975^{WT} cells (Figure 4.6C). Total colony number reflects cell survival, whereas larger colonies as was the case of H1975^{L858R} suggest greater proliferation with large numbers of cell per colony. SGX523 therefore appears to be inhibiting different characteristics of the agar colony assay.

Finally, using a random migration experiment, we established that cell motility was reduced by MET inhibition but was only significant in H1975^{L858R} cells. H1975$^{L858R/T790M}$ cells demonstrated reduced random migration also after treatment with SGX523, but this was not significantly different to baseline. Representative rose blots and quantification shown in Figure 4.7.

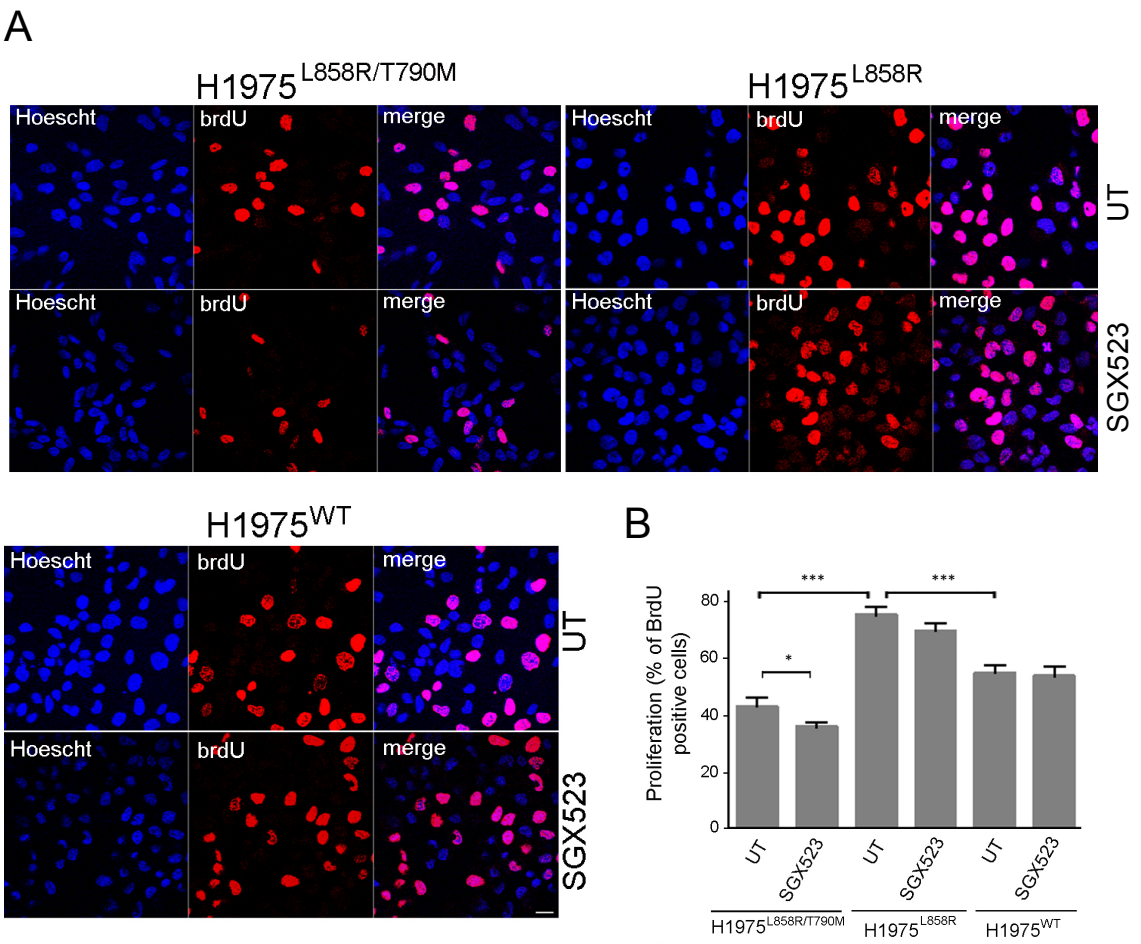

Figure 4.6. SGX523 inhibits proliferation in H1975$^{L858R/T790M}$ cells

BrdU Proliferation assay. A) Representative images of the three cell lines grown at 60% confluence on coverslips and treated or not with SGX523 for 24 hours. Scale bar, 20μm. BrdU positive nuclei (Anti-BrdU, Mouse Alexa Fluor 546) in the red channel show cycling cells, Hoechst dye is used a counterstain for all nuclei as a denominator (blue channel). B) Quantification was performed in ImageJ using a macro to count number of nuclei in red (BrdU +ve) versus blue (all nuclei) channels for 5-10 views per section, using a threshold approach to separate nuclei from background. Averages plotted as a percentage of BrdU +ve nuclei. H1975^{L858R} cells (top right panel) show the greatest % positive BrdU stained nuclei. Only H1975$^{L858R/T790M}$ cells however show significant inhibition of proliferation with SGX523 treatment as shown by the reduction in red stained nuclei and the quantification in the graph. SEM bars shown (*p <0.05, ***p<0.0001, N=5).

C

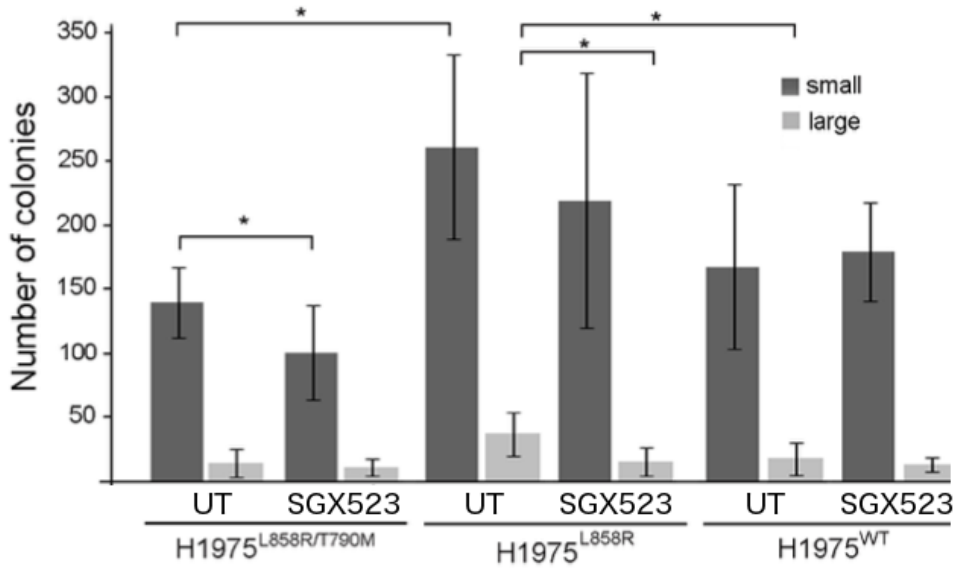

Fig 4.6. (ctd) SGX523 inhibits proliferation in H1975$^{L858R/T790M}$ cells

C) Anchorage-independent Agar Growth Assay. Soft agar colony formation in the H1975 derivate cell lines in the presence or absence of SGX523 (5μM). The graph shows the number of colonies after 3 weeks of growth. Quantification was performed in ImageJ using a macro to count number of colonies per field of view for 5-10 views per section, using a threshold approach to separate nuclei from background. Small colonies were defined as 100-1500μm circularity, and large colonies, >1500μm circularity. Number of colonies represents cell survival. Larger colonies suggest higher number of cell divisions/proliferation. Averages plotted. SGX523 treatment led to signficant reduction in small colony formation (dark grey) in H1975$^{L858R/T790M}$ cells. For large colonies (light grey), a signficant drug response was seen in H1975^{L858R} instead. SD Error bars shown (* p< 0.001 N=3). (Agar data kindly Provided by Dr. E. Ortiz-Zapater).

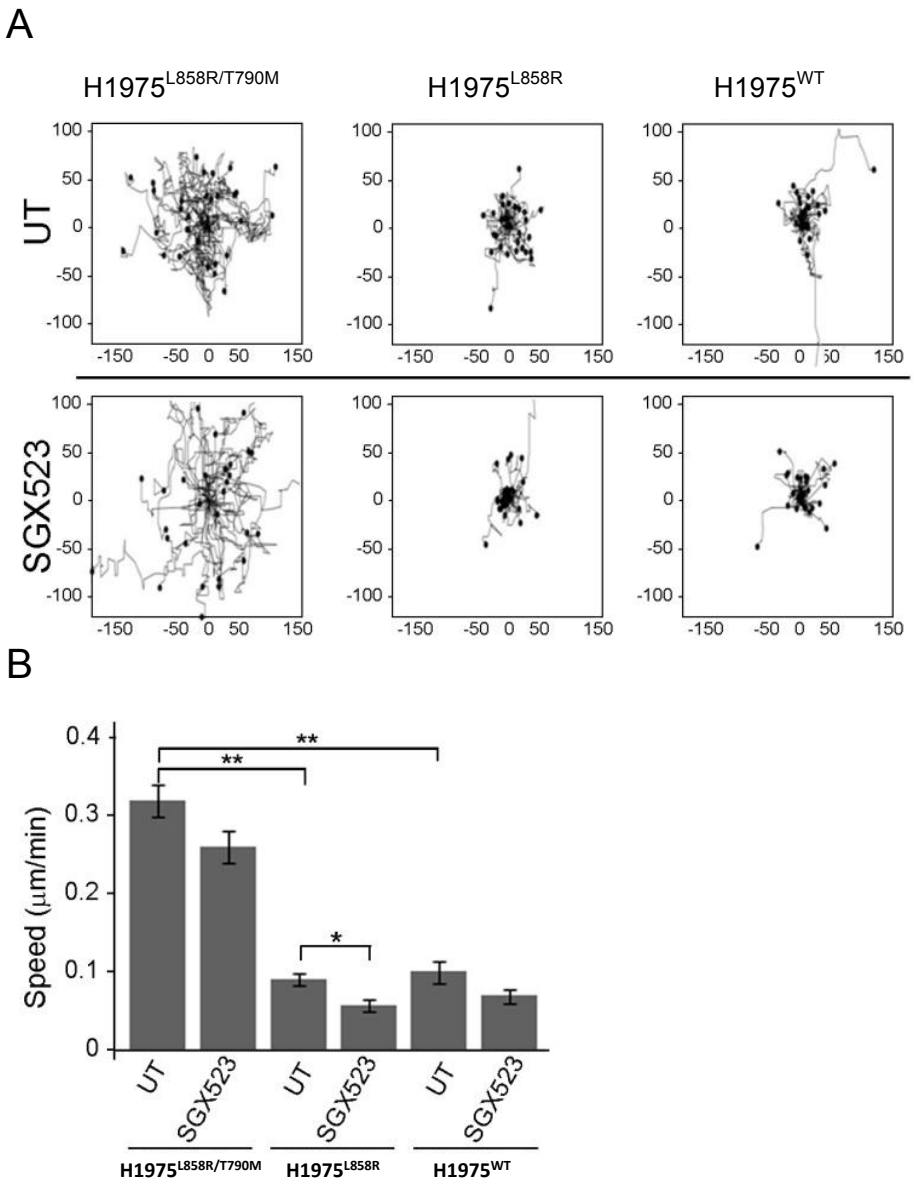

Figure 4.7. SGX523 inhibits random cell migration in H1975^{L858R}

A) Random migration assay of H1975 derived cells plated to low confluence in presence or absence of SGX523 (5μM) with timelapse microscopy >18h. Representative rose plots shown with tracks for all cells normalised to a common origin at the centre of the blot (velocity is μm/minute: x and y axis on plots are in μm. Tracks were made manually in ImageJ by isolating the centre of each cell of interest per frame and analysed by Mathematica notebook (3 fields of view, 10 cells per image). B) Bar graph showing speed quantification of random migration velocity. SD bars shown (*p<0.005, **p<0.0001, N=4). Greatest migrational velocity is shown by longer tracks as in the case of the H1975$^{L858R/T790M}$. Greatest change in track length were noted in the H1975^{L858R} cell line and hence were considered the most responsive to SGX523 in terms of migration.

4.2.6 Inhibition of MET changes the EGFR-MET interaction *in vitro*

In view of the observed differences in the interaction between MET and EGFR in our cells resulting from the *EGFR* mutations at baseline, we hypothesised that MET inhibition would alter the interaction between EGFR and MET in the different mutant cell lines. To test this we measured the changes in the interaction between MET and EGFR using FRET-FLIM, before and after MET inhibition by SGX523 (see Figure 4.8) As is demonstrated in the quantification of average FRET across all pixels, we found that the interaction between MET and EGFR in H1975$^{L858R/T790M}$ cells was significantly reduced in the presence of SGX523 (see Figure 4.8A and B). This is represented by the heat map images where the FRET interaction is changed from a predominantly high FRET, red pixel dominated image to a predominantly low FRET, blue pixel dominated image in the treated cells. By contrast, in the H1975^{L858R} cells, SGX523 led to a significant increase in EGFR-MET interaction compared to baseline, shown in the representative images as a switch from a blue heat map than the red treated heat map. There was no significant difference in the FRET between MET and EGFR before/after SGX523 treatment in the H1975^{WT} cells which had generally low FRET values, shown in the representative images as blue pixels. The intensity images (grayscale) show the EGFR and MET staining alone to confirm accurate staining of EGFR/MET. These FRET results provide evidence to support the hypothesis that MET kinase inhibition by SGX523 altered the direct interaction between MET and EGFR in a mutation-specific manner in these cells.

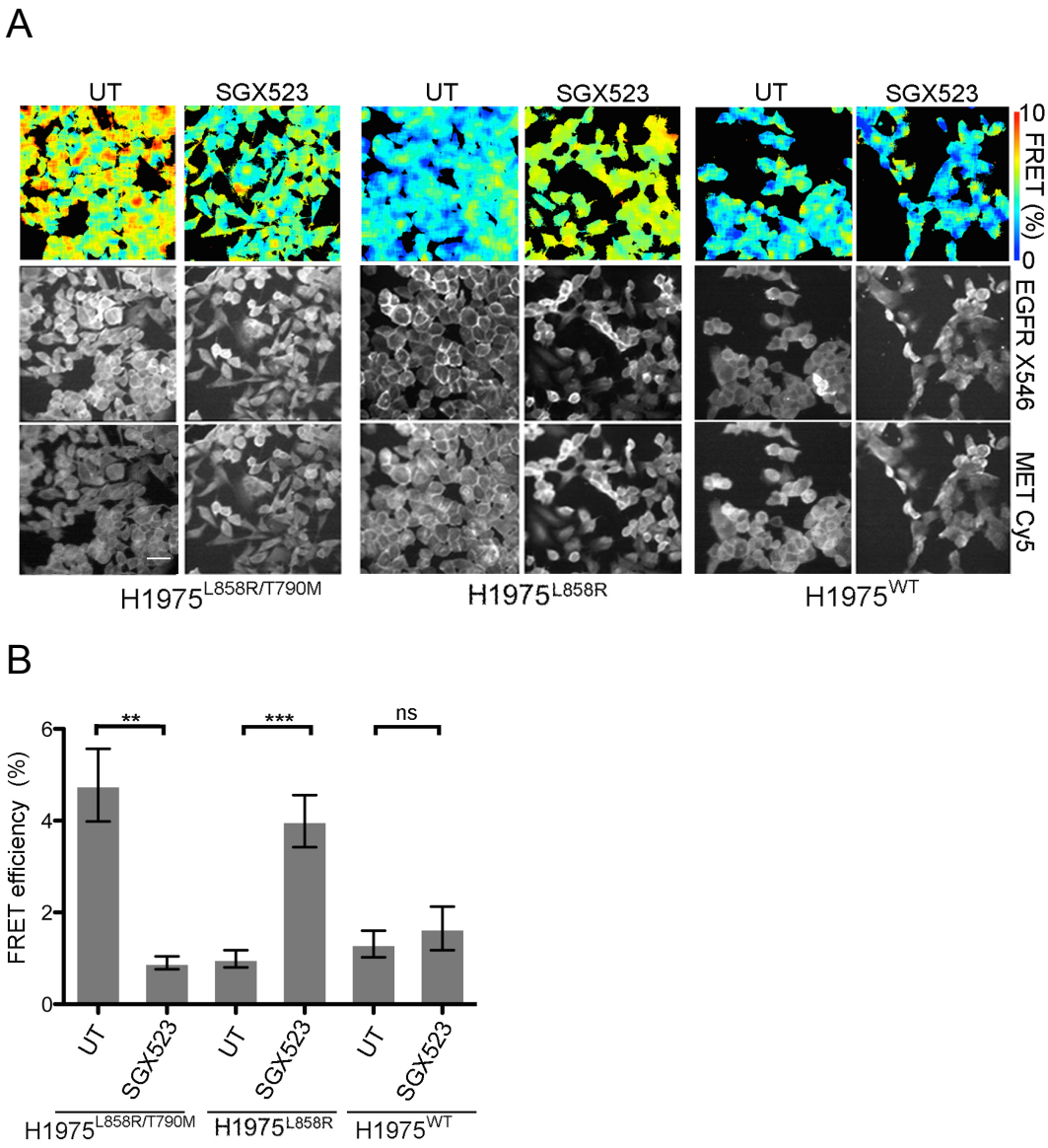

Figure 4.8. SGX523 changes the EGFR-MET interaction *in vitro*

A) Fluorescence lifetime imaging performed in the three H1975 derived cell lines plated to subconfluence on coverslips with or without treatment with SGX523 (5μM) for 24 hours. Representative pseudocolour lifetime images with FRET efficiency accompanied by corresponding grayscale donor (EGFR-Alexa Fluor 546) and acceptor (MET-Cyanine 5) intensity images are shown. Scale bar, 50μm. B) Bar chart showing quantification of average FRET efficiency of EGFR-MET interaction performed in H1975 derived cells in presence or not of SGX523. Interaction between EGFR and MET is reduced with SGX in H1975$^{L858R/T790M}$ and increased in H1975^{L858R} as in seen in the heat maps: becoming more blue (less FRET) or more red (more FRET) in line with the EGFR-MET dimer quantification. FRET measurement data was obtained in Tri2 for 3-5 fields of view per condition per experiment imaged. SEM bars shown (**p=0.001, ***p<0.0005, N=6). Quantification in Excel and GraphPad Prism. The variation indicated by the SEM highlights the consistent nature demonstrated by the data across multiple experiments.

4.2.7 Oral administration of SGX523 results in effective and sustained blockade of MET phosphorylation *in vivo*

To test whether the differential effects of SGX523 on MET and EGFR interaction could be reproduced *in vivo*, we utilised the xenograft model based on the H1975-derived mutant cell lines. $H1975^{L858R/T790M}$, $H1975^{L858R}$ and $H1975^{WT}$ cells were injected into the flanks of immunosuppressed BalbC mice and tumours were allowed to grow for 2 weeks. Mice were then subjected to 12 days of treatment with SGX523 or vehicle alone, administered daily by oral gavage. Figure 4.9 demonstrates timings of drug administration. The intention of this part of the *in vivo* study was to obtain tumour tissue from murine xenografts grown in the presence of SGX523 or mock treatment for each mutant and to be able to compare their growth and biology.

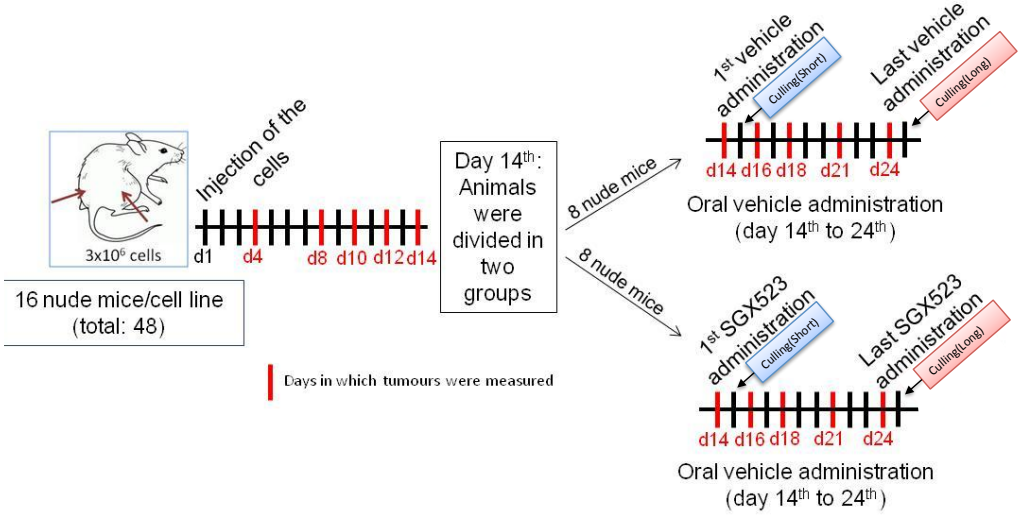

Figure 4.9. Time-line schematic of the murine *in vivo* model.
Red bars indicate days of tumour measurement. The time-line divides on day 14 to represent initiation of treatment and separation of mock versus treatment mice. Vehicle or SGX523 were administered by gavage daily. See Chapter 2 Methods and figure legends for details about tumour numbers in individual experiments.

Target tissue drug delivery was confirmed by WB and immunohistochemistry (IHC). A band at 140KDa corresponding to phosphorylated MET was visible in lysates coming from xenograft tumour specimens in the untreated cohort but not in the SGX523 treated samples (Figure 4.10A). Phospho-MET immunostaining of xenograft tumours from each group also confirmed loss of phospho-MET signal in SGX523 exposed mice only suggesting that the drug was delivered effectively to the tumours with complete and sustained suppression of MET phosphorylation (Figure 4.10B).

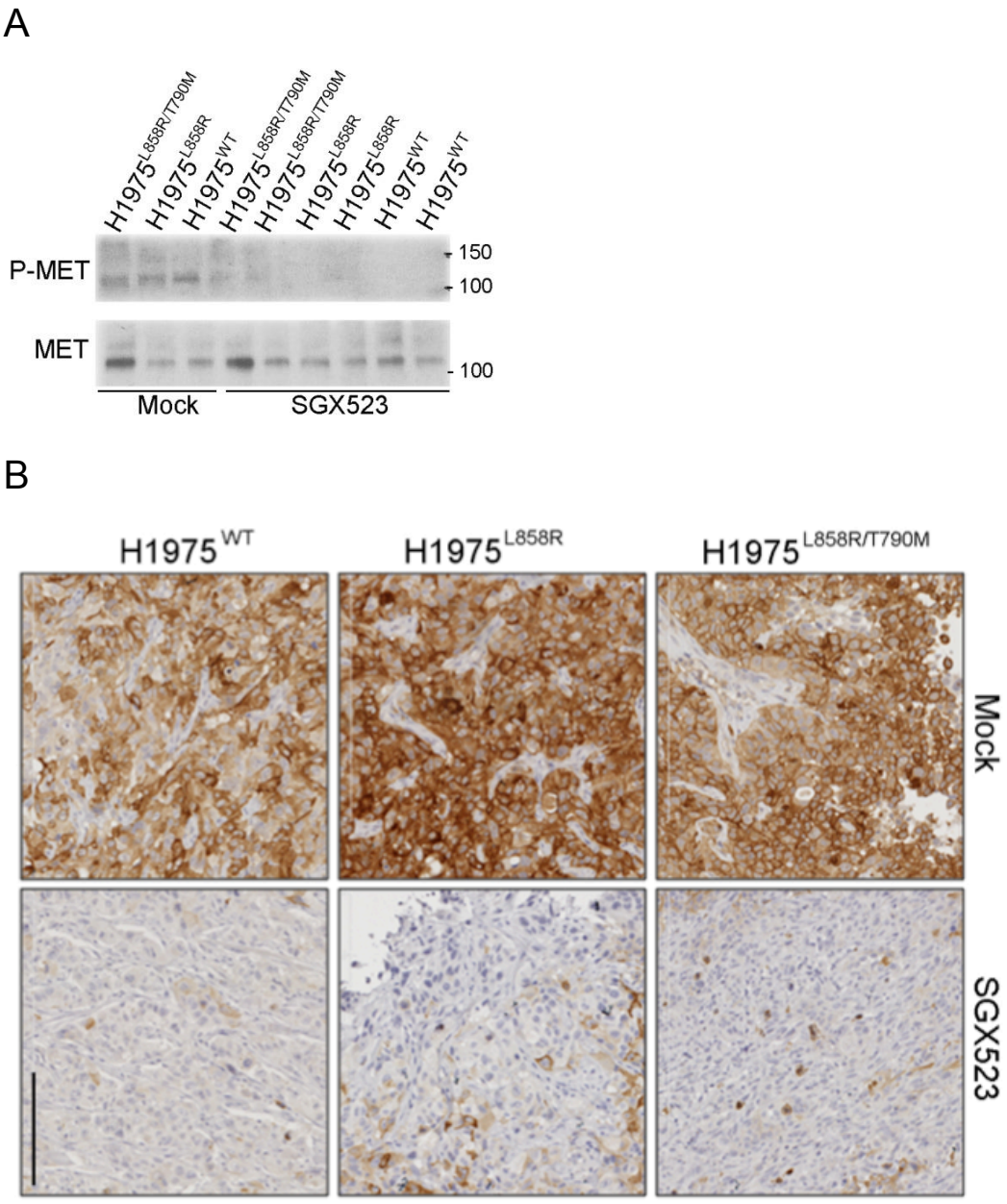

Figure 4.10. SGX523 effectively inhibits MET phosphorylation *in vivo* and reaches xenograft tumours when administered by gavage

A) WB of phospho- and total-MET in xenograft tumourlysates grown from each of the H1975 cell lines. Vehicle (mock) or SGX523 treated mice (60mg/kg) were used as indicated. B) Representative images of phospho-MET staining, in xenografts tumors grown from each H1975 derivate cell line coming from mice treated with vehicle (mock) or SGX523 as indicated. Scale bar, 250μm. The phospho-MET WB bands (2 samples per tumour type) and strong brown staining of the phospho-MET immunohistochemistry were convincingly eliminated by treatment with SGX523 confirming target tissue delivery.

4.2.8 *In vivo* effects of MET inhibition on tumour growth/proliferation

We then analysed the *in vivo* effect of oral administration of SGX523 on tumour growth and proliferation. Tumour volumes were measured every two days to establish whether there was a direct effect arising from the treatment compared between groups. This is shown in the linear graph of relative tumour growth normalized for each tumour type to 1 (Figure 4.11A). As was the case for the cells *in vitro*, The $H1975^{L858R/T790M}$-derived tumours in SGX523 treated mice grew more slowly (lower line) than in vehicle treated mice (upper line); this effect was evident after 4 days of SGX523 administration and was sustained up to 14 days, where continued separation of the growth curves were seen. $H1975^{L858R}$ and $H1975^{WT}$derived tumours lacked significant SGX523 responses over the 14-day growth period with both growth lines being closely apposed. This result was confirmed using a phospho-Histone H3 antibody and HRP developing (brown stained nuclei) as shown in (Figure 4.11B). As shown in the quantification, the proportion of phospho-histone H3 positive nuclei being significantly reduced after SGX523 treatment is only seen in the $H1975^{L858R/T790M}$ xenografts.

4.2.9 *In vivo* effects of MET inhibition on the tumour microenvironment

To characterise the differences in response to SGX523 between the tumour xenografts further, we compared haematoxylin and eosin (H&E) staining in the mock and SGX523-treated groups for each of the three xenograft tumours types. As per the quantifications, we observed significant reduction in staining for collagen by Masson's trichrome (MT) in $H1975^{L858R}$ as evidenced in the representative images by a reduced percentage of tumours with green collagen fibres between the cells (Figure 4.12A). Consistent with this, α-SMA was also significantly reduced in $H1975^{L858R}$. In this case the representative images show stromal tissue stained brown in a similar pattern to the MT images (Figure 4.12B). Finally the cd31 staining, which indicates endothelial cells in newly formed vessels, i.e. neo-angiogenesis (Figure 4.13) was also significantly reduced in the $H1975^{L858R}$ in the SGX523 treated tumours. A drug effect was not observed in the other xenografts for any of these three stains.

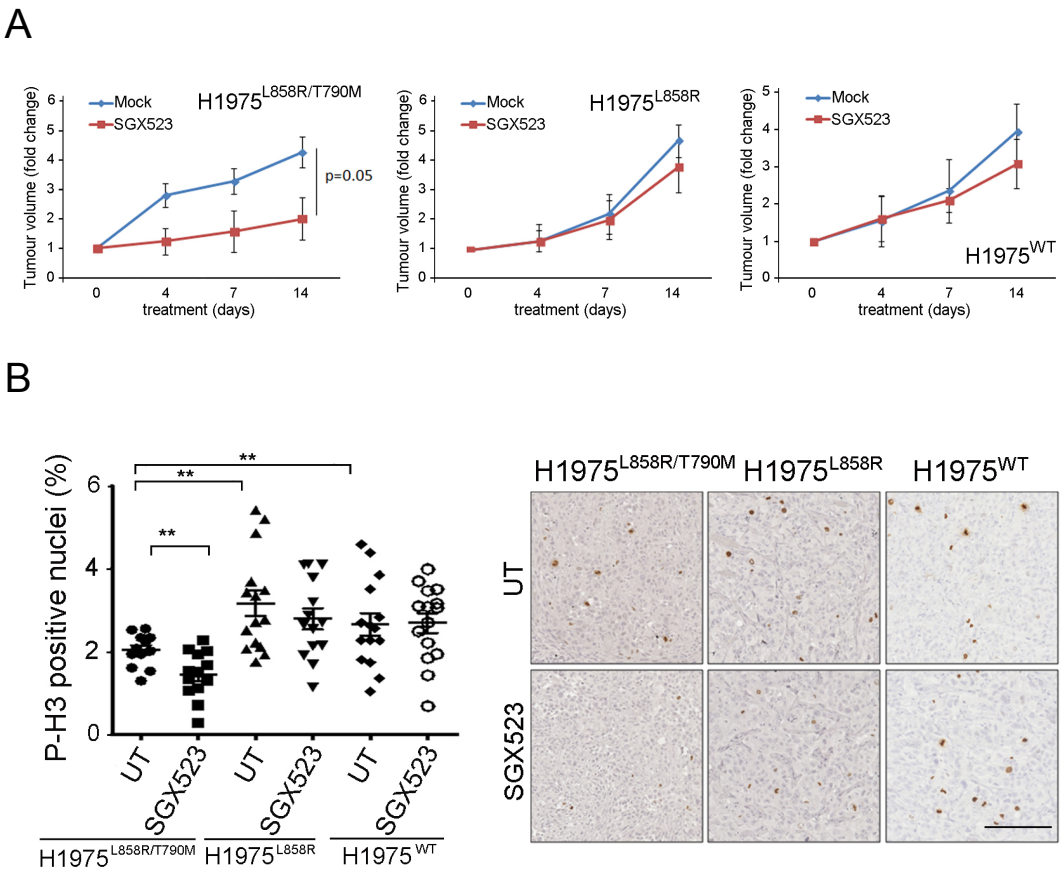

Figure 4.11. *In vivo* effects of MET inhibition on cell proliferation

Xenograft tumour growth curves. $3x10^6$ cells were injected into both flanks of immunocompromised BALB/c nude mice and tumours allowed to grow for 14 days at which point administration of SGX523 (60mg/kg) or mock vehicle was commenced. N=16 tumours (8 mice, bilateral tumours) per condition. A) Graphs showing the fold change in volumes in the xenografts tumours coming from the three H1975 derived cell lines during the 12 days of treatment. Tumours were measured at the indicated times using a calliper and volumes calculated ($0.4xAxB^2$ where A=long axis and B=short axis of the tumour). SD bars shown. N=8-10 tumours per condition. We can see separation of the growth curves in $H1975^{L858R/T790M}$ suggesting SGX523 treatment effect in terms of proliferation in this cell line only. B) Quantification and representative images of tumour immunohoistochemistry for phospho-histone H3 (P-H3) of xenografts tumours coming from each H1975 derived cell line in the presence or absence of SGX523. Quantification was performed in ImageJ using a macro to score % threshold area (brown staining in representative image) in relation to background tissue for 6-10 views per section. Again there was more phospho-Histone H3 staining in $H1975^{L858R}$ tumours suggesting greatest % of proliferating cells. This was significantly reduced by SGX523 in $H1975^{L858R/T790M}$ tumours. Averages and SEM bars shown (**p<0.05). N=12-15 tumours per condition. phospho-Histone H3 stained brown for actively proliferating cell nuclei. Scale bar, 250µm.

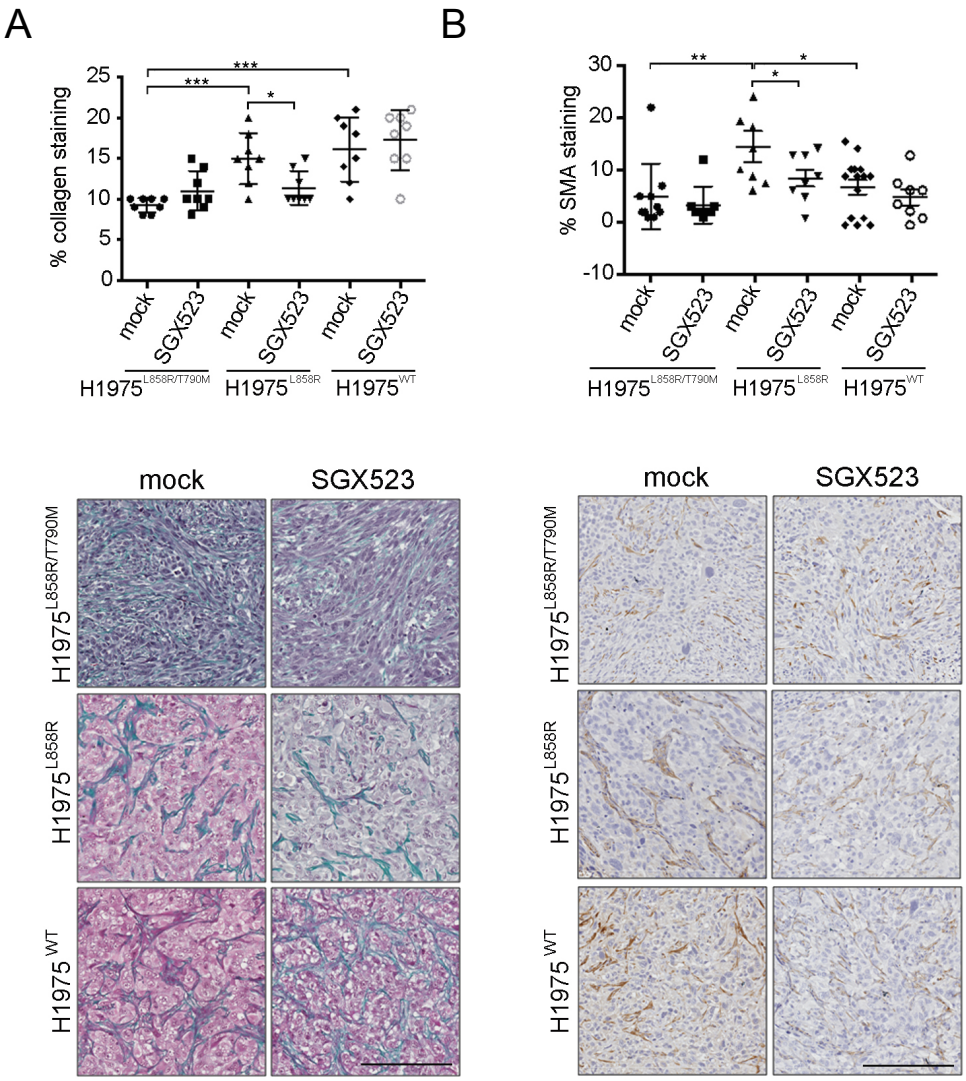

Figure 4.12. *In vivo* effects of MET inhibition on stroma remodelling
Xenograft immunohistochemistry from H1975-derivate mice treated with SGX523 or mock vehicle. Quantification and representative images shown for (A) Masson's trichrome (collagen stains green) and (B) α-smooth muscle actin (α-SMA) staining of xenografts tumours. Quantification of the staining is shown above the images in plots from Prism Graphpad. For Masson's trichrome, dominance of collagen-rich features in $H1975^{L858R}$ were scored to be highest by a consultant histopathologist (MM). Averages plotted using Prism Graph Pad. α-SMA quantification was performed in Hamamatsu Nanozoomer software according to % staining (brown staining in representative images) in relation to background tissue. Both markers of stromal deposition were significantly reduced in $H1975^{L858R}$. N=8 Tumours per condition. A) SD; B) SEM, *p<0.05, **p<0.01, ***p<0.001). Scale bar, 250 μm.

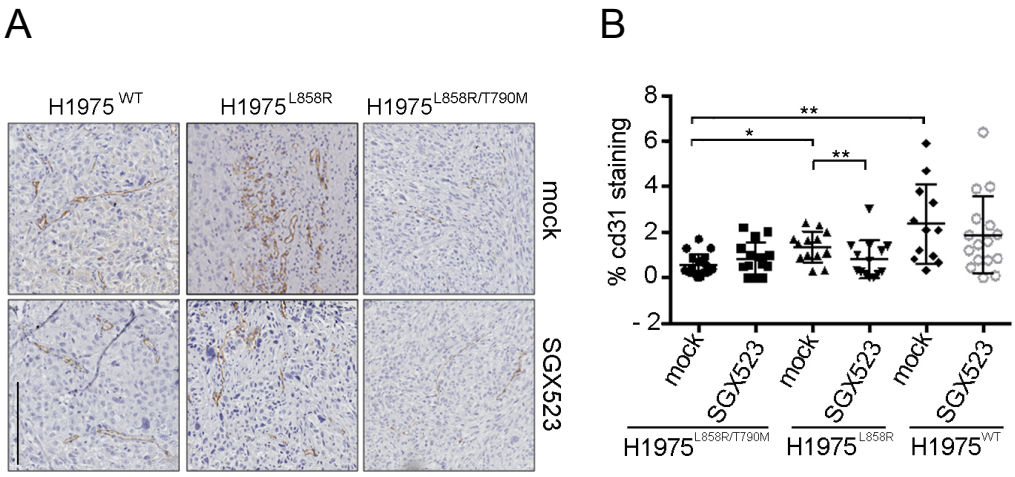

Figure 4.13. *In vivo* effects of MET inhibition on vascularisation
Xenograft immunohistochemistry from H1975-derivate mice treated with SGX523 (60mg/kg) or mock vehicle. Representative images and quantification shown for CD31 staining of xenografts tumours (FFPE). CD31 staining (brown) indicates neovascularisation. Scale bar, 250 μm. Quantification was performed in ImageJ using a macro to score % threshold area (brown staining in representative image) in relation to background for 6-10 views per tumour. Averages and SEM bars shown (*p<0.05, **p<0.01). CD31 indicating neovascularisation was significantly reduced in $H1975^{L858R}$ only. More heterogeneity for this marker was seen in $H1975^{WT}$ tumours. N=16 tumours per condition.

4.2.10 Validating an EGFR-MET FRET assay *in vivo*

We subjected the FRET antibodies validated earlier in this chapter (Section 4.2.3) to assessment in FFPE tissue. This is necessary since there is a high degree of autofluorescence in this tissue type and increase care required for antigen retrieval, both of which can impinge on FRET signal. Although the MET (AF276) antibody could be demonstrated to provide specific staining in FFPE prepared tissue (Figure 4.14), the staining intensity in FFPE specimens was considered unfavourable for successful detection of FRET with the pre-existing *in vitro* pair and hence an alternative strategy was sought. We hence determined an alternative pair of antibodies, both of which were intracellular. The first was the MET (D1C2) antibody, which had been recommended to us before by the histopathologist (MM) for other MET tissue staining within the group (seen in indirect staining in Figure 4.3). This was employed alongside an EGFR (Ab-15) antibody recommended by Professor Ng also previously utilised within his laboratory.

A customised azide/BCA-free preparation of the MET (D1C2) antibody was obtained from the manufacturer and separate aliquots labelled with Alexa Fluor 546 or Cyanine 5 dyes to establish whether the EGFR-MET pair would perform most reliably with MET as the donor or acceptor. Labelling reactions were undertaken with assistance of Dr Weitsman who also provided advice on modification to the antigen retrieval method (See Chapter 2 Methods) to provide enhanced staining of FFPE specimens with the FRET antibodies.

Figure 4.15 demonstrates staining of a mouse xenograft section from the mock group. Both EGFR (Ab-15) and MET (D1C2) provided adequate staining of FFPE prepared xenograft tissue. A low concentration of donor antibody in the presence or absence of an excess of acceptor was designed as is typical of FRET experiments. It was seen that the staining intensity of the EGFR (Ab-15) donor-pair was most favourable with the concentrations as specified and EGFR (Ab-15)-Alexa Fluor 546 selected as preferred donor and its concentration titrated accordingly against staining appearances in the Cy3 channel and FRET efficiency (see Figure 4.16).

A

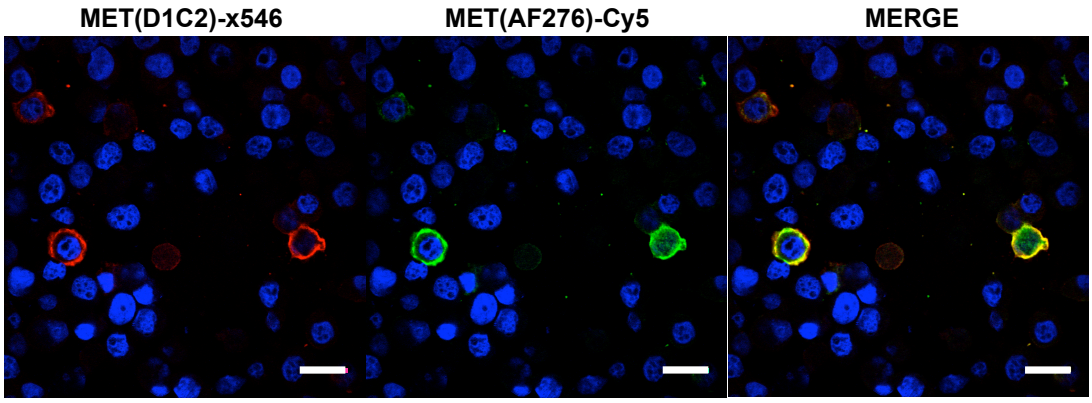

Figure 4.14. Directly labelled antibodies remain specific on FFPE MCF7 pellet
Antibody validation compared unlabelled and labelled antibody for use in FRET. MCF-7 cell pellet (FFPE) shown has been transfected with MET. Hoechst counterstain (blue) used to demonstrate cell nuclei. MCF-7 MET+ cells co-stained with MET (D1C2)-Alexa Fluor 546 (red channel) and MET (AF276)-Cyanine 5 (green channel) respectively. Co-localised signal (yellow) seen in merged channel shows that the antibodies retained specificity for MET on the FFPE processed cells. Scale bars, 20μm.

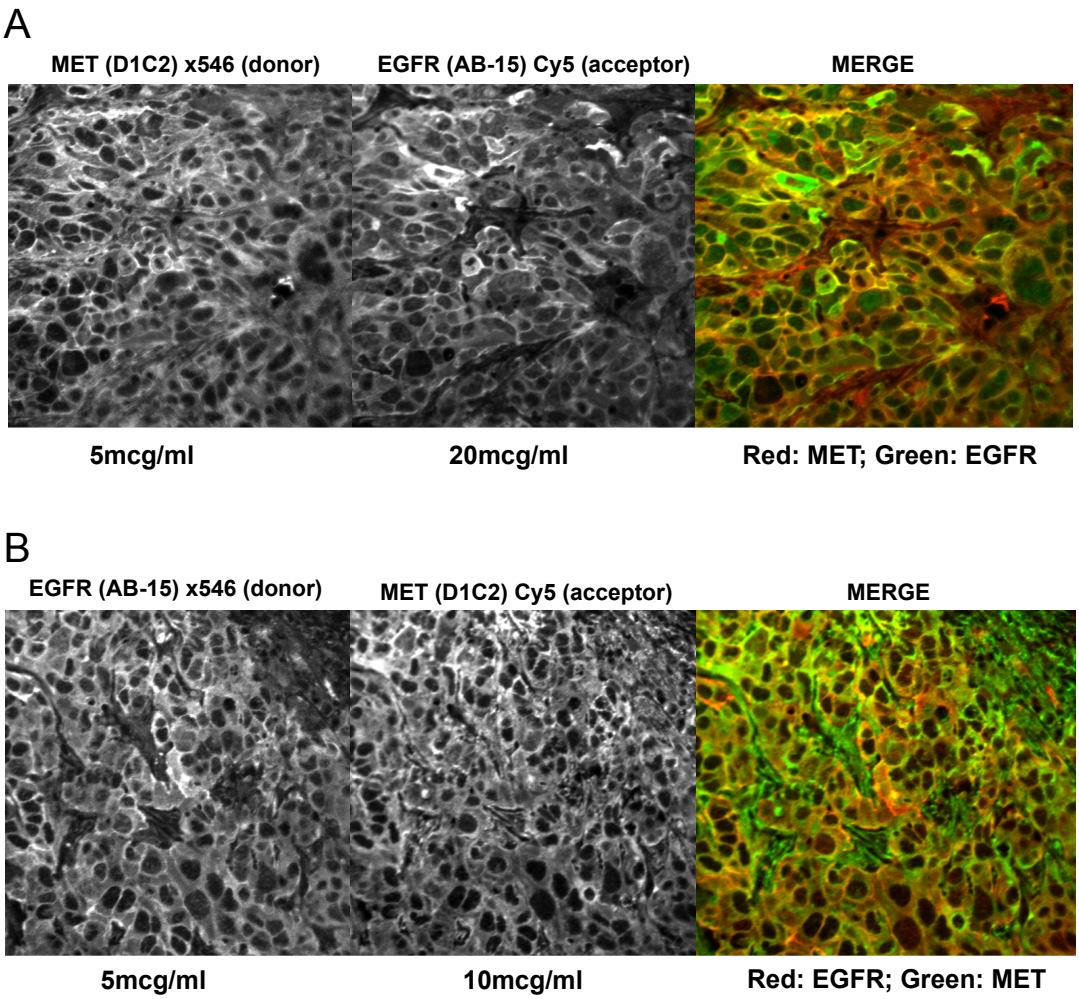

Figure 4.15. Donor:Acceptor staining intensity for EGFR vs MET donor in xenograft tumours (FFPE specimens)

Example antibody titration steps. Example intensity images in Cy3 and Cy5 chanels for specified antibody combinations for a donor and acceptor pair of labelled antibodies against EGFR and MET. A) MET Donor: MET (D1C2)-Alexa Fluor 546 (red channel) and EGFR (Ab-15)-Cyanine5 (green channel) versus B) EGFR Donor: EGFR (Ab-15)-Alexa Fluor 546 (red channel) and MET (D1C2)-Cyanine 5 (green channel) staining within FFPE processed murine xenograft tumours at the antibody concentrations specified. EGFR and MET Co-localisation is shown (yellow) in merged channels with good quality staining that would be consistent with that expected for each antibody. The epifluorescence images at these concentrations would be appropriate for FRET. Acceptor antibody is always required in excess. Imaging intensity for the combination in B was favourablle, with greater intensity even with lower concentrations of acceptor antibody.

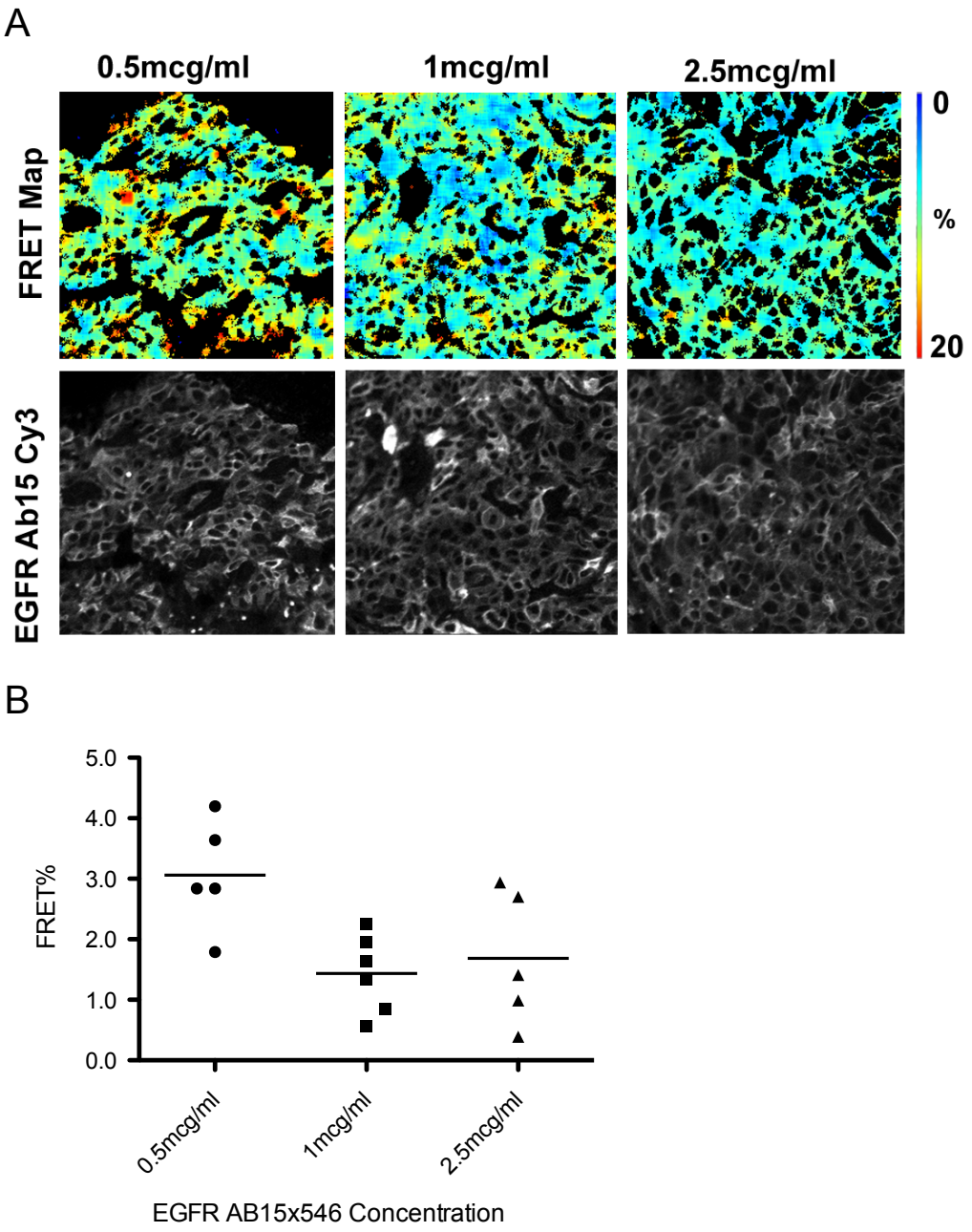

Figure 4.16 Optimising donor antibody concentration antibody *in vivo*
A) Representative FRET heat maps and grayscale images shown for Donor EGFR (Ab-15)-Alexa Fluor 546 staining in xenograft FFPE in presence or absence of dual staining with acceptor MET (D1C2)-Cyanine5. B) Quantification of FRET efficiency in the xenograft tumours at the donor antibody concentrations specified. Both show staining that favours the cell membranes with co-localisation (yellow) in merged channels. Acceptor antibody was used at 10mcg/ml. $P<0.05$ (0.5 vs 1mcg/ml). N=5 points per condition. Each point represents FRET efficiency from the average of pixels in one field of view.

4.2.11 Inhibition of MET changes the EGFR-MET interaction *in vivo*

We observed very similar results in the FRET assay optimized for use in the xenograft tissues (Figure 4.17) as we had in the *in vitro* data (Figure 4.8). These samples were different from the *in vitro* cells on coverslips in that they required processing to exclude autofluorescence both in terms of the methodology and also in a requirement for tri-exponential imaging to mask autofluorescence with an algorithm to exclude extremely low lifetimes correlating to such autofluorescence rather than that of the donor fluorophore. Again we observed the highest FRET between MET and EGFR in $H1975^{L858R/T790M}$ derived tumours, and this was again significantly reduced by SGX523 as reflected by a similar colour change from red to blue heat map pixels. In $H1975^{L858R}$ derived tumours, MET-EGFR interaction at baseline was low and increased significantly by SGX523. There was no significant FRET change in xenograft tissue derived from $H1975^{WT}$ cells. The FRET results were within narrow standard errors reflecting increased uniformity in the tumour sample lifetime readings coming from the xenografts (Figure 4.17).

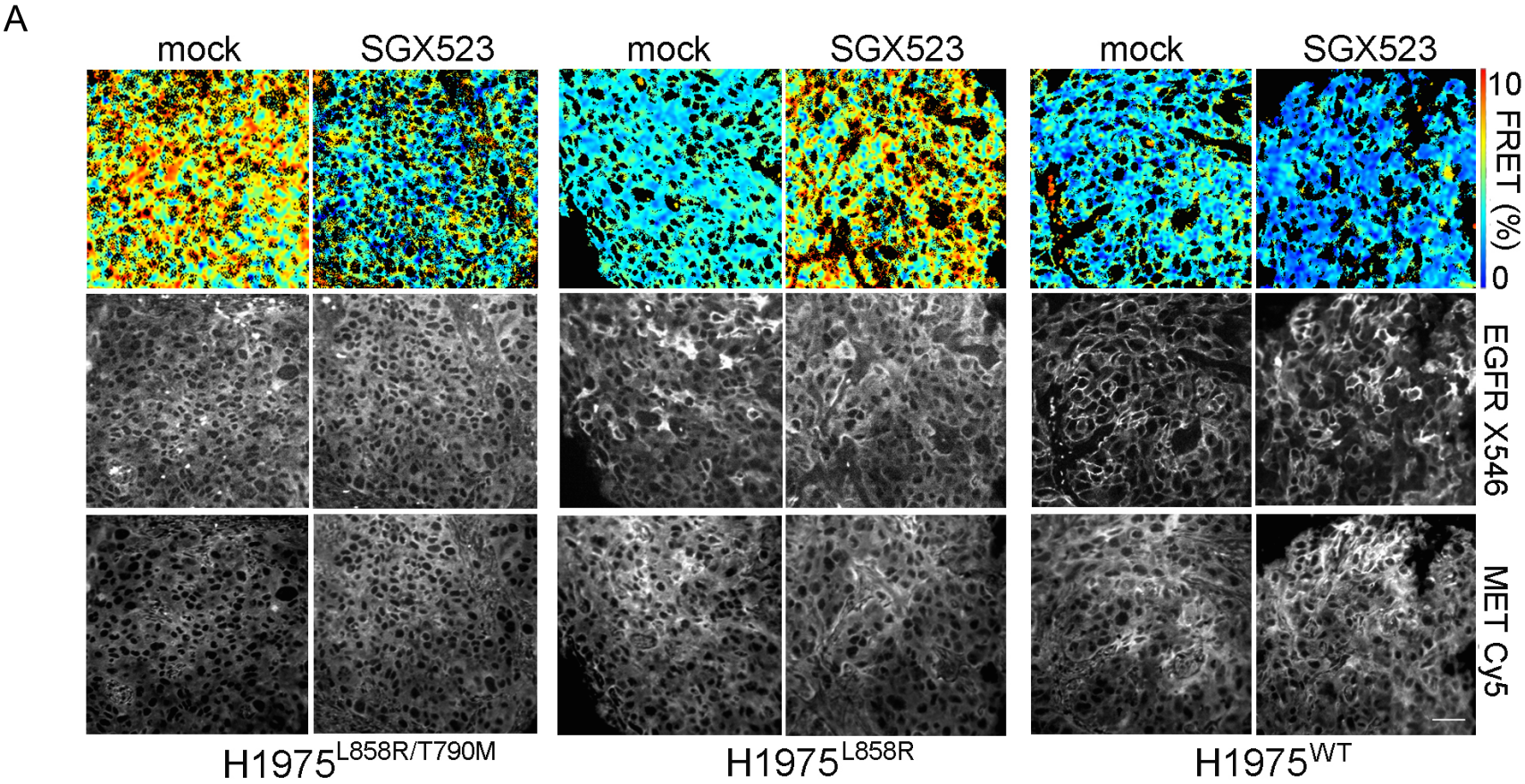

Figure 4.17. SGX523 changes the EGFR-MET interaction *in vivo*

A) Representative lifetime images for EGFR:MET FRET in xenograft tumours accompanied by corresponding grayscale donor (EGFR-Alexa Fluor 546) and acceptor (MET-Cyanine 5) intensity images. Red areas on the heat map correspond to high FRET and blue areas to low FRET. In $H1975^{L858R/T790M}$ we see a change to a more blue image with loss of EGFR-MET interaction with SGX523 and the blue heat map in $H1975^{L858R}$ becomes more red consistent with formation of an EGFR-MET dimer. Scale bar, 50μm.

B

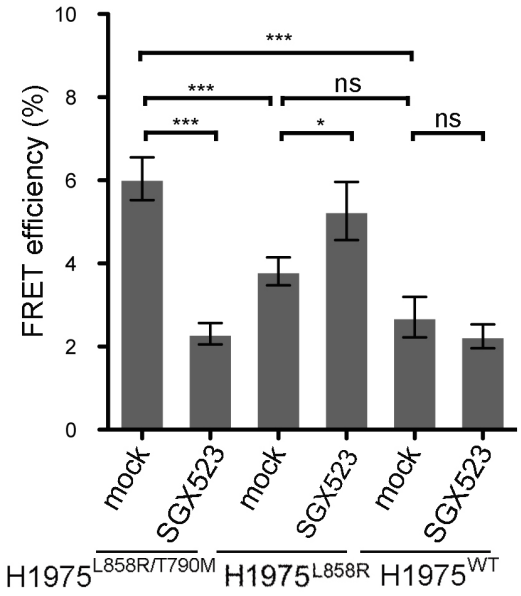

Figure 4.17. SGX523 changes the EGFR-MET interaction *in vivo* (Continued)
B) Quantification of average FRET of EGFR-MET interaction performed in xenograft tumours from each H1975 cell line in mice receiving mock or SGX523 treatment for 12 days. FRET efficiency is a quantitative measure of EGFR:MET interaction. Approximately 30 data points (within 4-6 tumours) per condition per experiment were imaged. SGX523 decreased FRET in $H1975^{L858R/T790M}$ and increased FRET in $H1975^{L858R.}$ Average and SEM bars shown (* $p<0.05$, *** $p<0.001$ N=2).

4.2.12 EGFR-MET FRET can be detected in human FFPE biopsies.

Finally we performed a brief validation of our FRET EGFR-MET assay in human tissue bank lung cancer biopsy specimens to establish if such an assay could be used to detect a FRET signal in human samples. Time and resource constraints prevented an extensive comparison of different samples but this proof of principle experiment demonstrated that FRET could be detected in human tumour samples that had been processed routinely by FFPE and stored in a tissue biobank. A range of FRET values were obtained within each tumour and between different tumours likely representing intra-tumoural and inter-patient heterogeneity. The range is demonstrated both in FRET but the demonstration of consistent donor lifetimes between different specimens is supportive of a robust assay with consistent performance of the assay across these intra- and inter-tumoral difference. The FRET results were similar for three tumours although the FRET pattern within each differed, likely indicating intra-tumoral heterogeneity (Figure 4.18).

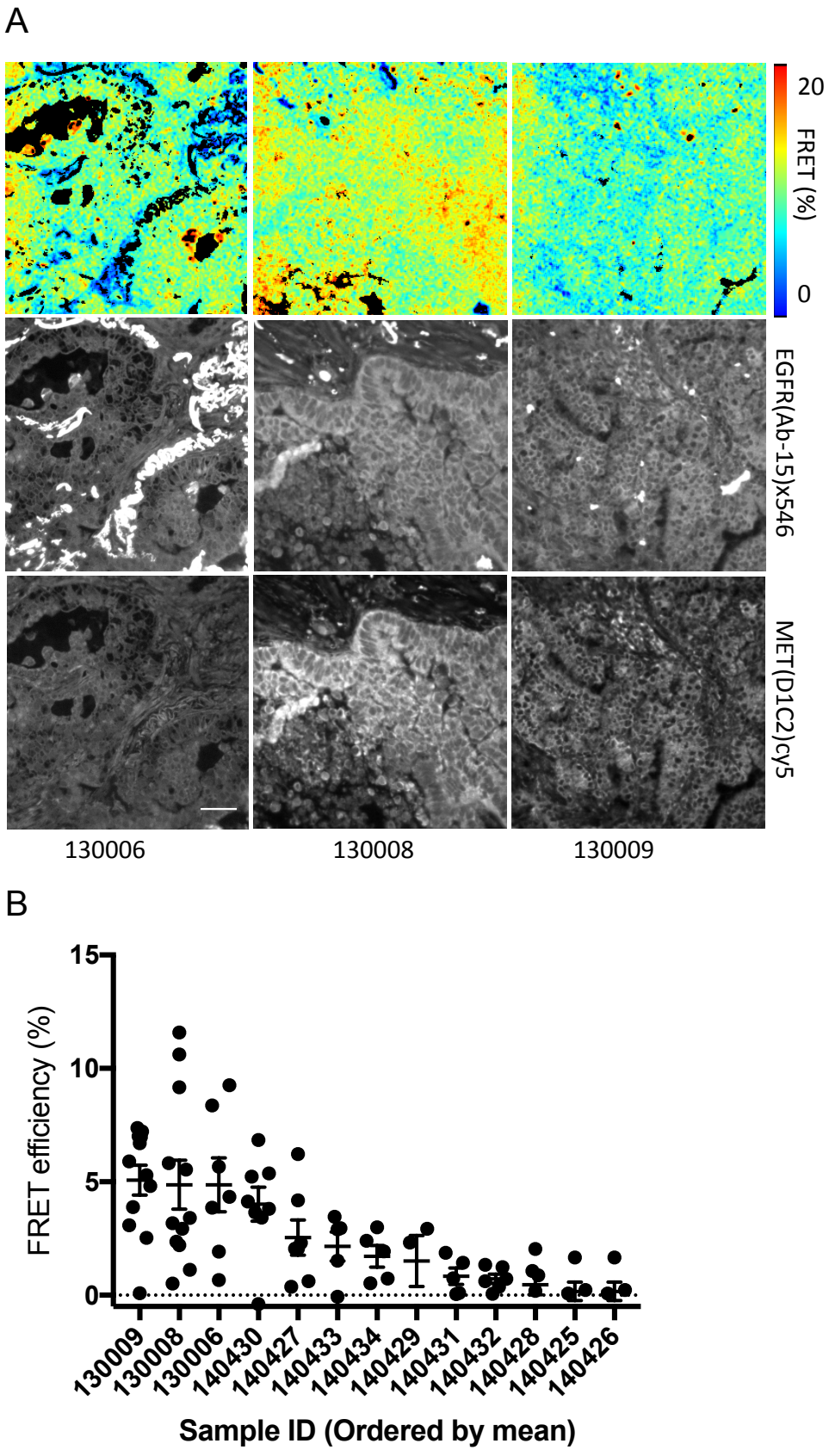

Figure 4.18. Proof-of-principle for EGFR-MET FRET assay in patient derived human lung cancer tissue bank specimens (FFPE)

Figure 4.18. Proof-of-principle for EGFR-MET FRET assay in patient derived human lung cancer tissue bank specimens (FFPE)
A) Representative FRET lifetime images for EGFR:MET FRET in three tissue biobank patient tumours accompanied by corresponding grayscale donor EGFR (Ab-15)-Alexa Fluor 546; 0.5mcg/ml and acceptor MET (D1C2)-Cyanine 5; 10mcg/ml) intensity images. Scale bar, 50μm. Lifetime images are tri-exponentially analysed and enable masking of artefactual lifetimes as is seen between the bright spots in the grayscale EGFR intensity images and the colour lifetime images (masked areas appear black). This is important as FFPE prepared specimens are more prone to artefact and autofluorescence due to processing techniques. Areas of high EGFR-MET FRET, corresponding to increased EGFR-MET interaction are indicated by red pixels. Low FRET is scored by blue pixels. B) Quantification of average FRET of EGFR-MET interaction performed in resection specimens from 13 human NSCLC tumours from the Guy's tissue bank (FFPE). FRET efficiency is a quantitative measure of EGFR:MET interaction. 8-12 data points per tumour per experiment were imaged. Average and SEM bars shown. N=13 patients. The range of values seen are likely to represent both intra-tumoural heterogeneity and variability between different patients.

4.2.13 Effects of MET inhibition on ERK, AKT and FAK signaling

In light of the differential effects of MET kinase inhibition between the different cell lines on MET and EGFR FRET, cell proliferation and stroma remodelling, we looked for differences in AKT, FAK and ERK to explain this. All have been linked to MET signaling and we expected also to see differential effects of MET kinase inhibition on this signaling pathway (Gusenbauer, Zanucco et al. 2015). We treated $H1975^{L858R/T790M}$, $H1975^{L858R}$ and $H1975^{WT}$ cells in normal replete medium, with SGX523 for 24 hours and assessed phosphorylation levels of ERK.

Figure 4.19A shows the western blots and the corresponding phosphorylated forms. SGX523 effect on MET was confirmed by the absence of a band for phosphorylated MET in each of the treated lanes. There was no effect on EGFR phosphorylation in response to the MET inhibition. There was a significant reduction in ERK phosphorylation in SGX523 treated $H1975^{L858R/T790M}$ cells as shown for the quantification for these western blots which represents the intensity of the phospho-ERK band compared to total ERK. This could account for the reduction that we saw in proliferation in this cell line, but as per the Western blot the inhibition of ERK phosphorylation was incomplete and was only observed in this $H1975^{L858R/T790M}$ cell line (Figure 4.19B). Analysis of xenograft tumour lysates obtained from SGX523 or vehicle-treated animals also showed reduction in the band for phosphorylated ERK in $H1975^{L858R/T790M}$-derived xenografts alone (Figure 4.19C). Bands for total levels of these proteins were comparable. We then looked for AKT and FAK as an alternative explanation for the different responses in inhibition of the stroma and migration in the other cell lines but we saw no change in phospho-AKT or FAK signals (Figure 4.19

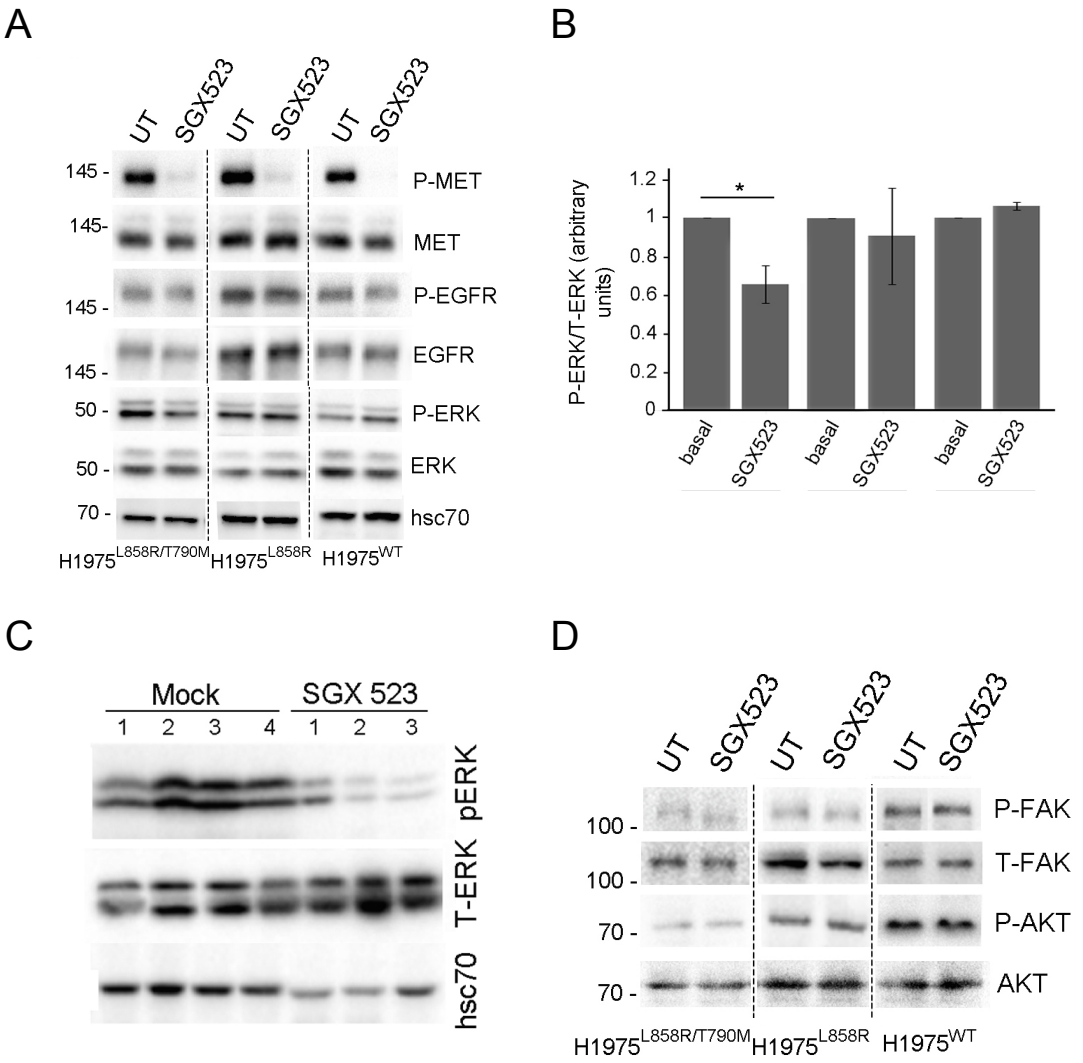

Figure 4.19. Effect of SGX523 on ERK phosphorylation in H1975$^{L858R/T790M}$
A) WB of phospho- and total EGFR, MET, AKT, ERK and FAK from cell lysates of the different H1975 cell lines treated or not with SGX523 for 24 hours. hsc70 levels are also shown as loading control. B) Quantification of the P-ERK vs T-ERK WBs shown in (A) in the three H1975 derivate cells. SD Bars shown. (*$p<0.05$, N=3). C) WB of phospho- and total-ERK in the extracts coming from the H1975$^{L858R/T790M}$ xenografts tumours in mock vehicle (lanes 1-4) and SGX523 treated mice in lanes 1-4 and SGX523 lanes 1-3 corresponding to different tumours from each of these respective treatment groups. hsc70 is also shown as loading control. D) WB of phospho- and total AKT and FAK from cell lysates of the different H1975 cell lines treated or not with SGX523 for 24 hours. The only change in signaling we observed from this data was a reduction in phospho-ERK in response to SGX523. This was not marked but was confirmed by densitrometry (see B) and also observed *in vivo* (C). No effect was seen for pAKT/pFAK blots in response to SGX523. ERK WB data kindly Provided by Dr. E. Ortiz-Zapater.

Since we had expected to see differences in AKT in response to MET inhibition we hypothesised that this could be due to an absence of ligand in these experiments. We proceeded to assess the cell lines for the signaling response (P-AKT and total AKT) to SGX523 treatment, using the respective ligands for EGFR/MET i.e. EGF and HGF, to mimic more closely the tissue microenvironment. Phosphorylation signal was visibly changed from baseline in pAKT blots following EGF exposure in all conditions. HGF increased pAKT signal in $H1975^{WT}$. In the other cell lines it was less easy to distinguish this visually. In $H1975^{L858R/T790M}$ there appeared to be a reduction in the EGF (and EGF + HGF) exposed samples with SGX523 treatment consistent with the crosstalk expected in this line. It was not possible to clearly delineate a response to SGX523 in the presence of ligand in the other cell lines, nor with HGF, even after densitometry. We concluded that the only ligand response in these two signaling pathways that resulted in a different response to SGX523 was the reduction in EGF-mediated signal in the $H1975^{L858R/T790M}$ cells consistent with the loss of the EGFR-MET dimer in this line. From this we could conclude that HGF is not able to overcome the inhibition produced by SGX523, and that EGF is not the ligand responsible for the differences in the other cell lines in response to SGX523 treatment.

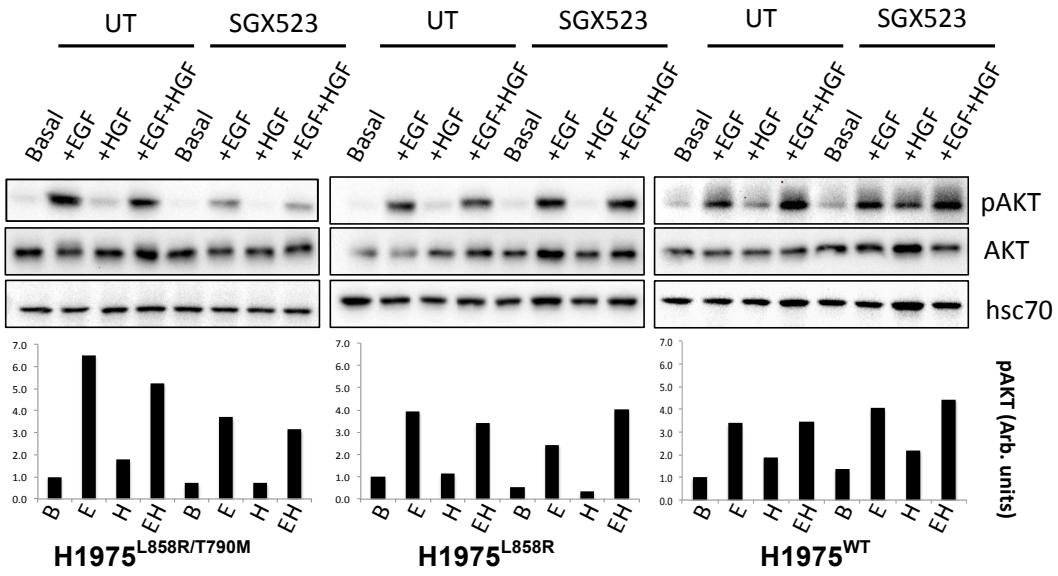

Figure 4.20. Response to EGF/HGF stimulation versus MET inhibition on AKT and phosphorylation *In vitro*

WB of phospho- and total AKT from cell lysates of the different H1975 derived cell lines treated or not with SGX523 (1h) in the presence or absence of EGF, HGF or both for 15 minutes. hsc70 levels were used as loading control. Quantifications are shown for phospho-AKT normalised to hsc70. The x-axis of the quantifications matches the labels above the Western blots, re-labelled with the following letters for clarity B-Basal, E-EGF, H-HGF or EH-EGF+HGF (untreated then SGX523 treated lanes accordingly). EGF alone or in combination with HGF increases the pAKT signal. HGF only increases pAKT in the case the $H1975^{WT}$ cell line but this is negligible when accounting for the loading control in HSC70. No change was observed from SGX523 treatment except modulation of a pAKT signal change seen in response to EGF in $H1975^{L858R/T790M}$ (N=2). This is reminiscent of HER2 which alone can activate ERK but requires dimerisation with HER3 for PI3K/AKT signaling and supports an interaction between EGFR and MET (Arteaga and Engelman 2014).

4.2.14 Summary

In summary, MET interacts with EGFR differently in cells that encode WT, L858R and L858R-T790M-EGFR and modulates the tumour cell behaviour as well as the interaction with the stroma. More importantly, the inhibition of MET by SGX523 modulates this interaction depending on the *EGFR* mutation. This interaction appears to be in opposite directions in L858R and EGFR L858R-T790M encoding cells *in vitro* and *in vivo*. Namely EGFR and MET are dimerised when *EGFR* is double mutated ($H1975^{L858R/T790M}$) but not with the single mutant form ($H1975^{L858R}$). MET therapy seemed to be active in both mutated cell lines but in the case of the single mutant ($H1975^{L858R}$), it enhanced formation of the EGFR-MET dimer where as in the presence of the double-mutant it reduced it ($H1975^{L858R/T790M}$). We saw downstream changes in ERK in $H1975^{L858R/T790M}$ that may account for the reduced proliferation but couldn't establish downstream pathways that accounted for the drug response in the other cell lines.

Unfortunately I had no further time/resources to explore downstream pathways more comprehensively. We were clear that the EGFR-MET dimer differed with the *EGFR* mutations. Another hypothesis would be that these dimers had consequences for an additional receptor depending on the EGFR mutant present. A good candidate to explore further would be HER3, which is a preferred heterodimer partner of EGFR and HER2 and has also been linked to *MET* amplification. I explore these themes further in the discussion that follows.

4.3 Discussion

In this section I focus on our observation that in a model of lung adenocarcinoma, EGFR-MET crosstalk depends on *EGFR* genotype and we believe as a consequence so does the response to MET inhibition.

4.3.1 Do EGFR and MET interact in lung adenocarcinoma?

Consistent with a wealth of existing literature that supports EGFR-MET crosstalk (Jo, Stolz et al. 2000, Puri and Salgia 2008, Tang, Du et al. 2008, Zhang, Staal et al. 2010), we used our *in vitro* model, to confirm EGFR and MET proximity at the cell membrane by immunofluorescence and interaction with co-immunoprecipitation (co-IP). This provided us with evidence that within our H1975 derived lung adenocarcinoma model based on the L858R and T790M *EGFR* driver and resistance mutations, EGFR and MET can exist alongside each other at the cell membrane. Our co-IP results supported a direct interaction between these receptors and additionally the conjectured *EGFR* mutational status dependent differences in this EGFR-MET crosstalk that we saw between the cell lines by FRET-FLIM.

In our FRET experiments we saw high levels of FRET in the $H1975^{L858R/T790M}$ cells and xenografts that were not seen in the $H1975^{L858R}$ cells or tumours. This would be consistent with a high proportion of EGFR existing as EGFR-MET dimers in the presence of the EGFR-TKI resistance mutation T790M. EGFR-MET dimerisation in $H1975^{L858R/T790M}$ is consistent with the existing literature of EGFR-MET crosstalk in lung adenocarcinoma and also our earlier results showing co-localisation of the two proteins at the membrane. Equivalent findings were seen *in vitro* and *in vivo* affirming the validity of this approach (Engelman, Zejnullahu et al. 2007).

Dimerisation is known to be a critical component of both EGFR and MET signaling. In the case of EGFR, we have already discussed how receptor homodimerisation and heterodimerisation are crucial to activation of the kinase domain and known to be influenced by *EGFR* mutations (Shan, Eastwood et al. 2012). MET is also recognized to signal as a dimer and is also sensitive to ligand independent dimerisation in the presence of mutations and genomic amplification (Wickramasinghe and Kong-Beltran 2005). However, little is known about the physical or structural nature of a putative EGFR-MET dimer. We could infer from the conformational changes seen in EGFR dimerisation in general that a similar mechanism might apply. For example this may occur through allosteric interactions mediated through the dimerisation arm or juxtamembrane regulatory regions as seen between EGFR and HER family homo- and heterodimerisation.

As discussed in chapter 3, L858R induces changes in the EGFR ectodomain structure that render the single mutant L858R EGFR in an extended, dimerisation-competent conformation which has also been shown to encourage EGFR homodimerisation (Valley, Arndt-Jovin et al. 2015, Valley, Arndt-Jovin et al. 2015). MET activation resembles that of the HER receptors, whereby autophosphorylation following HGF induced dimerisation ejects the activation loop into an extended conformation reorienting the alpha C helix to form a viable active site. We might have expected that the extended confirmation of EGFR L858R was more able to interact with MET. However this hypothesis does not match the observations from the FRET experiments where untreated $H1975^{L858R}$ cells/tumours had low levels of EGFR-MET interaction. In the case of $H1975^{L858R}$, EGFR structural changes may therefore favour EGFR homodimer formation in preference over the EGFR-MET heterodimer or even sterically preclude the interaction with MET.

In $H1975^{L858R/T790M}$, EGFR-MET dimerisation occurs basally. It is not clear why the L858R and T790M mutants behave differently in this respect but there is a free-energy difference between the two mutants that alters the propensity for transition between the active and inactive states and as well as the positioning of residues known to be important in EGFR homodimerisation. Such conformational changes could alter the dimerisation domains to favour interaction with MET in the presence of the L858R-T790M double mutation but not L858R alone (Yun, Mengwasser et al. 2008, Rickert, Patel et al. 2011, Sutto and Gervasio 2013).

It is also not clear whether an EGFR homodimer is required to activate MET (see Figure 4.21A) or whether union EGFR and MET monomers would suffice. In the case of the latter, it is possible that a MET ‘donor drives activation of EGFR as the acceptor or vice versa (Figure 4.21B & C). This is well aligned to the model of specialisation of EGFR mutants as discussed in chapter 3 since one of the orientations might be favoured by an EGFR mutant acting as a more efficient acceptor as is described for the EGFR L858R mutant (Red Brewer, Yun et al. 2013). This preference for a role as donor or acceptor might differ between the L858R and L858R-T790M mutants for the EGFR-MET interaction as it does for the EGFR homodimer.

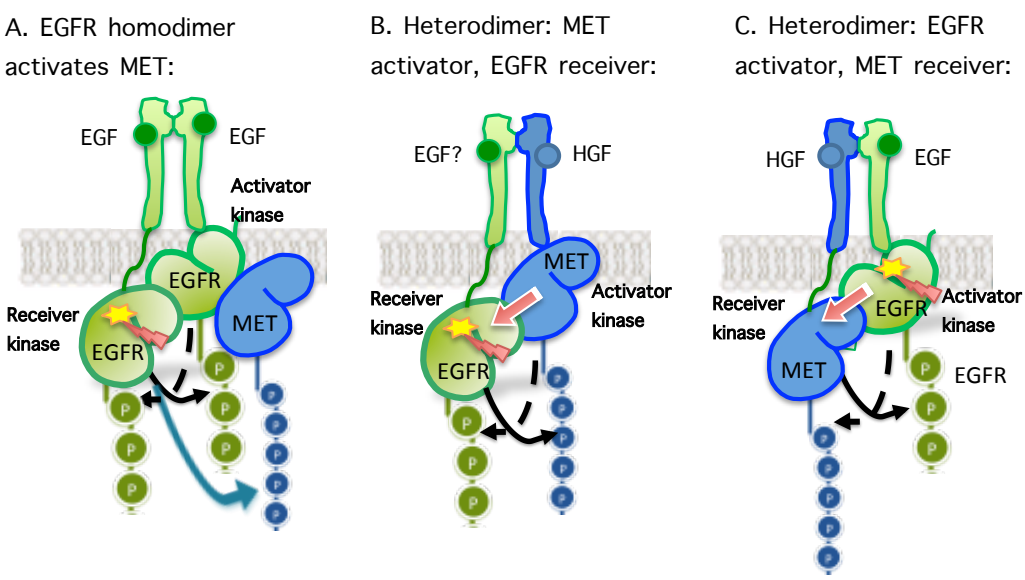

Figure 4.21 Models of EGFR-MET dimerisation.
Schematic of interaction between EGFR mutants to homodimerise with EGFR or heterodimerise with MET. Solid black arrow demonstrate transactivation of receiver kinase by activator. Dotted line shows possible reciprocal activation of the activator by the receiver. In A) the homodimeric EGFR complex may lead to MET activation. The models depicted in B) and C) suggest that EGFR and MET interact directly with transactivation that would result in phosphorylation. In B) MET is in the activator position whereas In C) EGFR is an activator. Additional allosteric interactions between partner kinase domains may act to alter the activation state. Adapted from (Littlefield and Jura 2013).

4.3.2 MET TKI effect on the EGFR-MET interaction

MET mediated resistance to EGFR TKI is primarily attributed to *MET* amplification. Use of MET therapies has potential in this group but is still poorly defined. A number of pre-clinical studies also demonstrate enhanced efficacy from dual EGFR and MET inhibition but there is also sparse data on the role of other EGFR TKI resistance mechanisms such as T790M. For example, in the H1975 and H8227 cell lines, both of which have increased MET expression, there is a synergistic response to combined EGFR and MET therapy - in H8227 this overcomes EGFR TKI resistance mediated by *MET* amplification whilst in H1975 it is an *EGFR* T790M gatekeeper resistance mutation that can be surmounted (Engelman, Zejnullahu et al. 2007, Wang, Li et al. 2010, Zhang, Staal et al. 2010).

We hypothesised that the different responses of each cell line to SGX523 would be due to the effect of this drug on MET in the direct physical interaction with EGFR. The physiological effects observed e.g. proliferation/stromal interaction following MET inhibition would then either represent the effect of SGX523 on one or both of:

1) MET inhibition modulates dimer formation between EGFR and MET which has consequences for EGFR and MET signaling.

2) MET inhibition prevents the capability of MET to phosphorylate EGFR within the heterodimer, which therefore alters the EGFR mediated signal.

According to our results from Figure 4.8 and Figure 4.17, MET inhibition does alter the interaction between EGFR and MET differently according to *EGFR* mutation status, thus supporting the first example. EGFR L858R-T790M preferentially bound to MET in the absence of SGX523, suggesting this is related to its activated form, whereas once bound to SGX523 the conformation of MET is unfavourable to EGFR binding. The reverse would thus be true of the EGFR L858R conformer. No such modulation was seen in H1975^{WT} suggesting that the altered binding by MET in its active or inactive form was related to the presence of mutated and not WT-EGFR.

Mechanistically, a possible explanation relates to the consequences of TKI binding on the kinase structure with relation to partnered N and C-lobes opposed around a cleft into which either ATP or such ATP-competitive inhibitors can bind (Stamos, Sliwkowski et al. 2002). ATP competitive inhibitors can present hydrogen bonds to the active site than mimic those of the adenine ring of ATP (Zhang, Yang et al. 2009). Inhibitors that stabilize the active conformation can promote dimerisation (Lu, Mi et al. 2012).

SGX523 preferentially binds an un-phosphorylated, inactive conformation of MET which upon binding results in occupation of the ATP binding site by a tyrosine residue (Buchanan, Hendle et al. 2009). This stabilises an unusual "DFG-In" conformation more usually associated with enzymatic activity (Buchanan, Hendle et al. 2009). SGX523 has a bivalent structure of which a quinolone moiety engages the MET hinge region resembling the binding of other ATP competitive inhibitors, which bind at this position but instead stabilizes an atypical activation loop conformation that internalises the kinase activation loop into the ATP binding pocket to preclude phosphotransfer at this site (Buchanan, Hendle et al. 2009). Thus whilst SGX523 is ATP-competitive, unlike other similar kinase inhibitors which target the ATP binding site in the active conformation, SGX523 binds the ATP binding site of an inactively conformed MET (Liu and Gray 2006). Interestingly, the DFG-in conformation is more often associated with an extended conformation that ejects the activation loop usually seen with the activated, phosphorylated form of MET (Rickert, Patel et al. 2011) This conformation could favour allosteric interaction with EGFR in $H1975^{L858R}$ cells.

The wider literature surrounding drug inhibition of receptor tyrosine kinases provides a number of examples of how these agents can alter the tendency of kinases to dimerise and in some cases paradoxically increase receptor-receptor interaction. For example there is evidence that EGFR homodimer formation can be enhanced by gefitinib or erlotinib treatment (Coban, Zanetti-Dominguez et al. 2015). In fact, various intermediates of EGFR oligomerisation are recognized following EGFR kinase inhibition (Bublil, Pines et al. 2010). HER2-HER3 dimer formation also occurs in breast cancer following treatment with Lapatinib (EGFR/HER2 directed TKI)(Scaltriti, Verma et al. 2009, Claus, Patel et al. 2014). This can also be associated with unexpected phenotypical responses to TKI treatment.

The clinical significance of TKI-induced dimers is further exemplified well by BRAF resistance arising as a consequence of transactivation of RAF dimers in the presence of ATP-competitive RAF inhibition (Poulikakos, Zhang et al. 2010). This paradox whereby TKI can increase tendency to dimerisation suggests our understanding of the mechanism of tyrosine kinase signaling and the translation of their blockade to cancer therapy is incomplete.

Beyond inducing or preventing dimer formation, inhibition of kinase activity, the primary goal of TKI should have inevitable consequences for crosstalk. Previous studies demonstrate that EGFR inhibitors can block MET phosphorylation and conversely that MET inhibitors can block EGFR phosphorylation (Lutterbach, Zeng et al. 2007, Guo,

Villen et al. 2008, Tanizaki, Okamoto et al. 2011). However, in all cell lines we saw complete inhibition of MET phosphorylation in response to SGX523 implying that any direct action arising from MET independently of EGFR would not appear to differ between the cell lines.

With regards to crosstalk mediated signaling, as demonstrated in Figure 4.22, the effect of SGX523 would differ between the two mutant cell lines in the following way:

1) In the case of H1975$^{L858R/T790M}$, SGX523-treated cells, the EGFR-MET dimer separates and consequently eliminates any signal that was emanating from MET acting on EGFR or EGFR acting on MET (cross-phosphorylation or allosteric interaction that promoted autophosphorylation). Inhibition of MET autophosphorylation would persist (MET kinase inactivated by SGX523).
2) Conversely, in the case of H1975^{L858R} there is now an EGFR-MET dimer. MET autophosphorylation signal is still lost (again, MET kinase is inactivated by SGX523) but MET can still act allosterically on EGFR via EGFR mediated signaling mediators. EGFR can now also allosterically alter the activity of MET.

In summary, in H1975$^{L858R/T790M}$ the EGFR-MET dimer is disrupted by SGX523 whilst in H1975^{L858R} it appears that EGFR L858R cannot bind with MET unless in an SGX523 bound conformation that is presumably inactive, although crosstalk may still proceed allosterically.

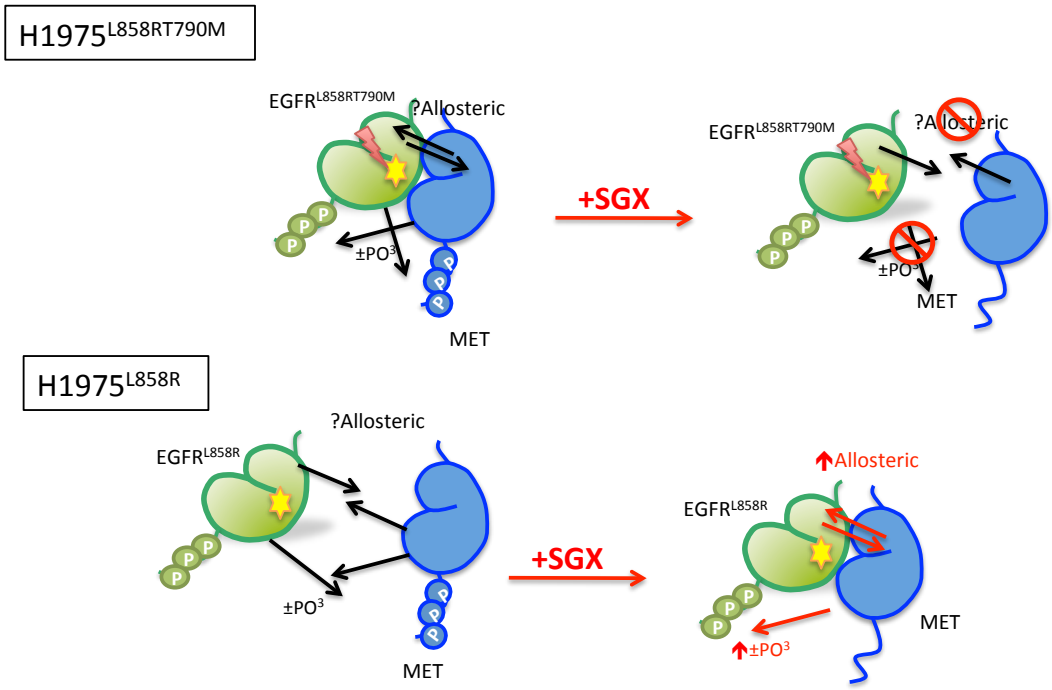

Figure 4.22 SGX523 effect on EGFR-MET heterodimers
The possible points of SGX523 interference with signaling downstream of EGFR and MET are highlighted. In H1975$^{L858R/T790M}$ untreated cells could cross-phosphorylate and interact allosterically. All such interactions are lost with breakage of the dimer and whilst EGFR could autophosphorylate as a homodimer, MET kinase activity is inhibited by SGX523. Conversely in the case of H1975^{L858R}, formation of the EGFR-MET dimer following SGX523 treatment, although not able to become activated due to MET kinase inhibition, allosteric interaction could still change the behaviour of the receptor.

4.3.3 MET inhibition and tumour cell traits?

In chapter 3 we observed an association between *EGFR* mutation type and cell phenotype, which resulted in different tendencies towards proliferation, migration and tumour microenvironment traits such as stroma formation. In this chapter we see that these phenotypes respond differently to MET inhibition across the cell lines. Since EGFR-MET interaction also differs with *EGFR* mutation status and SGX523, we expected that these features would be linked to the changes we saw in proliferation, migration etc. (Trusolino, Bertotti et al. 2010). We thus began to contemplate a model of how the EGFR and MET interaction when modified by targeted MET therapy could influence tumour cell traits.

Proliferation was only significantly inhibited in the 'double mutant' cell line H1975$^{L858R/T790M}$ as shown by the BrdU incorporation assay and agar colony formation and similarly in the xenograft model we only saw a significant reduction in growth and phospho-Histone H3 staining in xenografts coming from this this cell line. We observed that stromal markers of collagen, fibroblasts and cd31 were reduced in H1975^{L858R}

xenografts following SGX523 administration but with no effect in the other cell lines. The MET inhibition effects on proliferation are most consistent with the EGFR-MET dimer being an important determinant of proliferative growth that is responsive to MET inhibition since we saw loss of EGFR-MET dimer in H1975$^{L858R/T790M}$ cells and tumours with SGX523 treatment, along with suppression of proliferation. It is likely that there is redundancy between EGFR and MET, since we saw low amounts of EGFR-MET FRET in the more proliferative H1975^{L858R} cells/tumours, suggesting that here EGFR exerts a greater effect on cell cycling either as a homodimer independently of MET or in association with another receptor heterodimer pairing, for example HER3 as we discussed with the data on defective internalisation in Chapter 3. According to our FRET data, the apparent increase in the features of the tumour microenvironment (collagen, anti-SMA) in H1975^{L858R} xenografts is unlikely to have arisen through direct EGFR-MET interaction since we did not observe the EGFR-MET dimer under basal conditions in this mutant. The increased capacity for proliferation of *EGFR* L858R-driven cells may itself increase the degree of interaction with the stroma.

The effect of SGX523 on cell migration and the xenograft microenvironment were however most apparent in H1975^{L858R} and in this cell line, SGX523 also increased dimerisation of EGFR with MET. MET in this interaction is presumed to be inactive and dephosphorylated. The response to SGX523 could therefore reflect the inhibition of MET alone, independent of EGFR. Alternatively, the dephosphorylated, SGX523-bound form of MET could allosterically modulate EGFR in a more regulatory capacity.
It is also conceivable that MET inhibition has an effect on the tumour stroma independent to its direct activity on tumour cells, for example it has been shown that HGF enhances fibroblast migration towards an HGF gradient and HGF secretion by fibroblasts can stimulate the invasive activity of tumour cells (Qian, Mizumoto et al. 2003, Matsumoto and Nakamura 2006). We saw reduction of anti-SMA staining, a marker of fibroblasts in response to SGX523 suggesting that these cell types additionally were directly inhibited by MET inhibition, that may not have reflected a direct effect of the EGFR-MET dimer.

The complexity of these observations highlights how even exploring the interaction of a pair of molecules, whilst advantageous compared to analysis of a single protein e.g. *EGFR* mutations, still lacks clarity to explain the wider protein network. In any case, the different response to MET inhibition between the cell lines suggested that we were modifying not only MET, but that this effect also involved EGFR in one or more of the cell lines. Alternatively another signaling pathway that was regulated by the EGFR

mutant status was also altered by MET inhibition. The FRET data provided evidence to support the hypothesis that the EGFR-MET interaction could be responsible.

4.3.4 MET inhibition and downstream signaling in EGFR mutants

To validate and extend upon our observations and to understand how the EGFR and MET signals could be differentially transduced to traits of proliferation versus microenvironment interaction and invasiveness, we explored alterations in downstream signaling pathways in response to treatment that would explain the intracellular effector pathway through which this was acting. In the H1975$^{L858R/T790M}$ cells, where we observed EGFR-MET dimer presence at baseline, we expected that MET would modulate EGFR binding sites e.g. for AKT or ERK or alternatively, the interplay with MET could provide a secondary set of effector molecules through MET binding sites or other receptors (Engelman, Zejnullahu et al. 2007). It was thus surprising that we found only subtle differences in the most common downstream signaling pathways AKT and FAK, between the three cell lines.

We did see that SGX523 suppressed MET derived downstream activity through ERK but this occurred only in the H1975$^{L858R/T790M}$ cell line. ERK is an important mediator linked to EGFR and MET signaling and provided a plausible mechanism for the inhibition in proliferation we saw in the H1975$^{L858R/T790M}$ cells and tumours but not the other cell lines. There was not time to extend this work to other signaling pathways but this suggests that another downstream effector might be involved or alternatively there could be further complexity in the downstream changes seen in these pathways that meant that we did not see a clear signal change.

When we relate these findings back to the consequences of EGFR-MET interaction on downstream signaling as described above, we considered that the loss of the EGFR-MET dimer in H1975$^{L858R/T790M}$ with SGX523 treatment, occurred alongside a loss of ERK signal suggesting that an active EGFR L858R-T790M-MET dimer is favourable for effective ERK signaling. This observation was unique to H1975$^{L858R/T790M}$ suggesting that the dimer is relevant in the suppression of this pathway. We saw no effect here in AKT/FAK. In the case of the H1975^{L858R}, the induction of the EGFR-MET dimer by SGX523 resulted in no detectable alterations in downstream signaling such as ERK, AKT or FAK. This may imply an alternative pathway is effected or that the complexity/redundancy in the system preventing us from detecting a clear difference in signaling in response to SGX523 exposure. Alternatively there may be a paracrine consequence for EGFR-MET signaling in the context of MET inhibition or an effect of SGX523 on the stroma itself.

4.3.5 The challenges of using FRET-FLIM to develop a MET biomarker

Companion diagnostic biomarkers are important to enable more rapid and effective deployment of drugs in clinical trials by enhancing outcomes as a percentage of trial participants. There is potential to learn more about the differences between different MET inhibitors by studying subgroups of patients positive for different biomarkers to tell us more about which patients may or may not respond. Biomarkers indicative of resistance through MET activation may also become increasingly relevant with evolution of later generations of EGFR TKI where MET-mediated resistance remains a problem (Shi, Oh et al. 2016).

Our FRET-FLIM assay using EGFR and MET antibodies directly labelled with neighbouring fluorophores provides an alternative means by which to study the EGFR-MET interaction directly. Although nanoproximity approaches have been used to explore other EGFR/HER (Human Epidermal Growth Factor Receptor) family interactions in other cancers (Tao, Castel et al. 2014, Coban, Zanetti-Dominguez et al. 2015), to the best of our knowledge, this is the first work that utilises FRET-FLIM imaging to demonstrate EGFR-MET interaction and one of a limited number of studies using this approach in lung cancer. FRET-FLIM assays are unique in their study of dimer formation in that they are able to quantify interaction at the nanometre scale (5-10nm)(Kelleher, Fruhwirth et al. 2009). Using this technique of imaging antibodies with directly conjugated fluorophores in overlapping spectra, it is possible to measure the extent of fluorescence decay in the donor antibody-fluorophore conjugation when in close proximity to an acceptor fluorophore directly ligated to a partner antibody against another protein of interest.

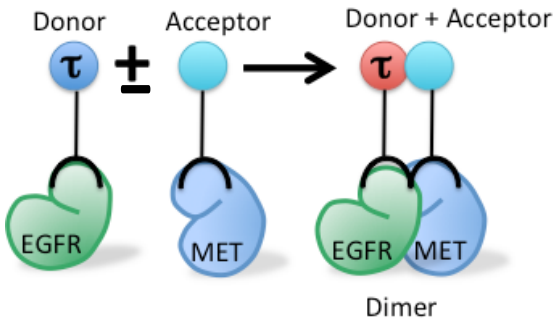

Figure 4.23. Schematic: EGFR-MET FRET Asssay

EGFR bound to antibody conjugated with donor fluorophore (e.g. Alexa Fluor 546) is measured in presence or absence of an antibody labelled with the acceptor fluorophore (e.g. Cyanine 5) targeted against the second protein of interest, i.e. MET. Binding of EGFR and MET is shown by interaction (FRET) between donor and acceptor fluorophores quantified by reduction of lifetime measurement (τ) in the donor fluorophore between donor alone and donor + acceptor lifetime images.

We designed and optimized an assay for an EGFR antibody-bound donor fluorophore (Alexa Flour 546) and a MET antibody bound acceptor (Cyanine 5). Initially an extracellular pair, EGFR (Ab-5)x546; MET (AF276)Cy5 provided specific staining when assessed on *in vitro* and FFPE specimens overexpressing EGFR/MET respectively. Poor FRET assay performance of this pair on FFPE tissue however, required converting to the intracellular pair. After searching for an appropriately specific MET antibody, a labelled version was then subjected to further validation to assess specificity using transient transfection for overexpression and review of donor:acceptor antibody concentrations/ratios most compatible with a FRET signal. Attempts to optimize a similar assay using a MET donor (and corresponding EGFR acceptor) identified this combination as a less effective FRET pair. In the interests of time and resource constraints, we proceeded with the EGFR (Ab-5)x546-MET(D1C2)cy5 combination. Tissue preparation including borohydride quenching steps to suppress autofluorescence and a purpose-made algorithm validated previously, capable of eliminating noise from residual autofluorescence was employed to mask any residual autofluorescence at the extremes of expected lifetime measurements observed in the FFPE specimens (Tao, Castel et al. 2014).

It is common for FRET assays to behave differently in the *in* vitro and *in vivo* settings in this way as a consequence of differences in EGFR-MET interaction with surrounding tissue. There is also often an increased problem with auto-fluorescence in formal fixed paraffin embedded (FFPE) specimens. For our FFPE tissue, we utilized a specialized algorithm for tri-exponential analysis with gating that masks out the very-low non-specific lifetimes typical of auto-fluorescence that had been developed in the lab previously and enabled more consistent data analysis. Overall there was good concordance between the data in each of these settings.

The increased FRET observed between EGFR and MET in the H1975$^{L858R/T790M}$ cell line represents an increased proportion of EGFR bound by MET. This is likely to reflect a greater affinity between this 'double mutant' form of EGFR with MET that exceeds that seen for the other EGFR mutants and WT. Alternative explanations of the differences observed could potentially have resulted from intrinsic differences in the behaviour of EGFR and MET in the three different cell types – either determined by EGFR directly or its interaction within a larger system of cancer-driven signaling. This may alter the quantities of EGFR and MET available to dimerise and thus a difference in the quantities of EGFR or MET and a different EGFR: MET ratio between the cell lines could be significant. Against this argument we found *MET* copy number and expression levels to be broadly similar between each of the cell types. EGFR levels

similarly were comparable and we considered it more likely that the presence of the designed mutations would be of greater significance, although this may have influenced the pattern of EGFR homodimers relative to EGFR-MET heterodimers. Given the promiscuity in receptor dimerisation and lateral signaling recognized with the EGFR family, it is possible that a third protein or receptor could influence the EGFR-MET interaction to a different degree depending on the *EGFR* mutation present i.e. one mutant form might be more sequestered by another molecule and therefore less able to interact with MET.

Additionally, our studies cannot discriminate between the binding of MET with monomeric EGFR as 1:1 or with an EGFR homodimer in a 1:2 or 1:many ratio or if EGFR and/or MET dimer: dimer or higher order oligomerisation is required for EGFR-MET crosstalk and how this differs depending upon the presence of *EGFR* mutations. This could be explored further with overexpression experiments in *in vitro* based assays, which quantify FRET in varying ratios of EGFR: MET availability. Other nanoproximity studies such as single molecule imaging could be of utility here. In the case of higher order oligomers, MET may facilitate or impede EGFR homodimer formation or modulate the kinase activity of EGFR molecules within the homodimer.

Furthermore, the FRET results for our chosen EGFR donor - MET acceptor pair representing the proportion of EGFR bound to MET, may differ when compared with the alternative (MET donor with EGFR acceptor pair), which would signify the proportion of MET bound to EGFR. The stoichiometry of the EGFR-MET crosstalk could be significant to the interpretation of this format of the assay. When FRET signal is low, there are fewer EGFR molecules dimerised with MET and the reverse with increased FRET. This does not tell us whether this reflects a change for example of 15% to 5% of the total EGFR pool or 70 to 50%. We have no data on the relative receptor concentrations of EGFR and MET and how this is affected by EGFR activation, by the presence of each mutation or MET inhibition. We could also consider that not all EGFR molecules are likely to be occupied by a MET heterodimer pairing (and vice versa) and that this may not be constant but instead dynamically altered by the presence of these mutations/kinase inhibitors. It could be possible to establish further information by choosing a MET donor to increase sensitivity although there is a time and cost implication to be considered in so doing. Nonetheless, the information that we have obtained remains useful but must be interpreted in the context of the wider biological system.

4.4 Summary

In summary, these results highlight the effects of *EGFR* mutation status and MET inhibition using the novel approach of FRET-FLIM imaging to explore the interaction between EGFR and MET. We noted that EGFR mutant status alters the propensity to EGFR-MET interaction, in that the EGFR L858R-T790M mutant interacted more readily than EGFR L858R or EGFR WT forms. This could be relevant to the differences observed between the phenotypes of each of the cell lines in Chapter 3.

The further important observation was that response in terms of changes in these cell phenotypes e.g. proliferation and migration *in vitro* and xenograft tumour growth and microenvironment following MET inhibition with SGX523 is dependent upon *EGFR* mutational status. We also saw that MET inhibition altered the EGFR-MET interaction as quantified by FRET-FLIM imaging.

Chapter 5. Discussion

This thesis adds important data to the literature on the mechanistic details of the EGFR-MET interaction. In this discussion I consider the possibilities on how this fits with existing structural data on EGFR dimerisation, how this might be useful in clinical studies, what an EGFR-MET assay would add to *EGFR* mutation testing and how this relates to MET targeted therapy.

5.1 Why does *EGFR* genotype influence EGFR-MET interaction?

EGFR mutations in lung cancer are widely studied in the context of sensitivity and resistance to EGFR Tyrosine Kinase Inhibitors (TKI). In chapter 3, I explored the hypothesis that *EGFR* mutations have a role to play beyond this in terms of tumour cell traits and EGFR activation. In Chapter 4, I developed an EGFR-MET FRET assay to provide new evidence that EGFR-MET interaction is determined by the same *EGFR* mutations that are important clinical determinants of EGFR TKI responsiveness and EGFR homodimerisation (Sharma, Bell et al. 2007, Rosell, Carcereny et al. 2012, Shan, Eastwood et al. 2012). In the case of the double mutant, H1975$^{L858R/T790M}$ EGFR and MET could interact whereas in H1975^{L588R} they could not.

EGFR mutation-determined EGFR-MET dimerisation could be the result of structural alterations arising from these activating *EGFR* mutations that are known from the literature to affect EGFR homodimerisation (Littlefield and Jura 2013). These likely relate to allosteric changes which result in an extended conformation, which align key catalytic regions to favour activation and expose the dimerisation arm (Shan, Eastwood et al. 2012, Valley, Arndt-Jovin et al. 2015). We hypothesised that the mechanism of EGFR heterodimerisation with MET could be similar to that of EGFR-EGFR homodimerisation. Structural studies such as x-ray crystallography would be required to demonstrate this definitively, however although not available FRET does validate their binding if not the mechanism.

In view of further evidence that specific EGFR mutants are unique in their capacity to dimerise with each other, EGFR WT and additionally other HER family receptors, we suggest that EGFR crosstalk with MET could similarly be influenced by *EGFR* genotype (Red Brewer, Yun et al. 2013). Interestingly this same data shows that some mutations act preferentially as ‘acceptors’ in an asymmetric pairing and are accordingly more likely to pair and become activated in association with WT EGFR. On this basis, we could deduce that likewise MET could be preferentially positioned in either an activator or donor position depending on the *EGFR* mutation present, which would alter

the signaling pathways transduced and potentially also signal permanence/recycling too as we saw for EGFR (Figure 3.3). EGFR-MET interaction may also depend on the activation status of EGFR prior to encountering MET, whereby the interaction is only effective when EGFR has already homodimerised leading to one activated MET monomer in the presence of more than one EGFR molecule in a one:many relationship (Figure 4.20).

5.2 Are EGFR-MET dimers central to the responsiveness of lung adenocarcinoma to MET inhibition?

The fact that we observed different phenotypic responses to MET inhibition in each cell line is consistent with the hypothesis that tumour cells with different EGFR mutants have different susceptibilities to MET inhibition. Chapter 4 also provided evidence linking EGFR-MET dimers to MET inhibition response. In the $H1975^{L858R/T790M}$ cell line we saw that the basal interaction between EGFR and MET is interrupted by SGX523 treatment. Conversely, in the $H1975^{L858R}$ cell line, EGFR and MET did not interact under resting conditions, but the addition of SGX523 results in an increase in EGFR-MET dimerisation. $H1975^{WT}$ cells had no substantial EGFR-MET interaction and are not modified by SGX523.

Our key findings of the phenotypical effects of MET inhibition on lung adenocarcinoma coming from the *in vitro* and *in vivo* studies were that with disruption of the EGFR L858R-T790M-MET dimer following SGX523 treatment there was reduction in proliferation and tumour growth. In the more proliferative $H1975^{L858R}$ cell lines in which the stromal components had been most significant, $EGFR^{L858R}$ functioned as an oncogenic driver without evidence for $EGFR^{L858R}$-MET binding until SGX523 treatment, which surprisingly had no consequence for proliferation or growth but did inhibit stromal deposition.

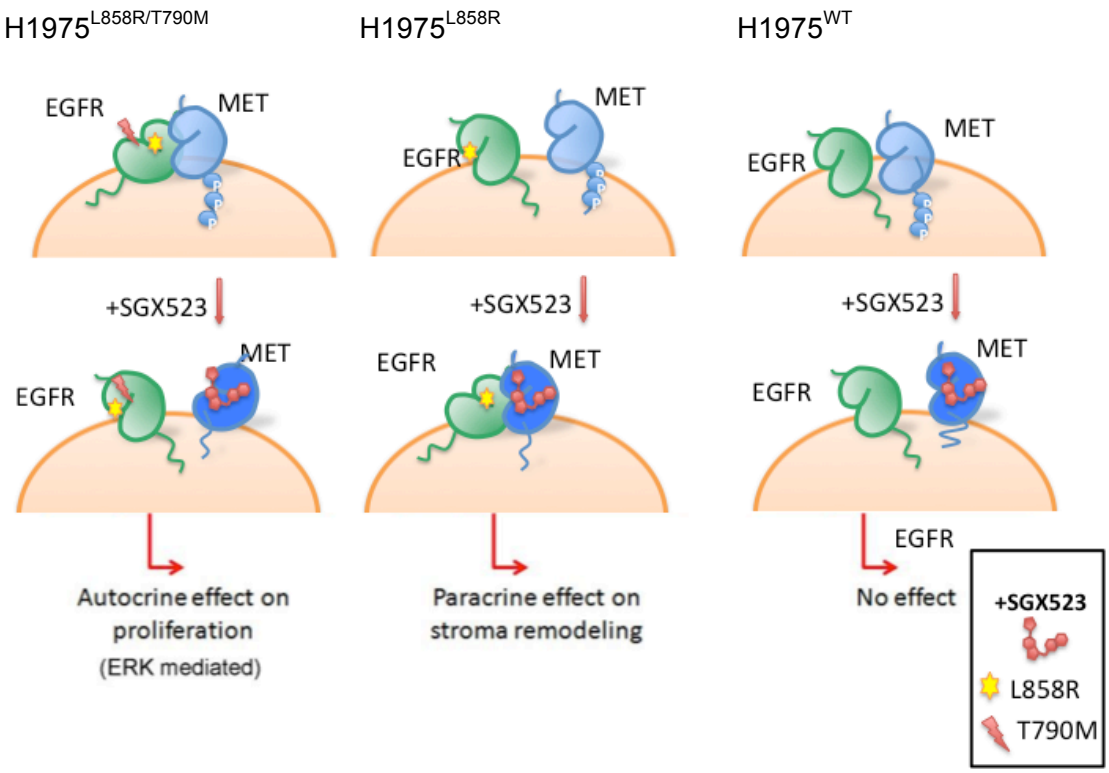

Figure 5.1 Effect of SGX523 on EGFR-MET heterodimerisation
Schematic model demonstrating the effect of SGX523 on EGFR-MET dimerisation pattern and consequences for tumour characteristics following treatment. In H1975$^{L858R/T790M}$ cells the EGFR L858R-T790M-MET dimer is disrupted alongside reduced proliferation. In H1975^{L858R} cells, EGFR L858R and MET do not interact until SGX523 binding to MET which presumably alters conformation to allow EGFR binding and with it reduces stromal deposition and migration. We observed no dimers in either scenario in H1975^{WT}.

These findings follow previous observations in our group that TKI therapy can increase or decrease EGFR dimerisation and that the likelihood of this happening differed between different EGFR mutants (Coban, Zanetti-Dominguez et al. 2015). The tendency for EGFR and MET to interact depending on the presence of the MET inhibitor could reflect conformational change in the MET kinase domain. In the untreated cells/tumours MET was more able to bind the double mutant form of EGFR. Since we did not see EGFR^{L858R}-MET dimer formation at baseline, we assumed that EGFR^{L858R} was only able to bind MET in its drug bound conformation arguing that the conformation of both EGFR and MET are both important determinants of the ability of EGFR and MET to dimerise and potentially function and that the SGX523 bound conformation of MET is altered in a way that favours interaction with EGFR L858R.

The different responses we observed to SGX523 between the cell lines in terms of phenotypical differences and to a lesser extent downstream signaling, suggested that these differences in EGFR-MET dimer formation are likely to determine specific downstream pathways between the mutant types. Changing the dominant downstream

pathway by influencing the EGFR-MET dimer could be a key component of how MET inhibition differs so notably between our EGFR mutants. Whether MET is bound to EGFR or not could alter the sites available for docking proteins to transduce a specific signal that results in a given cellular response. These sites could be within MET itself or alternatively be EGFR residues as part of an EGFR-MET dimer modulated allosterically by SGX523 through the EGFR-MET dimer.

Understanding the phenotypical responses to therapeutic agents in cell models helps us to appreciate the mechanisms in which these treatments could paralyse important tumour hallmarks – to slow or block growth, impede local or distant metastasis or prevent angiogenesis. They also suggest there is a specificity to particular treatment approaches that can govern the outcome expected and that should be incorporated into predictive assays that can be used to ascertain if a therapy is working or even determine which tumour types require targeting of an anti-proliferative agent rather than an anti-dimerisation agent for example.

Numerous MET inhibitors have been trialled in lung and other solid cancers ranging from the humanised monoclonal antibody onartuzumab ('METMab') to the small molecule inhibitor tivantinib. Most agents have failed in phase 3 trials (Scagliotti, von Pawel et al. 2015). In view of our data, and observations in the literature about the different mechanisms of action of different forms of MET targeted therapy, there may be different consequences for the EGFR-MET interaction depending on the particular kinase inhibitor selected and the conformation induced (some favour allosteric changes to active-like conformations whilst others compete at the ATP binding domain). Consequently there could be benefit in assessing the specific response to MET treatment for different classes of inhibitor. Small molecule kinase inhibitors are likely to have different effects to antibody-based therapies targeted against other parts of the receptor. Such therapies may then have more intricate effects than is currently appreciated.

5.3 Can we use EGFR/MET FRET assays on patient biopsies?

Having optimised our EGFR-MET FRET assay to the *in* vitro setting we thereafter made adjustments to the protocol to enable detection of FRET in FFPE specimens, This included enhancing the antigen retrieval technique, utilising a new donor:acceptor antibody pair and conducting the data analysis with a dedicated algorithm that subjected the data to tri-exponential fitting that excludes autofluorescence lifetimes. This approach demonstrated FRET signal in murine xenografts that had been prepared according to the standard FFPE preparation used for clinical specimens suggesting that human biopsy samples should be similarly amenable to this approach.

We thereafter processed several human tissue samples from human lung cancer tissue bank specimens as proof-of-principle that this approach could be employed in human specimens. In doing this we have repeated previous work by our collaborators that FRET-FLIM assays can be designed that would serve in biomarker studies (Tao, Castel et al. 2014). To our knowledge, this analysis of the EGFR-MET dimer and particularly examining FRET of HER family members in lung cancer specimens is novel and confirmed that FRET analysis could be reproducible in the context of standard clinical FFPE tissue processing techniques. In order to develop this assay into a clinical test, it would need to function in high throughput systems which may well need to be automated (Kelleher, Fruhwirth et al. 2009).

A number of governance steps would be required to bring such a FRET assay to clinical practice. Further validation in human specimens and development of the assay within the resource constraints of a clinical laboratory would be required. There would need to be validation in clinical studies in terms of the ability of an assay to detect a reliable signal from human cancer samples. It would also be necessary to understand which point of the natural history of a patient's tumour would be most useful to analyse with such approaches. Finally such a test must be demonstrated to be both an accurate and cost effective means to select targeted therapy. Thereafter, if there were particular subgroups of patients in whom differences in EGFR-MET crosstalk could be detected, it might be possible to determine a treatment strategy which differs in the same group and to protocolise such a therapy accordingly. For example responders versus non-responders to EGFR, MET and other kinase inhibitors (Kelleher, Fruhwirth et al. 2009, Tao, Castel et al. 2014). This would need approval by the appropriate research ethics, R & D and local and national technology appraisal boards including the MHRA. Beyond this appropriate training and clinical infrastructure investment would be required to develop this into a robust clinical service. Finally this has to be shown to be deliverable on the scales required of science delivered in a healthcare setting.

5.4 Would an EGFR: MET FRET assay offer more than *EGFR* genotype testing alone?

An outstanding question remains over whether it is sufficient to predict the efficacy of MET therapy using *EGFR* genotype alone, given that this approach would be achievable with current clinically utilised technology. Alternatively, and more likely, it will be necessary to explore such dedicated assays as we have explored to understand physiological EGFR-MET receptor crosstalk as a predictive biomarker.

Whilst thoracic oncology research has snowballed in recent years with significant developments such as the detection of *EGFR* activating mutations, this is likely to be barely the tip of the iceberg. There is increasing recognition of the complexity of mutational burden in lung cancer and furthermore of the diversity within individual patients and between different cases of lung cancer (de Bruin, McGranahan et al. 2014, Rizvi, Hellmann et al. 2015, Tan, Mok et al. 2015). This demands an increasingly personalized approach to therapeutic strategies and will require more effective diagnostic tools to classify and direct its treatment. FRET based assays provide one such example well suited to tackle the complexity of cancer by improving our understanding of interaction between individual players in a network of cancer signaling pathways (Kelleher, Fruhwirth et al. 2009, Fruhwirth, Fernandes et al. 2011). Consequently, there is clear potential to the translation of an assay of EGFR-MET interaction to a clinical test that exceeds the capability of existing approaches if we follow the hypothesis that the interaction between two molecules such as EGFR and MET is more important than for example protein levels or mutations status of either molecule in isolation.

Testing of *EGFR* mutation status could in principal provide a surrogate of the EGFR-MET interaction. In general there is comparatively little understanding of the role of EGFR when considering *MET* amplification. There is data that addition of a *MET* FISH positive result to any *EGFR* mutation is more useful as a prognostic marker compared to *EGFR* mutational status alone, alluding to the potential predictive role of EGFR and MET in partnership rather than sole testing of either target (Tanaka, Sueoka-Aragane et al. 2012). There are additionally other aberrations of MET signalling which may hinder EGFR-MET dimer formation that only an EGFR-MET FRET assay could detect (Gelsomino, Facchinetti et al. 2014). MET amplification is thought to be rare in EGFR-TKI naïve patients and whilst co-existence of *MET* amplification with T790M in patient specimens is recognized as uncommon, the extent of the scenarios in which EGFR and MET can contribute synergistically to tumorigenesis are not known (Bean, Brennan et al. 2007, Kubo, Yamamoto et al. 2009). Finally, testing *EGFR* mutations alone would

be unlikely to provide a sufficiently reliable surrogate of the EGFR-MET dimer as a therapeutic target as there may be other oncogenes present that also influence the EGFR-MET interaction.

An example of where a simple test has failed to appreciate the complexity of molecular signaling, has included the unexpected side effects seen with BRAF targeted tyrosine kinase inhibitors such as vemurafinib in melanoma whereby incomplete saturation of receptor by inhibitor results in RAF dimerisation and transactivation. This has led to attempts to design therapeutic approaches that dissociate RAF inhibition from paradoxical activation (Hey and Pritchard 2013, Samatar and Poulikakos 2014, Zhang, Spevak et al. 2015).

This could explain why dual targeting of EGFR-MET in clinical practice has not surmounted phase III clinical trials (Pérol 2014, Scagliotti, von Pawel et al. 2015), which is hampering the translation of these agents into novel therapies. It is plausible that this is because studies of MET targeted therapy have failed to select the appropriate subgroup of patients. Smaller studies continue to suggest a potential benefit of MET inhibitors by using newer predictive biomarkers and results in this area have been encouraging (Tanaka, Sueoka-Aragane et al. 2012). The preferred approaches to these 'partner tests' have evolved away from MET protein overexpression towards genomic aberrations such as *MET* copy number amplification, although the precise means of measuring this most accurately remains undetermined (Weingertner, Meyer et al. 2015). Newer literature has also identified a number of MET mutations, but neither is this an established method to predict treatment response (Paik, Drilon et al. 2015, Awad, Oxnard et al. 2016).

The priorities of improvements in assay development include better prognostication; the ability to rationalise use of these expensive agents; to identify those who would be at greatest risk of drug side effects relative to benefit from a given approach and rationalisation of drug design and testing. Thereafter having a test that is quick, easy, cost effective and deliverable within a clinical environment, whilst being accurate and acceptable to the patient in its means (e.g. blood sample or biopsy) are also important goals. This needs to be balanced against the wider cost implications of diagnostic and predictive partner tests, particularly in the current economic climate.

Considering the wider impact of this research on clinical practice and ultimately health policy, this data informs the need for more research into the potential of MET based therapies, the need for partner tests and what form they should take. Indeed, an

important consequence of such tests is that they should enable more rapid and effective development of drugs by enhancing outcomes as a percentage of trial participants as is shown by the difference between response rates in biomarker positive and negative patients in trials that assess the benefit of a drug based on a predictive biomarker as is now routinely the case for *EGFR* mutation testing and EGFR targeted therapy (Fukuoka, Wu et al. 2011, Rosell, Carcereny et al. 2012).

5.5 An H1975 derived model that elaborates upon TKI response

In summary, this chapter explores the wider significance of the findings related in this thesis whereby an NCI-H1975 based model of lung adenocarcinoma allowed us to observe how the EGFR mutations that define this model can alter tumour cell behaviour. I have discussed how the cell lines have enabled us to explore EGFR-MET dimerisation and its consequences for the potential therapeutic targeting of MET clinically. I have related this to the existing literature on MET targeted therapy and biomarkers in lung cancer and how an EGFR-MET signaling axis could add value to targeted therapy in patients with lung adenocarcinoma. Finally I have discussed the limitations of the model and suggest future avenues of research in this area.

The important outcomes of this PhD thesis include:

1) Through manipulation of the NCI-H1975 cell line we were able to directly compare the effects of *EGFR* mutations on EGFR-MET crosstalk and MET targeted therapy thus providing an important resource for future work in this area.
2) Design of a novel EGFR-MET FRET assay that allowed direct assessment of EGFR and MET interaction in a quantifiable manner. This has potential for improved understanding of the EGFR-MET interaction and could be extended to clinical applications ranging from prognostication to predicting response to treatment.
3) Thirdly, we have provided new evidence of the role of MET therapy in the presence of the *EGFR* oncogene. The need for further research in this area remains but our data suggests more efforts are required to understand the crosstalk between these pathways and the potential for assays addressing EGFR and MET to direct the combined inhibition of these targets.

The preparation of this data for publication and presentation in this thesis have provided an opportunity to reflect on further improvements that could be made to the model and approaches I would consider in future experiments. The major criticisms encountered in formal peer review of this work during the submission process, have included the potential for differences between the intrinsic EGFR L858R-T790M compared with transfected EGFR L858R and WT when instead transfecting with EGFR L858R-T790M may have been more comparable; the limitations of genomic manipulation using shEGFR compared with a CRISPR approach and thereafter the narrow focus on a pair of mutations within a single cell line.

All are valid concerns, which have contributed to the training provided within this fellowship. Reflecting further on this feedback within the wider group and at other scientific meetings reaffirms the strengths the model which has offered robust comparison between the mutations studied and has allowed consideration of the avenues which with additional time and resources may have been interesting to explore. The H1975 cell line approach is commonplace and robust in the EGFR translational science literature; whilst a CRISPR approach may have been desirable for increased accuracy of the mutational design of the cell lines, the polyclonality within our model may have reflected the heterogeneic nature of lung cancer more effectively. This could certainly be a direction of future research, potentially in combination with a transgenic e.g. FLOX mouse model. Using a non-cancer cell line such as HEK293, which does not have mutant EGFR, would also have been an interesting means of comparing the mutations in a purer population although would have been a less true representation of lung cancer *in vivo*.

With extended resources, we could also have combined the purer approach with multiple different mutations e.g. including del19 and *MET* amplification and additionally comparing these with other native lung cancer cell lines. It would be interesting to understand if the same patterns of dimerisation are observed with other activating or resistance mutations such as deletion in exon 19 and to probe the assay against these same mutations in other lung cancer cell lines and even to explore them in other models of cancer where EGFR or MET are known to be relevant.

Another element of the project, which could be expanded upon, would be the strategy of MET inhibition. A number of MET inhibitors are available and if resources allowed, comparing several of these would provide valuable insights as to how responses can differ between them. Our choice, SGX523, although clinically not viable, provided a highly selective tool to allow us to appreciate the role that the MET kinase contributed

to EGFR-MET interaction as directly assessed by FRET without off target effects (Buchanan, Hendle et al. 2009). There would be interest in extending this to other MET inhibitors and potentially to compare whether TKI and non-TKI inhibitors performed similarly in EGFR-MET dimer formation. Combinatorial approaches with EGFR inhibitors would also have been of considerable interest. In addition short hairpin elimination of MET and kinase dead MET mutants would have provided further validity to these approaches.

At the conception of this project some of these ideas and others were considered but the project presented was designed keeping in mind the need to maintain focus within the time and resource constraints suitable for a PhD thesis including guidance from local scientific peers and the MRC and Wellcome funding review bodies.

5.6 Future work and outstanding questions

Beyond these themes, a number of opportunities present themselves as new avenues of experiments to further elucidate the nature of the EGFR-MET interaction and with particular interest for the translation of the role of EGFR-MET crosstalk into clinical practice other ideas for translational research.

1) More detailed focus on the structural biology of the EGFR-MET dimer could reveal novel therapeutic approaches. For example there could be interest in exploring the structural determinants of EGFR-MET dimer with site directed mutagenesis aimed at disrupting domains important to dimerisation of one or both of these receptors. The impact of such structural alterations could be assessed using EGFR-MET FRET as a surrogate to predict clinical response.

2) Challenging the EGFR-MET FRET assay *ex vivo* as a screening tool for EGFR, MET or other related inhibitors (e.g. using pan-HER inhibitors) as a means of identifying potential agents for early clinical trials that might be more effective through manipulating the EGFR-MET dimer.

3) Finally developing the EGFR-MET FRET assay as a human biomarker for prognostic and predictive analysis of lung adenocarcinoma offers a novel avenue for translating this work to a clinically applicable tool.

Developing the EGFR-MET FRET assay further into a high throughput system would be an important step to any of these approaches, both experimentally, in terms of a system capable of rapidly assessing multiple experimental perturbations but also for use as a drug development screening tool or as a predictive biomarker applicable to meaningful numbers of clinical samples simultaneously (Kelleher, Fruhwirth et al. 2009).

Currently we depend on only a handful of clinical indices to dictate therapy (e.g. EGFR, KRAS, ALK, ROS). Novel biomarker tools such as FRET could prove vital to join up our knowledge of the wider promiscuity between receptor networks. Current approaches are based on the principal that a tumour tends to be addicted to a single oncogenic driver. It would be of interest to use FRET to understand where receptor crosstalk fits into this model. When does a passenger mutation emerge as a more significant driver and in what circumstances would this arise? Clinically this question is apparent in the example where *MET* amplification is seen to be enriched in samples from lung cancer brain metastasis - is MET therapy in the context of such lesions more relevant than the *EGFR* driver that led to the evolution of the first tumour? Single agent treatment approaches may not then be the most appropriate strategy - combining EGFR and MET therapies may help but understanding how to treat multiple targets with “Highly active anti-tumour therapy” may be the most difficult hurdle we are yet to face. Arrays of multiple FRET pairs, e.g. EGFR (WT)-MET, EGFR L858R-MET and beyond such as EGFR-HER3 assays could provide very interesting data on this front (Chmielecki and Pao 2010).

It would also be of interest to explore whether FRET would be most useful in early stage, fully resectable tumours or be better directed at tumour recurrence and those with advanced disease where other approaches have failed. In such circumstances one would want to compare the primary tumour with other metastatic lesions, potentially sampled more than once in the tumour evolution. FRET has also been demonstrated on liquid specimens and could thus be applied to circulating tumour cells as a blood test (Nedbal, Visitkul et al. 2015).

As medical therapies evolve, and the demand for those who are not surgically curable e.g. late stage disease; failed resection or advancing physiological age increase, this interesting question surrounding the extent to which we need to understand this system in more detail in order to find effective treatments becomes more relevant. We have little understanding of how many receptors or downstream mediators need to be inhibited to achieve sufficient tumour control. Similarly to what intricacy do we need to

understand the direction of a tumour cell to be able to understand the best clinical tests and select relevant therapies? Our knowledge has grown from classification to classification. At the outset this was 'cancer versus benign', 'metastatic versus non-metastatic'. We are now familiar with 'EGFR mutant versus non-mutant', 'L858R ± T790M or L858R with or without MET amplification or mutations. There will be increasing interest in newer technologies to assess these molecular aberrations, including approaches such as FRET to assess the wider promiscuity between receptor signaling pathways; capturing also the multiple signals likely to be seen with more complex treatment regimes that not only target classical inhibition e.g. kinase domain phosphorylation but that also look to modify protein-protein interaction more directly.

5.7 Summary

I have demonstrated that EGFR and MET interact directly and that their interaction is determined by *EGFR* genotype. MET TKI therapy modifies this interaction in a genotype specific manner and the response to MET TKI correlates with EGFR-MET dimerisation. Further work of interest would be to design clinical approaches to understand if this EGFR-MET interaction in MET targeted therapy can be translated, for example in the development of FRET EGFR-MET assays as a therapy partner test or to inform novel combinations of EGFR and MET therapies. Much is yet to be learned about the more complex interactions between these receptors, for example stoichiometry, directionality, specialised roles of particular mutants and the precise molecular nature of the interaction. Finally, considering EGFR and MET as a simplified paradigm of a wider system of derailed signaling in lung cancer, we can study the relevance of receptor interdependence. Through such an approach we might hope to understand how to tackle the wider complexities of the challenge of finding more effective lung cancer therapies as selectively applied according to predictive biomarkers.

Chapter 6. References

Alaoui-Jamali, M. A., D. J. Song, N. Benlimame, L. Yen, X. Deng, M. Hernandez-Perez and T. Wang (2003). "Regulation of multiple tumor microenvironment markers by overexpression of single or paired combinations of ErbB receptors." Cancer Res **63**(13): 3764-3774.

Amann, J., S. Kalyankrishna, P. P. Massion, J. E. Ohm, L. Girard, H. Shigematsu, M. Peyton, D. Juroske, Y. Huang, J. Stuart Salmon, Y. H. Kim, J. R. Pollack, K. Yanagisawa, A. Gazdar, J. D. Minna, J. M. Kurie and D. P. Carbone (2005). "Aberrant epidermal growth factor receptor signaling and enhanced sensitivity to EGFR inhibitors in lung cancer." Cancer Res **65**(1): 226-235.

Arteaga, C. L. (2007). "HER3 and mutant EGFR meet MET." Nat Med **13**(6): 675-677.

Arteaga, C. L. and J. A. Engelman (2014). "ERBB receptors: from oncogene discovery to basic science to mechanism-based cancer therapeutics." Cancer cell **25**(3): 282-303.

Awad, M. M., G. R. Oxnard, D. M. Jackman, D. O. Savukoski, D. Hall, P. Shivdasani, J. C. Heng, S. E. Dahlberg, P. A. Jänne, S. Verma, J. Christensen, P. S. Hammerman and L. M. Sholl (2016). "MET Exon 14 Mutations in Non–Small-Cell Lung Cancer Are Associated With Advanced Age and Stage-Dependent MET Genomic Amplification and c-Met Overexpression." Journal of Clinical Oncology.

Barber, P. R., I. D. C. Tullis, M. I. Rowley, C. D. Martins, G. Weitsman, K. Lawler, M. Coffey, N. Woodman, C. E. Gillett, T. Ng, B. Vojnovic, P. R. Barber, I. D. C. Tullis, M. I. Rowley, C. D. Martins, G. Weitsman, K. Lawler, M. Coffey, N. Woodman, C. E. Gillett, T. Ng and B. Vojnovic (2014). The Gray Institute open microscopes applied to radiobiology and protein interaction studies. Three-dimensional and multidimensional microscopy. T. Wilson and T. Wilson. Bellingham, Washington, S P I E - International Society for Optical Engineering. **8949**.

Bean, J., C. Brennan, J. Y. Shih, G. Riely, A. Viale, L. Wang, D. Chitale, N. Motoi, J. Szoke, S. Broderick, M. Balak, W. C. Chang, C. J. Yu, A. Gazdar, H. Pass, V. Rusch, W. Gerald, S. F. Huang, P. C. Yang, V. Miller, M. Ladanyi, C. H. Yang and W. Pao (2007). "MET amplification occurs with or without T790M mutations in EGFR mutant lung tumors with acquired resistance to gefitinib or erlotinib." Proc Natl Acad Sci U S A **104**(52): 20932-20937.

Beau-Faller, M., A. M. Ruppert, A. C. Voegeli, A. Neuville, N. Meyer, E. Guerin, M. Legrain, B. Mennecier, J. M. Wihlm, G. Massard, E. Quoix, P. Oudet and M. P. Gaub (2008). "MET gene copy number in non-small cell lung cancer: molecular analysis in a targeted tyrosine kinase inhibitor naive cohort." J Thorac Oncol **3**(4): 331-339.

Bell, D. W., I. Gore, R. A. Okimoto, N. Godin-Heymann, R. Sordella, R. Mulloy, S. V. Sharma, B. W. Brannigan, G. Mohapatra, J. Settleman and D. A. Haber (2005). "Inherited susceptibility to lung cancer may be associated with the T790M drug resistance mutation in EGFR." Nat Genet **37**(12): 1315-1316.

Benedettini, E., L. M. Sholl, M. Peyton, J. Reilly, C. Ware, L. Davis, N. Vena, D. Bailey, B. Y. Yeap, M. Fiorentino, A. H. Ligon, B. S. Pan, V. Richon, J. D. Minna, A. F. Gazdar, G. Draetta, S. Bosari, L. R. Chirieac, B. Lutterbach and M. Loda (2010). "Met activation in non-small cell lung cancer is associated with de novo resistance to EGFR inhibitors and the development of brain metastasis." Am J Pathol **177**(1): 415-423.

Boccaccio, C. and P. M. Comoglio (2006). "Invasive growth: a MET-driven genetic programme for cancer and stem cells." Nat Rev Cancer **6**(8): 637-645.

Bonine-Summers, A. R., M. E. Aakre, K. A. Brown, C. L. Arteaga, J. A. Pietenpol, H. L. Moses and N. Cheng (2007). "Epidermal Growth Factor Receptor Plays a Significant Role in Hepatocyte Growth Factor Mediated Biological Responses in Mammary Epithelial Cells." Cancer biology & therapy **6**(4): 561-570.

Brahmer, J., K. L. Reckamp, P. Baas, L. Crinò, W. E. E. Eberhardt, E. Poddubskaya, S. Antonia, A. Pluzanski, E. E. Vokes, E. Holgado, D. Waterhouse, N. Ready, J. Gainor, O. Arén Frontera, L. Havel, M. Steins, M. C. Garassino, J. G. Aerts, M. Domine, L. Paz-Ares, M. Reck, C. Baudelet, C. T. Harbison, B. Lestini and D. R. Spigel (2015). "Nivolumab versus Docetaxel in Advanced Squamous-Cell Non–Small-Cell Lung Cancer." New England Journal of Medicine **373**(2): 123-135.

Bublil, E. M., G. Pines, G. Patel, G. Fruhwirth, T. Ng, Y. Yarden, E. M. Bublil, G. Pines, G. Patel, G. Fruhwirth, T. Ng and Y. Yarden (2010). "Kinase-mediated quasi-dimers of EGFR." Faseb Journal **24**(12): 4744-4755.

Buchanan, S. G., J. Hendle, P. S. Lee, C. R. Smith, P. Y. Bounaud, K. A. Jessen, C. M. Tang, N. H. Huser, J. D. Felce, K. J. Froning, M. C. Peterman, B. E. Aubol, S. F. Gessert, J. M. Sauder, K. D. Schwinn, M. Russell, I. A. Rooney, J. Adams, B. C. Leon, T. H. Do, J. M. Blaney, P. A. Sprengeler, D. A. Thompson, L. Smyth, L. A. Pelletier, S. Atwell, K. Holme, S. R. Wasserman, S. Emtage, S. K. Burley and S. H. Reich (2009). "SGX523 is an exquisitely selective, ATP-competitive inhibitor of the MET receptor tyrosine kinase with antitumor activity *in vivo*." Mol Cancer Ther **8**(12): 3181-3190.

Burrell, R. A. and C. Swanton (2014). "Tumour heterogeneity and the evolution of polyclonal drug resistance." Molecular Oncology **8**(6): 1095-1111.

Camidge, D., S. Ou, G. Shapiro, G. Otterson, L. Villaruz, M. Villalona-Calero, A. Iafrate, M. Varella-Garcia, S. Dacic and S. Cardarella (2014). "Efficacy and safety of crizotinib in patients with advanced c-MET-amplified non-small cell lung cancer (NSCLC)." J Clin Oncol **32**(5).

Camidge, D. R., W. Pao and L. V. Sequist (2014). "Acquired resistance to TKIs in solid tumours: learning from lung cancer." Nat Rev Clin Oncol **11**(8): 473-481.

Campbell, M. R., D. Amin and M. M. Moasser (2010). "HER3 comes of age; New insights into its functions and role in signaling, tumor biology, and cancer therapy." Clinical cancer research : an official journal of the American Association for Cancer Research **16**(5): 1373-1383.

Cancer Genome Atlas Research, N. (2014). "Comprehensive molecular profiling of lung adenocarcinoma." Nature **511**(7511): 543-550.

Cappuzzo, F., P. A. Janne, M. Skokan, G. Finocchiaro, E. Rossi, C. Ligorio, P. A. Zucali, L. Terracciano, L. Toschi, M. Roncalli, A. Destro, M. Incarbone, M. Alloisio, A. Santoro and M. Varella-Garcia (2009). "MET increased gene copy number and primary resistance to gefitinib therapy in non-small-cell lung cancer patients." Ann Oncol **20**(2): 298-304.

Cappuzzo, F., A. Marchetti, M. Skokan, E. Rossi, S. Gajapathy, L. Felicioni, M. Del Grammastro, M. G. Sciarrotta, F. Buttitta, M. Incarbone, L. Toschi, G. Finocchiaro, A. Destro, L. Terracciano, M. Roncalli, M. Alloisio, A. Santoro and M. Varella-Garcia (2009). "Increased MET gene copy number negatively affects survival of surgically resected non-small-cell lung cancer patients." J Clin Oncol **27**(10): 1667-1674.

Capuani, F., A. Conte, E. Argenzio, L. Marchetti, C. Priami, S. Polo, P. P. Di Fiore, S. Sigismund and A. Ciliberto (2015). "Quantitative analysis reveals how EGFR activation and downregulation are coupled in normal but not in cancer cells." Nat Commun **6**.

Carey, K. D., A. J. Garton, M. S. Romero, J. Kahler, S. Thomson, S. Ross, F. Park, J. D. Haley, N. Gibson and M. X. Sliwkowski (2006). "Kinetic Analysis of Epidermal Growth Factor Receptor Somatic Mutant Proteins Shows Increased Sensitivity to the Epidermal Growth Factor Receptor Tyrosine Kinase Inhibitor, Erlotinib." Cancer Research **66**(16): 8163-8171.

Cassell, A. and J. R. Grandis (2010). "Investigational EGFR-targeted therapies in HNSCC." Expert opinion on investigational drugs **19**(6): 709-722.

Chen, X., J. Y. Zhou, J. Zhao, J. J. Chen, S. N. Ma and J. Y. Zhou (2013). "Crizotinib overcomes hepatocyte growth factor-mediated resistance to gefitinib in EGFR-mutant non-small-cell lung cancer cells." Anticancer Drugs **24**(10): 1039-1046.

Chen, Z., C. M. Fillmore, P. S. Hammerman, C. F. Kim and K.-K. Wong (2014). "Non-small-cell lung cancers: a heterogeneous set of diseases." Nat Rev Cancer **14**(8): 535-546.

Chmielecki, J. and W. Pao (2010). "Highly active antitumor therapy (HAATT) for epidermal growth factor receptor-mutant lung cancer." Clin Cancer Res **16**(22): 5371-5373.

Christensen, J. G., R. Schreck, J. Burrows, P. Kuruganti, E. Chan, P. Le, J. Chen, X. Wang, L. Ruslim, R. Blake, K. E. Lipson, J. Ramphal, S. Do, J. J. Cui, J. M. Cherrington and D. B. Mendel (2003). "A Selective Small Molecule Inhibitor of c-Met Kinase Inhibits c-Met-Dependent Phenotypes *in vitro* and Exhibits Cytoreductive Antitumor Activity *in vivo*." Cancer Research **63**(21): 7345-7355.

Chung, B. M., S. M. Raja, R. J. Clubb, C. Tu, M. George, V. Band and H. Band (2009). "Aberrant trafficking of NSCLC-associated EGFR mutants through the endocytic recycling pathway promotes interaction with Src." BMC Cell Biol **10**: 84.

Citri, A., K. B. Skaria and Y. Yarden (2003). "The deaf and the dumb: the biology of ErbB-2 and ErbB-3." Exp Cell Res **284**(1): 54-65.

Claus, J., G. Patel, T. Ng, P. Parker, J. Claus, G. Patel, T. Ng and P. Parker (2014). "A role for the pseudokinase HER3 in the acquired resistance against EGFR- and HER2-directed targeted therapy." Biochemical Society Transactions **42**(4): 831-836.

Claus, J., G. Patel, T. Ng and P. J. Parker (2014). "A role for the pseudokinase HER3 in the acquired resistance against EGFR- and HER2-directed targeted therapy." Biochem Soc Trans **42**(4): 831-836.

Coban, O., L. C. Zanetti-Dominguez, D. R. Matthews, D. J. Rolfe, G. Weitsman, P. R. Barber, J. Barbeau, V. Devauges, F. Kampmeier, M. Winn, B. Vojnovic, P. J. Parker, K. A. Lidke, D. S. Lidke, S. M. Ameer-Beg, M. L. Martin-Fernandez and T. Ng (2015). "Effect of phosphorylation on EGFR dimer stability probed by single-molecule dynamics and FRET/FLIM." Biophys J **108**(5): 1013-1026.

Couraud, S., G. Zalcman, B. Milleron, F. Morin and P.-J. Souquet (2012). "Lung cancer in never smokers – A review." European Journal of Cancer **48**(9): 1299-1311.

Cross, D. A. E., S. E. Ashton, S. Ghiorghiu, C. Eberlein, C. A. Nebhan, P. J. Spitzler, J. P. Orme, M. R. V. Finlay, R. A. Ward, M. J. Mellor, G. Hughes, A. Rahi, V. N. Jacobs, M. R. Brewer, E. Ichihara, J. Sun, H. Jin, P. Ballard, K. Al-Kadhimi, R. Rowlinson, T. Klinowska, G. H. P. Richmond, M. Cantarini, D.-W. Kim, M. R. Ranson and W. Pao (2014). "AZD9291, an irreversible EGFR TKI, overcomes T790M-mediated resistance to EGFR inhibitors in lung cancer." Cancer discovery **4**(9): 1046-1061.

Day, E., P. H. Dear and F. McCaughan (2013). "Digital PCR strategies in the development and analysis of molecular biomarkers for personalized medicine." Methods **59**(1): 101-107.

de Bruin, E. C., N. McGranahan, R. Mitter, M. Salm, D. C. Wedge, L. Yates, M. Jamal-Hanjani, S. Shafi, N. Murugaesu, A. J. Rowan, E. Grönroos, M. A. Muhammad, S. Horswell, M. Gerlinger, I. Varela, D. Jones, J. Marshall, T. Voet, P. Van Loo, D. M. Rassl, R. C. Rintoul, S. M. Janes, S.-M. Lee, M. Forster, T. Ahmad, D. Lawrence, M. Falzon, A. Capitanio, T. T. Harkins, C. C. Lee, W. Tom, E. Teefe, S.-C. Chen, S. Begum, A. Rabinowitz, B. Phillimore, B. Spencer-Dene, G. Stamp, Z. Szallasi, N. Matthews, A. Stewart, P. Campbell and C. Swanton (2014). "Spatial and temporal diversity in genomic instability processes defines lung cancer evolution." Science **346**(6206): 251-256.

Devarakonda, S., D. Morgensztern and R. Govindan (2015). "Genomic alterations in lung adenocarcinoma." The Lancet Oncology **16**(7): e342-e351.

Ekert, J. E., K. Johnson, B. Strake, J. Pardinas, S. Jarantow, R. Perkinson and D. C. Colter (2014). "Three-dimensional lung tumor microenvironment modulates therapeutic compound responsiveness *in vitro*--implication for drug development." PLoS One **9**(3): e92248.

Engelman, J. A., P. A. Janne, C. Mermel, J. Pearlberg, T. Mukohara, C. Fleet, K. Cichowski, B. E. Johnson and L. C. Cantley (2005). "ErbB-3 mediates phosphoinositide 3-kinase activity in gefitinib-sensitive non-small cell lung cancer cell lines." Proc Natl Acad Sci U S A **102**(10): 3788-3793.

Engelman, J. A., K. Zejnullahu, T. Mitsudomi, Y. Song, C. Hyland, J. O. Park, N. Lindeman, C. M. Gale, X. Zhao, J. Christensen, T. Kosaka, A. J. Holmes, A. M. Rogers, F. Cappuzzo, T. Mok, C. Lee, B. E. Johnson, L. C. Cantley and P. A. Janne (2007). "MET amplification leads to gefitinib resistance in lung cancer by activating ERBB3 signaling." Science **316**(5827): 1039-1043.

Ercan, D., C. Xu, M. Yanagita, C. S. Monast, C. A. Pratilas, J. Montero, M. Butaney, T. Shimamura, L. Sholl, E. V. Ivanova, M. Tadi, A. Rogers, C. Repellin, M. Capelletti, O. Maertens, E. M. Goetz, A. Letai, L. A. Garraway, M. J. Lazzara, N. Rosen, N. S. Gray, K. K. Wong and P. A. Janne (2012). "Reactivation of ERK signaling causes resistance to EGFR kinase inhibitors." Cancer Discov **2**(10): 934-947.

Feldman, M. E. and Y. Yarden (2014). "Steering tumor progression through the transcriptional response to growth factors and stroma." FEBS Lett **588**(15): 2407-2414.

Feng, Y., P. S. Thiagarajan and P. C. Ma (2012). "MET Signaling: Novel Targeted Inhibition and Its Clinical Development in Lung Cancer." Journal of Thoracic Oncology **7**(2): 459-467.

Fong, J. T., R. J. Jacobs, D. N. Moravec, S. B. Uppada, G. M. Botting, M. Nlend and N. Puri (2013). "Alternative signaling pathways as potential therapeutic targets for overcoming EGFR and c-Met inhibitor resistance in non-small cell lung cancer." PLoS One **8**(11): e78398.

Franklin, W. A., R. Veve, F. R. Hirsch, B. A. Helfrich and P. A. Bunn, Jr. (2002). "Epidermal growth factor receptor family in lung cancer and premalignancy." Semin Oncol **29**(1 Suppl 4): 3-14.

Fruhwirth, G. O., L. P. Fernandes, G. Weitsman, G. Patel, M. Kelleher, K. Lawler, A. Brock, S. P. Poland, D. R. Matthews, G. Keri, P. R. Barber, B. Vojnovic, S. M. Ameer-Beg, A. C. C. Coolen, F. Fraternali, T. Ng, G. O. Fruhwirth, L. P. Fernandes, G. Weitsman, G. Patel, M. Kelleher, K. Lawler, A. Brock, S. P. Poland, D. R. Matthews, G. Keri, P. R. Barber, B. Vojnovic, S. M. Ameer-Beg, A. C. C. Coolen, F. Fraternali and T. Ng (2011). "How Forster Resonance Energy Transfer Imaging Improves the Understanding of Protein Interaction Networks in Cancer Biology." Chemphyschem : A European journal of chemical physics and physical chemistry **12**(3): 442-461.

Fujita, T. (2013). "Targeted therapy for gastric cancer." Lancet Oncol **14**(6): 440-442.

Fukuoka, M., Y.-L. Wu, S. Thongprasert, P. Sunpaweravong, S.-S. Leong, V. Sriuranpong, T.-Y. Chao, K. Nakagawa, D.-T. Chu, N. Saijo, E. L. Duffield, Y. Rukazenkov, G. Speake, H. Jiang, A. A. Armour, K.-F. To, J. C.-H. Yang and T. S. K. Mok (2011). "Biomarker Analyses and Final Overall Survival Results From a Phase III, Randomized, Open-Label, First-Line Study of Gefitinib Versus Carboplatin/Paclitaxel in Clinically Selected Patients With Advanced Non–Small-Cell Lung Cancer in Asia (IPASS)." Journal of Clinical Oncology **29**(21): 2866-2874.

Gajiwala, K. S., J. Feng, R. Ferre, K. Ryan, O. Brodsky, S. Weinrich, J. C. Kath and A. Stewart (2013). "Insights into the aberrant activity of mutant EGFR kinase domain and drug recognition." Structure **21**(2): 209-219.

Garrett, T. P. J., N. M. McKern, M. Lou, M. J. Frenkel, J. D. Bentley, G. O. Lovrecz, T. C. Elleman, L. J. Cosgrove and C. W. Ward (1998). "Crystal structure of the first three domains of the type-1 insulin-like growth factor receptor." Nature **394**(6691): 395-399.

Gazdar, A. F. (2009). "Activating and resistance mutations of EGFR in non-small-cell lung cancer: role in clinical response to EGFR tyrosine kinase inhibitors." Oncogene **28 Suppl 1**: S24-31.

Gelsomino, F., F. Facchinetti, E. R. Haspinger, M. C. Garassino, L. Trusolino, F. De Braud and M. Tiseo (2014). "Targeting the MET gene for the treatment of non-small-cell lung cancer." Crit Rev Oncol Hematol **89**(2): 284-299.

Gherardi, E., W. Birchmeier, C. Birchmeier and G. Vande Woude (2012). "Targeting MET in cancer: rationale and progress." Nat Rev Cancer **12**(2): 89-103.

Gherardi, E., M. E. Youles, R. N. Miguel, T. L. Blundell, L. Iamele, J. Gough, A. Bandyopadhyay, G. Hartmann and P. J. G. Butler (2003). "Functional map and domain structure of MET, the product of the c-met protooncogene and receptor for hepatocyte growth factor/scatter factor." Proceedings of the National Academy of Sciences **100**(21): 12039-12044.

Go, H., Y. K. Jeon, H. J. Park, S.-W. Sung, J.-W. Seo and D. H. Chung (2010). "High MET Gene Copy Number Leads to Shorter Survival in Patients with Non-small Cell Lung Cancer." Journal of Thoracic Oncology **5**(3): 305-313.

Godin-Heymann, N., I. Bryant, M. N. Rivera, L. Ulkus, D. W. Bell, D. J. Riese, 2nd, J. Settleman and D. A. Haber (2007). "Oncogenic activity of epidermal growth factor receptor kinase mutant alleles is enhanced by the T790M drug resistance mutation." Cancer Res **67**(15): 7319-7326.

Goldstraw, P., K. Chansky, J. Crowley, R. Rami-Porta, H. Asamura, W. E. E. Eberhardt, A. G. Nicholson, P. Groome, A. Mitchell, V. Bolejack, P. Goldstraw, R. Rami-Porta, H. Asamura, D. Ball, D. G. Beer, R. Beyruti, V. Bolejack, K. Chansky, J. Crowley, F. Detterbeck, W. E. Erich Eberhardt, J. Edwards, F. Galateau-Sallé, D. Giroux, F. Gleeson, P. Groome, J. Huang, C. Kennedy, J. Kim, Y. T. Kim, L. Kingsbury, H. Kondo, M. Krasnik, K. Kubota, A. Lerut, G. Lyons, M. Marino, E. M. Marom, J. van Meerbeeck, A. Mitchell, T. Nakano, A. G. Nicholson, A. Nowak, M. Peake, T. Rice, K. Rosenzweig, E. Ruffini, V. Rusch, N. Saijo, P. Van Schil, J.-P. Sculier, L. Shemanski, K. Stratton, K. Suzuki, Y. Tachimori, C. F. Thomas Jr, W. Travis, M. S. Tsao, A. Turrisi, J. Vansteenkiste, H. Watanabe, Y.-L. Wu, P. Baas, J. Erasmus, S. Hasegawa, K. Inai, K. Kernstine, H. Kindler, L. Krug, K. Nackaerts, H. Pass, D. Rice, C. Falkson, P. L. Filosso, G. Giaccone, K. Kondo, M. Lucchi, M. Okumura, E. Blackstone, F. Abad Cavaco, E. Ansótegui Barrera, J. Abal Arca, I. Parente Lamelas, A. Arnau Obrer, R. Guijarro Jorge, D. Ball, G. K. Bascom, A. I. Blanco Orozco, M. A. González Castro, M. G. Blum, D. Chimondeguy, V. Cvijanovic, S. Defranchi, B. de Olaiz Navarro, I. Escobar Campuzano, I. Macía Videira, E. Fernández Araujo, F. Andreo García, K. M. Fong, G. Francisco Corral, S. Cerezo González, J. Freixinet Gilart, L. García Arangüena, S. García Barajas, P. Girard, T. Goksel, M. T. González Budiño, G. González Casaurrán, J. A. Gullón Blanco, J. Hernández Hernández, H. Hernández Rodríguez, J. Herrero Collantes, M. Iglesias Heras, J. M. Izquierdo Elena, E. Jakobsen, S.

Kostas, P. León Atance, A. Núñez Ares, M. Liao, M. Losanovscky, G. Lyons, R. Magaroles, L. De Esteban Júlvez, M. Mariñán Gorospe, B. McCaughan, C. Kennedy, R. Melchor Íñiguez, L. Miravet Sorribes, S. Naranjo Gozalo, C. Álvarez de Arriba, M. Núñez Delgado, J. Padilla Alarcón, J. C. Peñalver Cuesta, J. S. Park, H. Pass, M. J. Pavón Fernández, M. Rosenberg, E. Ruffini, V. Rusch, J. Sánchez de Cos Escuín, A. Saura Vinuesa, M. Serra Mitjans, T. E. Strand, D. Subotic, S. Swisher, R. Terra, C. Thomas, K. Tournoy, P. Van Schil, M. Velasquez, Y. L. Wu and K. Yokoi (2016). "The IASLC Lung Cancer Staging Project: Proposals for Revision of the TNM Stage Groupings in the Forthcoming (Eighth) Edition of the TNM Classification for Lung Cancer." Journal of Thoracic Oncology **11**(1): 39-51.

Greulich, H., T. H. Chen, W. Feng, P. A. Janne, J. V. Alvarez, M. Zappaterra, S. E. Bulmer, D. A. Frank, W. C. Hahn, W. R. Sellers and M. Meyerson (2005). "Oncogenic transformation by inhibitor-sensitive and -resistant EGFR mutants." PLoS Med **2**(11): e313.

Gridelli, C., P. Maione, F. Del Gaizo, G. Colantuoni, C. Guerriero, C. Ferrara, D. Nicolella, D. Comunale, A. De Vita and A. Rossi (2007). "Sorafenib and Sunitinib in the Treatment of Advanced Non-Small Cell Lung Cancer." The Oncologist **12**(2): 191-200.

Guessous, F., Y. Zhang, C. diPierro, L. Marcinkiewicz, J. Sarkaria, D. Schiff, S. Buchanan and R. Abounader (2010). "An orally bioavailable c-Met kinase inhibitor potently inhibits brain tumor malignancy and growth." Anticancer Agents Med Chem **10**(1): 28-35.

Guha, U., R. Chaerkady, A. Marimuthu, A. S. Patterson, M. K. Kashyap, H. C. Harsha, M. Sato, J. S. Bader, A. E. Lash, J. D. Minna, A. Pandey and H. E. Varmus (2008). "Comparisons of tyrosine phosphorylated proteins in cells expressing lung cancer-specific alleles of EGFR and KRAS." Proc Natl Acad Sci U S A **105**(37): 14112-14117.

Guo, A., J. Villen, J. Kornhauser, K. A. Lee, M. P. Stokes, K. Rikova, A. Possemato, J. Nardone, G. Innocenti, R. Wetzel, Y. Wang, J. MacNeill, J. Mitchell, S. P. Gygi, J. Rush, R. D. Polakiewicz and M. J. Comb (2008). "Signaling networks assembled by oncogenic EGFR and c-Met." Proc Natl Acad Sci U S A **105**(2): 692-697.

Gusenbauer, S., E. Zanucco, P. Knyazev and A. Ullrich (2015). "Erk2 but not Erk1 regulates crosstalk between Met and EGFR in squamous cell carcinoma cell lines." Mol Cancer **14**.

Hanahan, D. and R. A. Weinberg (2011). "Hallmarks of cancer: the next generation." Cell **144**(5): 646-674.

Hansen, A. R. and L. L. Siu (2013). "Epidermal Growth Factor Receptor Targeting in Head and Neck Cancer: Have We Been Just Skimming the Surface?" Journal of Clinical Oncology **31**(11): 1381-1383.

Harris, R. C., E. Chung and R. J. Coffey (2003). "EGF receptor ligands." Exp Cell Res **284**(1): 2-13.

Hata, A. N., M. J. Niederst, H. L. Archibald, M. Gomez-Caraballo, F. M. Siddiqui, H. E. Mulvey, Y. E. Maruvka, F. Ji, H.-e. C. Bhang, V. Krishnamurthy Radhakrishna, G. Siravegna, H. Hu, S. Raoof, E. Lockerman, A. Kalsy, D. Lee, C. L. Keating, D. A. Ruddy, L. J. Damon, A. S. Crystal, C. Costa, Z. Piotrowska, A. Bardelli, A. J. Iafrate, R. I. Sadreyev, F. Stegmeier, G. Getz, L. V. Sequist, A. C. Faber and J. A. Engelman (2016). "Tumor cells can follow distinct evolutionary paths to become resistant to epidermal growth factor receptor inhibition." Nat Med **22**(3): 262-269.

Hatanpaa, K. J., S. Burma, D. Zhao and A. A. Habib (2010). "Epidermal Growth Factor Receptor in Glioma: Signal Transduction, Neuropathology, Imaging, and Radioresistance." Neoplasia (New York, N.Y.) **12**(9): 675-684.

Herbst, R. S. (2004). "Review of epidermal growth factor receptor biology." Int J Radiat Oncol Biol Phys **59**(2 Suppl): 21-26.

Herbst, R. S., P. Baas, D.-W. Kim, E. Felip, J. L. Pérez-Gracia, J.-Y. Han, J. Molina, J.-H. Kim, C. D. Arvis, M.-J. Ahn, M. Majem, M. J. Fidler, G. de Castro, Jr., M. Garrido, G. M. Lubiniecki, Y. Shentu, E. Im, M. Dolled-Filhart and E. B. Garon (2016). "Pembrolizumab versus docetaxel for previously treated, PD-L1-positive, advanced non-small-cell lung cancer (KEYNOTE-010): a randomised controlled trial." The Lancet **387**(10027): 1540-1550.

Hey, F. and C. Pritchard (2013). "A new mode of RAF autoregulation: a further complication in the inhibitor paradox." Cancer Cell **23**(5): 561-563.

Hochreiter, B., A. P. Garcia and J. A. Schmid (2015). "Fluorescent proteins as genetically encoded FRET biosensors in life sciences." Sensors (Basel) **15**(10): 26281-26314.

Holbro, T., R. R. Beerli, F. Maurer, M. Koziczak, C. F. Barbas, 3rd and N. E. Hynes (2003). "The ErbB2/ErbB3 heterodimer functions as an oncogenic unit: ErbB2 requires ErbB3 to drive breast tumor cell proliferation." Proc Natl Acad Sci U S A **100**(15): 8933-8938.

Hubbard, S. R. (2009). "The Juxtamembrane Region of EGFR Takes Center Stage." Cell **137**(7): 1181-1183.

Hung, M.-S., I. C. Chen, J.-H. Lung, P.-Y. Lin, Y.-C. Li and Y.-H. Tsai (2016). "Epidermal Growth Factor Receptor Mutation Enhances Expression of Cadherin-5 in Lung Cancer Cells." PLoS ONE **11**(6): e0158395.

Hynes, N. E. and H. A. Lane (2005). "ERBB receptors and cancer: the complexity of targeted inhibitors." Nat Rev Cancer **5**(5): 341-354.

Infante, J. R., T. Rugg, M. Gordon, I. Rooney, L. Rosen, K. Zeh, R. Liu, H. A. Burris and R. K. Ramanathan (2013). "Unexpected renal toxicity associated with SGX523, a small molecule inhibitor of MET." Invest New Drugs **31**(2): 363-369.

Jackman, D., W. Pao, G. J. Riely, J. A. Engelman, M. G. Kris, P. A. Janne, T. Lynch, B. E. Johnson and V. A. Miller (2010). "Clinical definition of acquired resistance to epidermal growth factor receptor tyrosine kinase inhibitors in non-small-cell lung cancer." J Clin Oncol **28**(2): 357-360.

Jo, M., D. B. Stolz, J. E. Esplen, K. Dorko, G. K. Michalopoulos and S. C. Strom (2000). "Cross-talk between Epidermal Growth Factor Receptor and c-Met Signal Pathways in Transformed Cells." Journal of Biological Chemistry **275**(12): 8806-8811.

Johnson, B. E. (2016). "Divide and Conquer to Treat Lung Cancer." New England Journal of Medicine **375**(19): 1892-1893.

Junttila, M. R. and F. J. de Sauvage (2013). "Influence of tumour micro-environment heterogeneity on therapeutic response." Nature **501**(7467): 346-354.

Jura, N., N. F. Endres, K. Engel, S. Deindl, R. Das, M. H. Lamers, D. E. Wemmer, X. Zhang and J. Kuriyan (2009). "Mechanism for activation of the EGF receptor catalytic domain by the juxtamembrane segment." Cell **137**(7): 1293-1307.

Kalyankrishna, S. and J. R. Grandis (2006). "Epidermal Growth Factor Receptor Biology in Head and Neck Cancer." Journal of Clinical Oncology **24**(17): 2666-2672.

Kancha, R. K., N. von Bubnoff, C. Peschel and J. Duyster (2009). "Functional analysis of epidermal growth factor receptor (EGFR) mutations and potential implications for EGFR targeted therapy." Clin Cancer Res **15**(2): 460-467.

Karachaliou, N., C. Mayo-de Las Casas, C. Queralt, I. de Aguirre, B. Melloni, F. Cardenal, R. Garcia-Gomez, B. Massuti, J. M. Sanchez, R. Porta, S. Ponce-Aix, T. Moran, E. Carcereny, E. Felip, I. Bover, A. Insa, N. Reguart, D. Isla, A. Vergnenegre, F. de Marinis, R. Gervais, R. Corre, L. Paz-Ares, D. Morales-Espinosa, S. Viteri, A. Drozdowskyj, N. Jordana-Ariza, J. L. Ramirez-Serrano, M. A. Molina-Vila, R. Rosell and G. Spanish Lung Cancer (2015). "Association of EGFR L858R Mutation in Circulating Free DNA With Survival in the EURTAC Trial." JAMA Oncol **1**(2): 149-157.

Kawakami, H., I. Okamoto, T. Arao, W. Okamoto, K. Matsumoto, H. Taniguchi, K. Kuwata, H. Yamaguchi, K. Nishio, K. Nakagawa and Y. Yamada (2013). "MET amplification as a potential therapeutic target in gastric cancer." Oncotarget **4**(1): 9-17.

Kelleher, M. T., G. Fruhwirth, G. Patel, E. Ofo, F. Festy, P. R. Barber, S. M. Ameer-Beg, B. Vojnovic, C. Gillett, A. Coolen, G. Keri, P. A. Ellis and T. Ng (2009). "The potential of optical proteomic technologies to individualize prognosis and guide rational treatment for cancer patients." Target Oncol **4**(3): 235-252.

Kindler, H., T. Karrison, Y.-H. Carol Tan, B. Rose, M. Ahmad, C. Straus, R. Sargis and T. Seiwert (2017). "OA13.02 Phase II Trial of Pembrolizumab in Patients with Malignant Mesothelioma (MM): Interim Analysis." Journal of Thoracic Oncology **12**(1): S293-S294.

Kirisits, A., D. Pils and M. Krainer (2007). "Epidermal growth factor receptor degradation: an alternative view of oncogenic pathways." Int J Biochem Cell Biol **39**(12): 2173-2182.

Kiuchi, T., E. Ortiz-Zapater, J. Monypenny, D. R. Matthews, L. K. Nguyen, J. Barbeau, O. Coban, K. Lawler, B. Burford, D. J. Rolfe, E. de Rinaldis, D. Dafou, M. A. Simpson, N. Woodman, S. Pinder, C. E. Gillett, V. Devauges, S. P. Poland, G. Fruhwirth, P. Marra, Y. L. Boersma, A. Pluckthun, W. J. Gullick, Y. Yarden, G. Santis, M. Winn, B. N. Kholodenko, M. L. Martin-Fernandez, P. Parker, A. Tutt, S. M. Ameer-Beg and T. Ng (2014). "The ErbB4 CYT2 variant protects EGFR from ligand-induced degradation to enhance cancer cell motility." Sci Signal **7**(339): ra78.

Kong-Beltran, M., J. Stamos and D. Wickramasinghe "The Sema domain of Met is necessary for receptor dimerization and activation." Cancer Cell **6**(1): 75-84.

Kubo, T., H. Yamamoto, W. W. Lockwood, I. Valencia, J. Soh, M. Peyton, M. Jida, H. Otani, T. Fujii, M. Ouchida, N. Takigawa, K. Kiura, K. Shimizu, H. Date, J. D. Minna, M. Varella-Garcia, W. L. Lam, A. F. Gazdar and S. Toyooka (2009). "MET gene amplification or EGFR mutation activate MET in lung cancers untreated with EGFR tyrosine kinase inhibitors." Int J Cancer **124**(8): 1778-1784.

Kumar, A., E. T. Petri, B. Halmos and T. J. Boggon (2008). "Structure and clinical relevance of the epidermal growth factor receptor in human cancer." J Clin Oncol **26**(10): 1742-1751.

La Monica, S., C. Caffarra, F. Saccani, E. Galvani, M. Galetti, C. Fumarola, M. Bonelli, A. Cavazzoni, D. Cretella, R. Sirangelo, R. Gatti, M. Tiseo, A. Ardizzoni, E. Giovannetti, P. G. Petronini and R. R. Alfieri (2013). "Gefitinib Inhibits Invasive Phenotype and Epithelial-Mesenchymal Transition in Drug-Resistant NSCLC Cells with MET Amplification." PLoS ONE **8**(10): e78656.

Lakowicz, J. R. (2013). Principles of fluorescence spectroscopy, Springer Science & Business Media.

Lazzara, M. J., K. Lane, R. Chan, P. J. Jasper, M. B. Yaffe, P. K. Sorger, T. Jacks, B. G. Neel and D. A. Lauffenburger (2010). "Impaired SHP2-Mediated Extracellular Signal-Regulated Kinase Activation Contributes to Gefitinib Sensitivity of Lung Cancer Cells with Epidermal Growth Factor Receptor–Activating Mutations." Cancer Research **70**(9): 3843-3850.

Lee, J. K., S. Hahn, D. W. Kim, K. J. Suh, B. Keam, T. M. Kim, S. H. Lee and D. S. Heo (2014). "Epidermal growth factor receptor tyrosine kinase inhibitors vs conventional chemotherapy in non-small cell lung cancer harboring wild-type epidermal growth factor receptor: a meta-analysis." Jama **311**(14): 1430-1437.

Lemmon, M. A. (2009). "Ligand-induced ErbB receptor dimerization." Experimental cell research **315**(4): 638-648.

Lemmon, M. A. and J. Schlessinger (2010). "Cell signaling by receptor-tyrosine kinases." Cell **141**(7): 1117-1134.

Lemmon, M. A., J. Schlessinger and K. M. Ferguson (2014). "The EGFR family: not so prototypical receptor tyrosine kinases." Cold Spring Harb Perspect Biol **6**(4): a020768.

Liang, Z., J. Zhang, X. Zeng, J. Gao, S. Wu and T. Liu (2010). "Relationship between EGFR expression, copy number and mutation in lung adenocarcinomas." BMC Cancer **10**(1): 1-9.

Lievense, D. L. A., D. D. H. Sterman, D. R. Cornelissen and P. J. G. Aerts (2017). "Checkpoint Blockade in Lung Cancer and Mesothelioma." American Journal of Respiratory and Critical Care Medicine **0**(ja): null.

Littlefield, P. and N. Jura (2013). "EGFR lung cancer mutants get specialized." Proc Natl Acad Sci U S A **110**(38): 15169-15170.

Liu, Y. and N. S. Gray (2006). "Rational design of inhibitors that bind to inactive kinase conformations." Nat Chem Biol **2**(7): 358-364.

Lu, C., L. Z. Mi, T. Schurpf, T. Walz and T. A. Springer (2012). "Mechanisms for kinase-mediated dimerization of the epidermal growth factor receptor." J Biol Chem **287**(45): 38244-38253.

Lutterbach, B., Q. Zeng, L. J. Davis, H. Hatch, G. Hang, N. E. Kohl, J. B. Gibbs and B.-S. Pan (2007). "Lung Cancer Cell Lines Harboring MET Gene Amplification Are Dependent on Met for Growth and Survival." Cancer Research **67**(5): 2081-2088.

Lynch, T. J., D. W. Bell, R. Sordella, S. Gurubhagavatula, R. A. Okimoto, B. W. Brannigan, P. L. Harris, S. M. Haserlat, J. G. Supko, F. G. Haluska, D. N. Louis, D. C. Christiani, J. Settleman and D. A. Haber (2004). "Activating Mutations in the Epidermal Growth Factor Receptor Underlying Responsiveness of Non–Small-Cell Lung Cancer to Gefitinib." New England Journal of Medicine **350**(21): 2129-2139.

Ma, P. C., R. Jagadeeswaran, S. Jagadeesh, M. S. Tretiakova, V. Nallasura, E. A. Fox, M. Hansen, E. Schaefer, K. Naoki, A. Lader, W. Richards, D. Sugarbaker, A. N. Husain, J. G. Christensen and R. Salgia (2005). "Functional expression and mutations of c-Met and its therapeutic inhibition with SU11274 and small interfering RNA in non-small cell lung cancer." Cancer Res **65**(4): 1479-1488.

Ma, P. C., T. Kijima, G. Maulik, E. A. Fox, M. Sattler, J. D. Griffin, B. E. Johnson and R. Salgia (2003). "c-MET mutational analysis in small cell lung cancer: novel juxtamembrane domain mutations regulating cytoskeletal functions." Cancer Res **63**(19): 6272-6281.

Ma, P. C., G. Maulik, J. Christensen and R. Salgia (2003). "c-Met: structure, functions and potential for therapeutic inhibition." Cancer Metastasis Rev **22**(4): 309-325.

Maheswaran, S., L. V. Sequist, S. Nagrath, L. Ulkus, B. Brannigan, C. V. Collura, E. Inserra, S. Diederichs, A. J. Iafrate, D. W. Bell, S. Digumarthy, A. Muzikansky, D. Irimia, J. Settleman, R. G. Tompkins, T. J. Lynch, M. Toner and D. A. Haber (2008). "Detection of mutations in EGFR in circulating lung-cancer cells." N Engl J Med **359**(4): 366-377.

Matsubara, D., S. Ishikawa, O. Sachiko, H. Aburatani, M. Fukayama and T. Niki (2010). "Co-Activation of Epidermal Growth Factor Receptor and c-MET Defines a Distinct Subset of Lung Adenocarcinomas." The American Journal of Pathology **177**(5): 2191-2204.

Matsumoto, K. and T. Nakamura (2006). "Hepatocyte growth factor and the Met system as a mediator of tumor–stromal interactions." International Journal of Cancer **119**(3): 477-483.

Menis, J., M. G. Levra and S. Novello (2013). "MET inhibition in lung cancer." Translational Lung Cancer Research **2**(1): 23-39.

Merchant, M., X. Ma, H. R. Maun, Z. Zheng, J. Peng, M. Romero, A. Huang, N.-y. Yang, M. Nishimura, J. Greve, L. Santell, Y.-W. Zhang, Y. Su, D. W. Kaufman, K. L. Billeci, E. Mai, B. Moffat, A. Lim, E. T. Duenas, H. S. Phillips, H. Xiang, J. C. Young, G. F. Vande Woude, M. S. Dennis, D. E. Reilly, R. H. Schwall, M. A. Starovasnik, R. A. Lazarus and D. G. Yansura (2013). "Monovalent antibody design and mechanism of action of onartuzumab, a MET antagonist with anti-tumor activity as a therapeutic agent." Proceedings of the National Academy of Sciences **110**(32): E2987-E2996.

Mitsudomi, T. and Y. Yatabe (2010). "Epidermal growth factor receptor in relation to tumor development: EGFR gene and cancer." FEBS Journal **277**(2): 301-308.

Mitsui, K., M. Yonezawa, A. Tatsuguchi, S. Shinji, K. Gudis, S. Tanaka, S. Fujimori and C. Sakamoto (2014). "Localization of phosphorylated ErbB1-4 and heregulin in colorectal cancer." BMC Cancer **14**: 863.

Mok, T. S., Y. L. Wu, S. Thongprasert, C. H. Yang, D. T. Chu, N. Saijo, P. Sunpaweravong, B. Han, B. Margono, Y. Ichinose, Y. Nishiwaki, Y. Ohe, J. J. Yang, B. Chewaskulyong, H. Jiang, E. L. Duffield, C. L. Watkins, A. A. Armour and M. Fukuoka (2009). "Gefitinib or carboplatin-paclitaxel in pulmonary adenocarcinoma." N Engl J Med **361**(10): 947-957.

Morandell, S., T. Stasyk, S. Skvortsov, S. Ascher and L. A. Huber (2008). "Quantitative proteomics and phosphoproteomics reveal novel insights into complexity and dynamics of the EGFR signaling network." Proteomics **8**(21): 4383-4401.

Morgillo, F., C. M. Della Corte, M. Fasano and F. Ciardiello (2016). "Mechanisms of resistance to EGFR-targeted drugs: lung cancer." ESMO Open **1**(3).

Muller, S., A. Chaikuad, N. S. Gray and S. Knapp (2015). "The ins and outs of selective kinase inhibitor development." Nat Chem Biol **11**(11): 818-821.

Mulloy, R., A. Ferrand, Y. Kim, R. Sordella, D. W. Bell, D. A. Haber, K. S. Anderson and J. Settleman (2007). "Epidermal growth factor receptor mutants from human lung cancers exhibit enhanced catalytic activity and increased sensitivity to gefitinib." Cancer Res **67**(5): 2325-2330.

Murthy, U., M. Basu, A. Sen-Majumdar and M. Das (1986). "Perinuclear location and recycling of epidermal growth factor receptor kinase: immunofluorescent visualization using antibodies directed to kinase and extracellular domains." The Journal of Cell Biology **103**(2): 333-342.

Nakagawa, T., S. Takeuchi, T. Yamada, S. Nanjo, D. Ishikawa, T. Sano, K. Kita, T. Nakamura, K. Matsumoto, K. Suda, T. Mitsudomi, Y. Sekido, T. Uenaka and S. Yano (2012). "Combined therapy with mutant-selective EGFR inhibitor and Met kinase inhibitor for overcoming erlotinib resistance in EGFR-mutant lung cancer." Mol Cancer Ther **11**(10): 2149-2157.

Nedbal, J., V. Visitkul, E. Ortiz-Zapater, G. Weitsman, P. Chana, D. R. Matthews, T. Ng and S. M. Ameer-Beg (2015). "Time-domain microfluidic fluorescence lifetime flow cytometry for high-throughput Förster resonance energy transfer screening." Cytometry Part A **87**(2): 104-118.

Ng, T., M. Parsons, W. E. Hughes, J. Monypenny, D. Zicha, A. Gautreau, M. Arpin, S. Gschmeissner, P. J. Verveer, P. I. Bastiaens and P. J. Parker (2001). "Ezrin is a downstream effector of trafficking PKC-integrin complexes involved in the control of cell motility." EMBO J **20**(11): 2723-2741.

Ng, T., A. Squire, G. Hansra, F. Bornancin, C. Prevostel, A. Hanby, W. Harris, D. Barnes, S. Schmidt, H. Mellor, P. I. Bastiaens and P. J. Parker (1999). "Imaging protein kinase Calpha activation in cells." Science **283**(5410): 2085-2089.

Noro, R., A. Gemma, S. Kosaihira, Y. Kokubo, M. Chen, M. Seike, K. Kataoka, K. Matsuda, T. Okano, Y. Minegishi, A. Yoshimura and S. Kudoh (2006). "Gefitinib (IRESSA) sensitive lung cancer cell lines show phosphorylation of Akt without ligand stimulation." BMC Cancer **6**: 277.

Okuda, K., H. Sasaki, H. Yukiue, M. Yano and Y. Fujii (2008). "Met gene copy number predicts the prognosis for completely resected non-small cell lung cancer." Cancer Sci **99**(11): 2280-2285.

Olivero, M., M. Rizzo, R. Madeddu, C. Casadio, S. Pennacchietti, M. R. Nicotra, M. Prat, G. Maggi, N. Arena, P. G. Natali, P. M. Comoglio and M. F. Di Renzo (1996). "Overexpression and activation of hepatocyte growth factor/scatter factor in human non-small-cell lung carcinomas." Br J Cancer **74**(12): 1862-1868.

Ortiz-Zapater, E., R. W. Lee, W. Owen, G. Weitsman, G. Fruhwirth, R. G. Dunn, M. J. Neat, F. McCaughan, P. Parker, T. Ng and G. Santis (2017). "MET-EGFR dimerization in lung adenocarcinoma is dependent on EGFR mtations and altered by MET kinase inhibition." PLOS ONE **12**(1): e0170798.

Oser, M. G., M. J. Niederst, L. V. Sequist and J. A. Engelman (2015). "Transformation from non-small-cell lung cancer to small-cell lung cancer: molecular drivers and cells of origin." The Lancet Oncology **16**(4): e165-e172.

Paez, J. G., P. A. Janne, J. C. Lee, S. Tracy, H. Greulich, S. Gabriel, P. Herman, F. J. Kaye, N. Lindeman, T. J. Boggon, K. Naoki, H. Sasaki, Y. Fujii, M. J. Eck, W. R. Sellers, B. E. Johnson and M. Meyerson (2004). "EGFR mutations in lung cancer: correlation with clinical response to gefitinib therapy." Science **304**(5676): 1497-1500.

Paik, P. K., A. Drilon, P.-D. Fan, H. Yu, N. Rekhtman, M. S. Ginsberg, L. Borsu, N. Schultz, M. F. Berger, C. M. Rudin and M. Ladanyi (2015). "Response to MET Inhibitors in Patients with Stage IV Lung Adenocarcinomas Harboring MET Mutations Causing Exon 14 Skipping." Cancer Discovery **5**(8): 842-849.

Pao, W. and J. Chmielecki (2010). "Rational, biologically based treatment of EGFR-mutant non-small-cell lung cancer." Nat Rev Cancer **10**(11): 760-774.

Pao, W., V. A. Miller, K. A. Politi, G. J. Riely, R. Somwar, M. F. Zakowski, M. G. Kris and H. Varmus (2005). "Acquired resistance of lung adenocarcinomas to gefitinib or erlotinib is associated with a second mutation in the EGFR kinase domain." PLoS Med **2**(3): e73.

Park, J. H., Y. Liu, M. A. Lemmon and R. Radhakrishnan (2012). "Erlotinib binds both inactive and active conformations of the EGFR tyrosine kinase domain." Biochem J **448**(3): 417-423.

Park, K., E.-H. Tan, K. O'Byrne, L. Zhang, M. Boyer, T. Mok, V. Hirsh, J. C.-H. Yang, K. H. Lee, S. Lu, Y. Shi, S.-W. Kim, J. Laskin, D.-W. Kim, C. D. Arvis, K. Kölbeck, S. A. Laurie, C.-M. Tsai, M. Shahidi, M. Kim, D. Massey, V. Zazulina and L. Paz-Ares (2016). "Afatinib versus gefitinib as first-line treatment of patients with EGFR mutation-positive non-small-cell lung cancer (LUX-Lung 7): a phase 2B, open-label, randomised controlled trial." The Lancet Oncology **17**(5): 577-589.

Parsons, M., M. D. Keppler, A. Kline, A. Messent, M. J. Humphries, R. Gilchrist, I. R. Hart, C. Quittau-Prevostel, W. E. Hughes, P. J. Parker and T. Ng (2002). "Site-directed perturbation of protein kinase C- integrin interaction blocks carcinoma cell chemotaxis." Mol Cell Biol **22**(16): 5897-5911.

Patel, G. S., T. Kiuchi, K. Lawler, E. Ofo, G. O. Fruhwirth, M. Kelleher, E. Shamil, R. Zhang, P. R. Selvin, G. Santis, J. Spicer, N. Woodman, C. E. Gillett, P. R. Barber, B. Vojnovic, G. Keri, T. Schaeffter, V. Goh, M. J. O'Doherty, P. A. Ellis and T. Ng (2011). "The challenges of integrating molecular imaging into the optimization of cancer therapy." Integr Biol (Camb) **3**(6): 603-631.

Pérol, M. (2014). "Negative results of METLung study: an opportunity to better understand the role of MET pathway in advanced NSCLC." Translational Lung Cancer Research **3**(6): 392-394.

Peto, R., S. Darby, H. Deo, P. Silcocks, E. Whitley and R. Doll (2000). "Smoking, smoking cessation, and lung cancer in the UK since 1950: combination of national statistics with two case-control studies." BMJ **321**(7257): 323-329.

Pines, G., W. J. Köstler and Y. Yarden (2010). "Oncogenic mutant forms of EGFR: Lessons in signal transduction and targets for cancer therapy." FEBS Letters **584**(12): 2699-2706.

Pinheiro, L. B., V. A. Coleman, C. M. Hindson, J. Herrmann, B. J. Hindson, S. Bhat and K. R. Emslie (2012). "Evaluation of a Droplet Digital Polymerase Chain Reaction Format for DNA Copy Number Quantification." Analytical Chemistry **84**(2): 1003-1011.

Pirker, R. and M. Filipits (2012). "Cetuximab in non-small-cell lung cancer." Translational Lung Cancer Research **1**(1): 54-60.

Politi, K., M. F. Zakowski, P.-D. Fan, E. A. Schonfeld, W. Pao and H. E. Varmus (2006). "Lung adenocarcinomas induced in mice by mutant EGF receptors foundin human lung cancers respondto a tyrosine kinase inhibitor orto down-regulation of the receptors." Genes & Development **20**(11): 1496-1510.

Poulikakos, P. I., C. Zhang, G. Bollag, K. M. Shokat and N. Rosen (2010). "RAF inhibitors transactivate RAF dimers and ERK signalling in cells with wild-type BRAF." Nature **464**(7287): 427-430.

Puri, N. and R. Salgia (2008). "Synergism of EGFR and c-Met pathways, cross-talk and inhibition, in non-small cell lung cancer." J Carcinog **7**: 9.

Qian, L. W., K. Mizumoto, N. Maehara, K. Ohuchida, N. Inadome, M. Saimura, E. Nagai, K. Matsumoto, T. Nakamura and M. Tanaka (2003). "Co-cultivation of pancreatic cancer cells with orthotopic tumor-derived fibroblasts: fibroblasts stimulate tumor cell invasion via HGF secretion whereas cancer cells exert a minor regulative effect on fibroblasts HGF production." Cancer Lett **190**(1): 105-112.

Reck, M., D. F. Heigener, T. Mok, J.-C. Soria and K. F. Rabe (2013). "Management of non-small-cell lung cancer: recent developments." The Lancet **382**(9893): 709-719.

Red Brewer, M., C. H. Yun, D. Lai, M. A. Lemmon, M. J. Eck and W. Pao (2013). "Mechanism for activation of mutated epidermal growth factor receptors in lung cancer." Proc Natl Acad Sci U S A **110**(38): E3595-3604.

Regales, L., M. N. Balak, Y. Gong, K. Politi, A. Sawai, C. Le, J. A. Koutcher, D. B. Solit, N. Rosen, M. F. Zakowski and W. Pao (2007). "Development of New Mouse Lung Tumor Models Expressing EGFR T790M Mutants Associated with Clinical Resistance to Kinase Inhibitors." PLoS ONE **2**(8): e810.

Reiter, J. L., D. W. Threadgill, G. D. Eley, K. E. Strunk, A. J. Danielsen, C. S. Sinclair, R. S. Pearsall, P. J. Green, D. Yee, A. L. Lampland, S. Balasubramaniam, T. D. Crossley, T. R. Magnuson, C. D. James and N. J. Maihle (2001). "Comparative genomic sequence analysis and isolation of human and mouse alternative EGFR transcripts encoding truncated receptor isoforms." Genomics **71**(1): 1-20.

Rickert, K. W., S. B. Patel, T. J. Allison, N. J. Byrne, P. L. Darke, R. E. Ford, D. J. Guerin, D. L. Hall, M. Kornienko, J. Lu, S. K. Munshi, J. C. Reid, J. M. Shipman, E. F. Stanton, K. J. Wilson, J. R. Young, S. M. Soisson and K. J. Lumb (2011). "Structural basis for selective small molecule kinase inhibition of activated c-Met." J Biol Chem **286**(13): 11218-11225.

Riemenschneider, M. J., D. W. Bell, D. A. Haber and D. N. Louis (2005). "Pulmonary Adenocarcinomas with Mutant Epidermal Growth Factor Receptors." New England Journal of Medicine **352**(16): 1724-1725.

Rittmeyer, A., F. Barlesi, D. Waterkamp, K. Park, F. Ciardiello, J. von Pawel, S. M. Gadgeel, T. Hida, D. M. Kowalski, M. C. Dols, D. L. Cortinovis, J. Leach, J. Polikoff, C. Barrios, F. Kabbinavar, O. A. Frontera, F. De Marinis, H. Turna, J.-S. Lee, M. Ballinger, M. Kowanetz, P. He, D. S. Chen, A. Sandler and D. R. Gandara (2017). "Atezolizumab versus docetaxel in patients with previously treated non-small-cell lung cancer (OAK): a phase 3, open-label, multicentre randomised controlled trial." The Lancet **389**(10066): 255-265.

Rizvi, N. A., M. D. Hellmann, A. Snyder, P. Kvistborg, V. Makarov, J. J. Havel, W. Lee, J. Yuan, P. Wong, T. S. Ho, M. L. Miller, N. Rekhtman, A. L. Moreira, F. Ibrahim, C. Bruggeman, B. Gasmi, R. Zappasodi, Y. Maeda, C. Sander, E. B. Garon, T. Merghoub, J. D. Wolchok, T. N. Schumacher and T. A. Chan (2015). "Mutational landscape determines sensitivity to PD-1 blockade in non–small cell lung cancer." Science **348**(6230): 124-128.

Rosell, R., E. Carcereny, R. Gervais, A. Vergnenegre, B. Massuti, E. Felip, R. Palmero, R. Garcia-Gomez, C. Pallares, J. M. Sanchez, R. Porta, M. Cobo, P. Garrido, F. Longo, T. Moran, A. Insa, F. De Marinis, R. Corre, I. Bover, A. Illiano, E. Dansin, J. de Castro, M. Milella, N. Reguart, G. Altavilla, U. Jimenez, M. Provencio, M. A. Moreno, J. Terrasa, J. Munoz-Langa, J. Valdivia, D. Isla, M. Domine, O. Molinier, J. Mazieres, N. Baize, R. Garcia-Campelo, G. Robinet, D. Rodriguez-Abreu, G. Lopez-Vivanco, V. Gebbia, L. Ferrera-Delgado, P. Bombaron, R. Bernabe, A. Bearz, A. Artal, E. Cortesi, C. Rolfo, M. Sanchez-Ronco, A. Drozdowskyj, C. Queralt, I. de Aguirre, J. L. Ramirez, J. J. Sanchez, M. A. Molina, M. Taron, L. Paz-Ares, P.-C. Spanish Lung Cancer Group in collaboration with Groupe Francais de and T. Associazione Italiana Oncologia (2012). "Erlotinib versus standard chemotherapy as first-line treatment for European patients with advanced EGFR mutation-positive non-small-cell lung cancer (EURTAC): a multicentre, open-label, randomised phase 3 trial." Lancet Oncol **13**(3): 239-246.

Ruparel, M. and S. M. Janes (2016). "Lung cancer screening: what we can learn from UKLS?" Thorax **71**(2): 103-104.

Samatar, A. A. and P. I. Poulikakos (2014). "Targeting RAS-ERK signalling in cancer: promises and challenges." Nat Rev Drug Discov **13**(12): 928-942.

Scagliotti, G., J. von Pawel, S. Novello, R. Ramlau, A. Favaretto, F. Barlesi, W. Akerley, S. Orlov, A. Santoro, D. Spigel, V. Hirsh, F. A. Shepherd, L. V. Sequist, A. Sandler, J. S. Ross, Q. Wang, R. von Roemeling, D. Shuster and B. Schwartz (2015). "Phase III Multinational, Randomized, Double-Blind, Placebo-Controlled Study of Tivantinib (ARQ 197) Plus Erlotinib Versus Erlotinib Alone in Previously Treated Patients With Locally Advanced or Metastatic Nonsquamous Non-Small-Cell Lung Cancer." J Clin Oncol **33**(24): 2667-2674.

Scaltriti, M., C. Verma, M. Guzman, J. Jimenez, J. L. Parra, K. Pedersen, D. J. Smith, S. Landolfi, S. Ramon y Cajal, J. Arribas and J. Baselga (2009). "Lapatinib, a HER2 tyrosine

kinase inhibitor, induces stabilization and accumulation of HER2 and potentiates trastuzumab-dependent cell cytotoxicity." Oncogene **28**(6): 803-814.

Schlessinger, J. (2002). "Ligand-Induced, Receptor-Mediated Dimerization and Activation of EGF Receptor." Cell **110**(6): 669-672.

Schuler, M., Y.-L. Wu, V. Hirsh, K. O'Byrne, N. Yamamoto, T. Mok, S. Popat, L. V. Sequist, D. Massey, V. Zazulina and J. C. H. Yang (2016). "First-Line Afatinib versus Chemotherapy in Patients with Non–Small Cell Lung Cancer and Common Epidermal Growth Factor Receptor Gene Mutations and Brain Metastases." Journal of Thoracic Oncology **11**(3): 380-390.

Sequist, L. V., V. A. Joshi, P. A. Janne, A. Muzikansky, P. Fidias, M. Meyerson, D. A. Haber, R. Kucherlapati, B. E. Johnson and T. J. Lynch (2007). "Response to treatment and survival of patients with non-small cell lung cancer undergoing somatic EGFR mutation testing." Oncologist **12**(1): 90-98.

Sequist, L. V., J.-C. Soria, J. W. Goldman, H. A. Wakelee, S. M. Gadgeel, A. Varga, V. Papadimitrakopoulou, B. J. Solomon, G. R. Oxnard, R. Dziadziuszko, D. L. Aisner, R. C. Doebele, C. Galasso, E. B. Garon, R. S. Heist, J. Logan, J. W. Neal, M. A. Mendenhall, S. Nichols, Z. Piotrowska, A. J. Wozniak, M. Raponi, C. A. Karlovich, S. Jaw-Tsai, J. Isaacson, D. Despain, S. L. Matheny, L. Rolfe, A. R. Allen and D. R. Camidge (2015). "Rociletinib in EGFR-Mutated Non–Small-Cell Lung Cancer." New England Journal of Medicine **372**(18): 1700-1709.

Sequist, L. V., B. A. Waltman, D. Dias-Santagata, S. Digumarthy, A. B. Turke, P. Fidias, K. Bergethon, A. T. Shaw, S. Gettinger and A. K. Cosper (2011). "Genotypic and histological evolution of lung cancers acquiring resistance to EGFR inhibitors." Science translational medicine **3**(75): 75ra26-75ra26.

Shan, Y., M. P. Eastwood, X. Zhang, E. T. Kim, A. Arkhipov, R. O. Dror, J. Jumper, J. Kuriyan and D. E. Shaw (2012). "Oncogenic mutations counteract intrinsic disorder in the EGFR kinase and promote receptor dimerization." Cell **149**(4): 860-870.

Sharma, S. V., D. W. Bell, J. Settleman and D. A. Haber (2007). "Epidermal growth factor receptor mutations in lung cancer." Cancer **7**: 169-181.

Shi, P., Y.-T. Oh, G. Zhang, W. Yao, P. Yue, Y. Li, R. Kanteti, J. Riehm, R. Salgia, T. K. Owonikoko, S. S. Ramalingam, M. Chen and S.-Y. Sun (2016). "Met gene amplification and protein hyperactivation is a mechanism of resistance to both first and third generation EGFR inhibitors in lung cancer treatment." Cancer Letters **380**(2): 494-504.

Sholl, L. M., D. L. Aisner, M. Varella-Garcia, L. D. Berry, D. Dias-Santagata, Wistuba, II, H. Chen, J. Fujimoto, K. Kugler, W. A. Franklin, A. J. Iafrate, M. Ladanyi, M. G. Kris, B. E. Johnson, P. A. Bunn, J. D. Minna and D. J. Kwiatkowski (2015). "Multi-institutional oncogenic driver mutation analysis in lung adenocarcinoma: The Lung Cancer Mutation Consortium experience." J Thorac Oncol.

Shtiegman, K., B. S. Kochupurakkal, Y. Zwang, G. Pines, A. Starr, A. Vexler, A. Citri, M. Katz, S. Lavi, Y. Ben-Basat, S. Benjamin, S. Corso, J. Gan, R. B. Yosef, S. Giordano and Y. Yarden (2007). "Defective ubiquitinylation of EGFR mutants of lung cancer confers prolonged signaling." Oncogene **26**(49): 6968-6978.

Siegel, R. L., K. D. Miller and A. Jemal (2016). "Cancer statistics, 2016." CA: A Cancer Journal for Clinicians **66**(1): 7-30.

Singh, A. and J. Settleman (2010). "EMT, cancer stem cells and drug resistance: an emerging axis of evil in the war on cancer." Oncogene **29**(34): 4741-4751.

Sohn, J., S. Liu, N. Parinyanitikul, J. Lee, G. N. Hortobagyi, G. B. Mills, N. T. Ueno and A. M. Gonzalez-Angulo (2014). "cMET Activation and EGFR-Directed Therapy Resistance in Triple-Negative Breast Cancer." J Cancer **5**(9): 745-753.

Sordella, R., D. W. Bell, D. A. Haber and J. Settleman (2004). "Gefitinib-sensitizing EGFR mutations in lung cancer activate anti-apoptotic pathways." Science **305**(5687): 1163-1167.

Spigel, D. R., K. L. Reckamp, N. A. Rizvi, E. Poddubskaya, H. J. West, W. E. E. Eberhardt, P. Baas, S. J. Antonia, A. Pluzanski, E. E. Vokes, E. Holgado, D. M. Waterhouse, N. Ready, J. F. Gainor, O. R. Aren, L. Horn, L. Paz-Ares, C. Baudelet, B. J. Lestini and J. R. Brahmer (2015). "A phase III study (CheckMate 017) of nivolumab (NIVO; anti-programmed death-1 [PD-1]) vs docetaxel (DOC) in previously treated advanced or metastatic squamous (SQ) cell non-small cell lung cancer (NSCLC)." Journal of Clinical Oncology **33**(15_suppl): 8009-8009.

Stamos, J., M. X. Sliwkowski and C. Eigenbrot (2002). "Structure of the epidermal growth factor receptor kinase domain alone and in complex with a 4-anilinoquinazoline inhibitor." J Biol Chem **277**(48): 46265-46272.

Steinway, S. N., H. Dang, H. You, C. B. Rountree and W. Ding (2015). "The EGFR/ErbB3 Pathway Acts as a Compensatory Survival Mechanism upon c-Met Inhibition in Human c-Met+ Hepatocellular Carcinoma." PLoS One **10**(5): e0128159.

Stewart, E. L., S. Z. Tan, G. Liu and M.-S. Tsao (2015). "Known and putative mechanisms of resistance to EGFR targeted therapies in NSCLC patients with EGFR mutations—a review." Translational Lung Cancer Research **4**(1): 67-81.

Suda, K., R. Onozato, Y. Yatabe and T. Mitsudomi (2009). "EGFR T790M mutation: a double role in lung cancer cell survival?" J Thorac Oncol **4**(1): 1-4.

Surati, M., P. Patel, A. Peterson and R. Salgia (2011). "Role of MetMAb (OA-5D5) in c-MET active lung malignancies." Expert Opin Biol Ther **11**(12): 1655-1662.

Sutto, L. and F. L. Gervasio (2013). "Effects of oncogenic mutations on the conformational free-energy landscape of EGFR kinase." Proceedings of the National Academy of Sciences of the United States of America **110**(26): 10616-10621.

Takezawa, K., V. Pirazzoli, M. E. Arcila, C. A. Nebhan, X. Song, E. de Stanchina, K. Ohashi, Y. Y. Janjigian, P. J. Spitzler, M. A. Melnick, G. J. Riely, M. G. Kris, V. A. Miller, M. Ladanyi, K. Politi and W. Pao (2012). "HER2 Amplification: A Potential Mechanism of Acquired Resistance to EGFR Inhibition in EGFR-Mutant Lung Cancers That Lack the Second-Site EGFRT790M Mutation." Cancer Discov.

Tan, C.-S., B.-C. Cho and R. A. Soo (2016). "Next-generation epidermal growth factor receptor tyrosine kinase inhibitors in epidermal growth factor receptor -mutant non-small cell lung cancer." Lung Cancer **93**: 59-68.

Tan, D. S. W., T. S. K. Mok and T. R. Rebbeck (2015). "Cancer Genomics: Diversity and Disparity Across Ethnicity and Geography." Journal of Clinical Oncology.

Tanaka, A., N. Sueoka-Aragane, T. Nakamura, Y. Takeda, M. Mitsuoka, F. Yamasaki, S. Hayashi, E. Sueoka and S. Kimura (2012). "Co-existence of positive MET FISH status with EGFR mutations signifies poor prognosis in lung adenocarcinoma patients." Lung Cancer **75**(1): 89-94.

Tang, Z., R. Du, S. Jiang, C. Wu, D. S. Barkauskas, J. Richey, J. Molter, M. Lam, C. Flask, S. Gerson, A. Dowlati, L. Liu, Z. Lee, B. Halmos, Y. Wang, J. A. Kern and P. C. Ma (2008). "Dual MET-EGFR combinatorial inhibition against T790M-EGFR-mediated erlotinib-resistant lung cancer." Br J Cancer **99**(6): 911-922.

Tanizaki, J., I. Okamoto, K. Sakai and K. Nakagawa (2011). "Differential roles of trans-phosphorylated EGFR, HER2, HER3, and RET as heterodimerisation partners of MET in lung cancer with MET amplification." British journal of cancer **105**: 807-813.

Tao, J. J., P. Castel, N. Radosevic-Robin, M. Elkabets, N. Auricchio, N. Aceto, G. Weitsman, P. Barber, B. Vojnovic, H. Ellis, N. Morse, N. T. Viola-Villegas, A. Bosch, D. Juric, S. Hazra, S. Singh, P. Kim, A. Bergamaschi, S. Maheswaran, T. Ng, F. Penault-Llorca, J. S. Lewis, L. A. Carey, C. M. Perou, J. Baselga, M. Scaltriti, J. J. Tao, P. Castel, N. Radosevic-Robin, M. Elkabets, N. Auricchio, N. Aceto, G. Weitsman, P. Barber, B. Vojnovic, H. Ellis, N. Morse, N. T. Viola-Villegas, A. Bosch, D. Juric, S. Hazra, S. Singh, P. Kim, A. Bergamaschi, S. Maheswaran, T. Ng, F. Penault-Llorca, J. S. Lewis, L. A. Carey, C. M. Perou, J. Baselga and M. Scaltriti (2014). "Antagonism of EGFR and HER3 Enhances the Response to Inhibitors of the PI3K-Akt Pathway in Triple-Negative Breast Cancer." Science Signaling **7**(318).

Thatcher, N., F. R. Hirsch, A. V. Luft, A. Szczesna, T. E. Ciuleanu, M. Dediu, R. Ramlau, R. K. Galiulin, B. Bálint, G. Losonczy, A. Kazarnowicz, K. Park, C. Schumann, M. Reck, H. Depenbrock, S. Nanda, A. Kruljac-Letunic, R. Kurek, L. Paz-Ares and M. A. Socinski "Necitumumab plus gemcitabine and cisplatin versus gemcitabine and cisplatin alone as first-line therapy in patients with stage IV squamous non-small-cell lung cancer (SQUIRE): an open-label, randomised, controlled phase 3 trial." The Lancet Oncology **16**(7): 763-774.

The Cancer Genome Atlas Research, N. (2014). "Comprehensive molecular profiling of lung adenocarcinoma." Nature **511**(7511): 543-550.

Travis, W. D., E. Brambilla, M. Noguchi, A. G. Nicholson, K. Geisinger, Y. Yatabe, C. A. Powell, D. Beer, G. Riely, K. Garg, J. H. M. Austin, V. W. Rusch, F. R. Hirsch, J. Jett, P.-C. Yang and M. Gould (2011). "International Association for the Study of Lung Cancer/American Thoracic Society/European Respiratory Society: International Multidisciplinary Classification of Lung Adenocarcinoma." Proceedings of the American Thoracic Society **8**(5): 381-385.

Travis, W. D., E. Brambilla and G. J. Riely (2013). "New Pathologic Classification of Lung Cancer: Relevance for Clinical Practice and Clinical Trials." Journal of Clinical Oncology **31**(8): 992-1001.

Trusolino, L., A. Bertotti and P. M. Comoglio (2010). "MET signalling: principles and functions in development, organ regeneration and cancer." Nat Rev Mol Cell Biol **11**(12): 834-848.

Tsai, M. F., T. H. Chang, S. G. Wu, H. Y. Yang, Y. C. Hsu, P. C. Yang and J. Y. Shih (2015). "EGFR-L858R mutant enhances lung adenocarcinoma cell invasive ability and promotes malignant pleural effusion formation through activation of the CXCL12-CXCR4 pathway." Sci Rep **5**: 13574.

Turke, A. B., Y. Song, C. Costa, R. Cook, C. L. Arteaga, J. M. Asara and J. A. Engelman (2012). "MEK inhibition leads to PI3K/AKT activation by relieving a negative feedback on ERBB receptors." Cancer Res **72**(13): 3228-3237.

Turke, A. B., K. Zejnullahu, Y. L. Wu, Y. Song, D. Dias-Santagata, E. Lifshits, L. Toschi, A. Rogers, T. Mok, L. Sequist, N. I. Lindeman, C. Murphy, S. Akhavanfard, B. Y. Yeap, Y. Xiao, M. Capelletti, A. J. Iafrate, C. Lee, J. G. Christensen, J. A. Engelman and P. A. Janne (2010). "Preexistence and clonal selection of MET amplification in EGFR mutant NSCLC." Cancer Cell **17**(1): 77-88.

Uchida, A., S. Hirano, H. Kitao, A. Ogino, K. Rai, S. Toyooka, N. Takigawa, M. Tabata, M. Takata, K. Kiura and M. Tanimoto (2007). "Activation of downstream epidermal growth factor receptor (EGFR) signaling provides gefitinib-resistance in cells carrying EGFR mutation." Cancer Science **98**(3): 357-363.

Valley, C. C., D. J. Arndt-Jovin, T. M. Jovin, M. P. Steinkamp, A. I. Chizhik, N. Karedla, W. S. Hlavacek, B. S. Wilson, K. A. Lidke and D. S. Lidke (2015). "Inside-Out Signaling of Oncogenic EGFR Mutants Promotes Ligand-Independent Dimerization." Biophysical Journal **108**(2, Supplement 1): 351a.

Valley, C. C., D. J. Arndt-Jovin, N. Karedla, M. P. Steinkamp, A. I. Chizhik, W. S. Hlavacek, B. S. Wilson, K. A. Lidke and D. S. Lidke (2015). "Enhanced dimerization drives ligand-independent activity of mutant EGFR in lung cancer." Mol Biol Cell.

Vassal, G., M.-c. Ledeley, C. Tournigand, T. Aparicio, I. Ray-Coquard, L. Taillandier, B. Escudier, B. You, A. Goncalves, C. Lombard Bohas, J. F. Seitz, T. Andre, J.-P. Merlio, L. Arnould, G. Ferretti, Y. Menu, T. Mortier, E. Lonchamp, C. Mahier - Ait Oukhatar and D. Moro-Sibilot (2015). "Activity of crizotinib in relapsed MET amplified malignancies: Results of the French AcSe Program." ASCO Meeting Abstracts **33**(15_suppl): 2595.

Vigna, E. and P. M. Comoglio (2014). "Targeting the oncogenic Met receptor by antibodies and gene therapy." Oncogene.

Vivanco, I., H. I. Robins, D. Rohle, C. Campos, C. Grommes, P. L. Nghiemphu, S. Kubek, B. Oldrini, M. G. Chheda, N. Yannuzzi, H. Tao, S. Zhu, A. Iwanami, D. Kuga, J. Dang, A. Pedraza, C. W. Brennan, A. Heguy, L. M. Liau, F. Lieberman, W. K. Yung, M. R. Gilbert, D. A. Reardon, J. Drappatz, P. Y. Wen, K. R. Lamborn, S. M. Chang, M. D. Prados, H. A. Fine, S. Horvath, N. Wu, A. B. Lassman, L. M. DeAngelis, W. H. Yong, J. G. Kuhn, P. S. Mischel, M. P. Mehta, T. F. Cloughesy and I. K. Mellinghoff (2012). "Differential sensitivity of glioma- versus lung cancer-specific EGFR mutations to EGFR kinase inhibitors." Cancer Discov **2**(5): 458-471.

Wang, D. D., L. Ma, M. P. Wong, V. H. F. Lee and H. Yan (2015). "Contribution of EGFR and ErbB-3 Heterodimerization to the EGFR Mutation-Induced Gefitinib- and Erlotinib-Resistance in Non-Small-Cell Lung Carcinoma Treatments." PLoS ONE **10**(5): e0128360.

Wang, W., Q. Li, T. Yamada, K. Matsumoto, I. Matsumoto, M. Oda, G. Watanabe, Y. Kayano, Y. Nishioka, S. Sone and S. Yano (2009). "Crosstalk to Stromal Fibroblasts Induces Resistance of Lung Cancer to Epidermal Growth Factor Receptor Tyrosine Kinase Inhibitors." Clinical Cancer Research **15**(21): 6630-6638.

Wang, X., K. Li, H. Chen, D. Wang, Y. Zhang and C. Bai (2010). "Does hepatocyte growth factor/c-Met signal play synergetic role in lung cancer?" Journal of cellular and molecular medicine **14**: 833-839.

Wang, Z., P. a. Longo, M. K. Tarrant, K. Kim, S. Head, D. J. Leahy and P. a. Cole (2011). "Mechanistic insights into the activation of oncogenic forms of EGF receptor." Nature structural & molecular biology **18**: 1388-1393.

Weber, F., K. Fukino, T. Sawada, N. Williams, K. Sweet, R. M. Brena, C. Plass, T. Caldes, G. L. Mutter, M. A. Villalona-Calero and C. Eng (2005). "Variability in organ-specific EGFR mutational spectra in tumour epithelium and stroma may be the biological basis for differential responses to tyrosine kinase inhibitors." Br J Cancer **92**(10): 1922-1926.

Weingertner, N., N. Meyer, A.-C. Voegeli, D. Guenot, S. Renaud, G. Massard, P.-E. Falcoz, A. Olland, B. Mennecier, M.-P. Gaub, V. Lindner, J.-P. Ghnassia, E. Quoix, M.-P. Chenard and M. Beau-Faller (2015). "Correlation between MET protein expression and MET gene copy number in a Caucasian cohort of non-small cell lung cancers according to the new IASLC/ATS/ERS classification." Pathology - Journal of the RCPA **47**(4): 320-328.

Wickramasinghe, D. and M. Kong-Beltran (2005). "Met activation and receptor dimerization in cancer: a role for the Sema domain." Cell Cycle **4**(5): 683-685.

Wiehr, S., O. von Ahsen, L. Rose, A. Mueller, J. G. Mannheim, V. Honndorf, D. Kukuk, G. Reischl and B. J. Pichler (2013). "Preclinical evaluation of a novel c-Met inhibitor in a gastric cancer xenograft model using small animal PET." Mol Imaging Biol **15**(2): 203-211.

Wilson, T. R., J. Fridlyand, Y. Yan, E. Penuel, L. Burton, E. Chan, J. Peng, E. Lin, Y. Wang, J. Sosman, A. Ribas, J. Li, J. Moffat, D. P. Sutherlin, H. Koeppen, M. Merchant, R. Neve and J. Settleman (2012). "Widespread potential for growth-factor-driven resistance to anticancer kinase inhibitors." Nature **487**(7408): 505-509.

Wood, S. L., M. Pernemalm, P. A. Crosbie and A. D. Whetton (2014). "The role of the tumor-microenvironment in lung cancer-metastasis and its relationship to potential therapeutic targets." Cancer Treat Rev **40**(4): 558-566.

Worsham, M. J., H. Ali, J. Dragovic and V. P. Schweitzer (2012). "Molecular Characterization of Head and Neck Cancer: How Close to Personalized Targeted Therapy?" Molecular diagnosis & therapy **16**(4): 209-222.

Xu, K. P. and F. S. Yu (2007). "Cross talk between c-Met and epidermal growth factor receptor during retinal pigment epithelial wound healing." Invest Ophthalmol Vis Sci **48**(5): 2242-2248.

Xu, L., E. Kikuchi, C. Xu, H. Ebi, D. Ercan, K. A. Cheng, R. Padera, J. A. Engelman, P. A. Janne, G. I. Shapiro, T. Shimamura and K. K. Wong (2012). "Combined EGFR/MET or EGFR/HSP90 inhibition is effective in the treatment of lung cancers codriven by mutant EGFR containing T790M and MET." Cancer Res **72**(13): 3302-3311.

Xu, L., M. B. Nilsson, P. Saintigny, T. Cascone, M. H. Herynk, Z. Du, P. G. Nikolinakos, Y. Yang, L. Prudkin, D. Liu, J. J. Lee, F. M. Johnson, K. K. Wong, L. Girard, A. F. Gazdar, J. D. Minna, J. M. Kurie, Wistuba, II and J. V. Heymach (2010). "Epidermal growth factor receptor regulates MET levels and invasiveness through hypoxia-inducible factor-1alpha in non-small cell lung cancer cells." Oncogene **29**(18): 2616-2627.

Yakes, F. M., J. Chen, J. Tan, K. Yamaguchi, Y. Shi, P. Yu, F. Qian, F. Chu, F. Bentzien, B. Cancilla, J. Orf, A. You, A. D. Laird, S. Engst, L. Lee, J. Lesch, Y.-C. Chou and A. H. Joly (2011). "Cabozantinib (XL184), a Novel MET and VEGFR2 Inhibitor, Simultaneously Suppresses Metastasis, Angiogenesis, and Tumor Growth." Molecular Cancer Therapeutics **10**(12): 2298-2308.

Yano, S., W. Wang, Q. Li, K. Matsumoto, H. Sakurama, T. Nakamura, H. Ogino, S. Kakiuchi, M. Hanibuchi, Y. Nishioka, H. Uehara, T. Mitsudomi, Y. Yatabe, T. Nakamura and S. Sone (2008). "Hepatocyte Growth Factor Induces Gefitinib Resistance of Lung Adenocarcinoma with Epidermal Growth Factor Receptor–Activating Mutations." Cancer Research **68**(22): 9479-9487.

Yarden, Y. and M. X. Sliwkowski (2001). "Untangling the ErbB signalling network." Nat Rev Mol Cell Biol **2**(2): 127-137.

Yen, H. Y., Y. C. Liu, N. Y. Chen, C. F. Tsai, Y. T. Wang, Y. J. Chen, T. L. Hsu, P. C. Yang and C. H. Wong (2015). "Effect of sialylation on EGFR phosphorylation and resistance to tyrosine kinase inhibition." Proc Natl Acad Sci U S A **112**(22): 6955-6960.

Yousaf-Khan, U., C. van der Aalst, P. A. de Jong, M. Heuvelmans, E. Scholten, J.-W. Lammers, P. van Ooijen, K. Nackaerts, C. Weenink, H. Groen, R. Vliegenthart, K. ten Haaf, M. Oudkerk and H. de Koning (2017). "Final screening round of the NELSON lung cancer screening trial: the effect of a 2.5-year screening interval." Thorax **72**(1): 48-56.

Yu, H. A., S. K. Tian, A. E. Drilon and et al. (2015). "Acquired resistance of egfr-mutant lung cancer to a t790m-specific egfr inhibitor: Emergence of a third mutation (c797s) in the egfr tyrosine kinase domain." JAMA Oncology **1**(7): 982-984.

Yun, C.-H., T. J. Boggon, Y. Li, M. S. Woo, H. Greulich, M. Meyerson and M. J. Eck (2007). "Structures of Lung Cancer-Derived EGFR Mutants and Inhibitor Complexes: Mechanism of Activation and Insights into Differential Inhibitor Sensitivity." Cancer Cell **11**(3): 217-227.

Yun, C. H., K. E. Mengwasser, A. V. Toms, M. S. Woo, H. Greulich, K. K. Wong, M. Meyerson and M. J. Eck (2008). "The T790M mutation in EGFR kinase causes drug resistance by increasing the affinity for ATP." Proc Natl Acad Sci U S A **105**(6): 2070-2075.

Zhang, C., W. Spevak, Y. Zhang, E. A. Burton, Y. Ma, G. Habets, J. Zhang, J. Lin, T. Ewing, B. Matusow, G. Tsang, A. Marimuthu, H. Cho, G. Wu, W. Wang, D. Fong, H. Nguyen, S. Shi, P. Womack, M. Nespi, R. Shellooe, H. Carias, B. Powell, E. Light, L. Sanftner, J. Walters, J. Tsai, B. L. West, G. Visor, H. Rezaei, P. S. Lin, K. Nolop, P. N. Ibrahim, P. Hirth and G. Bollag (2015). "RAF inhibitors that evade paradoxical MAPK pathway activation." Nature **526**(7574): 583-586.

Zhang, J., P. L. Yang and N. S. Gray (2009). "Targeting cancer with small molecule kinase inhibitors." Nat Rev Cancer **9**(1): 28-39.

Zhang, X., J. Gureasko, K. Shen, P. A. Cole and J. Kuriyan (2006). "An allosteric mechanism for activation of the kinase domain of epidermal growth factor receptor." Cell **125**(6): 1137-1149.

Zhang, X., J. Gureasko, K. Shen, P. A. Cole and J. Kuriyan (2006). "An Allosteric Mechanism for Activation of the Kinase Domain of Epidermal Growth Factor Receptor." Cell **125**(6): 1137-1149.

Zhang, Y. W., B. Staal, C. Essenburg, S. Lewis, D. Kaufman and G. F. Vande Woude (2013). "Strengthening Context-Dependent Anti-Cancer Effects on Non-Small Cell Lung Carcinoma by Inhibition of Both MET and EGFR." Mol Cancer Ther.

Zhang, Y. W., B. Staal, C. Essenburg, Y. Su, L. Kang, R. West, D. Kaufman, T. Dekoning, B. Eagleson, S. G. Buchanan and G. F. Vande Woude (2010). "MET kinase inhibitor SGX523 synergizes with epidermal growth factor receptor inhibitor erlotinib in a hepatocyte growth factor-dependent fashion to suppress carcinoma growth." Cancer Res **70**(17): 6880-6890.

Zillhardt, M., J. G. Christensen and E. Lengyel (2010). "An Orally Available Small-Molecule Inhibitor of c-Met, PF-2341066, Reduces Tumor Burden and Metastasis in a Preclinical Model of Ovarian Cancer Metastasis." Neoplasia (New York, N.Y.) **12**(1): 1-10.

Zucali, P. A., M. G. Ruiz, E. Giovannetti, A. Destro, M. Varella-Garcia, K. Floor, G. L. Ceresoli, J. A. Rodriguez, I. Garassino, P. Comoglio, M. Roncalli, A. Santoro and G. Giaccone (2008). "Role of cMET expression in non-small-cell lung cancer patients treated with EGFR tyrosine kinase inhibitors." Ann Oncol **19**(9): 1605-1612.